

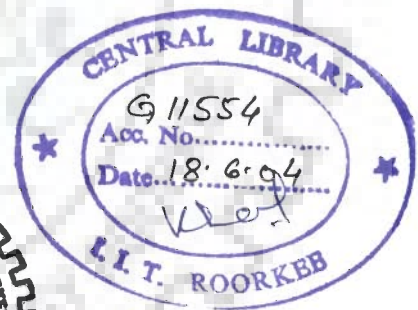
# BIOMASS CHARACTERIZATION AND GASIFICATION IN A FLUIDIZED BED

## A THESIS

*Submitted in fulfillment of the  
requirements for the award of the degree  
of*  
DOCTOR OF PHILOSOPHY  
*in*  
CHEMICAL ENGINEERING

By

**P. B. GANGAVATI**



DEPARTMENT OF CHEMICAL ENGINEERING  
INDIAN INSTITUTE OF TECHNOLOGY ROORKEE  
ROORKEE-247 667 (INDIA)

FEBRUARY, 2002



INDIAN INSTITUTE OF TECHNOLOGY  
ROORKEE

CANDIDATE'S DECLARATION

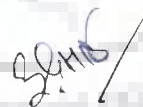
I hereby certify that the work which is being presented in the thesis entitled "BIOMASS CHARACTERIZATION AND GASIFICATION IN A FLUIDIZED BED" in fulfillment of the requirement for the award of the Degree of Doctor of Philosophy submitted in the Department of Chemical Engineering of the Indian Institute of Technology, Roorkee is an authentic record of my own work carried out during a period from August 1998 to February 2002 under the supervision of Dr. I.M. Mishra, Professor and Dr. B. Prasad, Assistant Professor, Department of Chemical Engineering, Indian Institute of Technology Roorkee, Roorkee.


The matter embodied in this thesis has not been submitted by me for the award of any other degree of this or any other Institute/University.

  
(P.B. GANGAVATI)


This is to certify that the above statement made by the candidate is correct to the best of our knowledge.


Date : February 14, 2002

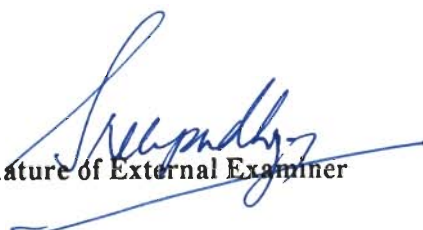
  
(I.M. MISHRA)  
Supervisor

  
(B. PRASAD)  
Supervisor

The Ph.D. Viva-Voce examination of Shri P.B. Gangawati, Research Scholar, has been held on 14.08.2002

  
Signature of Supervisor(s)

  
Signature of H.O.D.  
Prof. & Head

  
Signature of External Examiner

## ACKNOWLEDGEMENTS

---

I express my deep sense of gratitude to Dr. I. M. Mishra, Professor and Dr. B. Prasad, Assistant Professor, Department of Chemical Engineering, Indian Institute of Technology Roorkee, Roorkee for their suggestions, guidance and supervision at each level of this research work. I remain ever obliged for their kind inspiration, encouragement and wholehearted help without which this work would not have been completed.

I am thankful to Professor I. M. Mishra Head and Professor Surendra Kumar, former Head of Chemical Engineering Department for having provided me the departmental facilities.

I thank sincerely Dr. I. D. Mall, and Dr. Shri Chand, both Associate Professors for their encouragement and kind advice. I remember thankfully Late Dr. Desh Deepak for his kind encouragement.

My special thanks are due to Sarvashri B. K. Arora, Jugendra Singh, Bhag Singh, Harbans Singh, Ayodhya Prasad Singh, Satya Pal Singh, Sukh Pal Singh and Bhagwan Pal Singh of different laboratories of the Chemical Engineering Department for their generous, timely help and cooperation during the experimental phase of the work. My special thanks are also due to Shri Suresh Chand of Alternate Hydro Energy Center and Shri Anil Kumar Saini of Institute Instrumentation Center for kind help during experiments/analysis. Shri Suresh Singh took pains to type the manuscript, my thanks to him.

Shri Y.K. Atray deserves my heartfelt thanks for his vast help in the fabrication and initial testing of the gasifier unit.

I sincerely thank the Chairman of Shri Basaveshwar Vidya Vardhak Sangh, Bagalkot, the Principal, Basaveshwar Engineering College Bagalkot and the Directorate of Technical Education, Government of Karnataka for sponsoring me under Quality Improvement Programme. I am thankful to the Professor and coordinator and the staff at the QIP Centre, Indian Institute of Technology Roorkee for their

cooperation I am also thankful to the Professor and Head and colleagues of Mechanical Engineering Department at Basaveshwar Engineering College for their kind cooperation for making my study leave realized.

I am thankful to my friends, Mr. Inderjeet Singh, Dr. Abdal Kareem (Jordan), Mr. N.S. Khan, Mr. Anurag Garg, Mr. Salam Jibareel (Iraq), Mr. Alemayehu (Ethiopia) and Dr. A.K. Singh, for cheering me up and helping at the time of need. Mr. Madian, J. Safi (Syria) deserves special thanks for his pain taking help in some calculations.

My sincere thanks are due to Professor J. Corella of University Complutense of Madrid, Professor A.E. Ghaly of Dalhousie University, Dr. J. van Doorn and Dr. J. Neeft of ECN-Netherlands, Dr. Diblasi of University of Napoli, Professor Walawender W.P., Dr. P. Hasler of Verenum Research Zurich, and Dr. A.K. Jain of PAU Ludhiana for encouraging me by sending their paper reprints/suggestions.

I am very thankful to Smt. and Professor Arun Verma, and Smt. I. M. Mishra for their kind well wishes, encouragement and the care of us they took through out the study period.

I remember my father, late Dr. B.H. Gangavati who did not live long enough to see me even graduating. His ideals keep inspiring me always to try to do the best possible. Blessings of my mother Smt. Pramilabai helped me overcome difficulties. Wife Smt. Sadhana and Son Sudeep constantly encouraged me by enduring every difficulty throughout the period.

It was my proud privilege to be associated, as a student, with a renowned engineering teacher, academician and administrator Dr. I. M. Mishra. Dr. B. Prasad has impressed me by his scientific and positive approach in overcoming difficulties. I hope this experience helps me during the time to come, for the overall success of my participation in the Quality Improvement Programme.

I thank one and all for the kind help and suggestions received during the course of this work.

**P. B. GANGAVATI**

# ABSTRACT

---

The exploitation of renewable energy sources for meeting the ever increasing energy requirements has become more demanding for those developing countries which are importing significant amounts of crude petroleum, natural gas and petroleum products. Among the several alternative renewable energy sources, biomass occupies a unique place.

Biomass materials like agricultural, agro-processing and forestry residues are available in abundance in India. Some of them pose disposal problems due to their low fodder and fertilizer values, e.g. rice husk, bagasse, sawdust and pressmud (a waste from sugar industry), etc. Thermal gasification for energy utilization of such waste biomass materials is an attractive proposition. The well developed moving bed gasifiers have not been found suitable for such materials. A fluidized bed gasifier accepts the biomass of low bulk density and high ash content such as agricultural/agro-industrial and forestry wastes.

The present experimental study was undertaken to understand the fluidization behaviour, thermal degradation behaviour and kinetics of five most commonly and abundantly available agricultural, agro-industrial and forestry residues in India. These included village rice husk, mill rice husk, sawdust, bagasse and pressmud. Further, in the study, the village rice husk and sawdust were employed for studying their gasification characteristics in a fluidized bed gasifier.

## **Experimental Programme**

### **Fluidization Experiments**

The fluidization behaviour of the five biomass materials as binary mixtures with inert carrier solids like sand and bauxite were studied under cold flow atmosphere conditions in a set-up comprising of a vertical plexiglass fluidizing column of 76 mm id

and 1000 mm high and fitted with a multiorifice type distributor plate. Experiments were conducted for different weight percent of biomass content in the bed mixture (charge).

### **Thermal Degradation Behaviour and Kinetics**

The biomass materials were subjected to thermal analysis in a Stanton Redcraft thermo analyzer. Two heating rates ( $20^{\circ}\text{Cmin}^{-1}$  and  $40^{\circ}\text{Cmin}^{-1}$ ) and two experimental atmospheres (nitrogen and air) were used to obtain TGA, DTG and DTA thermograms. Thermal degradation characteristics and the kinetic parameters namely, activation energy, pre-exponential factor and order of reaction were obtained from these thermograms. Available integral and differential methods like these proposed by Coats and Redfern, Agarwal and Sivasubramanian, Horowitz and Metzger, Freeman and Carroll, Reich and Stivala and Piloyan and Novikova were used to determine kinetic parameters.

### **Fluidized Bed Gasification of Village Rice Husk and Sawdust**

Fluidized bed gasification of village rice husk and sawdust were conducted in a 100 mm id, 1650 mm total height fluidized bed gasifier unit developed in the laboratory. The unit comprised of the fluidized bed reactor, the biomass feeding unit, high efficiency cyclone and an after burner. A multiorifice type distributor plate was used to support the fluidizing solids and to distribute the fluidizing and gasifying air. The gasification experiments were conducted at four fluidization velocities ( $0.53$ ,  $0.59$ ,  $0.68$  and  $0.73 \text{ ms}^{-1}$ ) and at five equivalence ratios ( $0.20$ ,  $0.25$ ,  $0.30$ ,  $0.35$  and  $0.40$ ). Gas and tar sampling trains as per latest procedures were used. The gas was compositionally analysed using a gas chromatograph. The tar content of the raw gas was analysed gravimetrically.

The performance of the gasifier under different operating conditions of fluidization velocity and equivalence ratio was evaluated in terms of temperature profile in the reactor, gas composition, gas heating value, gas yield, carbon conversion

efficiency, tar and particulate content of the gas and the thermal efficiency of the gasifier for the two feedstocks.

## **Results and Discussion**

### **Preliminary Experiments**

In the preliminary experiments, the properties of the five biomass were determined to assess their suitability and feasibility for use as fuels/feedstocks for gasification. Their low bulk density values ( $< 200 \text{ kgm}^{-3}$ ) indicated that they were unsuitable as feedstocks for a moving bed gasifier. A fluidized bed gasifier accepts them as feedstocks. All the five biomass fuels had a low nitrogen content and a sufficiently good heating value.

### **Fluidization Behaviour of Biomass Materials**

Attempts to fluidize a biomass material alone as a single component bed charge indicated that a low bulk density (bulk density  $< 200 \text{ kgm}^{-3}$ ), complex shaped biomass material was not fluidizable easily and that an inert solid (carrier solid) must be added to the bed charge to make a binary mixture to facilitate its fluidization. Significant hysteresis was observed in the plots of pressure drop versus superficial air velocity (increasing and decreasing mode).

Fluidization of binary mixtures of carrier solid (sand or bauxite bed with  $H/D=1$ ) and 1 to 9 wt% of each biomass material indicated good fluidization of the bed charge upto a biomass content of 8 wt%. The quality of fluidization deteriorated with each one percent increase in the biomass content of the bed charge (visually observed) and that the mixture was not fluidizable beyond 8wt% of the biomass content in the bed. It was also observed that with increase in the biomass content in the bed mixture, the value of minimum fluidization velocity also increased.

### **Thermal Degradation Characteristics of Biomass Materials**

TGA, DTG and DTA curves showed the several distinct zones during which the thermal degradation process of the biomass. A natural break in the slope of the

TGA curve is indicative of a change in the rate of weight loss due to drying, devolatilization and degradation of biomass components namely hemicellulose, cellulose and lignin. The nature of TGA, DTG and DTA curves clearly indicated the number of reaction (degradation) zones for the thermal degradation of the five biomass materials under different experimental conditions. From the thermograms, the rates of degradation and weight of residue at the end of the degradation could be determined.

For village rice husk, four reaction zones were identified, while only three reaction zones could be seen for mill rice husk. During pyrolysis, the maximum rates of degradation for village rice husk were 11.7 and 23.1 wt% min<sup>-1</sup> at heating rates of 20 and 40°Cmin<sup>-1</sup> respectively. The thermal degradation in air showed only two distinct temperature zones for both village rice husk and mill rice husk with 14.9-17.5 wt%min<sup>-1</sup> at 20°Cmin<sup>-1</sup> and 37-39.51 wt%min<sup>-1</sup> at 40°Cmin<sup>-1</sup> heating rates, in the first reaction zone. The degradation rates in the second reaction zones were lower.

For sawdust, a five clear temperature (reaction) zones could be identified. The maximum rates of degradation were 29.7 and 56.9 wt%min<sup>-1</sup> at 20 and 40°Cmin<sup>-1</sup> heating rates respectively. The residues were 17.5% at 20°Cmin<sup>-1</sup> and 25.0% at 40°Cmin<sup>-1</sup>. During thermal degradation in air, four distinct degradation zones, other than the one of drying, were identified. Maximum rates of degradation were during second reaction zone with the values of 46.6 wt% min<sup>-1</sup> and 51.6 wt%min<sup>-1</sup> for 20 and 40°Cmin<sup>-1</sup> heating rates respectively.

The thermal degradation of bagasse in nitrogen indicated three reaction zones with the second zone having the maximum degradation rates of 22.5 wt%min<sup>-1</sup> and 49.6 wt%min<sup>-1</sup> for 20 and 40°Cmin<sup>-1</sup> heating rates respectively. Air degradation had five reaction zones. Pressmud, a sugar mill waste, showed distinct degradation behaviour in comparison to other biomass materials. Pyrolysis behaviour showed poor devolatilization with maximum degradation rates of 9.7 wt%min<sup>-1</sup> and 14.0 wt%min<sup>-1</sup> at 25 and 40°Cmin<sup>-1</sup> respectively. However in an oxidizing environment rate of



degradation was as high as  $90 \text{ wt\%min}^{-1}$  at  $10^\circ\text{Cmin}^{-1}$  which showed that pressmud has the potential to be considered as a feedstock for gasification.

### **Kinetics of Thermal Degradation**

TGA curves were used to determine kinetics of thermal degradation of the biomass materials in nitrogen and air atmospheres using differential and integral methods. In all six methods as proposed by Coats and Redfern (1964), Agarwal and Sivasubramanian (1987), Horowitz and Metzger (1963), Piloyan and Novikova (1967), Reich and Stivala (1982) and Freeman and Carroll (1958) were used to determine kinetic parameters assuming a simple, single-step, irreversible reaction. The entire degradation zone was also represented by a single-step, irreversible reaction using Agarwal and Sivasubramanian approximation for the integral analysis of kinetics. For all the biomass materials, at the two heating rates and under nitrogen and air atmospheres, the kinetic parameters were determined by using a least-square best-fit approach. For the integral method of Coats and Redfern, and Agarwal and Sivasubramanian, the  $n$  was varied from zero to 3.0 to obtain the best-fit linear relation to determine the activation energy  $E$ , and the pre-exponential factor,  $k_0$ . For any  $n$ , the value of  $E$  obtained by Coats and Redfern method and Agarwal and Sivasubramanian method were the same. The pre-exponential factor, however, differed slightly. From the results it was clear that the entire range of degradation could be represented by a single-step, irreversible reaction using Agarwal and Sivasubramanian (1987) approximation for integration, with reasonable confidence for all the biomass materials. It was found that as the value of  $n$  increased, the activation energy also increased for the best fit correlation using integral method. Therefore, it is not the activation energy alone, but the value of order of reaction  $n$  which gave the best fit for the TGA data, alongwith  $E$  and  $k_0$  should be taken for the design of pyrolysis and gasification reactor.

The kinetic parameters indicated that the best fit kinetic parameters varied in the range  $0.50 < n < 2.50$ ,  $27.84 < E < 132.9 \text{ kJmol}^{-1}$  and  $3.21 \times 10^1 < k_0 < 1.414 \times 10^{12} \text{ min}^{-1}$  for all the biomass materials. For air degradation, the values of  $E$  are found to be

higher than those for pyrolysis at any value of  $n$ . The values of  $n$ ,  $E$  and  $k_0$  are found to be within the range reported by other investigators.

### **Fluidized Bed Gasification of Village Rice Husk and Sawdust**

The performance of the gasifier-unit, as a whole, was found to be satisfactory for both village rice husk and sawdust gasification.

The average bed temperature varied between 575 to 782°C for village rice husk gasification and 680 to 791°C for sawdust gasification. The average free board temperatures were found to be lower than the average bed temperatures by 79 to 131°C for village rice husk and 81 to 92°C for sawdust. This was because of the absence of any external heat source to assist the gasification process, as has been employed by other investigators. Gasifier temperatures increased with increase in the equivalence ratio and/or with increase in the fluidization velocity.

As the equivalence ratio increased, the concentration of  $\text{CO}_2$  increased and the concentrations of fuel gases viz.,  $\text{CO}$ ,  $\text{H}_2$ ,  $\text{CH}_4$  and  $\text{C}_2\text{H}_m$  decreased. Increase in fluidization velocity lead to the similar effect. Among the fuel gases,  $\text{CO}$  had the highest concentration (11.2-19.4% vol. for VRH; 12.8-19.9% vol. For SD) followed by  $\text{H}_2$  (2.7-2.8% vol. for VRH; 3.1-4.3% vol. for SD), and  $\text{CH}_4$  (1.5-2.3%vol. for VRH; 2.0 – 2.7% vol. for SD). The gas higher heating value (HHV) ranged from 2.35 to 3.85  $\text{MJNm}^{-3}$  (gas at normal temperature and pressure) for village rice husk (VRH) and 2.81 to 4.14  $\text{MJNm}^{-3}$  for sawdust (SD). The higher heating value of the product gas from both village rice husk and sawdust decreased linearly with increase in the equivalence ratio and fluidization velocity. The gas yield varied from 1.8 to 2.14  $\text{Nm}^3 \text{kg}^{-1}$  DAF for village rice husk and 1.88 to 2.13  $\text{nm}^3 \text{kg}^{-1}$  DAF for sawdust. In both cases, the gas yield increased with equivalence ratio (ER) upto  $\text{ER}=0.35$  and thereafter it decreased. The energy output (the energy value of the gas per kg of VRH or SD) were found to be in the range of 4.7 to 7.3  $\text{MJkg}^{-1}$  DAF for VRH and 5.6 to 8.1  $\text{MJkg}^{-1}$  DAF for SD. Carbon conversion efficiency varied from 52.03 to 65.94% for VRH and 57.18 to 66.93% for SD.

The gravimetric method allowed the determination of high boiling tar compounds only. The tar content of the raw product gas slightly decreased with increase in equivalence ratio for both village rice husk and sawdust. Fluidization velocity did not seem to affect the tar content. Particulate matter content of the gas did not exhibit any specific trend with either equivalence ratio or fluidization velocity. The gasifier thermal efficiency ranged from 51.43 to 72.30% for sawdust gasification and 36.39 to 57.04% for village rice husk gasification.



# LIST OF CONTENTS

CHAPTER	TITLE	PAGE NO.
	CANDIDATE'S DECLARATION	i
	ACKNOWLEDGEMENTS	ii
	ABSTRACT	iv
	CONTENTS	xi
	LIST OF FIGURES	xvii
	LIST OF TABLES	xxiii
	LIST OF ABBREVIATIONS AND SYMBOLS	xxix
<b>CHAPTER 1</b>	<b>INTRODUCTION</b>	<b>1</b>
	1.1 Biomass	1
	1.2 Availability of Biomass	2
	1.3 Physico-Chemical and Thermal Characteristics of Biomass Materials	4
	1.4 Thermochemical Conversion of Biomass	5
	1.5 Types of Biomass Gasifiers	11
	1.6 Chemistry of Biomass Gasification	12
	1.7 Fluidized Bed Gasification	15
	1.8 Effect of Equivalence Ratio	19
	1.9 Present Status of Research on Fluidized Bed Thermal Gasification in India	23
	1.10 Aims and Objectives of the Proposed Work	24
<b>CHAPTER II</b>	<b>LITERATURE REVIEW</b>	<b>25</b>
	2.1 Fluidization of Binary Mixtures of Particles	25

2.2	Fluidization of Biomass Materials	33
2.3	Thermal Degradation/Decomposition of Biomass Using Thermogravimetric Analysis	41
2.4	Determination of Kinetic Parameters During Pyrolysis	49
2.4.1	Single Reaction Models	50
2.4.1.1	Integral method	51
2.4.1.2	Differential method	54
2.4.1.3	Maximum rate method using DTG and/DTA data	57
2.4.2	Multi Reaction Models	58
2.4.2.1	Distributed activation energy model (DAEM)	59
2.4.2.2	Individual volatile product model (IVPM)	61
2.4.2.3	Functional group model (FGM)	61
2.5	Studies on Fluidized Bed Gasification of Biomass	62
2.5.1	Air Gasification	62
2.5.2	Steam Gasification	67
2.5.3	Gasification with Steam and Oxygen Mixtures	77
2.5.4	Modified Fluidized Bed Gasifiers	78
<b>CHAPTER III</b>	<b>EXPERIMENTAL</b>	<b>81</b>
3.1	Biomass Materials : Collection and Storage	81
3.2	Physico-Mechanical Characteristics of Biomass Materials	82
3.2.1	Bulk Density	82
3.2.2	Particle Density	82
3.2.3	Particle Size	82

3.2.4	Packed Bed Voidage	82
3.2.5	Angle of Repose	82
3.2.6	Angle of Slide	83
3.2.7	Carrier Solids and their Properties	83
3.3	Physico-Chemical and Thermochemical Characteristics of Biomass Materials	84
3.3.1	Proximate Analysis	84
3.3.2	Ultimate Analysis	85
3.3.3	Heating Values	86
3.3.4	Ash Deformation and Fusion Temperatures	86
3.4	Cold-flow Fluidization	86
3.4.1	Experimental Set-up	86
3.4.2	Minimum Fluidization Velocity of Carrier Solids	88
3.4.3	Fluidization of a Biomass when Fluidized Alone	89
3.4.4	Minimum Fluidization Velocity of Mixtures of Carrier Solid and Biomass	89
3.5	Thermal Degradation Studies	90
3.6	Experimental Set-up for the Fluidized Bed Thermal Gasification of Biomass with Air	90
3.6.1	The Fluidized Bed Reactor	91
3.6.2	Air Supply Unit	96
3.6.3	The Biomass Feeding Unit	97
3.6.4	Cyclone	100
3.7	Gasification Measurements	100
3.7.1	Temperature Measurements	100
3.7.2	Pressure Drop and Flow Rate Measurements	102
3.7.3	Feed Rate of Biomass	105

3.8	Gasification Runs	105
3.8.1	Start-Up of the Gasifier	108
3.8.2	Steady State Operation of the Gasifier	108
3.8.3	Shut Down of the Gasifier	109
3.9	Sampling of Gas	110
3.9.1	Gas Sampling Train	110
3.9.2	Gas Sampling	110
3.9.3	Compositional Analysis of Gas	112
3.10	Tar Sampling	112
3.10.1	Tar Sampling Train	112
3.10.2	Tar Sampling	114
3.10.3	Determination of Particulates	118
3.10.4	Gravimetric Analysis of Tar	119
<b>CHAPTER IV</b>	<b>RESULTS AND DISCUSSION</b>	<b>120</b>
4.1	Fluidization Behaviour of Biomass Materials	120
4.1.1	Physico-Mechanical Properties of Biomass Materials	120
4.1.2	Fluidization Characteristics	123
4.2	Thermal Degradation Behaviour and Kinetics Using Thermogravimetric Analysis	147
4.2.1	Biomass Materials and Test Conditions	147
4.2.2	Thermal Degradation Characteristics	147
4.2.2.1	Village rice husk	147
4.2.2.2	Mill rice husk	151
4.2.2.3	Sawdust	157
4.2.2.4	Bagasse	163
4.2.2.5	Pressmud	169

4.3	Kinetics of Biomass Thermal Decomposition	174
4.3.1	Integral and Differential Methods for the Use with Thermogravimetry	174
4.3.2	Kinetics of Pyrolysis	176
	4.3.2.1 Village rice husk	178
	4.3.2.2 Mill rice husk	181
	4.3.2.3 Sawdust	185
	4.3.2.4 Bagasse	188
	4.3.2.5 Pressmud	191
4.3.3	Kinetics of Thermal Degradation in Oxidizing (Air) Atmosphere	195
	4.3.3.1 Village rice husk and mill rice husk	195
	4.3.3.2 Sawdust	202
	4.3.3.3 Bagasse	205
	4.3.3.4 Pressmud	208
4.4	Fluidized Bed Gasification of Village Rice Husk and Sawdust	211
4.4.1	Physico Chemical Properties of the Biomass	211
	4.4.1.1 Proximate analysis	211
	4.4.1.2 Ultimate analysis	212
4.4.2	Thermochemical Properties of the Biomass	214
	4.4.2.1 Heating values	214
	4.4.2.2 Ash deformation and fusion temperatures	214
4.4.3	Biomass Gasification in the Fluidized Bed	215
	4.4.3.1 Gasifier temperature	215
	4.4.3.2 Gas composition	228



4.4.3.3	Gas higher heating value	234
4.4.3.4	Gas yield	239
4.4.3.5	Energy output	245
4.4.3.6	Carbon conversion	246
4.4.3.7	Tar content of the gas	250
4.4.3.8	Particulate matter in the gas	257
4.4.3.9	Effect of residence time of gas on gas yield and gasifier efficiency	257
4.4.3.10	Gasifier thermal efficiency	261
<b>CHAPTER V</b>	<b>CONCLUSIONS AND RECOMMENDATIONS</b>	<b>267</b>
5.1	Preliminary Experiments	267
5.1.1	Physicomechanical Properties	267
5.1.2	Physicochemical Properties	268
5.1.3	Thermochemical Properties	268
5.2	Fluidization Behaviour of Biomass Materials	269
5.3	Characteristics and Kinetics of Thermal Degradation	270
5.4	Kinetics of Thermal Degradation	272
5.5	Fluidized Bed Gasification of Village Rice husk and Sawdust	273
5.6	Recommendations	275
	<b>REFERENCES</b>	<b>277</b>

# LIST OF FIGURES

FIG. NO.	TITLE	PAGE NO.
1.1	Gasification Processes and their Products	10
1.2	Types of Biomass Gasifiers	13
1.3	Gasification Reactor Types with their Temperature and Solids Conversion Profiles.	14
1.4	Biomass Adiabatic Reaction Temperatures Showing Pyrolysis, Gasification and Combustion Regions for Air and Oxygen Reactions.	21
1.5	Equilibrium Composition for Adiabatic Air/Biomass Equilibrium.	22
2.1.1	A Model of the Segregating/Mixing System	26
2.1.2	Segregation Pattern for Large Jetsam Fraction	27
2.1.3	Variation of Mixing Index with Gas Velocity	29
2.1.4	Effect of Mixing/Segregation State on the Relationship Between Bed Pressure Drop and Superficial Gas Velocity (Idealized) (a) Completely Mixed; (b) Completely Segregated; (c) Partial Mixing	31
2.2.1	Pressure Drop in the Bed Versus Superficial Gas Velocity. Silica Sand ( $d_p = - 297 + 200 \mu\text{m}$ ) and Sawdust (40 Vol%, $d_p = - 1000 + 400 \mu\text{m}$ )	38
3.1	Schematic of the Experimental Assembly for Cold Flow Fluidization Experiments	87
3.2	Schematic Diagram of the Fluidized Bed Gasifier Unit	92
3.3	Fluidized Bed Gasifier : Constructional Details	93
3.4	A View of the Distributor Plate	95
3.5	Details of the Biomass Feeding Screw Conveyors	98
3.6	Details of the Cyclone	101

3.7	Locations of the Thermocouples and the Pressure Measuring Taps in the Gasifier System	103
3.8	The Orifice Meter for Measuring Gas Flow	104
3.9	A Schematic of the Gas Sampling Train	111
3.10	A Schematic View of the Tar Sampling Train	113
3.11	Details of the Thimble Holder Assembly of the Tar Sampling Train	115
3.12	Schematic of Tar Protocol	117
4.1.1	Variation of Pressure Drop with Superficial Air Velocity for Fluidization of Sand ( $d_p = - 500 + 350 \mu\text{m}$ )	126
4.1.2	Variation of Pressure Drop with Superficial Air Velocity for Fluidization of Sand ( $d_p = - 500 + 350 \mu\text{m}$ ) for Different Bed Height to Diameter Ratios.	127
4.1.3(a)	Variation of Pressure Drop with Superficial Air Velocity for Fluidization of Sand of Different Particle Sizes	128
4.1.3(b)	Variation of Pressure Drop with Superficial Air Velocity for Fluidization of Carrier Solids of Different Densities but Same Particle Size. ( $d_p = - 850 + 710 \mu\text{m}$ )	129
4.1.4	Variation of Pressure Drop with Superficial Air Velocity for Sand and Bauxite of Same Particle Sizes and their Mixtures (1:1 Vol., $H/D=1$ )	130
4.1.5	Variation of Pressure Drop with Superficial Air Velocity for Fluidization of Sand and Mill Rice Husk; Sand ( $d_p = -500 + 350\mu\text{m}$ ) and 3 wt% Mill Rice Husk, $H/D$ for Sand Bed =1)	132
4.1.6 (a)	Variation of Pressure Drop with Superficial Air Velocity for Fluidization of Sand and Mill Rice Husk Mixtures (i) Sand and 1wt% Mill Rice Husk, (ii) Sand and 4 wt% Mill Rice Husk	133
4.1.6(b)	Variation of Pressure Drop with Superficial Air Velocity for Fluidization of Sand and Mill Rice Husk Mixtures (i) Sand and 8 wt% Mill Rice Husk, (ii) Sand and 9 wt% Mill Rice Husk	134

4.1.7(a)	Variation of Pressure Drop with Superficial Air Velocity for Fluidization of Sand and Bagasse Mixtures (i) Sand and 1wt% Bagasse, (ii) Sand and 4 wt% Bagasse	135
4.1.7(b)	Variation of Pressure Drop with Superficial Air Velocity for Fluidization of Sand and Bagasse Mixtures (i) Sand and 8 wt% Bagasse, (ii) Sand and 9 wt% Bagasse	136
4.1.8(a)	Variation of Pressure Drop with Superficial Air Velocity for Fluidization of Sand and Pressmud Mixtures (i) Sand and 1 wt% Pressmud, (ii) Sand and 4 wt% Pressmud	137
4.1.8(b)	Variation of Pressure Drop with Superficial Air Velocity for Fluidization of Sand and Pressmud Mixtures (i) Sand and 8 wt% Pressmud, (ii) Sand and 9 wt% Pressmud	138
4.1.9	Variation of Minimum Fluidization Velocity with Percent Volume of Sawdust in Bed Mixture.	142
4.1.10	Variation of Minimum Fluidization Velocity with Percent Volume of Village Rice Husk in Bed Mixture.	143
4.1.11	Variation of Minimum Fluidization Velocity with Percent Volume of Mill Rice Husk in Bed Mixture.	144
4.1.12	Variation of Minimum Fluidization Velocity with Percent Volume of Pressmud in Bed Mixture.	145
4.1.13	Variation of Minimum Fluidization Velocity with Percent Volume of Baggase in Bed Mixture.	146
4.2.1(a)&(b)	Thermogravimetric and Differential Thermal Analysis of Village Rice Husk in (a) Nitrogen and (b) Air ; Heating Rate = 20°C min <sup>-1</sup>	148
4.2.2(a)&(b)	Thermogravimetric and Differential Thermal Analysis of Village Rice Husk in (a) Nitrogen and (b) Air ; Heating Rate = 40°C min <sup>-1</sup>	149
4.2.3(a)&(b)	Thermogravimetric and Differential Thermal Analysis of Mill Rice Husk in (a) Nitrogen, and (b) Air; Heating Rate=25°Cmin <sup>-1</sup>	153

4.2.4(a)&(b)	Thermogravimetric and Differential Thermal Analysis of Mill Rice Husk in (a) Nitrogen and (b) Air ; Heating Rate = 40°C min <sup>-1</sup>	154
4.2.5(a)&(b)	Thermogravimetric and Differential Thermal Analysis of Sawdust in (a) Nitrogen and (b) Air; Heating Rate = 20°C min <sup>-1</sup>	158
4.2.6(a)&(b)	Thermogravimetric and Differential Thermal Analysis of Sawdust in (a) Nitrogen and (b) Air; Heating Rate = 40°C min <sup>-1</sup>	159
4.2.7(a)&(b)	Thermogravimetric and Differential Thermal Analysis of Bagasse in (a) Nitrogen and (b) Air; Heating Rate = 20°C min <sup>-1</sup>	164
4.2.8(a)&(b)	Thermogravimetric and Differential Thermal Analysis of Bagasse in (a) Nitrogen and (b) Air; Heating Rate = 40°C min <sup>-1</sup>	165
4.2.9(a)&(b)	Thermogravimetric and Differential Thermal Analysis of Press mud in (a) Nitrogen, Heating Rate = 25°C min <sup>-1</sup> and (b) Air ; Heating Rate = 20°C min <sup>-1</sup>	170
4.2.10(a)&(b)	Thermogravimetric and Differential Thermal Analysis of Press mud in (a) Nitrogen and (b) Air ; Heating Rate = 40°C min <sup>-1</sup>	171
4.4.1(a)	Temperature Profile of the Fluidized Bed Gasifier, Feed Stock: Village Rice Husk Fluidization Air Velocity = 0.53 ms <sup>-1</sup>	220
4.4.1(b)	Temperature Profile of the Fluidized Bed Gasifier, Feed Stock: Village Rice Husk Fluidization Air Velocity = 0.59 ms <sup>-1</sup>	221
4.4.1(c)	Temperature Profile of the Fluidized Bed Gasifier, Feed Stock: Village Rice Husk Fluidization Air Velocity = 0.68 ms <sup>-1</sup>	222
4.4.1(d)	Temperature Profile of the Fluidized Bed Gasifier, Feed Stock: Village Rice Husk Fluidization Air Velocity = 0.73 ms <sup>-1</sup>	223
4.4.2(a)	Temperature Profile of the Fluidized Bed Gasifier, Feed Stock: Sawdust Fluidization Air Velocity = 0.53 ms <sup>-1</sup>	224

4.4.2(b)	Temperature Profile of the Fluidized Bed Gasifier, Feed Stock: Sawdust Fluidization Air Velocity = $0.59 \text{ ms}^{-1}$	225
4.4.2(c)	Temperature Profile of the Fluidized Bed Gasifier, Feed Stock: Sawdust Fluidization Air Velocity = $0.68 \text{ ms}^{-1}$	226
4.4.2(d)	Temperature Profile of the Fluidized Bed Gasifier, Feed Stock: Sawdust Fluidization Air Velocity = $0.73 \text{ ms}^{-1}$	227
4.4.3	Variation of Gas Composition with ER and Fluidization Air Velocity: Village Rice Husk Gasification	231
4.4.4	Variation of Gas Composition with ER and Fluidization Air Velocity: Sawdust Gasification	232
4.4.5	Comparison of Gas Composition at Different Equivalence Ratios Reported by Different Workers with the Present Work	233
4.4.6(a)	Variation of Product Gas Heating Value with ER and Fluidization Air Velocity, Feed Stock: Village Rice Husk	236
4.4.6(b)	Variation of Product Gas Heating Value with ER and Fluidization Air Velocity, Feed Stock: Sawdust	237
4.4.7(a)	Variation of Gas Yield with ER and Fluidization Air Velocity, Feed Stock: Village Rice Husk	242
4.4.7(b)	Variation of Gas Yield with ER and Fluidization Air Velocity, Feed Stock: Sawdust	243
4.4.8	Comparison of Gas Yield at Different Equivalence Ratios with Some Reported Values	244
4.4.9(a)	Variation of Carbon Conversion Efficiency with Equivalence Ratio: Village Rice Husk Gasification	248
4.4.9(b)	Variation of Carbon Conversion Efficiency with Equivalence Ratio: Sawdust Gasification	249
4.4.10 (a)	Variation of Tar Content of Product Gas with Equivalence Ratio, Feed Stock: Village Rice Husk	252

4.4.10 (b)	Variation of Tar Content of Product Gas with Fluidization Air Velocity, Feed Stock: Village Rice Husk	253
4.4.11 (a)	Variation of Tar Content of Product Gas with Equivalence Ratio, Feed Stock: Sawdust	254
4.4.11 (b)	Variation of Tar Content of Product Gas with Fluidization Air Velocity, Feed Stock: Sawdust	255
4.4.11 (c)	Variation of Tar Content of Product Gas with Equivalence Ratio Compared with Values Reported by Narvaez et al. (1996)	256
4.4.12(a)	Variation of Gas Yield with Residence Time and Fluidization Velocity, Feed Stock: Village Rice Husk	259
4.4.12(b)	Variation of Gas Yield with Residence Time and Fluidization Velocity, Feed Stock: Sawdust	260
4.4.13(a)	Variation of Gasifier Thermal Efficiency with Fluidization Air Velocity : Village Rice Husk Gasification	264
4.4.13(b)	Variation of Gasifier Thermal Efficiency with Fluidization Air Velocity : Sawdust Gasification	265

# LIST OF TABLES

TABLE NO.	TITLE	PAGE NO.
1.1	All-India Potential Availability (Million Tonnes) of Agriculture-Based Biomass	2
1.2	Estimation of Biomass Produced in India	3
1.3	Density and Proximate Analyses of Biomass Materials.	6
1.4	Elemental Analyses of Biomass	7
1.5	Important Chemical Reactions of the Gasification Processes.	12
1.6	Operation and Efficiency Parameters, Constructive Features and Biomass Characteristics (Pilot Plant Gasifiers).	17
1.7	Operation and Efficiency Parameters, Constructive Features and Biomass Characteristics (Demonstration and Commercial Units)	18
1.8	Present Status of Research on Thermal Gasification of Biomass in India	23
2.2.1	Mixtures of Biomass and Second Solid Used in Fluidized-Bed Gasifiers	39
2.2.2	Fluidization Characteristics of Rice Husk, its Ash and Char	40
2.4.1	Integral Method Equations for Determining Kinetic Parameters for Single, Irreversible Reaction, Using Thermogravimetric Data	52
2.4.2	Differential Method Equations for Determining Kinetic Parameters for Single, Irreversible Reaction, Using Thermogravimetric Data	56
2.5.1	Air Gasification of Biomass in Fluidized Beds – Literature Citations	68
2.5.2	Reactor Constructional Details and Operating Conditions in Fluidized Bed Air Gasification of Biomass	73
3.1.1	Village Rice Husk Feed Rates and Air Supply Rates in Fluidized Bed Gasification Experiments	106



3.1.2	Sawdust Feed Rates and Air Supply Rates in Fluidized Bed Gasification Experiments	107
4.1.1(a)	Physico-mechanical Properties of Biomass Materials	122
4.1.1(b)	Characteristics of Carrier Solids	122
4.2.1 (a)	Thermal Degradation in the Initial Degradation Zone (Nitrogen : 50 mlmin <sup>-1</sup> )	152
4.2.1 (b)	Thermal Degradation in the Second Reaction Zone (Nitrogen : 50 mlmin <sup>-1</sup> )	152
4.2.1 (c)	Thermal Degradation in the Third Reaction Zone (Nitrogen : 50 mlmin <sup>-1</sup> )	152
4.2.1 (d)	Thermal Degradation in the Fourth Reaction Zone (Nitrogen : 50 mlmin <sup>-1</sup> )	152
4.2.2(a)	Thermal Degradation in the First Reaction Zone (Air : 50 mlmin <sup>-1</sup> )	155
4.2.2(b)	Thermal Degradation in Second Reaction Zone (Air : 50 mlmin <sup>-1</sup> )	155
4.2.3(a)	Thermal Degradation of Sawdust in First Reaction Zone (Nitrogen : 50 mlmin <sup>-1</sup> )	161
4.2.3(b)	Thermal Degradation of Sawdust in Second and Third Reaction Zones (Nitrogen : 50 mlmin <sup>-1</sup> )	161
4.2.4(a)	Thermal Degradation of Sawdust in First Reaction Zone (Air : 50 mlmin <sup>-1</sup> )	161
4.2.4(b)	Thermal Degradation of Sawdust (Air : 50 mlmin <sup>-1</sup> )	161
4.2.5(a)	Thermal Degradation of Bagasse in First Reaction Zone (Nitrogen : 50 mlmin <sup>-1</sup> )	167
4.2.5(b)	Thermal Degradation of Bagasse (Nitrogen : 50 mlmin <sup>-1</sup> )	167
4.2.6(a)	Thermal Degradation of Bagasse in the First Reaction Zone (Air : 50 mlmin <sup>-1</sup> )	167
4.2.6(b)	Thermal Degradation of Bagasse (Air : 50 mlmin <sup>-1</sup> )	167

4.2.7(a)	Initial Thermal Degradation of Pressmud (Nitrogen : 50 mlmin <sup>-1</sup> )	173
4.2.7(b)	Thermal Degradation of Pressmud (Nitrogen : 50 mlmin <sup>-1</sup> )	173
4.2.8(a)	Initial Thermal Degradation of Pressmud (Air : 60 mlmin <sup>-1</sup> )	173
4.2.8(b)	Thermal Degradation of Pressmud (Air : 60 mlmin <sup>-1</sup> )	173
4.3.1(a)	Kinetic Parameters for Village Rice Husk Pyrolysis from Thermogravimetric Analysis (Nitrogen : 50 mlmin <sup>-1</sup> ) Heating Rate : 20°Cmin <sup>-1</sup>	179
4.3.1(b)	Kinetic Parameters for Village Rice Husk Pyrolysis from Thermogravimetric Analysis (Nitrogen : 50 mlmin <sup>-1</sup> ) Heating Rate : 40°Cmin <sup>-1</sup>	180
4.3.2(a)	Kinetic Parameters for Mill Rice Husk Pyrolysis from Thermogravimetric Analysis (Nitrogen : 50 mlmin <sup>-1</sup> ) Heating Rate : 25°Cmin <sup>-1</sup>	182
4.3.2(b)	Kinetic Parameters for Mill Rice Husk Pyrolysis from Thermogravimetric Analysis (Nitrogen : 50 mlmin <sup>-1</sup> ) Heating Rate : 40°Cmin <sup>-1</sup>	183
4.3.3(a)	Kinetic Parameters for Sawdust Pyrolysis from Thermogravimetric Analysis (Nitrogen : 50 mlmin <sup>-1</sup> ) Heating Rate : 20°Cmin <sup>-1</sup>	186
4.3.3(b)	Kinetic Parameters for Sawdust Pyrolysis from Thermogravimetric Analysis (Nitrogen : 50 mlmin <sup>-1</sup> ) Heating Rate : 40°Cmin <sup>-1</sup>	187
4.3.4(a)	Kinetic Parameters for Bagasse Pyrolysis from Thermogravimetric Analysis (Nitrogen : 50 mlmin <sup>-1</sup> ) Heating Rate : 20°Cmin <sup>-1</sup>	189
4.3.4(b)	Kinetic Parameters for Bagasse Pyrolysis from Thermogravimetric Analysis (Nitrogen : 50 mlmin <sup>-1</sup> ) Heating Rate : 40°Cmin <sup>-1</sup>	190

4.3.5(a)	Kinetic Parameters for Pressmud Pyrolysis from Thermogravimetric Analysis (Nitrogen : 50 mlmin <sup>-1</sup> ) Heating Rate : 25°Cmin <sup>-1</sup>	192
4.3.5(b)	Kinetic Parameters for Pressmud Pyrolysis from Thermogravimetric Analysis (Nitrogen : 50 mlmin <sup>-1</sup> ) Heating Rate : 40°Cmin <sup>-1</sup>	193
4.3.6(a)	Kinetic Parameters for Village Rice Husk Thermal Degradation from TGA/DTG Data (Air : 50 mlmin <sup>-1</sup> ) Heating Rate : 20°Cmin <sup>-1</sup>	196
4.3.6(b)	Kinetic Parameters for Village Rice Husk Thermal Degradation from TGA/DTG Data (Air : 50 mlmin <sup>-1</sup> ) Heating Rate : 40°Cmin <sup>-1</sup>	197
4.3.7(a)	Kinetic Parameters for Mill Rice Husk Thermal Degradation from TGA/DTG Data (Air : 50 mlmin <sup>-1</sup> ) Heating Rate : 20°Cmin <sup>-1</sup>	199
4.3.7(b)	Kinetic Parameters for Mill Rice Husk Thermal Degradation from TGA/DTG Data (Air : 60 mlmin <sup>-1</sup> ) Heating Rate : 40°Cmin <sup>-1</sup>	200
4.3.8(a)	Kinetic Parameters for Sawdust Thermal Degradation from TGA/DTG Data (Air : 50 mlmin <sup>-1</sup> ) Heating Rate : 20°Cmin <sup>-1</sup>	203
4.3.8(b)	Kinetic Parameters for Sawdust Thermal Degradation from TGA/DTG Data (Air : 50 mlmin <sup>-1</sup> ) Heating Rate : 40°Cmin <sup>-1</sup>	204
4.3.9(a)	Kinetic Parameters for Bagasse Thermal Degradation from TGA/DTG Data (Air : 50 mlmin <sup>-1</sup> ) Heating Rate : 20°Cmin <sup>-1</sup>	206
4.3.9(b)	Kinetic Parameters for Bagasse Thermal Degradation from TGA/DTG Data (Air : 50 mlmin <sup>-1</sup> ) Heating Rate : 40°Cmin <sup>-1</sup>	207

4.3.10(a)	Kinetic Parameters for Pressmud Thermal Degradation from TGA/DTG Data (Air : 50 mlmin <sup>-1</sup> ) Heating Rate : 20°Cmin <sup>-1</sup>	209
4.3.10(b)	Kinetic Parameters for Pressmud Thermal Degradation from TGA/DTG Data (Air : 50 mlmin <sup>-1</sup> ) Heating Rate : 40°Cmin <sup>-1</sup>	210
4.4.1(a)	Proximate Analysis of Biomass Materials	213
4.4.1(b)	Ultimate Analysis	213
4.4.2(a)	Heating Value of Biomass Materials	213
4.4.2(b)	Ash Deformation and Fusion Temperatures	213
4.4.3(a)	Temperature Measurements in the Fluidized Bed Gasification Experiments, Feed Stock : Village Rice Husk	216
4.4.3(b)	Temperature Measurements in the Fluidized Bed Gasification Experiments, Feed Stock : Sawdust	217
4.4.4(a)	Average Gas Composition of Producer Gas, Feed Stock : Village Rice Husk	229
4.4.4(b)	Average Gas Composition of Producer Gas, Feed Stock : Sawdust	230
4.4.5	Higher Heating Value of the Gas Produced	235
4.4.6	Comparison of Higher Heating Value of the Gas Reported by Different Workers	238
4.4.7(a)	Gas Production Rate, Normalized Gas Production Rate and Gas Yield, Feed Stock : Village Rice Husk	240
4.4.7(b)	Gas Production Rate, Normalized Gas Production Rate and Gas Yield, Feed Stock : Sawdust	241
4.4.8	Carbon Conversion Efficiencies for Village Rice Husk and Sawdust Gasification.	247
4.4.9(a)	Tar Content of the Producer Gas, Feed Stock : Village Rice Husk	251
4.4.9(b)	Tar Content of the Producer Gas, Feed Stock : Sawdust.	251

4.4.10	Gas Residence Time for Village Rice Husk and Sawdust Gasification	258
4.4.11(a)	Gasifier Thermal Efficiency for Village Rice Husk Gasification Experiments	262
4.4.11(b)	Gasifier Thermal Efficiency for Sawdust Gasification Experiments	263

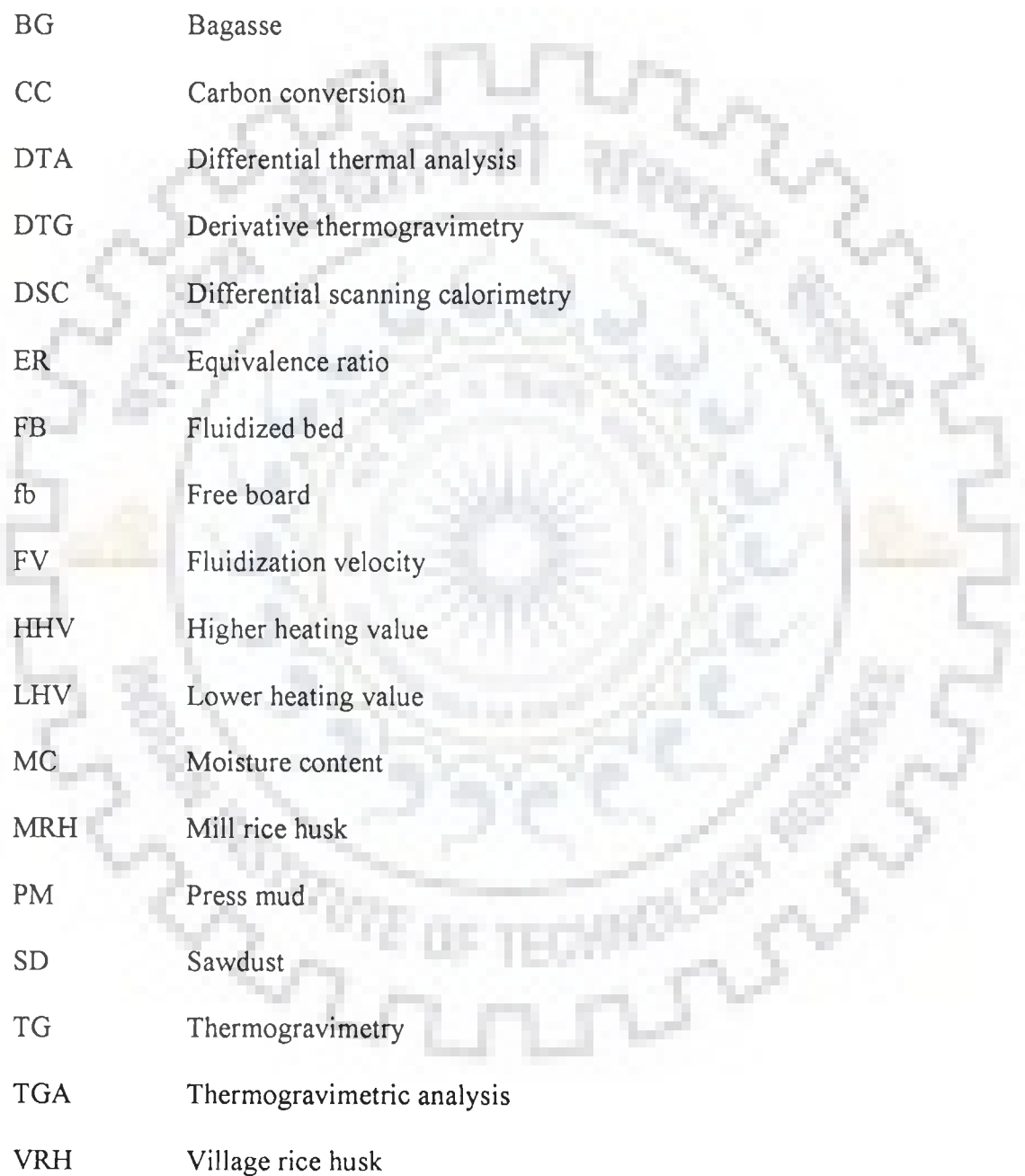


# LIST OF ABBREVIATIONS AND SYMBOLS

---

---

## ABBREVIATIONS



BG	Bagasse
CC	Carbon conversion
DTA	Differential thermal analysis
DTG	Derivative thermogravimetry
DSC	Differential scanning calorimetry
ER	Equivalence ratio
FB	Fluidized bed
fb	Free board
FV	Fluidization velocity
HHV	Higher heating value
LHV	Lower heating value
MC	Moisture content
MRH	Mill rice husk
PM	Press mud
SD	Sawdust
TG	Thermogravimetry
TGA	Thermogravimetric analysis
VRH	Village rice husk

## ENGLISH SYMBOLS

a	Heating rate ( $\text{Kmin}^{-1}$ or $^{\circ}\text{Cmin}^{-1}$ )
Ar	Archimedes number (-)
d	Diameter (mm)
E	Activation energy ( $\text{kJmol}^{-1}$ )
g	Acceleration of gravity ( $\text{ms}^{-2}$ )
G	Galileo number (-)
$k_0$	Pre exponential factor ( $\text{s}^{-1}$ or else depending upon the order of reaction)
M	Mixing index (-)
n	Order of reaction (-)
R	Universal gas constant ( $\text{kJmol}^{-1}\text{K}^{-1}$ ).
Re	Reynolds number (-)
$\text{Re}_{mf}$	Reynolds number at minimum fluidization (-)
T	Absolute temperature (K)
$u_{bf}$	Velocity of beginning of fluidization ( $\text{ms}^{-1}$ )
$u_{cf}$	Velocity of complete fluidization ( $\text{ms}^{-1}$ )
$U_{mf}, u_{mf}$	Minimum fluidization velocity ( $\text{ms}^{-1}$ )
$u_p$	Fictitious minimum fluidization velocity of straw ( $\text{ms}^{-1}$ )
$U_s, U$	Superficial gas velocity ( $\text{ms}^{-1}$ )
$u_{vf}$	Minimum fluidization velocity of straw-sand mixture ( $\text{ms}^{-1}$ ).
x	Mass fraction of particle

## GREEK SYMBOLS

$\beta$	Heating rate ( $\text{Kmin}^{-1}$ )
$\varepsilon$	Bed voidage (-)
$\rho$	Density ( $\text{kgm}^{-3}$ )
$\mu$	Viscosity of gas ( $\text{Nsm}^{-2}$ )
$\rho_b$	Bulk density ( $\text{kgm}^{-3}$ )
$\varepsilon_{mf}$	Bed voidage at minimum fluidization (-)
$\rho_p$	Particle density ( $\text{kgm}^{-3}$ )
$\Delta P$	Pressure drop ( $\text{N-m}^{-2}$ )





---

---

## INTRODUCTION

### 1.1 BIOMASS

The exploitation of the renewable energy sources for meeting the ever-increasing energy requirements has become more demanding for those developing countries, which are importing significant amounts of crude petroleum and its products. Among the several alternative renewable energy sources, biomass occupies a unique place.

Biomass is the name given to the plant matter, which is created by photosynthesis where in the Sun's energy converts water and carbon dioxide into organic matter. Thus biomass materials are the products of plant growth. These include energy plantations, agricultural and agro-industrial wastes and residues, forestry residues and animal waste matter. In the Indian context, animal waste and cattle wastes have been treated as a separate category and not as a part of biomass (Mohan and Meshram, 1998). Woody biomass obtained from natural forests and agro-forestry plantations, etc. is a high-valued commodity with diverse uses as timber, raw material for pulp and paper, fuel wood etc. (Kishore, 1995, Jorapur and Rajavanshi, 1995).

Biomass can be interpreted as 'stored solar energy', and is benign in terms of carbon sequestration. Because of its excellent storage properties, it competes well with all other forms of soft energies like wind, solar, ocean thermal, tidal, etc. The biomass is also attractive, as a fuel, for power generation because of its many similarities to fossil fuels like, ability to generate 'firm' power as well as power on demand and broadly similar combustion characteristics. Thus the substitution of fossil fuels in the power generation sector by biomass fuels could be brought about, without major transitional economic costs and adjustments. Therefore unlike many other renewable energy technologies (e.g. solar power generation), the biomass based energy technology is a true 'replacement' technology.

## 1.2 AVAILABILITY OF BIOMASS

In India, about 70% of the population lives in villages and about 75% of the energy needs of the rural India are met from biomass. The replacement of biomass as a source of energy in rural India by oil would put an additional burden of import of an estimated 15 million tonnes of crude oil every year, costing over Rs.  $6 \times 10^4$  million (Mohan and Meshram, 1998).

Agriculture based biomass potential in India is estimated to be around 270 million tonnes, depending on various conversion factors used for calculating the biomass yield. Agriculture-based biomass availability is steadily increasing over the years as may be seen from Table 1.1

**Table 1.1 : All-India Potential Availability (million tonnes) of Agriculture-Based Biomass (TEDDY, 2000-2001)**

Biomass	1980/81	1990/91	1995/96
Rice husk	26.8	37.1	39.8
Wheat straw	48.4	73.5	83.3
Maize cobs	2.1	2.7	2.8
Pearl millet straw	8.9	11.4	9.0
Sugarcane bagasse	51.4	80.4	93.4
Coconut shell	0.8	1.3	1.9
Coconut fibre	0.9	1.6	2.3
Coconut pith	1.4	2.4	3.4
Groundnut shell	1.7	2.5	2.6
Cotton stalks	23.5	22.3	27.3
Jute sticks.	3.9	3.1	2.7
Total	169.8	238.1	268.5

Note :

The conversion factors used are listed below:

Rice husk – yield of clean rice x 0.5  
Wheat straw-grain yield x 1.33  
Maize cobs-grain yield x 0.3  
Straw from pearl millet – grain yield x 1.66  
Bagasse – weight of cane x 0.33  
One coconut – 135 g shell, 164 g fibre, and 246 g pith  
Groundnut shell – kernel yield x 0.33  
Cotton stalks – 3 tonnes/hectare  
Jute sticks – 3 tonnes/hectare

Mohan and Meshram (1998) and Tripathi et al.(1998) have estimated the availability of main agro-residues in India and is shown in Table 1.2.

**Table 1.2 : Estimation of Biomass Produced in India**

Crop	Type of Residue	Ratio of Production to Residue		Quantity Million Tonnes	
		Mohan and Meshram (1998)	Tripathi et al. (1998)	Mohan and Meshram (1998) for 1996-97	Tripathi et al. (1998) for 2000-2001
Rice	Straw	1.50	-	120.0	-
	Husk	0.30	1:0.25	24.0	24.1
Sugarcane	Bagasse	0.30	-	81.0	-
	Tops	0.05	-	13.5	-
	Trash	0.10	-	27.0	-
	Press mud	-	-	-	-
Maize	Cobs	0.30	1:0.3	3.0	3.2

There are large quantities of residues associated with agricultural production and processing industries. Sugar mills in India generate about 0.33 tonne of bagasse per ton of sugar cane crushed. Thus the availability of cane bagasse is around 100 million tones. About 90% of the bagasse produced in the sugar mills is used in the boilers for the production of steam and power. Indian sugar mills, using double sulphitation process for juice and syrup clarification, produce about 12 million tonnes of press mud (filter cake) as a waste. Press mud has about 68-75% of moisture, 24-28% of combustibles and 6-8% of ash. It is very rich in micro nutrients for agricultural crops: nitrogen, 1.9%, phosphorous 1.8%, potassium 0.9%, calcium 4.3%, magnesium 0.7%, sulfur 3.2%, sodium 0.1%, manganese 0.034%, zinc 0.0089% and copper 0.0053% (Mishra et al., 1998). In Asia-Pacific region residues are in plenty, the generation being equivalent to about 65% of energy use in these countries (Hall, 1991). Often these are left to decompose naturally in huge heaps or are disposed of by burning (Bhattacharya, 1993). It has been reported that 90% of the straw produced in the state

of Punjab in India is disposed off by burning (Jenkins and Bhatnagar, 1991). Decomposition and combustion of residues result in the release of their carbon content to the atmosphere and contribute to global warming (Bhattacharya, 1993). In India, it is estimated that more than eight million tonnes of the residues will be produced in the year 2000-2001, with a primary energy potential of about 1200 peta joules (Tripathi et al., 1998).

If the surplus biomass is to be used for power generation alone, it could save over 70 million tonnes of coal every year, and reduce over 160 million tonnes of net CO<sub>2</sub> emissions into the atmosphere. This can also generate an additional employment of 20-30 crore man days every year in rural areas through involvement of people in local collection, storage, handling and transportation of biomass for power projects (Mohan & Meshram, 1998).

### **1.3 PHYSICO-CHEMICAL AND THERMAL CHARACTERISTICS OF BIOMASS MATERIALS**

The important physico-chemical and thermal characteristics of biomass materials are :

- (i) Density – particle and bulk
- (ii) Shape
- (iii) Angle of repose and slide
- (iv) Proximate analysis – moisture, fixed carbon, volatile matter, and ash
- (v) Ultimate (elemental) analysis – carbon(C), hydrogen (H), oxygen (O), sulfur, chlorine
- (vi) Ash deformation and fusion temperatures
- (vii) Heating value – lower and higher

The kinetics of thermal degradation – drying, pyrolysis, char formation, char gasification and combustion are very important as these will dictate the design of the equipment for thermal degradation. Iyer et al. (1997) have compiled information on

physico-chemical and thermal characteristics of a large number of biomass materials. These can be taken as average characteristics, since the characteristics of each biomass will vary depending upon the variety/species of the biomass, the geographical location of its availability, etc. They have given the comparative assessment of biomass materials with wood and coal as follows :

Component (wt% dry basis)	Biomass*	Wood	Coal
Fixed carbon	10-20	15-20	60-80
Volatile matter	60-85	70-85	20-30
Ash Content	1-20	1-3	5-40

\* Agro and forest-residues except wood.

Table 1.3 presents the density and proximate analyses of different biomass materials used in thermal gasification. It may be seen that very few data are available for wheat straw, almond shells and sawdust, whereas a number of workers have reported data for rice husk/rice hull.

Table 1.4 presents the ultimate analysis of rice husk, wheat straw and sawdust as reported by different workers.

#### 1.4 THERMOCHEMICAL CONVERSION OF BIOMASS

The conversion of biomass into more valuable and cleaner gaseous form, is normally achieved through two entirely different processes, namely, biochemical processes and thermochemical processes (Brandon et al., 1984, Sharma et al., 1988).

The biochemical processes include anaerobic digestion and alcoholic fermentation. Anaerobic decomposition of biomass yields methane through bacterial fermentation or ethanol from yeast (*S.Cerevisiae*) fermentation. Biomass is a mixture of three main components namely, cellulose, hemicellulose and lignin and some other minor components like inorganic compounds (Shafizadeh, 1985). Anaerobic digestion is a slow rate process and is suitable only for cellulose components. Complete biomass conversion to energy is possible only through thermochemical processes like pyrolysis, gasification or combustion (Mukunda and Paul, 1994).

Table 1.3 : Density and Proximate Analyses of Biomass Materials

Biomass	Density, kg m <sup>-3</sup>		Proximate Analysis				Heating Value, MJ kg <sup>-1</sup>		Reference	
	Bulk Density	True Particle	Fixed carbon (dry %)	Volatile Matter (dry %)	Ash (dry %)	Moisture (wet %)	Low (dry basis)	High (dry basis)		
Rice/Paddy Husk	100	735	-	-	-	-	-	-	Houston (1972)	
	150	740	15.80	73.21	10.99	11.90	-	-	Peel and Santos (1980)	
	100	750	-	-	-	-	-	-	Govind rao (1980)	
			16.55	63.69	19.76	11.51	-	13.00*	Peiyi (1983)	
			18.80	65.00	16.20	7.12	-	14.00*	Nagh et al. (1983)	
			15.8	63.60	20.60	6.50-9.10	-	14.89	Rossi (1984)	
			16.67	65.47	17.86	7.10	15.25	16.14	Jenkins (1985)	
			21.00	60.00	19.00	-	-	-	Xu et al (1985)	
			15.22	60.69	16.23	-	-	12.70*	Kapur et al. (1985)	
			13.98	62.35	23.67	4.10	-	14.09	Preto et al. (1987)	
			21.00	60.00	19.00	-	-	-	Bingyan et al. (1987)	
			12-15	65-67	15-18	3-4	-	12.56*	Chakraborti et al. (1988)	
			19.90	60.64	19.48	-	13.24	13.38	Grover (1989)	
			16.68	60.67	21.10	9.96	-	-	Hartiniati et al. (1989)	
			15-20	60-69	15-21	-	-	-	Sen and Ghosh (1992)	
		235	19.90	64-66.1	17.60	-	13.24	13.38*	Anuradha et al. (1992)	
		100	-	16.67	61.11	22.22	10	-	12.54*	Jain et al. (1994)
		120	-	12.00	72.20	15.80	10.0	-	15.60	Sanchez and Lora (1994)
		86-110	-	17.6	60.64	19.46	-	-	-	Jha (1996)
				12.4-14.2	63-67.6	18.2-24.6	-	13.24-14.22	-	
			-	-	19.8	-	13.31	14.61	Mansaray and Ghaly (1997)	
		20	65.7	16.69	9.2	-	-	-	Natarajan (1998)	
	235	17.6	60.64	19.46	-	-	-	-		
			12.5	71.00	16.50	-	14.10	15.50	Bhatnagar (1996)	
	110	-	14.7-18	19.2	-	-	-	13.1-14.8*	Iyer et al. (1997)	
Bagasse			16.87	75.10	8.03	-	19.37	19.50	Anuradha (1990)	
			9.20	86.40	4.40	6.4	-	16.70	Sanchez and Lora (1994)	
			4.26	93.20	2.54	-	-	19.19*	Jha (1996)	
			15.00	82.0	3.00	-	-	17.30*	Iyer et al. (1997)	
Wheat Straw		75-80	17.90	66.8	15.30	7.80	13.40	-	Herguido et al. (1992)	
		-	17.61	78.8	3.59	10-11	18-71	-	Ergudenler et al (1997)	
		-	11.7-20.0	72-80.6	7.7-8.0	-	16.8-17.2*	-	Iyer et al. (1997)	
Almond Shells	1200	-	19.35	79.40	1.17	8.84	-	-	Rapagna and Latif (1997)	
	-	-	19.30	79.4	2.30	-	-	17.6*	Iyer et al. (1997)	
Saw dust	-	-	14.10	84.60	1.30	8.50	18.80	-	Herguido et al. (1992)	
	-	-	15.2	84.2	0.60	12.90	-	18.0	Sanchez and Lora (1994)	
	-	-	16.5-25.0	70-82.3	1.2-5.6	-	-	17.7-20.5*	Iyer et al. (1997)	

\* High or low Heating value is not known.

Note : Bulk density depends on the size of the material.

Table 1.4 : Elemental Analyses of Biomass

Biomass	Elements, %							Reference
	C	H	O	N	S	Cl	Ash	
Rice/	41.00	5.00	37.60	0.60	0.30	-	15.50	Kaupp (1982)
Paddy-	35.49	4.56	30.44	0.51	Trace	-	17.49	Peiyi (1983)
Husk/	40.94	4.30	35.86	0.40	0.02	0.12	18.34	Jenkins and Ebeling (1985)
Hull	37.80	4.70	33.50	0.27	0.03	-	23.70	Preto et al. (1987)
	40.20	5.00	35.40	2.00	0.10	-	17.30	Chakraborti et al. (1988)
	39.94	5.46	38.86	0.11	0.02	-	-	Hartiniati et al. (1989)
	35.50	5.70	39.80	0.50	-	-	15.50	Bridgwater (1991)
	38.00	4.00	38.00	0.40	0.02	-	20.00	Anuradha et al. (1992)
	37.80	4.73	35.53	0.46	-	-	21.48	Boateng et al. (1992)
	36.42-37.03	4.91-5.25	35.88-40.94	0.09-0.59	-	-	16.69-22.20	Iyer et al. (1997)
Wheat Straw	43.70*	6.10*	-	0.40*				Herguido et al. (1992)
Pine saw dust	47.36 50.00	5.84 5.70	46.76 44.10	0.00 0.1-0.3	0.04 0.03	- -	0.50 -	Prasad and Kuester (1988) Narvaez et al. (1996)
Saw dust	44.63-52.28	5.20-5.88	40.85-45.90	0.47-2.08	-	-	1.20-1.51	Iyer et al.(1997)

\* Ash free basis

In the thermochemical conversion processes, biomass is subjected to a high temperature and depending on the quantity of oxygen supplied, the processes such as pyrolysis, gasification and combustion occur (Reed, 1981). Pyrolysis is the thermal (Pyro) decomposition (lysis) of biomass in the absence of oxygen at temperatures 200 to 600°C to yield energetically dense products, charcoal, liquid (tar, an aqueous solution of organics) and gaseous products (Maschio et al., 1992, Srivastava et al., 1996). Pyrolysis is an intermediate step in the gasification or combustion process.

Combustion is defined as a series of free radical reactions in which carbon and hydrogen in the biomass fuel react with oxygen to form carbon dioxide and water with the liberation of heat. To ensure complete combustion of a fuel, oxygen is supplied in excess of stoichiometric requirement. This minimises the production of carbon monoxide and maximises the heat release (Tillman, 1987). Direct combustion of biomass, as a fuel, is an age-old practice and has poor thermal efficiency. Even then, biomass combustion is the source of basic energy for domestic cooking and other heating needs in the rural house holds as well as in a variety of traditional industries in the developing countries (Bhattacharya, 1993). The thermal efficiency of open air combustion of biomass in such applications has been reported to be low (about 8-15%). It is also reported to be associated with many health risks (Uma et al., 1996). Recent developments in biomass combustion technology include bubbling fluidized bed and the circulating fluidized bed combustor technologies. In the mid-1980s, about 110 fluidized bed boilers utilizing biomass as a fuel were operating world wide (La Nauze, 1996). In the early 1990s, a total of 223 circulating fluidized bed combustor units were reported to be in operation (Engstrom and Lee, 1991).

Thermal gasification is the process of converting biomass into a gaseous fuel by means of partial oxidation at high temperature (usually 700 to 850°C). In this process, a



combustible gas is obtained from a biomass by the reaction of the fuel with a gasifying medium, usually air (Beenackers and van Swaaij, 1984). The gas so obtained is generally called producer gas and is mainly composed of carbon monoxide and hydrogen. It also contains carbon dioxide, water vapour, nitrogen (from air) and small amounts of hydrocarbons along with tars and ash. The quality of the gas depends much on the gasification medium and the type of the gasifier employed. The application of the gas depends upon the degree of its 'clean-ness'. A 'tar-and dust-laden' gas can be directly used for combustion in furnaces. A gas 'cleaned, scrubbed and cooled' to near ambient air conditions, finds application in internal combustion engines as a substitute fuel (Prasad and Sharma, 1986).

The final products of the gasification depend on the type of gasification process. The gasification processes are classified based on the gasification medium (gasifying agent) employed (Fig. 1.1). With air as the gasifying agent, the gas generated is of low energy value, about 3 to 5.5 MJNm<sup>-3</sup>, due to nitrogen dilution. This process is called 'Low joule gasification' (Beenackers and Bridgewater, 1989). Such a gas cannot be economically transported over long distances (Walawender et al., 1985a), but it can be used locally in boilers, engines and turbines. The gasification process in which oxygen is used as the gasifying agent is known as 'Medium joule gasification'. Such a gasification process leads to nitrogen-free gas and hence is of higher energy content, about 10-18 MJNm<sup>-3</sup>. This gas is suitable for limited pipeline distribution as well as synthesis gas for conversion to ammonia, methanol and gasoline (Reed, 1981). However, such a technology needs a costly and energy intensive air separation plant. It also calls for additional safety precautions. In medium joule gasification, the cost of oxygen constitutes to about 25 to 35% of the cost of the gas (van Fredersdoff and Elliott, 1963). This has encouraged development work on air gasification.

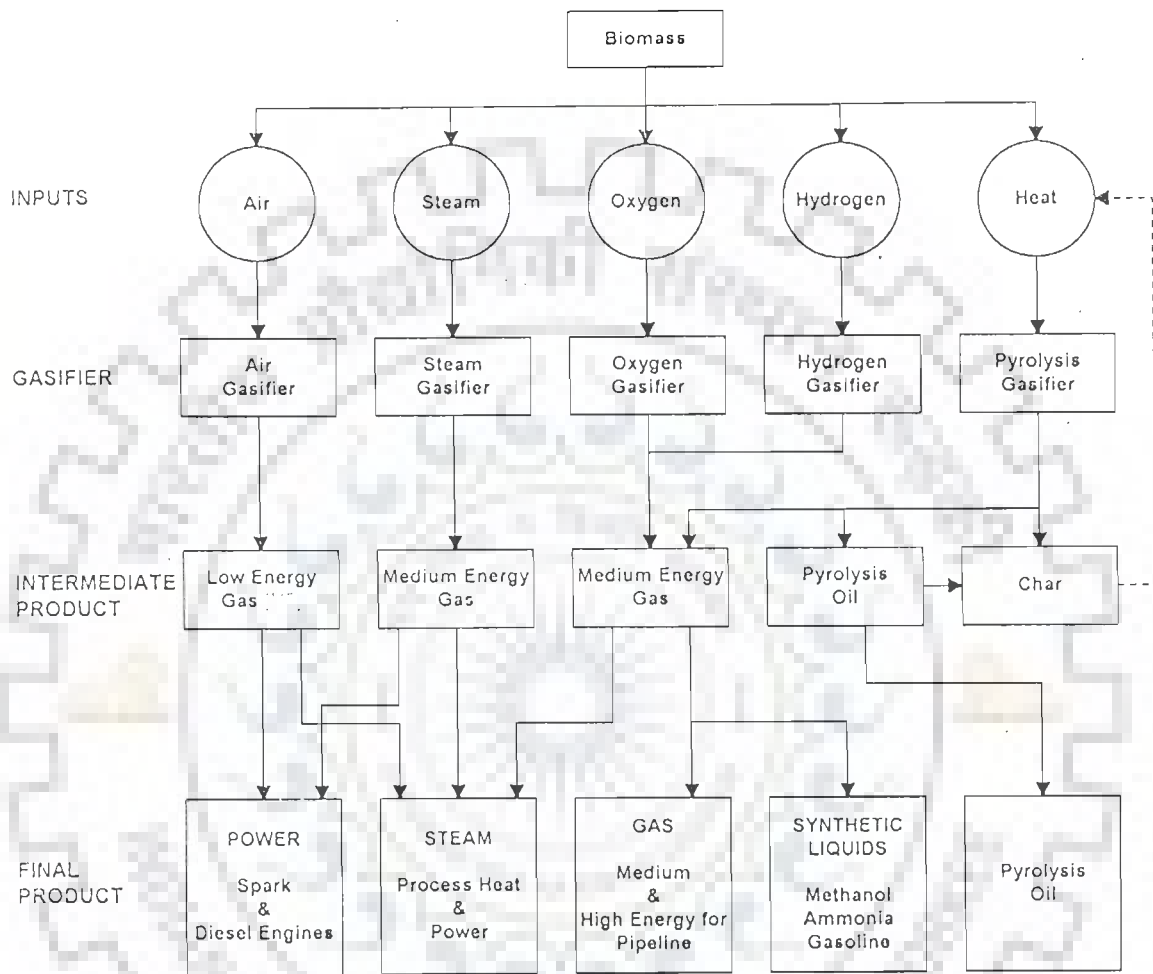


Fig. 1.1 Gasification processes and their products (Reed, 1981)

## 1.5 TYPES OF BIOMASS GASIFIERS

The gasification process may be classified on the following basis :

- a) Gasifying agent : Air, Oxygen, Steam
- b) Heat supply method: Direct, Indirect like circulating gas, circulating sand, heat transfer through walls and chemical energy of reaction.
- c) Process pressure: Atmospheric, Pressurised.
- d) Solid-gas contact principle-Reactor type : Fixed bed, Moving bed - up draft, down draft and cross draft, Fluidized bed (bubbling, spouted, circulating), Entrained bed and Stirred bed .

The choice of the gasification process and reactor (gasifier) type generally depends on the type of the biomass feedstock and the desired gas quality. In the moving bed down draft gasifier, the biomass slowly descends downwards as a packed bed. The three subtypes of the moving bed gasifiers are the counter-current type, co-current type and cross-current type moving bed gasifiers. The producer gas from counter current gasifier has a temperature of about 400<sup>0</sup>C, is rich in hydrocarbons (Dibiasi et al., 1999) and is suitable for direct thermal applications (Patil and Rao, 1993). The co-current moving bed gasifier produces a gas of about 500-600<sup>0</sup>C which generally contains less tar. After cleaning and cooling, the gas can be used in diesel engines (Prasad and Sharma, 1986).

The thermal gasification of biomass, especially of high ash content, in a moving bed gasifier, encounters the problems of slagging and cinderling of ash. (Moreno and Goss, 1983, Hos and Groeneveld, 1987). The cross current gasifier produces a gas that has a composition and temperature some where in between the values of the corresponding parameters of the counter and co-current gasifiers. As this gas provides no special advantage over the gas from the other two, this type of gasifier is not popular commercially.

Depending upon the type of the gasifier and the mode of biomass-air contact, the thermal processes like drying, pyrolysis, oxidation and reduction may take place. These processes as detailed by Iyer et al. (1997), are shown in Fig. 1.2.

van Swaij (1981) has shown the gasification reactor types with temperature and solid conversion profiles. This is reproduced here as Fig. 1.3. It may be seen that in the fluidized bed gasifier, the temperature and solids conversion remain uniform throughout the fluid-bed.

## 1.6 CHEMISTRY OF BIOMASS GASIFICATION

Chemistry of biomass gasification is generally described by representing biomass as carbon (assumed) leading to solid-gas and gas-phase reactions, as given in Table 1.5.

**Table 1.5 : Important Chemical Reactions of the Gasification Processes (Iyer et al., 1997)**

Reaction	Reaction Heat kJmol <sup>-1</sup>	Process	Equation number
C+heat→CH <sub>4</sub> + condensable hydrocarbons + char	-	Devolatilization	(1.1)
Heterogeneous Reactions			
C+O <sub>2</sub> →CO <sub>2</sub>	-393.80	Combustion	(1.2)
C+2H <sub>2</sub> →CH <sub>4</sub>	-74.95	Hydro gasification	(1.3)
C+H <sub>2</sub> O →CO+H <sub>2</sub>	131.40	Water-gas	(1.4)
C+CO <sub>2</sub> →2CO	+172.69	Boudouard	(1.5)
Homogeneous reactions			
CO+H <sub>2</sub> O→H <sub>2</sub> +CO	-41.20	Water-gas shift	(1.6)
CO+3H <sub>2</sub> →CH <sub>4</sub> +H <sub>2</sub> O	-206.30	Methanation	(1.7)
CO <sub>2</sub> +4H <sub>2</sub> →CH <sub>4</sub> +2H <sub>2</sub> O	-165.10	Methanation	(1.8)

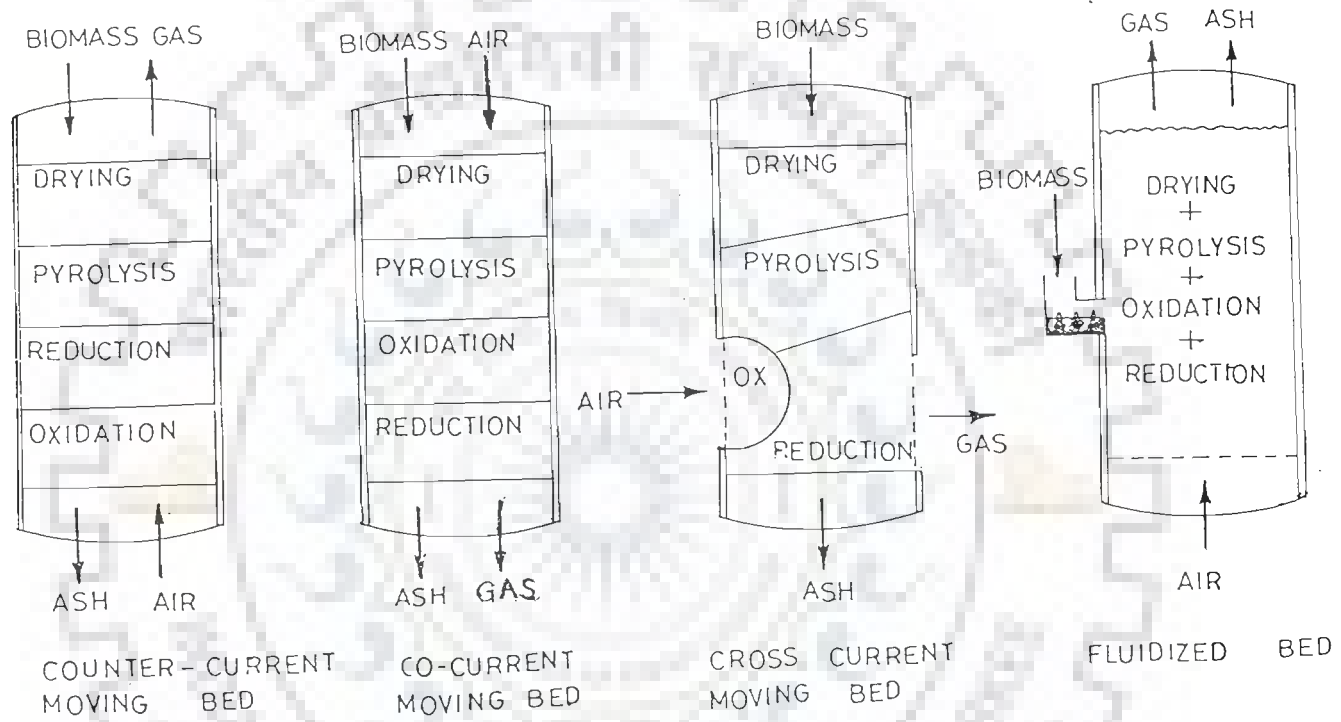
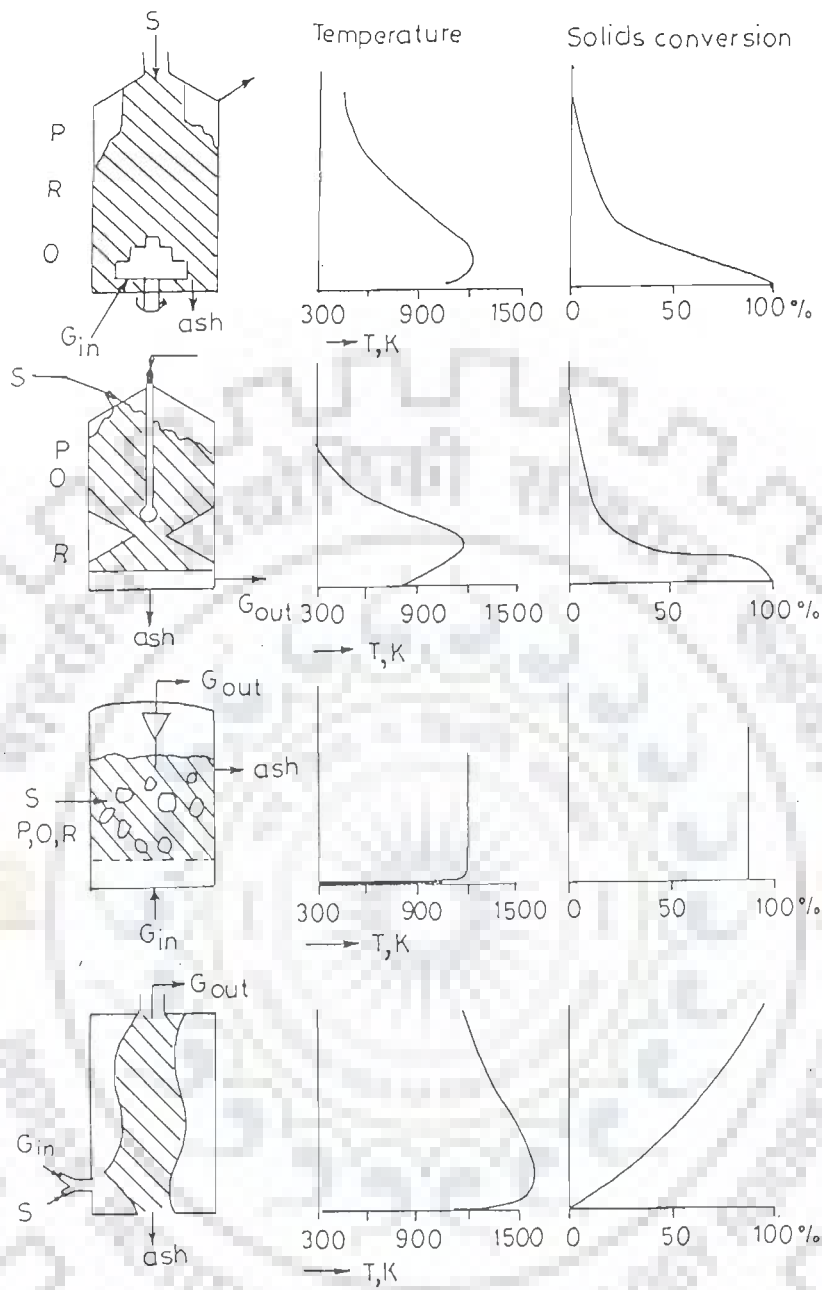


Fig. 1.2 Types of biomass gasifiers (Iyer et al., 1997)



S = Solids feedstock input  
 $G_{in}$  = Gasification agent input  
 $G_{out}$  = Product gas out  
 P = Pyrolysis zone  
 O = Oxidation zone  
 R = Reduction zone

Fig. 1.3 Gasification reactor types with their temperature and solids conversion profiles (van Swaij, 1981)

The thermal energy needed by the gasification process is supplied by the highly exothermic combustion reaction (Eq.1.2). the reaction of hydrogen with carbon (Eq. 1.3) and the reaction of hydrogen and carbon monoxide, the methanation reaction (Eq. 1.7) are also exothermic reactions and hence supply heat to the gasification process. These reactions are interrelated by the water-gas shift reaction (Eq. 1.6) and the equilibrium of this reaction controls the water-gas and Boudouard reactions. The water-gas reaction (Eq.1.4) and the Boudouard reaction (Eq. 1.5) are endothermic and represent conversion of carbon into combustible carbon monoxide gas formation. These reactions derive the heat energy supplied by the combustion reaction. These reactions are favoured, thermodynamically and kinetically, by high temperatures (Desrosiers, 1981). Therefore a decreased yield of CH<sub>4</sub> and C<sub>2</sub>-hydrocarbons results if the hydrogasification and methanation reactions proceed at a lower rate. The production of H<sub>2</sub> and CO is favoured. The objective of the biomass gasification is to convert it into a combustible quality gas of maximum heating value. This is achieved in low temperature gasification to produce CH<sub>4</sub> according to the overall reaction:



## 1.7 FLUIDIZED BED GASIFICATION

Fluidized bed gasification is advantageous for fine biomass particles like sawdust, rice husk/hull, bagasse etc., which owing to their peculiar shape, low bulk density and fine size, can not be used in a moving bed gasifier. Normally the biomass is mixed with an inert solid in such proportions as may be easily fluidised (<10% by weight of biomass). The fluidizing velocity is kept normally about 1.3-1.5 U<sub>mfr</sub> (minimum fluidizing velocity) of the biomass-inert mixture. The feed enters above the inert bed and gets mixed with the fluidizing inert solid. Steam may also be used in the gasification. The fluidizing gas passes through a distributor. Depending upon the type of biomass used in the gasifier, 800 - 1000°C temperature is obtained in the bed.

The produced gas may contain small quantities of tar and large quantities of ash particles. The gas is normally treated in a cyclone/scrubber depending upon its end-use.

The fluidised bed gasification offers uniform high temperature condition (isothermal) of operation, and is considered best suited for agro-residues and other solid wastes which contain high ash and have low bulk density (Schoeters et al., 1989; Sanchez and Lora., 1994; Sridhar et al., 1996).

Gasification allows the use of the biomass fuel in Brayton–Rankine combined co-generation cycles. For biomass integrated gasifier/gas turbine combined cycle (BIG/GT-CC) systems, fluidized bed gasifiers using such biomass as saw dust, rice husk, bagasse, etc. may be advantageous over moving bed gasifiers due to following reasons (Gomez et al., 1995, Gangawati et al., 2000b).

- High fuel flexibility – low density and fine-granulometry biomass fuels may be used. In the downdraft gasifiers due to low packing density of the biomass, feeding gets disrupted due to frequent bridging and tunnelling.
- Intensive heat transfer rate due to the mixture of the inert hot material with the fuel to be gasified in isothermal (~850°C) bed conditions. In downdraft gasifiers, temperatures as high as 1200°C normally exists in the oxidation zone due to which , ash sintering, and clinkering have been observed.
- High carbon conversion for limited particle residence times.
- High volumetric heat release density,  $\text{kJm}^{-3}\text{s}^{-1}$ .

Fluidized bed gasifiers can be classified into two types:

- (i) Bubbling Fluidized Bed (BFB) Gasifiers
- (ii) Circulating Fluidized Bed (CFB) Gasifiers

BFB gasifiers are the first generation gasifiers whereas CFB gasifiers are the second generation gasifiers. Gomez et al. (1995) have listed operational and efficiency parameters, construction features and biomass characteristics of pilot plant gasifiers as reported in literature upto 1994 (Table 1.6 and 1.7).



**Table 1.6 : Operation and Efficiency Parameters, Constructive Features and Biomass Characteristics (Pilot Plant Gasifiers)**  
(Gomez et al., 1995)

Biomass	Gasifier type	Capacity MW th	Operation pressure Mpa	Bed temperature °C	Reactor diameter mm	Gasification agent	Biomass moisture %	Air factor	Gas heating value MJNm <sup>-3</sup>	Static bed height mm	Gas composition, % by volume			Reactor height mm	Gasifier efficiency	References
											CO	H <sub>2</sub>	CH <sub>4</sub>			
Wheat husk	BFB	-	0.1	950	230	Air	-	-	3.00-3.50	-	12.20	5.60	3.30	-	-	Clark and Goodman, 1985
Rice straw	BFB	-	0.1	755	660	Air	-	-	5.30 (HHP)	-	13.00	9.20	6.30	2300	-	Lamorey et al., 1985
Wood wastes (Lurgi)	CFB	2.50	0.1	820	-	Air-steam	15.0	-	5.86	-	18.70	14.10	3.50	-	80.2	Mehrling and Reimert, 1986
Bagasse pellets	BFB	-	0.1	650-850	480	Air-steam	9.2	-	5.60 (HHV)	250-380	17.90	4.70	5.60	2700	57.0-62.0	Baptista, 1986
Wood wastes (IGT)	BFB	0.89	2.2	837	-	Air-steam	10.8	0.170	10.00	-	10.70	32.50	14.30	-	77.0	Evans et al., 1987
Wood shavings and bark	CFB	2.00	0.1	750-900	-	Preheated air	30.3-35.0	-	4.00-7.00	-	-	-	-	-	-	Rensfeld, 1988
Cotton stalks	BFB	1.70	0.1	725	844	Air	-	0.250-0.300	6.80	800	-	-	-	-	-	Maniatis and Kiritisis, 1992
Wood powder	CFB	0.75	0.1	864-974	410	Air	-	0.200	7.19	-	16.10	13.24	7.32	4000	74.0	Bingyan et al., 1993
Wood and wood wastes	BFB	1.70	0.1	743	300	Air	12.8-16.8	0.298	5.20-8.20 (HHV)	600	15.30	9.00	3.70	4000	84.8	Czernik et al., 1994
Bagasse	BFB	-	2.1	850	-	Oxygen	-	-	12.60	-	26.11	18.30	17.30	-	67.0	Overend et al., 1994

**Table 1.7 : Operation and Efficiency Parameters, Constructive Features and Biomass Characteristics  
(Demonstration and Commercial Units)  
(Gomez et al., 1995)**

Biomass	Gasifier type	Capacity MW th	Operation pressure Mpa	Bed temperature °C	Reactor diameter mm	Gasification agent	Biomass moisture %	Air facto	Gas heating value MJ/Nm <sup>3</sup>	Static bed height mm	Gas composition, % by volume			Reactor height mm	Gasifier efficiency	References
											CO	H <sub>2</sub>	CH <sub>4</sub>			
Wood shavings (TPS)	CFB	65	0.18	-	-	Pre-heated air	35.0	-	-	-	-	-	-	43	Strom et al., 1982	
Bark (Lurgi)	CFB	16	0.10	800	-	Air	15.0	-	-	-	30.0	28.8	8.2	-	Mehring and Reimert, 1986	
Wood waste (Omnifuel)	BFB	23	0.10	760	-	Air	-	-	4.99 (HHV)	-	11.0	7.5	6.3	-	Omnifuel, 1990	
Wood wastes (Bioflow)	CFB	18	2.40	950-1000	-	Preheated air	45.0-55.0	-	5.00	-	-	-	-	82-83	Lundqvist, 1993	
RDF pellets (Studvik)	CFB	20	3.5 (kPa)	800-900	-	Air	1.6-11.9	-	7.00-8.50 (HHV)	-	9.0-13.0	7.0-9.0	6.0-9.0	94.96	Campagnola, 1994	

Natarajan et al. (1998) have also given the constructional details of BFB gasifiers and combustors used by different researchers alongwith the operating parameters for rice husk as the biomass feed. They have also summarized the main observations and results obtained by different research workers in literature on rice husk gasification in fluidized beds. Several other reports are available in literature on fluidized bed gasification using different biomass materials as the feedstock, e.g. feedlot manure (Raman, et al., 1980 a,b), luan wood chips (Sakoda et al., 1981), sawdust (Flanigan et al., 1982), Guayule and portuguese cork, oak, *Euphorbia lathyris*, sawdust, Russian thistle, cellulose and wood (Prasad and Kuester, 1988), wood shavings, cacao hulls, refuse derived fuel and *Euphorbia Tirucalli* pellets (Schoeters et al., 1989), pine sawdust (Corella et al., 1991), pine (*Pinus pinaster*) sawdust , pine wood chips, cereal straw , and thistles (*Cynara Cardumculus*) (Herguido et al., 1992), corn cobs (Jiang and Morey, 1992), rice husk, bagasse, sawdust, spent coffee seeds, rice husk and cane bagasse (Sanchez and Lora., 1994), almond shells (Rapagna and Latif, 1997), wheat straw (Ergundenler et al., 1997), pine wood (Gil et al., 1999). Some of these studies were with air and others with air and steam for gasification.

Of late, a number of investigations on fluidized bed steam gasification have been reported (Boateng et al., 1992, Corella et al., 1991, Rapagna and Latif, 1997), a majority of them focussing on the analysis of the produced gas resulting from different biomass feedstock.

## 1.8 EFFECT OF EQUIVALENCE RATIO

The reactions given by Eqs. (1.1 to 1.9) in Table 1.5 may be used to predict the equilibrium composition of the gases produced. As may be seen, this equilibrium composition depends upon the rate of air entering the gasifier per unit mass of the biomass.

The amount of air entering the reactor is normally related to a term called “Equivalence Ratio” (ER), defined as,

$$ER = \frac{(\text{weight of oxygen/weight of dry fuel})_{\text{entering}}}{(\text{weight of oxygen/weight of dry fuel})_{\text{stoichiometric}}}$$

Oxygen in the above definition may be replaced by air as well. The stoichiometric amount of oxygen or air required for complete combustion of the biomass varies from one biomass to the other. Gumz (1950) has given a graphical presentation of the composition of the gases produced in a gasifier fed with coal. For biomass gasification, ER is normally kept between 0.2 and 0.4. Below an ER of 0.2, pyrolysis predominates the process and above an ER of 0.4, combustion predominates. When the hot raw gas from the gasifier is to be burnt in a furnace without any cooling, the gasifier can be operated at the minimum ER (~0.20) as the tar formed during the pyrolysis can then be burnt in the vapour state in the furnace, thus providing maximum possible heat recovery from the hot raw gas. For use in engines, raw gas is to be stripped off its tar content (<100 mgNm<sup>-3</sup>) and in these situations, ER to be used depends on the temperature along the gasifier. Desrosiers (1981) has distinguished pyrolysis, gasification and combustion for biomass for air and oxygen reactions. Fig. 1.4 shows the plot between ER and the adiabatic reaction temperature. The equilibrium composition for adiabatic air/biomass equilibrium as given by Desrosiers (1981) is reproduced in Fig.1.5. Narvaez et al. (1996) have shown that the amount of fuel gases. (H<sub>2</sub>, CO, CH<sub>4</sub>, and C<sub>2</sub>H<sub>2</sub>) decreases as ER increases from 0.20 to 0.45. Similar trends have been found by other workers also, as shown in their paper.

In a fluidised bed gasifier, the gas composition deviates from the equilibrium composition, depending upon the temperature distribution in the fluidised bed gasifier (i.e. the solid bed and the free board height), average gas residence time and its distribution in the gasifier.

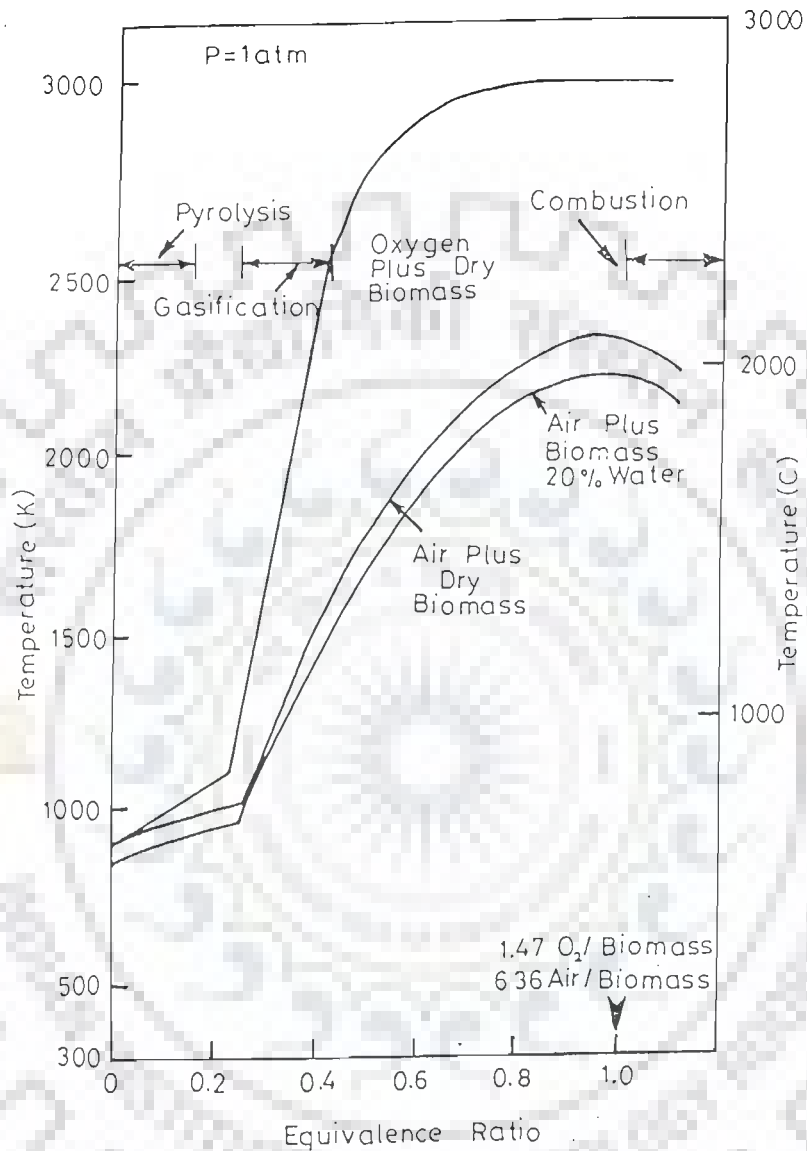


Fig. 1.4 Biomass adiabatic reaction temperatures showing pyrolysis, gasification and combustion regions for air and oxygen reactions (Desrosiers, 1981)

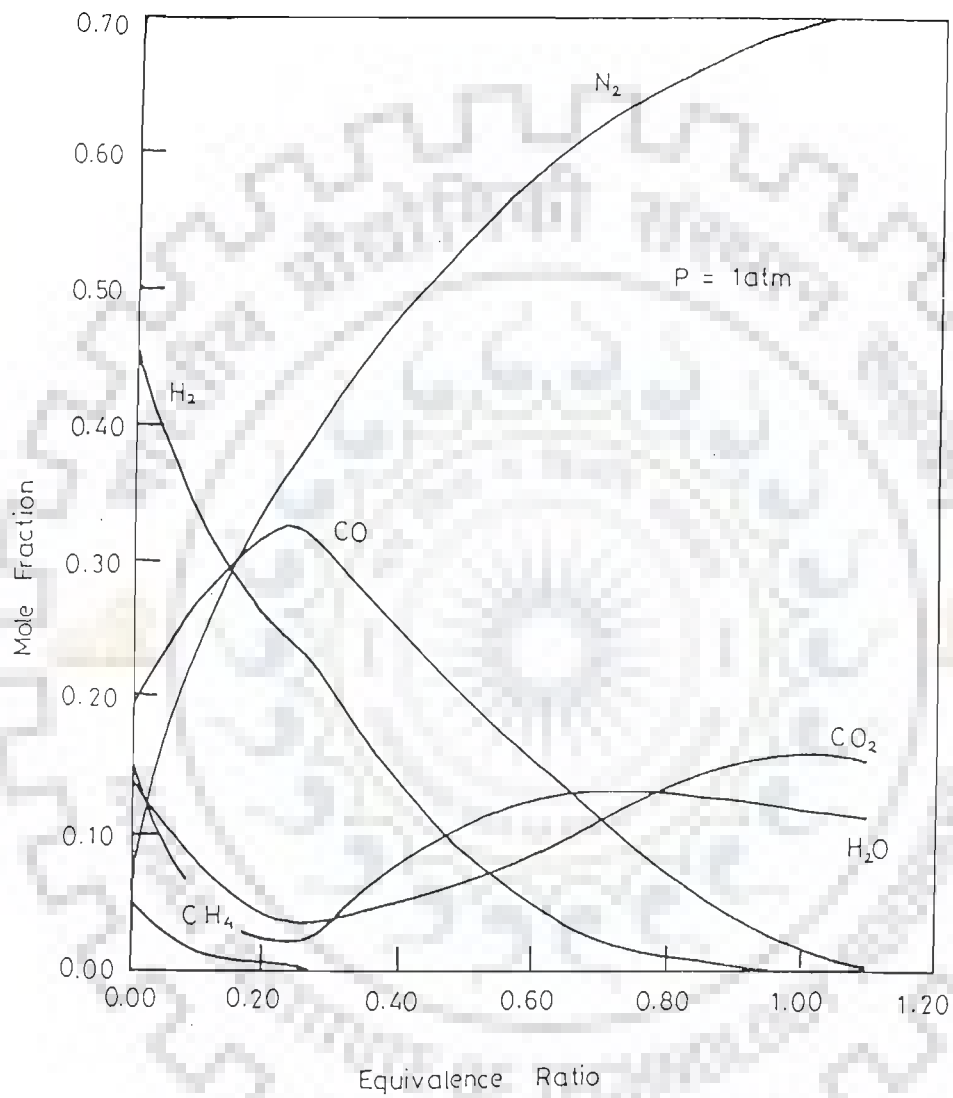


Fig. 1.5 Equilibrium composition for adiabatic air/biomass equilibrium (Desrosiers, 1981)

## 1.9 PRESENT STATUS OF RESEARCH ON FLUIDIZED BED THERMAL GASIFICATION IN INDIA

As seen in Section 1.5, a number of investigators in other countries have reported their findings on thermal gasification of biomass in fluidized beds. However, in India, only one research group (Natarajan et al., 1998) have reported their results on the fluidized bed gasification of rice husk. Table 1.8 presents the status of research work on thermal gasification of biomass in India.

**Table 1.8 : Present Status of Research on Thermal Gasification of Biomass in India**

Institution	Type of Gasifier	Feedstock	Application	Reference
Indian Institute of Technology, Roorkee (Formerly University of Roorkee)	Closed top downdraft	Wood	Power generation	Prasad and Sharma (1986), Sharma (1988)
Deptt. of Mech. Engg., IIT-Bombay	Downdraft	Wood	Power generation	Parikh (1989)
Deptt. of Chemical Engg., IIT-Delhi	Downdraft gasifier and Thermo-chemical characterisation	Wood	Power generation	Grover et al.(1989) Iyer et al. (1997)
SPRERI Vallabh Vidyanagar	Downdraft	Woody agricultural residues	Power generation	Patel and Rao (1993)
Deptt. of Aerospace Engg., IISc, Bangalore	Open top down-draft	Wood	Power generation	Mukunda et al.(1994) Indo-Swiss Program)
NARI Maharashtra Phaltan	Throatless downdraft	Sugarcane leaves	Power generation	Jorapur and Rajavanshi(1995) funded by Rock Feller Foundation USA
TERI, New Delhi	Throatless downdraft	Wood	Power generation, drying	Raman et al. (1995)
Anna University Chennai	Fluidized bed gasifier	Rice husk	Power generation	Natarajan(1998) (Indo-Swiss Program)

Bridgwater (1990) has compiled the activities on thermal gasification of biomass undertaken by different institutions in various countries the world-over. This covers the activities initiated at the erstwhile University of Roorkee, now Indian Institute of Technology, (IIT), Roorkee. Considering the biomass availability in the country and the suitability of the utilization of the fluidized bed gasification of agro-forestry-based biomass, the present research work has been undertaken. This work is a part of the research work on biogasification and thermal gasification of biomass currently undertaken at the Department of Chemical Engineering, IIT, Roorkee.

#### **1.10 AIMS AND OBJECTIVES OF THE PROPOSED WORK**

Based on the literature survey as detailed in Chapter-II, and the works reported in India, the aims and objectives of the work covered in this thesis may be specified as follows:

1. To characterize and analyse different biomass materials for their physico-mechanical and chemical properties.
2. To study the fluidization characteristics of different biomass materials (agro/forestry-/industry-derived biomass) mixed with different fluidizing media (inert solids) in different volumetric (or mass) proportions.
3. To study the thermal degradation characteristics of a few biomass materials using thermo-gravimetric and differential thermal analyses-under inert (nitrogen) and oxidizing (air) atmospheres.
4. To study the thermal degradation (pyrolysis and gasification) kinetics of a few biomass materials.
5. To study the thermal gasification characteristics of a few biomass materials in a fluidized bed gasifier and to study the effect of equivalence ratio (ER) on their gasification characteristics.



---

## LITERATURE REVIEW

Biomass gasification studies abound in literature. However, not many studies are reported on fluidized bed gasification of biomass. In the following paragraphs, literature citations on fluidization characteristics of binary mixtures, mixtures of sand/bauxite with biomass, thermogravimetric analyses of biomass and the fluidized bed gasification of biomass have been reported and critically reviewed.

### 2.1 FLUIDIZATION OF BINARY MIXTURES OF PARTICLES

Davidson and Harrison (1971) have reported the mechanism of particle mixing as observed in a gas-fluidized bed of uniform particles. In such a bed, particle movement is caused solely by the bubbles, which produce a characteristic “drift” displacement. Bubbles also carry particles in their wake, some spillage or wake shedding with local exchange, from bottom to top of the bed.

Otero and Corella (1971 a,b) were, probably, the first investigators to have observed the problems of segregation while fluidizing the mixtures of solids with different sizes and densities. They observed two fluidization velocities- the minimum fluidization velocity and the maximum fluidization velocity in such mixtures (1971a) and that the segregation occurred while fluidizing such mixtures (1971b).

Rowe et al. (1972) carried out experimental studies in two-dimensional fluidized beds with two solid components, which were coloured differently for ease of observation. With particles differing in size and/or in density, they observed segregation of particles at low gas velocities especially when there was appreciable particle density difference. With sufficient increase in the gas velocity, segregation started disappearing tending the particles to get well mixed, although some segregation may still remain. For binary systems, Rowe and coworkers called the component

tending to settle to the bottom as “Jetsam” and that tending to float as “Flotsam”. In general, the heavier component tends to settle while the lighter one rises. They studied the segregation and mixing patterns by using different initial packing patterns of components. They photographed the bubble movement in the bed and presented typical segregation patterns for low jetsam concentration.

Gibilaro and Rowe (1974) proposed a mathematical model based on the proposed mechanisms of segregation and mixing as exemplified by the photographic evidences. They proposed circulation and exchange of particles between two assumed phases of the bed- a bulk phase and a wake phase of particles, which travel upwards with the bubbles. Overall circulation corresponds to the bubble-induced convection and exchange between the phases is an analogue of wake growth and wake shedding or particle spillage. This circulation and exchange is modeled in Fig. 2.1.1 and is expressed by a pair of differential equations applying simultaneously to the two phases. The solutions of this model are shown graphically in Fig. 2.1.2, giving typical segregation patterns for low jetsam concentrations.

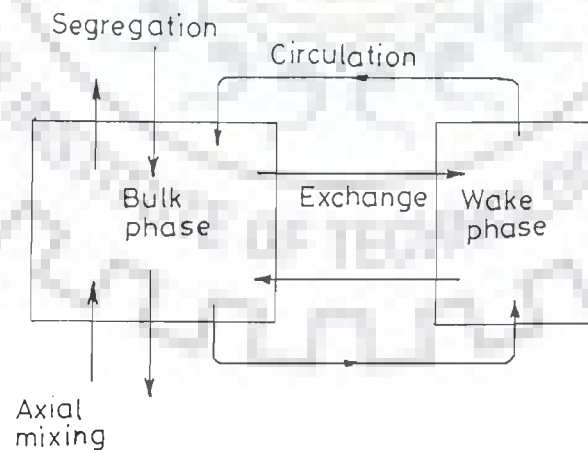


**Fig. 2.1.1 A model of the segregating/mixing system (Gibilaro and Rowe, 1974)**

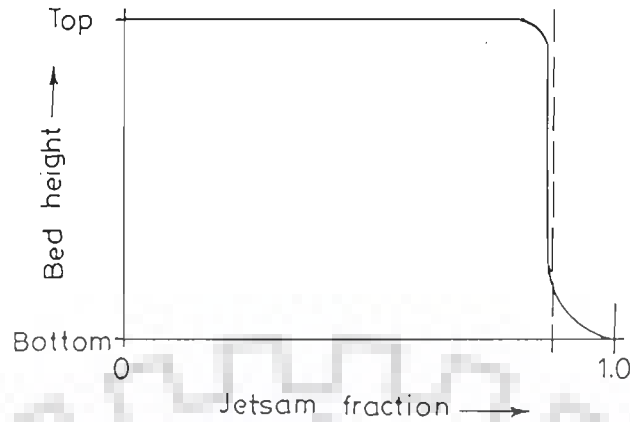


**Fig. 2.1.2 Segregation pattern for large jetsam fraction (Gibilaro and Rowe, 1974)**

Wen and Yu (1966) modified the Ergun (1952) equation of pressure drop through the particle bed of a single component to make it more useful, as it eliminated the terms of voidage and shape factor (which can be hardly determined), for the prediction of minimum fluidization velocity.

$$Ar = 24.5 Re_{mf} + 1650 Re_{mf}^2 \quad (2.1.1)$$

$$\text{where, } Ar = d^3 \delta_f (\delta_s - \delta_f) g / \mu^2 \quad (2.1.2)$$

$$Re_{mf} = \frac{d \delta_f U_{mf}}{\mu} \quad (2.1.3)$$

and f and s represent the fluid and the solid, respectively.

For non-single component systems, the above equation of Wen and Yu (1966) does not hold true. Bed comprising of particles of different sizes exhibits peculiar behavior when fluidized. When a small amount of fines is added to coarser material, the minimum fluidization velocity is reduced resulting in increased bubble flow. Cheung et al. (1974) presented a simple correlation for minimum fluidization velocity for binary mixtures having the diameter ratio up to 3.

$$(U_{mf})_{mixture} = (U_{mf})_s \left( \frac{(U_{mf})_l}{(U_{mf})_s} \right) X_s^2 \quad (2.1.4)$$

where, s and l refer to respectively, the small and large particles.  $X_s$  is the mass fraction of the smaller particles.

Rowe and Nienow (1975) have presented a semi-theoretical equation to obtain the minimum fluidization velocity of the multi-component mixtures from the known minimum fluidization velocity and voidage of mono-sized particles of a known diameter, and the mass fraction of particles of different diameters in a mixture, which had a known voidage. This equation is given as,

$$(U_{mf})_{mixture} = (U_{mf})_1 \left[ (\epsilon / \epsilon_1)^3 \left( \frac{1 - \epsilon_1}{1 - \epsilon} \right)^{2-n} \right]^{1/n} \left[ x_1 + \frac{d_1}{d_2} x_2 + \dots \right]^{(1-3/n)} \quad (2.1.5)$$

where 1 refers to the mono-sized particles of diameter  $d_1$ .  $x_1, x_2, \dots$  are the mass fractions of particles of diameter  $d_1, d_2, \dots$  in the mixture which has a voidage  $\epsilon$ . The exponent n is a function of the Reynolds regime of flow and takes a value little greater than unity.

Equation (2.1.5), however, is not applicable for beds having particles of different density. Particle density difference is a much stronger factor than size difference in having a well-mixed fluidized bed. Whilst size difference could still make a homogeneous fluidized bed, a small density difference may make the bed tend to segregate. When a binary mixture is fluidized, dynamic mixing-segregation equilibrium is set-up, which is mainly a function of the density and size of the solid particles and of the gas flow rate. The flow rate of the gas, which passes through the bed in the form of bubbles, determines the equilibrium segregation pattern.

Rowe and Nienow (1976) defined a mixing index, M as the ratio of the proportion of jetsam dispersed in the upper part of the bed to the total jetsam fraction present (i.e.  $M = x/\bar{x}$ ). Using the data on binary mixtures available to them, they

showed that the mixing index varies with the gas velocity in S-shaped form and gave a logistic equation of the form,

$$M = 1/[1 + \exp(-Z)] \quad (2.1.6)$$

where

$$Z = \left( \frac{U - U_{T0}}{U - U_F} \right) \exp(U/U_{T0}) \quad (2.1.7)$$

$U$  = Superficial gas velocity

$U_F$  = Minimum fluidization velocity of flotsam

$U_{T0}$  = Critical velocity above which mixing predominates (at  $M = 1/2$ )

The normalized data showing the variation of mixing index with gas velocity is shown in Fig. 2.1.3.

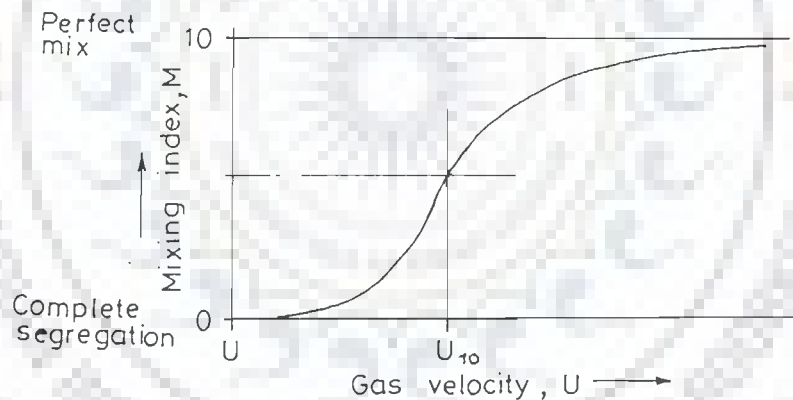


**Fig. 2.1.3** Variation of mixing index with gas velocity (Rowe and Nienow, 1976)

Chen and Keairns (1975) conducted fluidization experiments with six mixtures consisting of two-component, three-component, and wide-size distribution particles of different size and/or different density in both a pressurized system (upto 660 kPa) and a

low pressure (101-142 kPa) unit. They used 100 mm tempered glass and 114 mm steel pipes of different lengths with a perforated distributor plate with 96 holes of 1.6 mm diameter of equal spacing ( $\approx 6.35$  mm). The distributor plate was designed to provide  $\Delta P_{\text{grid}}/\Delta P_{\text{bed}} \geq 1$  and was covered with 74  $\mu\text{m}$  screen to prevent fine particles from falling through or plugging the orifice. The particle size ranged between 150 to 2800  $\mu\text{m}$  and density from 720 to 2800  $\text{kgm}^{-3}$ . They found that the segregation of particles in a fully fluidized bed occurs for mixtures of different size (e.g. dolomite) and of different density (e.g. char-dolomite mixture), and that the segregation at low velocity was rapid and reached the steady state in less than 30 s. They reported more than 95% separation of agglomerated ash particles in a fluidized bed combustor/gasifier when a velocity close to the minimum fluidization velocity of the agglomerated ash particles was used in the char/ash separator.

Vaid and Sengupta (1978) reported experimental studies on minimum fluidization velocities in beds of mixed solids (two, three, four and five component mixtures) in liquid fluidized beds. They showed that the fluidization behaviour of a bed of solids of mixed size and/or densities indicated that for a range of velocities between  $U_{\text{bf}}$  (the velocity of beginning of fluidization) and  $U_{\text{cf}}$  (the velocity of complete fluidization) the bed was only partially fluidized. They showed the analogy between this phenomenon and that of the fractional crystallization of a multicomponent solution. Based on the experimental data on liquid-solid fluidized beds and for gas-solid systems reported in the literature, they proposed the following correlations,

$$\text{Re}_{\text{bf}} = [ (18.1)^2 + 0.0192 \text{Ga} ]^{0.8} - 18.1 \quad (2.1.8)$$

$$\text{and } \text{Re}_{\text{cf}} = [ (24)^2 + 0.0546 \text{Ga} ]^{0.5} - 24 \quad (2.1.9)$$

Chiba et al. (1979) studied the fluidization of binary mixtures and classified the mixing state in the fluidized bed of binary system into that of (a) complete mixing, (b) complete segregation, and (c) partial mixing. When a binary mixture of two components, are fluidized, a component (say A) fluidizes at the lower gas velocity  $U_{\text{A}}$ ,

and the other (say B) at a higher gas velocity  $U_B$ . These authors reported an empirical equation for the estimation of the minimum fluidization velocity of complete and partial mixing beds. Fig. 2.1.4 shows the characteristic bed pressure drop-superficial gas velocity curves corresponding to these three states of mixing. Here, case (A) is the complete mixing bed composed of small particles having nearly the same sizes and densities. Case (B) is the segregated bed composed of particles whose sizes and densities are greatly different. Case (C) is the intermediate case of partial mixing bed. Most of the mixing states of the fluidized beds of binary components systems belong to this case.

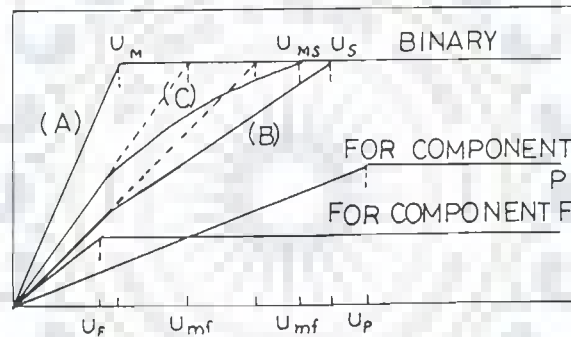


**Fig. 2.1.4** Effect of mixing/segregation state on the relationship between bed pressure drop and superficial gas velocity (idealized) (A) completely mixed; (B) completely segregated; (C) partial mixing (Chiba et al., 1979)

Chiba et al. (1979) have defined apparent fluidization velocities for segregating systems of the two components and complete mixing. Experimental values have been found to be extremely sensitive to voidage, which is a function both of bed composition and experimental technique. They found that the Eq. (2.1.4), given by Cheung et al. (1974) empirically, gives the best indication of the shape of the well-mixed  $U_{mg}$  ( $U_M$  or  $U_{MS}$  with fast defluidization) versus composition curve, provided  $U_F$  and  $U_P$  are known.

Here the subscripts M, MS, F and P represent completely mixed bed, partially mixed-partially segregated bed, the fluidized component minimum fluidization velocity and the packed component minimum fluidization velocity as explained in Fig. 2.1.4.

Yang and Keairns (1982) defined a hypothetical minimum fluidization velocity of the mixture as the intersection of the horizontal line representing the bed pressure drop, calculated by dividing the total bed weight by the bed cross sectional area, with the pressure drop curve after the maximum pressure drop is attained. However, this definition is useless, as the coarse particles cannot fluidize at that gas velocity. Noda et al. (1986) conducted experiments and compared their observations with a mechanistic model to study the fluidization characteristics of binary mixtures of particles with large size ratio. They used particles of different shapes such as wood chips, rubber sheets, glass beads, iron beads, soyabeans and small beans as coarse particles and nearly spherical fine particles of sands and glass beads as a fluidizing medium. Extending the modified Ergun equation as proposed by Wen and Yu (1966) for a single-component system as,

$$Ar = A Re_{mf}^2 + B Re_{mf} \quad (2.1.10)$$

Where,

$$Ar = d^3 \rho_g \left( \bar{\rho} - \rho_g \right) g / \mu^2 \quad (2.1.11)$$

$$Re_{mg} = \bar{d} \rho_g U_{mg} / \mu \quad (2.1.12)$$

$$\bar{\rho} = 1 / \left[ \frac{w_f}{\rho_f} + \frac{w_e}{\rho_e} \right] \quad (2.1.13)$$

$$\bar{d} = 1 / \bar{\rho} \left[ \frac{w_f}{d_f \nu_f} + \frac{w_e}{d_e \rho_e} \right] \quad (2.1.14)$$

f = fluidizing media (solid)

e = coarse particles



They correlated their experimental data and gave the parameters, A and B, as follows:

$$A = 36.2 \left( \frac{d_e \rho_f}{d_f \rho_o} \right)^{-0.196} \quad (2.1.15a)$$

$$B = 1397 \left( \frac{d_e \rho_f}{d_f \rho_o} \right)^{0.296} \quad (2.1.15b)$$

or

$$B = 6443.2 \left( \frac{d_e \rho_f}{d_f \rho_o} \right)^{-1.86} ; \quad d_e/d_f > 3, \rho_o/\rho_f \approx 1 \quad (2.1.16)$$

Eqs. (2.1.15a,b) is valid for general cases where the bed is completely mixed after both the components are fluidized. For specific cases where the bed is partially mixed after both components are fluidized, equation (2.1.16) is valid. The average particle diameter and the average density of bed particles were obtained using the correlations (Equations 2.1.12 and 2.1.13) as proposed by Goosens et al. (1971).

## 2.2 FLUIDIZATION OF BIOMASS MATERIALS

Most of the biomass used in the fluidized bed gasification do not fluidize easily. These materials are of low density, have peculiar shapes and surface characteristics, are hygroscopic in nature and are of varied sizes. The shape, size, density and moisture-absorbing capacity affect the quality of fluidization and its characteristics. This, in turn, affects the quality of thermal gasification. To improve the quality of fluidization and the gasification of biomass particles in a fluidized bed, a second solid, called carrier solid, is added to the biomass bed. Sand, bauxite and alumina particles have been mostly used as the carrier solids for biomass fluidization.

When a mixture of two solids of different sizes, shapes and densities are fluidized, the bed does not exhibit the uniform concentration of the solids as in the initial well mixed stage and segregation of the solids appears. The fluidization studies

reported in section 2.1 above did not use any biomass material for fluidization nor did they report such pronounced differences in particle diameters, densities and shapes as are encountered in sand/bauxite/alumina-biomass mixtures.

Although many investigators used biomass with a carrier solid for fluidized bed gasification studies, (Raman et al., 1980, Sakoda et al., 1981, Schoeters et al., 1981, Walawender et al., 1981, Feldman et al., 1984, Hemati et al., 1985, Singh et al., 1986, Font et al., 1986, Aarsen et al., 1986). Only Font et al. (1986) and Aarsen et al. (1986) have reported the minimum fluidization velocity of the mixture. Most of the gasification studies have been conducted at superficial air velocities in the range of 9.8-37  $\text{cm s}^{-1}$ ; although for woodchips/saw dust, the superficial velocities used were 320 and 450  $\text{cm s}^{-1}$ , with sand as the carrier solid.

Raman et al. (1980) used manure of two sizes;  $-0.9+2.39$  mm and  $-2.38+1.41$  mm with sand of 0.55mm for gasification in a fluidized bed. They studied gasification superficial gas velocities equal to at 2.5 to 3 times  $U_{mf}$  ( $U_{mf} = 11 \text{ cm s}^{-1}$ ) of sand particles.

Sakoda et al. (1981) studied the gasification of biomass in a fluidized bed. They used 5mm cubes of luan chips and 5mm size peanut shells in a 37mm inner diameter fluidization column. Microspherical alumina particles were used as carrier solid and nitrogen gas was used as the fluidizing medium. Nitrogen was used because both luan chips and peanut shells had more than 40% oxygen as the elemental constituent of the biomass.

Schoeters et al. (1981) used a mixture of wood shavings and sand particles ( $-710+425 \mu\text{m}$ ) and carried out fluidization at superficial gas velocity in the range of 1.8-2.5  $U_{mf}$ .

Walawendar et al.(1981) studied the fluidization of manure ( $-1.41+0.42$  mm) particles, and silica sand ( $-595+297 \mu\text{m}$ ) and calcite ( $-2.8+0.3$  mm) mixture.

Feldman and his group (1984) carried out experiments with woodchips and woodchips/sawdust of various sizes using sand as the fluidizing carrier medium. Hemati et al.(1985) reported results of a mixture of sawdust of size  $-400+345 \mu\text{m}$  with  $-315+250 \mu\text{m}$  size sand fluidized at velocities in the range of  $9.8-21.0 \text{ cms}^{-1}$ .

Singh et al. (1984) conducted fluidization experiments using cottonwood branches of  $-597+297 \mu\text{m}$  size and mixture of silica sand (75%) of size  $-597+297 \mu\text{m}$  and calcite (25wt.%) of  $-2.8+0.3 \text{ mm}$  size with air superficial velocities of  $15-20 \text{ cms}^{-1}$ .

Xu et al.(1985) and Flanigan et al.(1987)reported that the fluidization of rice husk or its char alone was difficult but the mixture of husk and sand and/or ash showed good fluidization characteristics. They observed that the bed oscillated between fluidization and severe channeling at high air superficial velocities. Ground husk was found to be easier to fluidize and that the fluidization behavior of husk and its ash was found to be superior to that of husk and sand mixture. They reported that the minimum fluidization and terminal velocities of sand and husk ash were about  $16.5$  and  $82 \text{ cms}^{-1}$ , respectively and that the minimum fluidization velocity of whole husk and sand mixture (1:12weight ratio) was approximately equal to the terminal velocity of sand ( $82 \text{ cms}^{-1}$ ), and that of char and sand mixture (1:10 weight ratio) was equal to that of sand (of  $234 \mu\text{m}$  size). Based on their experiments, they showed that mixture of 3-7 kg of sand /kg of ground husk exhibited good fluidization characteristics at the air superficial velocities of  $27$  to  $36 \text{ cms}^{-1}$ . The bed expansion was found to be about 2.5 times that of the static bed height at twice the minimum fluidization velocity.

Font et al. (1986) have carried out fluidization of almond shells with calcined (at  $950^{\circ}\text{C}$ ) sand of  $-210+105 \mu\text{m}$  size. They used a range of shell particle sizes,  $-105+63 \mu\text{m}$  to  $-500+297 \mu\text{m}$ . They reported that the  $u_{mf}$  of the mixture of particles of different size ranges varied between  $1.8$  to  $8.7 \text{ cms}^{-1}$ . Aarsen et al.(1986) used the particles of beechwood of the  $-3+1 \text{ mm}$  size range with  $325 \mu\text{m}$  size aluminum particles and reported  $U_{mf}$  of  $21.0 \text{ cms}^{-1}$ .

Hemati et al.(1990) carried out experimental study to establish mixing and segregation conditions of wood sawdust and coal particles in a fluidized bed of sand or alumina particles. With an increase in the fluidization velocity, uniformity of mixing was found to increase. For fluidization at velocities less than  $U/U_{mf} = 2.5$ , strong segregation occurred between sawdust and sand particles, however, for  $U/U_{mf} > 2$ , the bed became homogeneous for coal-sand mixing. The particle size was found to have practically no influence on mixing for sand and coal. It was also found that within a minute, dynamic equilibrium was established between mixing and segregation.

Bilbao et al. (1987) have conducted fluidization experiments on sand/straw binary mixtures. They found that the applications of the equations, available in literature, for predicting the minimum fluidization velocity have been unsuccessful due to following reasons :

- (i) The fluidization of sand/straw mixture containing more than 15 weight % straw could not be achieved.
- (ii) Since straw does not fluidize on its own, its minimum fluidization velocity  $U_p$  cannot be determined *a priori*.
- (iii) The  $U_{mf}$  values obtained by using the methods of Chiba et al. (1979) (Plot of  $\Delta P$  vs.  $U$  for different initial states of the bed) are always lower than the actual velocity needed to fluidize the mixtures. Therefore, it is not convenient to use equations where  $U_{mf}$  has been obtained from the above methods.

Bilbao et al. used sand of three sizes between 0.158 and 0.346 mm and straw of five sizes between 0.346 and 1.788 mm and conducted fluidization experiments in a glass column of 80 mm i.d, with a porous plate as gas distributor and air as the fluidizing medium at room temperature. They extrapolated their plots for  $U_{vf}$  vs.  $X_F$  for  $X_F=0$  to obtain  $U_p$  values and correlated as  $U_p = 50 d_p^{0.84}$ . They showed that all the plots obtained can be fitted to the equation.

$$U_{vf} = U_P - (U_P - U_F)X_F \quad (2.2.1)$$

where  $U_F$  values are those experimentally obtained or calculated from the correlation due to Wen and Yu (1966).

$$Re_{mf} = \left\{ \sqrt{C_1^2 + C_2 Ar} \right\} - C_1 \quad (2.2.2)$$

with the values of  $C_1 = 27.2$  and  $C_2 = 0.0408$  as recommended by Grace (1981).

They have also shown that this equation for  $Re_{mf}$  could be used for determining  $U_P$  if the values of  $C_1 = 4.5$  and  $C_2 = 0.12$  are assumed.

Aznar et al.(1992 a,b) have conducted detailed experiments on the fluidization of agricultural and forestry residues with a second fluidizing solid. In their paper (1992 a), they presented preliminary data and results for sand-sawdust mixtures. They did extensive work on the fluidization of mixtures with straw of small and large sizes and other biomass like woodchips, pine thinnings, sawdust, char and ground up thistle from energy plantations with beach and silica sand of different sizes and densities, dolomite and a commercial catalytic cracker as the second (carrier) solid. They studied the fluidization characteristics of a number of biomass mixtures with the carrier solids in two columns of 140 mm and 300 mm inside diameter and one meter high, made of transparent methacrylate. The gas distributor plates had special bubble caps with 0.6-0.8mm diameter horizontally drilled holes. The H/D ratio of the bed was varied between 1 and 2. The characteristics of the biomass and fluidizing carrier solids and operating parameters reported by different researchers till then have been detailed by them, as reproduced in Table 2.2.1.

These authors defined the minimum fluidization velocity,  $U_{mf}$  as the intersecting point between the horizontal line corresponding to the maximum curve of pressure drop ( $\Delta P$ ) versus superficial velocity ( $u$ ). They also showed that higher values of  $u_{mf}$  are obtained with the rapid defluidization method or homogeneous fixed bed than with slow defluidization or initially desegregated fixed bed. They also defined a minimum

velocity of complete (or maximum) fluidization ( $u_{cf}$ ) at which the entire bed (biomass + second solid) was in motion, independently of where this velocity started or whether or not all the biomass was segregated in the upper or lower part of the bed. The movement of biomass was different (small pegs, for example) from the movement of the carrier solid. The velocity of complete fluidization,  $u_{cf}$ , was, however, determined from visual observation. They found that  $H/D$  (height of the bed to the diameter of the column) ratio between 1 and 2 did not have any effect on  $u_{mf}$  and  $u_{cf}$ . Based on the works with different sizes of the carrier solid and those of the biomass with different mass percent in the mixture, they concluded that no correlation for  $u_{mf}$  or  $u_{cf}$  could be proposed. Fig. 2.2.1 illustrates the fluidization characteristics of such mixtures and the definitions of various fluidization velocities.

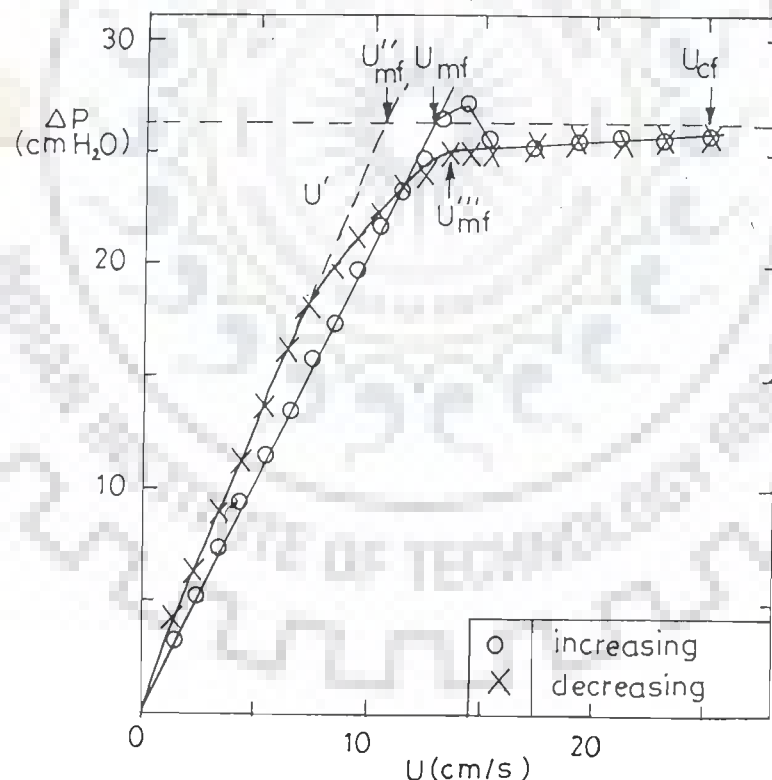


**Fig. 2.2.1** Pressure drop in the bed versus superficial gas velocity. Silica sand ( $d_p$  : - 297 + 200  $\mu\text{m}$ ) and saw dust (40 vol%,  $d_p$  : - 1000 + 400  $\mu\text{m}$ ) (Aznar et al., 1992a)

**Table 2.2.1 : Mixtures of Biomass and Second Solid Used in Fluidized-Bed Gasifiers (Aznar et al., 1992a)**

Biomass		Second solid		$U_{mf}$ of mixture	$U_s$ ( $cms^{-1}$ )	Reference
Type	Size	Type	Size			
Feedlot Manure	-0.9 + 2.39 mm -2.38 + 1.41 mm	Sand $U_{mf} = 11 cms^{-1}$	0.55 mm	28-33		Raman et al. (1972)
Wood chips and peanut hulls	5 mm (cube)	$Al_2O_3$	-450 + 370 $\mu m$	-	-	Sakoda et al. (1981)
Manure	-1.41 + 0.42 mm	Silica sand and calcite	-595 + 297 $\mu m$ -2.8+0.3 mm	-	37	Walawender et al. (1981)
Wood shavings	-	Sand	-710 + 425 $\mu m$	-	1.8-2.5 $U_{mf}$	Schoeters et al.(1981)
Wood chips	-3.8 + 0.6 cm	Sand	-840 + 297 $\mu m$	-	450	Feldman et al.(1984)
Wood chips/sawdust	Various sizes	Sand	-	-	320	Paisley et al. (1984)
Sawdust	-400 + 345 $\mu m$	Sand	-315 + 250 $\mu m$ $U_{mf} = 7 cms^{-1}$	-	9.8-21.0	Hemati et al. (1985)
Almond Shells	-105+ 63 $\mu m$ to -500 + 297 $\mu m$	Sand calcined at 950°C	-210 + 105 $\mu m$	1.8 to 8.7		Font et al. (1986)
Beechwood	-3 + 1 mm	Aluminum	325 $\mu m$	21.0		Aarsen et al. (1986)
Cottonwood branches	-597 + 297 $\mu m$	Silica sand (75 wt%) and calcite (25 wt%)	-2.8+0.3 mm	-	15-20	Singh et al. (1986)

Note :  $U_s$  = Superficial gas velocity,  $cms^{-1}$   
 $U_{mf}$  = Minimum fluidization velocity,  $cms^{-1}$

Sen and Ghosh (1992) have studied the fluidization characteristics of rice husk, husk char and ash, as also of their mixtures. They used a 76 mm diameter and 900 mm high perspex column having a multiorifice distributor at its base for fluidization experiments with a static bed depth of 150mm ( $H/D = 2$ ). Higher  $H/D$  ratios promoted channeling. Particles in the size range of 0.21 to 2.0 mm were used in the experiments. The plots of pressure drop versus superficial air velocity did not show the usual fluid-bed characteristics, with whole husk showing a poor behavior. No sharp break at the

region of onset of fluidization was found. The fluidization behavior of whole husk char was found to be better than that of the husk but not as good as that of the ash. Channeling was found with the mixture of char, ash and husk at low air velocities. Good mixing with little classification among the different particles was observed at bubbling velocities. They found that the minimum fluidization velocity of ash was around 65% of that of husk and the bubbling bed was found at about 50% of the bubbling velocity for husk. Aggregative beds were found at a velocity of about 2.5 times that of minimum fluidization velocity. The fluidization characteristics of husk, char and ash as compiled by Sen and Ghosh are reproduced below in Table 2.2.2.

**Table 2.2.2 : Fluidization Characteristics of Rice Husk, its Ash and Char  
(Sen and Ghosh, 1992)**

Material	Minimum fluidizing velocity, cms <sup>-1</sup>	Bubbling Velocity, cms <sup>-1</sup>	Entrainment Velocity, cms <sup>-1</sup>	Remarks
Ground husk	26	72	80	-
Whole husk	46	100	110	-
Ground husk ash	18	33	55	Comparatively finer particles were carried over.
Whole husk ash	30	51	70	-
Char(devolatilised husk)*	45	1000	115	-
Ash (70% and char mixture)*	-	100	100	Mainly finer particles of ash were carried over
Char (70%) and husk mixture	-	100	100	Mainly finer particles of char were carried over

\* Material prepared from whole husk.



Gangavati et al.(2000) studied the fluidization characteristics of sand(size:-500+350  $\mu\text{m}$ ; -850+710  $\mu\text{m}$ ) and bauxite (size: -500+420  $\mu\text{m}$ ; -850+710  $\mu\text{m}$ ) and the mixtures of these solids with rice husk and sawdust in different mass proportions varying from 1 to 8 % (by mass). They used thick plexiglass tube of 76mm inner diameter as the fluidizing column and a multiorifice distributor with 1.5mm diameter holes drilled in a triangular pitch. They used the carrier solid bed of H/D ratio = 1, 1.25 and 1.5 and found that H/D ratio in this range had no effect on fluidization characteristics. They found that the particle mixtures containing up to 8 mass % of the biomass with the carrier solids, showed good fluidization, when the fluidization was started with the well-mixed binary mixture. Above 8 mass % of the biomass content in the bed, proper quality of fluidization was not observed.

### **2.3 THERMAL DEGRADATION/DECOMPOSITION OF BIOMASS USING THERMOGRAVIMETRIC ANALYSIS**

The characteristics of thermal degradation of fuels and biomass materials are often studied using the data obtained from thermogravimetric analysis (TGA) and differential thermal analysis (DTA). Thermal degradation data obtained at different heating rates provide valuable information on the thermal degradation/decomposition of different fuels. Several investigators have used this technique to study the solid-state reactions, devolatilization characteristics and kinetics of thermal degradation of fuels and biomass (Freeman and Carroll, 1958; Coats and Redfern, 1967; Ramaih and Goring, 1967; Ramiah, 1970; Tia et al., 1991; Ghaly et al., 1993; Antal and Varhegyi, 1995; Nassar et al., 1996; Mansaray and Ghaly, 1998, 1999; Sharma and Rao, 1999; Diblasi and Branca, 1999; Katyal and Iyer, 2000; Singamsetti and Rao, 2000; Katyal, 2001). Thermogravimetric analysis is one of the most commonly used methods for studying devolatilization reactions (Raman et al., 1981). In thermal analysis experiments, a fuel (solid) mass is heated or cooled at a predetermined temperature-

time programme and the weight of the solid mass sample is continuously monitored and recorded as a function of temperature. Slow heating is normally resorted to maintain stability within the instrument. At high heating rate, the evolution of volatiles is very fast with low repolymerization. The TGA method provides the net weight loss of the sample and calculation of kinetic parameters is based on simplifying assumptions to represent the otherwise complex reactions occurring during thermal degradation of biomass.

Different research groups have used static (isothermal) and dynamic (non-isothermal, at different heating rates) TGA. The data obtained from dynamic mode experiments are greatly influenced by the configuration of the instrument and the experimental parameters like heating rate, sample size, purge gas flow rate and pressure (Raman et al., 1981). Antal (1982, 1985) has presented a comprehensive review of works reported on pyrolysis of cellulose and lignocellulosic materials. Antal et al. (1995) presented a 'State of the Art' on cellulose pyrolysis kinetics. He reported that although the Pyrolysis Chemistry was very involved and exceedingly complex, a simple, first order, high activation energy ( $238 \text{ kJmol}^{-1}$ ) model accurately described the pyrolytic decomposition of an extraordinary variety of cellulosic materials. This model accurately mimics the weight loss behavior of cellulose over a wide range of heating rates. They reported that the vapor – solid interactions (secondary reactions) are effectively the only source of char formed during the pyrolysis of pure cellulose. These reactions, probably catalyzed by water vapour, result in high yield of charcoal from biomass. They also reported the strong catalytic effect of mineral matters naturally present in whole biomass in the decomposition of the cellulose component. The use of fine particles of the biomass and a small sample size normally take care of heat and mass transport problems affecting the thermal decomposition. Under non-isothermal, constant heating rate conditions, intra-particle temperature gradients are minimized by using such particle sizes so as to give small Biot number (Antal and Varhegyi, 1995).

Sample sizes of about 0.5 mg are found to be adequate to offset extra-particle temperature gradient and the limitations of external heat transfer effects (Varhegyi et al., 1989, 1994). Cooley and Antal (1988) suggested the use of low heating rates ( $1-5 \text{ Kmin}^{-1}$ ) during avicel cellulose pyrolysis by thermogravimetry in flowing helium, argon and nitric oxide atmospheres with sample sizes between 5 and 7 mg. Antal and Varhegyi (1995) concluded that the decomposition of small samples of pure cellulose at low to moderate heating rates was dominated by a single rate limiting step which is well described by a single step, high activation energy, first-order model.

Raman et al. (1981) carried out devolatilization studies on feedlot manure using thermogravimetric analysis. The analysis of the data revealed that the total weight percent devolatilized was mainly influenced by the size fraction while the temperature at which the maximum rate of devolatilization occurred was mainly influenced by the heating rate. They used 0.5 – 1.5 mg samples of three size fractions, namely,  $-37 + 44$ ,  $-88 + 125$  and  $-420 + 840 \mu\text{m}$ , at the two heating rates of 60 and  $160 \text{ Kmin}^{-1}$  under dry nitrogen atmosphere as proposed by Pitt (1962), modified by Anthony et al. (1974) and on assumed value of  $k_0 = 1.67 \times 10^{13} \text{ s}^{-1}$  given by Benson (1968).

Hamad (1981) described thermal characteristics of rice hulls and found that upon heating above  $200^\circ\text{C}$  upto  $450^\circ\text{C}$ , 90% of the total volatile matter was separated. Decomposition was found to be rapid and temperature-dependent. Experiments were conducted in the absence of air as well as in the presence of oxygen. Presence of oxygen increased the weight loss over that for the absence of air.

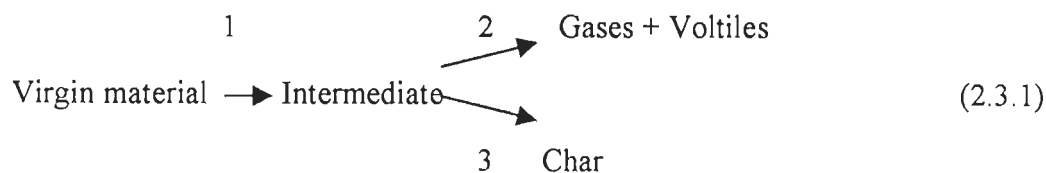
Nassar (1985) was probably the first to have conducted experiments on a large number of non-woody plants (bagasse, rice straw and rice hulls) for their thermal degradation characteristics by using differential thermal analysis (DTA) and thermogravimetric analysis (TGA) under oxidizing and inert atmospheres. He found that degradation patterns for rice straw and hulls (non-woody plants) were similar, and that the degradation pattern for bagasse was similar to hardwood. The rate of

degradation of non-woody plants was found to be faster than wood because of their porous structure. Using pseudo-first order rate kinetics, he found two values of the activation energy with a transition temperature of 335°C. The activation energies of rice straw and hull were found to be lower than that for bagasse. This was attributed to the effect of the inorganic matter (silica in this case) in the rice straw and hulls.

Ghaly and coworkers (1990, 1991, 1992, 1993) used TGA and DTA methods to study the thermal degradation characteristics of wheat straw, cereal straws and oat straw in air and nitrogen. They observed two reaction zones on the TGA and DTA curves and determined the order of reaction, activation energy, and pre-exponential factor for each zone separately by applying thermo-analytical techniques to the reaction kinetics.

Lipska-Quinn et al. (1985) and Bining and Jenkins (1992) studied the thermochemical reaction kinetics of rice straw. Bining and Jenkins used high heating rates, (i.e. 50 and 100 Kmin<sup>-1</sup>) and reported activation energy values for rice straw (110-175 kJmol<sup>-1</sup>) with first order reaction kinetics. Lipska-Quinn et al. (1985) investigated the thermal degradation in nitrogen in terms of heating rate and temperature. They found that the heating rates above 20 Kmin<sup>-1</sup> markedly increased the rate of thermal degradation of the rice straw and its components and also lowered the initial degradation temperature. Boateng et al. (1990) reported their results on the devolatilization of rice hulls by TGA: the devolatilization started at about 190°C and terminated at approximately 530°C. The temperature at which maximum devolatilization began and ended was affected by the heating rate.

Kaufopanos et al. (1989) have studied the kinetics of the pyrolysis of biomass and biomass components over a wide range of pyrolysis conditions including isothermal and non-isothermal heating conditions over an operative temperature range from 200 to 700°C and 5 to 80°Cmin<sup>-1</sup> heating rates. They proposed a new model to describe the kinetic rate of the pyrolysis of lignocellulosic materials as



They proposed that first reaction step resulting in the formation of the intermediate is of zero-order and is not associated with any weight loss. The intermediate so formed was supposed to undergo decomposition through two competitive pyrolysis reactions. They assumed that the three reactions follow the Arrhenius law for the temperature dependence of specific reaction rate. They reported the applicability of their model with sufficient accuracy to fit the experimental data on reaction rate and char yield. They reported that the biomass pyrolysis can be analysed by considering the biomass as the sum of its main components : cellulose, hemicellulose and lignin. It was found that the pyrolysis phenomenon for particles less than 1 mm in diameter is kinetically controlled.

Bilbao et al. (1990) have studied the kinetics of weight loss in the thermal decomposition of Pinaster pine and barley straw in a nitrogen environment. They conducted thermal degradation experiments under isothermal (200-350°C) and dynamic non-isothermal (1.5-80°C min<sup>-1</sup> heating rates) conditions. They analysed their experimental data assuring a single, irreversible, first order decomposition reaction. They found out the rate constant for each temperature and heating rate. They observed that for a given temperature of the system, an increase in the heating rate gives rise to an increase in the kinetic constant obtained, mainly at low temperatures. This was also the observation with xylan and lignin, but contrary to what was obtained with cellulose. For Pinaster pine they reported the following values for kinetic constants (n=1)

$$T < 290^{\circ}\text{C} : k_{1,5} = 0.017 \text{ min}^{-1}$$

$$290 < T < 325^{\circ}\text{C} : k_{1,5} = 3.61 \times 10^4 \text{ min}^{-1} ; E = - 68.85 \text{ KJ mol}^{-1}$$

$$>> 325^{\circ}\text{C} : k_{1,5} = 9.96 \times 10^{17} \text{ min}^{-1} ; E = - 222.1 \text{ KJmol}^{-1}$$

where  $k_{1.5}$  is the pre-exponential factor for Arrhenius equation at heating rate of  $1.5^\circ\text{C min}^{-1}$ . The rate of degradation at any heating rate is obtained as :

$$\left(\frac{dx_s}{dt}\right)_\beta = k_{1.5} (A_s - x_s) + \alpha (\beta - 1.5) \quad (2.3.2)$$

Where  $\beta =$  heating rate,  $^\circ\text{C min}^{-1}$

$x_s =$  conversion,  $A_s$  is the pyrolysable fraction, and,

$\alpha =$  a constant over a given temperature range.

For  $T < 290^\circ\text{C}$ ,  $\alpha = 0.017^\circ\text{C min}^{-1}$

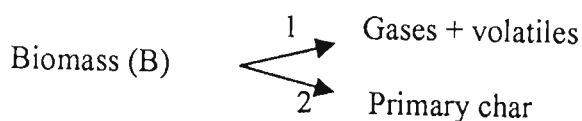
$T < 290^\circ\text{C}$ ,  $\alpha = 0.0043^\circ\text{C min}^{-1}$

$\beta > 5^\circ\text{C min}^{-1}$

Bilbao et al. have found good agreement between experimentally obtained degradation rate and theoretically predicted values.

Williams and Besler (1993) pyrolysed rice husk in a thermogravimetric analyzer and static batch reactor in nitrogen atmosphere to determine the effect of temperature and heating rate on their devolatilization. They used heating rates from  $5$  to  $80\text{Kmin}^{-1}$  and temperatures up to  $700^\circ\text{C}$ . They found two main areas of weight loss and a lateral shift in the thermograms with the increase in heating rates. They found that the thermograms of the major components of the rice husks – hemi cellulose, lignin and two forms of cellulose – could be directly correlated with the devolatilization of the rice husks. The static batch reactor pyrolysis under identical conditions to the TGA showed the evolution of  $\text{CO}$ ,  $\text{CO}_2$  and  $\text{H}_2\text{O}$  at lower temperatures, and lower concentrations of  $\text{CO}$ ,  $\text{CO}_2$ ,  $\text{H}_2\text{O}$ ,  $\text{H}_2$ ,  $\text{CH}_4$ ,  $\text{C}_2\text{H}_6$  and oil at higher temperatures.

Ahuja et al. (1996) proposed a primary reaction kinetic model for the pyrolysis of small particles of wood as,



They assumed that the two reactions follow the Arrhenius law. They studied these primary reactions in small particles through TGA and isothermal heating. They assumed the same order of reaction for the two competing reactions. Using TGA data, they showed the order of reaction is 1.1 and the values for the activation energies for both reactions varied between 86-93 kJmol<sup>-1</sup> for both acacia wood and eucalyptus wood. Using the primary reaction kinetics of small particles they proposed a chain growth model for heterogeneous secondary reactions for the pyrolysis of large wood particles and the parameters determined by non linear optimization. The model takes both the volatile retention time and cracking and repolymerization reactions of the vapours with the decomposing solid as well as auto catalysis into consideration. The extent of the secondary reactions is strongly influenced by the time and the ratio of the auto catalytic (propagation) reaction rate to non catalytic (initiation reaction rate). The reaction at any point in the particle is governed by the temperature at that point and consists of primary and heterogeneous secondary reactions.

Ahuja et al. (1997) studied the kinetics of biomass and sewage sludge pyrolysis using TGA and a sealed reactor. They used a competitive model consisting of weight loss and char formation reactions to simulate the experimental curves obtained by TGA. They used three heating rates, viz. 10, 20 and 40 Kmin<sup>-1</sup> for acacia wood, bagasse, rice husk and sewage sludge. Their results showed that the activation energies for weight loss and char forming steps were comparable implying that both the reactions were competitive in nature. The activation energies for all the biomass materials showed an increase with increasing heating rate. Rice husk and sewage sludge yielded higher amounts of char on moisture-and ash-free basis in a sealed reactor as compared to acacia and bagasse due to the catalytic effect of the inorganics present in higher amounts in these samples.

Jain et al. (1997a,b, 1999) carried out thermal analysis of paddy husk and cellulose using TGA and used a two stage model to correlate the data. They found that

the order of reaction of 1 may be assumed for the entire range of temperature, although an order of reaction 1.5 in the low temperature stage, and 2.0 at high temperature stage seemed to be most appropriate.

Teng et al. (1997) reported the pyrolysis of rice hulls in a TG Analyzer from room temperature to 900°C at heating rates of 10, 20, 60 and 100 Kmin<sup>-1</sup>. The global mass loss during rice hull pyrolysis was modeled by a combination of the volatile evolution of four independent parallel lumps- one for moisture and the other three for non-moisture volatiles. The decomposition of each lump was characterized by a single first-order reaction with respect to the amount of volatiles yet to evolve. The moisture lump evolved mainly at low temperatures with activation energy of 48 kJmol<sup>-1</sup>. The activation energies of the other three lumps, attributed to the decompositions of hemicellulose, cellulose and lignin, were found to be 154, 200 and 33 kJmol<sup>-1</sup>, respectively. The model used was that of Antal and Varhegyi (1995). Excellent agreement between the experimental data and the model predictions were shown.

Sharma and Rajeshwar Rao (1999) studied the pyrolysis of rice husk in both grain and powder form in nitrogen and CO<sub>2</sub> (only for rice husk samples) atmospheres at heating rates of 5, 10, 25, 50 and 100 Kmin<sup>-1</sup>, using TG analyzer. Isothermal studies were carried out for rice husk samples in nitrogen atmospheres at temperatures of 250, 275, 300, 350, 400, 450 and 500°C using a microbalance. They reported two distinct zones with a transition at 350°C, with reaction orders of 1.5 in the lower temperature zone and 2.0 in the higher temperature zone. The results obtained from non-isothermal and isothermal studies were found to be consistent. Using the generalized rate equation proposed by Gaur and Reed (1994), they presented a method to predict the pyrolysis rates at any heating rate condition.

Jain et al. (1999) reported the physical characteristics, proximate analysis, elemental analysis, chemical analysis and thermal decomposition of paddy husk. TG data were obtained under air and oxygen (5%) – nitrogen (95%) atmospheres at heating



rates of 10 and 100 Kmin<sup>-1</sup>. They reported that none of the single stage models reported in literature provide an acceptable correlation of the experimental data; the multistage models similar to the ones proposed by Milosavljevic and Suuberg (1995) were found to be reasonably accurate.

Singamsetti and Rajeshwar Rao (2000) presented experimental results on the pyrolysis of rice husk under both isothermal and non-isothermal heating conditions under nitrogen atmospheres. They found that the reaction order was 2.0 with the activation energy of 53 kJmol<sup>-1</sup>, if the isothermal data were used. With non- isothermal data , they reported two distinct temperature zones as reported earlier by Sharma and Rajeshwar Rao (1999). A second order reaction was found to give the best fit with the experimental data. The activation energy values were found to be in the range of 75-110 kJmol<sup>-1</sup> in the lower temperature range and 6-30 kJmol<sup>-1</sup> in the higher temperature range. This suggests that the reaction is chemically controlled in the lower temperature zone, and diffusion controlled in the higher temperature zone.

Katyal and Iyer (2000) and Katyal (2001) conducted thermal decomposition studies on pigeon pea stalk using TG analyzer and a pilot-plant-scale equipment. They reported that this biomass material could be effectively utilized either after pyrolysis or after partial pyrolysis by thermal gasification of reactive char to generate producer gas. Using TGA data, Katyal (2001) found that the initial and final temperature of active pyrolysis significantly affected the kinetic models.

#### **2.4 DETERMINATION OF KINETIC PARAMETERS DURING PYROLYSIS**

A number of models have been propounded by different researchers to explain thermal degradation kinetics and to determine kinetic parameters for biomass materials using thermogravimetric data. Most of the models have either been adopted or extended from the models developed for coal, polymers, and/or for cellulose. The chemistry of the biomass devolatilization and gasification is not well understood. Fluid dynamical

and reaction complexities add to the woes of the researchers, whereas mechanistic and theoretical approach may lead to too involved and complex expressions. Oversimplified approaches could lead to erroneous results. Anthony (1974) observed that the simple first-order reaction model led some research workers to incorrectly reject chemical reaction as the rate-limiting step in the devolatilization of pulverized coal. This is primarily due to low activation energies resulting from a single step parameter estimation (Berkowitz, 1960).

Most of the researchers have used simple, single step, single irreversible reactions to explain thermal degradation of biomass and to determine the kinetic parameters using TG trace. For single reaction mechanism, either integral and/or differential approach has been used. Integral approach is easier and gives more accurate results than the differential approach, although the processing of TG data may become more difficult. In single reaction models, first-order or n-order reaction kinetics has been tested. In multi-reaction models, several consecutive and/or series reactions are proposed. The reaction rate expressions are then solved and used in conjunction with differential method or the integral method to determine the rate constants.

#### 2.4.1 Single Reaction Models

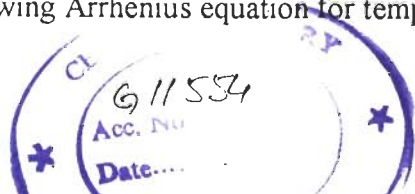
For a single step pyrolysis of solid biomass, a typical irreversible reaction of the type :



can be assumed to be valid. For this reaction, the decomposition of the solid can be represented by a general rate expression as,

$$\frac{dx}{dt} = kf(x) \quad (2.4.2)$$

where  $x$  is the fraction of  $A$  decomposed at time,  $t$  and  $f(x)$  is a function of  $x$  depending on the reaction mechanism, and  $k$  is the specific reaction rate constant following Arrhenius equation for temperature dependence as,



$$k = k_o \exp(-E/RT) \quad (2.4.3)$$

where  $k_o$  is the preexponential or frequency factor,  $E$  is the activation energy,  $R$  is the universal gas constant and  $T$  is the absolute temperature.  $x$  is normally obtained from TG trace as  $x = (W_o - W)/(W_o - W_f)$  where  $W_o$  is the initial weight of the solid,  $W$  is the solid weight at time  $t$  and  $W$  tends to  $W_f$  as  $t$  approaches infinity. Since in non-isothermal TGA, a linear constant heating rate, say  $\beta$   $Ks^{-1}$ , i.e.

$$\beta = \frac{dT}{dt}$$

is imposed, Eq. (2.4.2) can be written as

$$\frac{dx}{dT} = \frac{k_o}{\beta} \exp(-E/RT) f(x) \quad (2.4.4)$$

#### 2.4.1.1 Integral Method

Eq. 2.4.4 can be integrated between the initial (ambient) temperature  $T_o$  and any final temperature  $T$  and conversion between  $0$  and  $x$ , respectively, i.e.

$$\int_0^x \frac{dx}{f(x)} = \frac{k_o}{\beta} \int_{T_o}^T \exp(-E/RT) dT \quad (2.4.5)$$

For simple reactions,  $f(x) = (1-x)^n$ . Left hand side (LHS) of the above equation can be integrated depending upon the order of the reaction; the right hand side (RHS) integrand is not solvable analytically.

The L.H.S. integrand of Eq. (2.4.5) can be written as

$$\int \frac{dx}{f(x)} = \left( \frac{1 - (1-x)^{1-n}}{1-n} \right) ; n \neq 1 \quad (2.4.6)$$

$$\text{and} \quad = \left( \frac{1}{1-x} \right) ; n = 1 \quad (2.4.7)$$

Since the TG trace gives the relationship between weight loss (or  $x$ ) and  $T$ , this relationship is used to integrate Eq. (2.4.5) for determining the values of  $k_o$ ,  $E$  and the order of the reaction. In practice,  $f(x)$  is first determined by assuming the value of  $n$

and from its change with temperature; E and  $k_0$  are calculated so as to satisfy Equation (2.4.5). Several approximate integrations have been proposed in literature (Coats and Redfern, 1964, Piloyan and Novikova, 1967, Gorbachev, 1975. Lee and Beck, 1984, Li, 1985, Agarwal and Sivasubramanian, 1987). Chen and Nuttal (1979) rearranged the approximations of Gorbachev (1975). Some of these approximations and those using the maximum rate of conversion  $(dx/dT)_m$  at temperature  $T_m$  and that using two TG curves (Reich, 1965) have been given by Nishizaki (1980). These and other equations are summarized in Table 2.4.1.

**Table 2.4.1 : Integral Method Equations for Determining Kinetic Parameters, for Single, Irreversible Reaction, using Thermogravimetric Data**

Investigators	Equations
Van Krevelen et al. (1951)	$\ln \left( \frac{1 - (1-x)^n}{1-n} \right) = \ln \left[ \frac{k_0 R}{\beta E} \left( \frac{0.368}{T_m} \right) \right]^{E/RT_m} (T_{m+1}); n \neq 1$ $\ln [\ln x] = \frac{E}{R(T_{m+1})} \ln T ; n = 1 \quad (2.4.8)$ <p><math>T_m</math> = temperature at maximum conversion rate, i.e.</p> $\left( \frac{dx}{dT} \right)_m = (1-x_m) E / RT_m^2$
Horowitz and Metzger (1963)	$\ln \left\{ \ln \left( \frac{1 - (1-x)^{1-n}}{1-n} \right) \right\} = \frac{E\theta}{RT_m^2}; n \neq 1 \quad (2.4.9)$ $\ln(-\ln(1-x)) = \frac{E\theta}{RT_m^2}; n = 1$ <p><math>\theta = T - T_m</math>;</p> <p><math>T_m</math> = Temperature at <math>x = \frac{1}{e} = 0.368</math></p>
Reich and Levi (1963)	$\ln f(x) = -\frac{E}{RT} + \ln(k_0 \Delta T)$ $f(x) = -\ln(1-x) ; n = 1 \quad (2.4.10)$ $= x ; n = 0$ <p><math>\Delta T</math> = Temperature intervals for reading of x</p>

Investigators	Equations
Reich (1965)	$E = 4.6 \log \frac{(\beta_2 - \beta_1) \left( \frac{T_1}{T_2} \right)^2}{\left( \frac{1}{T_1} - \frac{1}{T_2} \right)} \quad (2.4.11)$
Ozawa (1965)	$-\log \beta_1 - 0.457 \frac{E}{RT_1} = -\log \beta_2 - 0.457 \left( \frac{E}{RT_2} \right)$ $\log(x^{1-n} - 1) = \log \beta; n \neq 1 \quad (2.4.12)$ $\log(nx) = \log \beta; n = 1$
Coats and Redfern (1964)	$F(x) = \ln \left\{ \frac{k_o R}{\beta E} \left( 1 - \frac{2RT}{E} \right) \right\} - \frac{E}{RT} \quad (2.4.13)$
Piloyan and Novikova (1967)	$F(x) = \ln \frac{k_o R}{\beta E} - \frac{E}{RT}; 0.05 < x < 0.5 \quad (2.4.14)$
Akita and Kase (1967) Skala, (1987) Williams (1985)	$\ln \left( \frac{\beta}{T_m^2} \right) = \ln \left( \frac{Rk_o}{E} \right) - \frac{E}{RT_m} \quad (2.4.15)$ $\left( \frac{dx}{dt} \right)_m = (1 - x_m) \frac{E}{RT_m^2}$
Gorbachev (1975)	$F(x) = \ln \frac{k_o R}{\beta E} \left( \frac{1}{1 + 2RT/E} \right) - \frac{E}{RT} \quad (2.4.16)$
Reich and Stivala (1978, 1980, 1982)	$\ln \left[ \frac{1 - (1 - x_i)^{1-n}}{1 - (1 - x_{i+1})^{1+n}} \right] \left( \frac{T_{i+1}}{T_i} \right)^2 = -\frac{E}{R} \left( \frac{1}{T_i} - \frac{1}{T_{i+1}} \right) \quad (2.4.17)$
Lee and Beck (1984)	$F(x) = \ln \left\{ \frac{k_o R}{\beta E} \left( \frac{1}{1 + 2RT/E} \right) \right\} - \frac{E}{RT}; 40 < E < 250 \text{ kJ/mol}$ $300 < T < 1000 \text{ K} \quad (2.4.18)$
Li (1985)	$F(x) = \ln \left\{ \frac{k_o R}{\beta E} \left( \frac{1 - 2(RT/E)}{1 - 6(RT/E)} \right) \right\} - \frac{E}{RT} \quad (2.4.19)$
Agarwal and Sivasubramanian (1987)	$F(x) = \ln \left\{ \frac{k_o R}{\beta E} \left( \frac{1 - 2(RT/E)}{1 - 5(RT/E)} \right) \right\} - \frac{E}{RT}; 40 < E < 250 \text{ kJ/mol}$ $300 < T < 1000 \text{ K} \quad (2.4.20)$
<b>Note:</b>	$F(x) = \ln \left[ \frac{1}{T^2} \int \frac{dx}{f(x)} \right] = \ln \left[ \frac{1}{T^2} \left\{ \frac{1 - (1-x)^{1-n}}{1-n} \right\} \right]; n \neq 1 \quad (2.4.21)$ $= \ln \left[ \frac{1}{T^2} \{-\ln(1-x)\} \right]; n = 1 \quad (2.4.22)$

### 2.4.1.2 Differential Method

The differential method for determining kinetic parameters starts with the Equation (2.4.2). In weight terms, the equation is rewritten as,

$$-\frac{dw}{dt} = k(w - w_f)^n \quad (2.4.23)$$

and which together with Eqs. (2.4.3) and (2.4.4), is transformed for pseudo-first order reaction as,

$$\left( -\frac{1}{(w - w_f)} \frac{dw}{dT} \right) = \frac{k_o}{\beta} \exp\left(\frac{-E}{RT}\right) \quad (2.4.24)$$

at any constant heating rate,  $\beta = \frac{dT}{dt}$

Taking log of both sides of Eq. (2.4.24) one gets

$$\ln\left( -\frac{1}{(w - w_f)} \frac{dw}{dT} \right) = \ln \frac{k_o}{\beta} - \frac{E}{RT} \quad (2.4.25)$$

In terms of time, Eq. (2.4.26) is written as,

$$\ln\left( -\frac{1}{(w - w_f)} \frac{dw}{dt} \right) = \ln k_o - \frac{E}{RT} \quad (2.4.26)$$

This is the equation proposed by Tang (1967).

For  $n^{\text{th}}$  order reaction, Eq. (2.4.24) may be transformed as,

$$-\left[ \frac{1}{(w_o - w_f)^n} \frac{dw}{dt} \right] = k_o \exp(-E/RT) \quad (2.4.27)$$

Taking log of both sides, one gets

$$-n \ln (w_o - w_f) + \ln \left( -\frac{dw}{dt} \right) = \ln k_o - \frac{E}{RT} \quad (2.4.28)$$

Differentiating Eq. (2.4.28) with respect to T, one gets

$$\frac{d}{dT} \ln \left( -\frac{dw}{dt} \right) - \frac{d}{dT} \{n \ln (w_o - w_f)\} = + \frac{E}{RT^2}$$

$$\text{or } \frac{E}{RT^2} dT = d \ln \left( -\frac{dw}{dt} \right) - n d \{ \ln(w_o - w_f) \} \quad (2.4.29)$$

In small incremental form, Eq. (2.4.29) may be written as,

$$-\frac{E}{R} \Delta \left( \frac{1}{T} \right) = \Delta \ln \left( -\frac{dw}{dt} \right) - n \Delta \{ \ln(w_o - w_f) \}$$

$$\text{Or } + \frac{E}{R} \frac{\Delta(1/T)}{\Delta \ln(w_o - w_f)} = - \frac{\Delta \ln(-dw/dt)}{\Delta \ln(w_o - w_f)} + n \quad (2.4.30)$$

This equation can also be written as,

$$\frac{\Delta \ln \left( + \frac{dx}{dt} \right)}{\Delta \ln(1-x)} = - \frac{E}{R} \frac{\Delta(1/T)}{\Delta \ln(1-x)} + n \quad (2.4.31)$$

The plot of  $\frac{\Delta \ln \left( + \frac{dx}{dt} \right)}{\Delta \ln(1-x)}$  against  $\frac{\Delta(1/T)}{\Delta \ln(1-x)}$  gives a straight line with a slope of  $(-E/R)$

and intercept  $n$ . Thus, the activation energy and the order of reaction could be obtained.

This Eq. (2.4.31) was first derived by Freeman and Carroll (1958).

The Equations derived by Kissinger (1957), Friedman (1965) and Chatterjee (1965) are given in Table 2.4.2.

**Table 2.4.2 : Differential Method Equations for Determining Kinetic Parameters  
for Single Irreversible Reaction using Thermogravimetric Data**

Investigators	Equations
Freeman and Carroll (1958)	$\frac{\Delta \log(\beta dx/dT)}{\Delta \log(1-x)} = n - \frac{E}{2.3R} \frac{\Delta(1/T)}{\Delta \log(1-x)} \quad (2.4.31)$ <p>where <math>\Delta</math> = difference value</p>
Kissinger (1957)	$\ln(1-x)_m^{n-1} = 1 + (n-1) \frac{2RT_m}{E}; n \neq 1 \quad (2.4.32)$ $\ln(1-x)_m = \left(1 - \frac{2RT_m}{E}\right); n = 1$ <p>where <math>(1-x)_m</math> is the value at <math>T_m</math> where the conversion rate is maximum;</p> $\frac{d\left(\ln\left(\frac{\beta}{T_m^2}\right)\right)}{d\left(\frac{1}{T_m}\right)} = -E/R \quad (2.4.33)$ $n = 1.26 S^{1/2} \quad (2.4.34)$ <p>where S is the shape index defined as</p> $S = \left(\frac{d^2x}{dt^2}\right)_1 / \left(\frac{d^2x}{dt^2}\right)_2$
Friedman (1965)	$\ln \beta \left(\frac{dx}{dT}\right) = \ln k_0 f(x) - E/RT \quad (2.4.35)$ $f(x) = [1-(1-x)]^n$
Chatterjee (1965)	$\log \left(\frac{-dW}{dt}\right)_1 - \log \left(\frac{-dW}{dt}\right)_2 = n(\log W_1 - \log W_2) \quad (2.4.36)$ <p>Where <math>W_1</math> and <math>W_2</math> are the residual weights at the same temperature of two initial sample weights, respectively</p>
Piloyan et al. (1966)	$\ln \Delta T = C - E/RT; 0.05 < x < 0.8 \quad (2.4.37)$
Tang (1967) & Nassar (1985)	$\ln \left[ -\frac{1}{(W - W_f)} \frac{dW}{dT} \right] = \ln \frac{k_0}{\beta} - \frac{E}{RT}; n = 1 \quad (2.4.38)$



### 2.4.1.3 Maximum Rate Method using DTG and/DTA Data

Kissinger (1957), Piloyan et al. (1966), Akita and Kase (1967) and Teng et al. (1997) have used DTA/DTG data to determine the kinetic parameters for chemical reactions. At the DTG peak, the rate of degradation (chemical reaction) is maximum and this temperature is taken as  $T_m$ . Kissinger defined a shape index,  $S$  to measure the amount of asymmetry in an endothermic differential thermal analysis peak. Using the single reaction model of the type solid – solid gas they manipulated the reaction rate equation to obtain a differential equation :

$$\frac{d\left(\ln\left(\frac{\beta}{T_m^2}\right)\right)}{d\left(\frac{1}{T_m}\right)} = -E/R \quad (2.4.33)$$

where  $T_m$  has been obtained as the peak DTA endothermic temperature at which the rate of reactions is maximum. Eq. (2.4.36) has been shown to be valid regardless of reaction order. Thus the activation energy can be obtained for a simple decomposition reaction regardless of reaction order by making DTA patterns at a number of heating rates,  $\beta$ . Kissinger defined a shape index for the DTA peak as the ratio of the slopes to tangents to the curve at inflection points. The reaction order has been correlated as,

$$n = 1.26 S^{1/2} \quad (2.4.34)$$

Piloyan et al. (1966) proposed a simple method to determine activation energy for thermal decomposition from DTA peak data which obviated the need to have several DTA curves with various heating rates. They proposed that the deviation of temperature in a DTA peak ( $\Delta T$ ) from the base line of DTA curve at any temperature can be related by

$$\ln \Delta T = C - E/RT; 0.05 < x < 0.8 \quad (2.4.37)$$

where  $C$  is a constant. Thus from a single peak the values of  $\Delta T$  at various temperatures can be obtained and plotted on a semi log graph to obtain the value of  $E$  from the slope.

Akita and Kase (1967) used the DTG or differential scanning calorimetry (DSC) data to study the pyrolysis kinetics of materials. For the first order reaction i.e.  $f(x) = (1-x)$ , they manipulated Eq. (2.4.4) by setting the double differential  $d^2 x/dt^2 = 0$  at  $T = T_m$  to yield

$$\left(\frac{dx}{dt}\right)_m = (1 - x_m) E / RT_m^2 \quad (2.4.39)$$

where  $m$  denotes the state of the maximum rate.

Rewriting Eq. (2.4.4) for the maximum rate conditions using first-order kinetics and combining with equation (2.4.39), gives

$$\ln\left(\frac{\beta}{T_m^2}\right) = \ln\left(\frac{Rk_o}{E}\right) - \frac{E}{RT_m} \quad (2.4.40)$$

By plotting  $\ln(\beta/T_m^2)$  versus  $1/T_m$  at different heating rates, a straight line is obtained, and the values of  $E$  and  $k_o$  can be obtained from the slope and intercept, respectively.

#### 2.4.2 Multi Reaction Models

The kinetics of volatile evolution during pyrolyses of solid hydrocarbons, including coal and biomass, have been successfully modelled by several independent parallel reactions of first order with respect to the amount of volatile yet to evolve (Soloman et al., 1988, Suuberg et al., 1979, Antal and Varhegyi, 1995, Teng et al., 1997). Antal and Varhegyi (1995) have suggested that the amounts of cellulose and hemi-cellulose present in a biomass sample could be quantitatively determined from TG data combined with a kinetic analysis.

Ramiah (1970) studied the thermal degradation of cellulose, hemi cellulose and lignin between room temperature and 600°C using TGA and DTA. He performed static and dynamic TGA and found that the activation energy,  $E$  for thermal degradation for different cellulosic, hemicellulosic, and lignin samples was in the range 150-250, 62-108, and 54-79 kJmol<sup>-1</sup>, respectively. DTA showed an endothermic tendency around

100°C in a flowing nitrogen and stationary air atmosphere. This endothermic behaviour was found to be absent in flowing oxygen atmosphere. The nature of DTA curves was dependent on the source of the samples and the presence of non-cellulosic impurities. While the presence of flowing oxygen made the degradation process occurring via two sharp exothermic processes, the thermal degradation, in the presence of flowing nitrogen and stationary air, occurred via a sharp endothermic (at 320°C) and a sharp exothermic (at 360°C) processes.

#### 2.4.2.1 Distributed Activation Energy Model (DAEM)

Pitt (1962) assumed that a large number of independent irreversible, parallel reactions occur during the devolatilization of coal. He assumed that each of these parallel reactions to be of first –order with respect to the unvolatilized material. Thus, for the  $i^{\text{th}}$  reaction,

$$\frac{dm_i}{dt} = k_i (m_i^* - m_i) \quad (2.4.41)$$

where  $m_i$  is the volatile matter resulting from the  $i^{\text{th}}$  reaction and  $k_i$  is the rate constant. Using the Arrhenius equation,

$$k_i = k_{o,i} \exp\left(\frac{-E_i}{RT}\right) \quad (2.4.42)$$

Pitt assumed that  $k_{o,i}$ , the pre-exponential factor, was the same for all the reactions, and that the activation energy  $E_i$  could be expressed as the continuous distribution function,  $f(E)$ .  $V_i^*$ , the potential volatile loss from the  $i^{\text{th}}$  reaction was given as the incremental value of the potential total volatile loss, as

$$V_i^* = dv^* = V^* f(E) dE \quad (2.4.43)$$

$$\text{where } \int_0^{\infty} f(E) dE = 1$$

With the above simplifying assumptions, the integration of the Eq. (2.4.41) gives,

$$\frac{W - W_f}{W_o - W_f} = \frac{V^* - V}{V^*} = \int_0^\infty \exp\left\{\int_0^t k_o \exp\left(\frac{-E}{RT}\right) dt\right\} f(E) dE \quad (2.4.44)$$

For isothermal conditions, Pitt constructed an  $f(E)$  curve which best represented his data by assuming the term  $\exp[k_o t \exp(-E/RT)]$  as a step function which was zero for  $E < RT \ln(k_o t)$  and unity for  $E \geq RT \ln(k_o t)$ .

For non-isothermal condition, Anthony et al. (1974) assumed that the function  $f(E)$  could be represented by a Gaussian distribution with a mean activation energy,  $E_{av}$  and a standard deviation,  $\sigma$ , i.e.

$$f(E) = \frac{1}{\sqrt{2\pi}\sigma} \exp\left[-\frac{(E - E_{av})^2}{2\sigma^2}\right] \quad (2.4.45)$$

Using a value of  $k_o = 1.67 \times 10^{13} \text{ s}^{-1}$  given by Bensen (1968) using transition state theory and the experimental value of  $V^*$ , they showed that the number of parameters needed to characterize the devolatilization curve could be reduced to two with little effect on the validity of the model with the experimental data.

Suuberg (1979) used the assumptions of Pitt (1962) and Anthony et al. (1974) and gave the nonisothermal weight loss of a coal particle as,

$$1 - x = \frac{1}{g\sqrt{\pi}} \int_{-\infty}^{\infty} \exp\left[-\frac{A}{Z} \exp(-Z)\right] \exp\left[-\left(\frac{Z - Z_o}{g}\right)^2\right] dz \quad (2.4.46)$$

and

$$g = \sigma \sqrt{2\pi / RT}, \quad Z = E / RT, \quad Z_o = E_o / RT, \quad A = \frac{k_o T}{a} \quad (2.4.47)$$

Where  $E_o$  = mean activation energy, and

$\sigma$  = Standard deviation.

Using approximations, he showed that the Eq. (2.4.46) reduces to

$$1 - x = \frac{1}{\sqrt{\pi}} \int_{-\infty}^{\infty} \exp(-y^2) dy \quad (2.4.48)$$

$$= \frac{1}{2} \text{erfc}(y) \quad (2.4.49)$$

where  $y = (z-z_0)/g$ , and

$$Y_c = (Z_c - Z_0)/g$$

$Z_c$  is estimated from

$$\frac{A}{Z_c} \exp(Z_c) = 0.5 \quad (2.4.50)$$

For a range of values of  $A$ ,  $Z_0$  and  $g$ , Eq. (2.4.47) was found to give an error of <5% in comparison to Eq. (2.4.39).

#### 2.4.2.2 Individual Volatile Product Model (IVPM)

This model uses multiple independent parallel first order reactions to describe the evolution of volatile products. Several researchers (Suuberg et al., 1979; Solomon et al., 1988; Antal and Varhegyi, 1995, and Teng et al., 1997) have shown this model to be applicable to pyrolysis of solid hydrocarbons, including coal and biomass. Teng et al. (1997) have shown that the pyrolysis of rice hull can be modelled as a combination of volatile evolution of four independent parallel lumps: one for moisture and the other three for non-moisture volatiles. The volatile evolutions were determined by the resolution of individual DTG peas. For each lump of volatile evolution, they used the Eq. (2.4.40) proposed by Akita and Kase (1967). They reported excellent agreement between the experimental data and model predictions.

#### 2.4.2.3 Functional Group Model (FGM)

This model proposed by Gavalas et al. (1981) envisioned coal as an ensemble of functional groups organized into tightly bound aromatic ring clusters connected by weaker aliphatic and ether bridges. Using the approximation of Agarwal and Sivasubramanian (1987), the formation of gaseous volatiles and tar upto time  $t$  are found to be:

$$Y_i = Y_{i0} \exp \left\{ -\frac{k_{oi}RT^2}{\beta E_i} \left[ \frac{1 - 2RT/E_i}{1 - 5(RT/E_i)^2} \right] \exp(-E_i/RT) \right\} \quad (2.4.51)$$

$$X_c = X_{io} \exp\left\{-\frac{k_{oc}RT^2}{\beta E_c} \left[\frac{1-2RT/E_c}{1-5(RT/E_c)^2}\right] \exp(-E_c/RT)\right\} \quad (2.4.52)$$

Where  $Y_i$  = fraction of  $i^{\text{th}}$  component, and

$X_\tau$  = fraction of coal forming tar yet to be converted

$\tau$  = tar component

The particle weight retained,  $w$  at any time of the pyrolysis process is described as,

$$w = w_o(1 - X_\tau) \sum_{i=1}^N Y_i + w_o X_\tau \sum_{i=1}^N Y_i \quad (2.4.53)$$

and the total weight loss is, therefore,  $(w_o - w)$  at any time  $t$ .

## 2.5 STUDIES ON FLUIDIZED BED GASIFICATION OF BIOMASS

### 2.5.1 Air Gasification

Raman et al. (1980) conducted gasification studies with dried feedlot manure as feedstock in a 229 mm inside diameter fluidized bed reactor. The reactor had a free board of 410 mm inside diameter. A burner with a duty of  $47.5 \text{ MJhr}^{-1}$  located at the bottom of the reactor (Plenum) generated the gas for fluidization, by the combustion of propane under starving air conditions. Supplementary heat (as needed) for operation was transferred across the walls of a radiant jacket surrounding the reactor. A burner with a duty of  $105.5 \text{ MJhr}^{-1}$  supplied heat to the jacket using natural gas as the fuel. Sand was used as the inert bed material. The objective of the study was to assess the effects of parameters namely superficial gas velocity, feed size fraction and the reactor temperature. These were studied with reference to the product gas composition, higher heating value of the product gas, and the product gas volumetric yield. Considerable scatter was observed in the gas yield with different batches of feed for a given operating condition and was attributed to the difference in the segregation phenomena between batches of feed. The superficial gas velocity and the gas residence time did not appear to have a significant influence on the gas composition and heating value for a given feed size fraction and a given gasification temperature. However the feed size

fraction had an influence on the composition, heating value and yield of the product gas. The yield of product gas increased and the maximum in the heating value curve (in the plot of temperature v/s heating value) shifted to the left as the size fraction became smaller. The gas yield and the energy recovery increased with increase in the reactor temperature. The concentrations of hydrogen and methane increased whereas the concentrations of carbon dioxide, carbon monoxide decreased with increase in temperature. The results obtained agreed approximately with those predicted by the thermochemical calculations as well as obtained experimentally for municipal waste by other investigators.

Sakoda et al. (1981) conducted experiments to explore the possibility of a gasification process for biomass material by use of a high temperature fluidized bed. Luann chips (a wood material from a tropical area) and peanut shells (agricultural waste) were used as feed materials. Gasification of these materials was carried out in a fluidized bed in the temperature range 400-1000°C. The feasibility of a process to gasify these materials was discussed based on the experimental results. It was observed that the yield of the product gas from the high temperature carbonization of biomass material reached 87%, even when steam was not used for the reaction. The maximum heating value of the gas produced by means of the heat carrier method was 3870 kcalNm<sup>-3</sup> when the gasification temperature was about 900°C.

Flanigan et al. (1982) conducted experimental tests on a 150 mm inside diameter and 1980 mm high-fluidized bed gasifier. Sawdust was fed into the reactor from a location near the top of the reactor. Electric strip heaters heated the reactor externally. It was found that temperature was the important single parameter. Once sufficient thermal energy was made available for gasification, residence time became the dominating parameter. It was concluded that, the residence time should be varied to optimize the gasification process.

Cherian et al. (1983) conducted gasification studies on a fluidized bed gasifier. A variety of feedstock was gasified in a 150 mm internal diameter and 1950 mm long fluidized bed reactor. The experimental results obtained were analyzed to determine the effects of different parameters such as air-fuel ratio, gas-fuel ratio and bed temperature on the energy content of the gas and the thermal efficiency of the process. The fuels used were charcoal, elm, lignite, manure, peat, oak sawdust with and without catalyst and straw. The gas yield was of the low-Btu type, the best values obtained ranged from approximately  $4.85 \text{ MJNm}^{-3}$  (130 Btu/scf) to  $7.46 \text{ MJNm}^{-3}$  (200 Btu/scf). For all these yields it was noted that nitrogen made up over 50% of the volume.

Xu et al. (1985) conducted basic experiments elucidating thermochemical and fluidization characteristics of rice hulls. A fluidized bed gasifier was constructed and tested utilizing ground rice hulls as feed material. The size of the gasifier was 150 mm in diameter and 2400 mm high. The products gas the char, and tar production rate and the exit gas composition were measured at various bed temperatures; rice hull feed rates and air velocity. The optimum operating conditions were obtained with reaction temperatures of  $704^{\circ}\text{C}$  to  $815^{\circ}\text{C}$ , an air to feed ratio of 0.747 to  $0.871 \text{ Nm}^3\text{kg}^{-1}$  of rice hulls, a rice hull feed rate 13.6 to  $18.2 \text{ kgh}^{-1}$  and a superficial air velocity of  $0.61$  to  $0.76 \text{ ms}^{-1}$ . The carbon conversion was as high as 75 percent. The heating value of the product gas varied between  $4.476$  and  $7.46 \text{ MJNm}^{-3}$ .

Schoeters et al. (1989) conducted experimental studies on fluidized bed gasification of biomass using a bench scale reactor. The lower section of the reactor was of 150 mm inside diameter while the upper (free board) section was of 300 mm inside diameter. The total reactor height was 1000 mm. The unit was externally heated with two electric heating blankets (2 kW each) one for the bed and the other for the free board section. A perforated plate distributor was used. The effect of the major process variables, such as air factor, volumetric throughput, steam and oxygen addition and feedstock properties on the gasifier performance were investigated. The experiments



revealed that the major parameter for the proper functioning of a fluidized bed gasifier was the control of the free board temperature. A high free board temperature resulted in higher reaction rates and a shift in the equilibrium value of some gasification reactions, e.g. the homogeneous water gas shift reaction. As the free board temperature increased, the higher heating value of produced gas decreased. The air factor, defined as the ratio of the amount of oxygen added to the amount of oxygen necessary for the stoichiometric combustion, affected the higher heating value of the gas, gas yield and thermal efficiency. Above an air factor of 0.4, the higher heating value of the gas decreased, while the gas yield increased with increase in air factor. The thermal efficiency showed a maximum value for air factor between values 0.3 and 0.6.

Jiang and Morey (1992) studied self-sustained air gasification of corncobs using a gasifier-combustor system to provide data for validating their numerical gasifier model. The gasifier was made from 3.2 mm thick stainless steel sheet and was 1270 mm high from the distributor plate to the top. There was an air plenum under the air distributor, which was connected to a start up combustor. The start up combustor provided necessary start up heat through propane + air combustion and once the self sustained corncob gasification was attained, the propane was shut off. Experiments were conducted operating the gasifier at two bed temperature values, viz. 647 and 747°C (low and high). The performance of the gasifier was analyzed using the gas samples. Tar sampling and analysis could not be conducted because of the difficulty in sampling. It was observed that at the low bed temperature, the chemical energy content (LHV) of the producer gas, the energy yield per unit area of bed cross section, utilization of reactor volume as the fluidized bed and the gas residence time in the bed are high. The fuel feed rate, discharge rate of unburned particles and ash, collected in the stack were also high. Further, at high bed temperature, the chemical energy content (LHV) of the producer gas, the energy yield per unit area of bed cross section, utilization of reactor volume as the fluidized bed and gas residence time in the bed were low. The fuel feed rate, discharge rate of unburned particles, ash, tar yield and

particulate emission collected in the stack were also low. The mass energy conversion from solid fuel to producer gas and sensible heat output rate in the stack were high.

Sanchez and Lora (1994) have reported the research on the fluidized bed gasification of biomass carried out in the State University of Campinas. They have conducted experiments to investigate the influence of the air factor on bed temperature, gas calorific value, and reactor efficiency. Gasification experiments were conducted in a 200 mm inside diameter, 2000 mm high reactor that was continuously fed using a screw conveyor. A multiorifice type distributor plate was used at the bottom of the reactor to distribute air. The bed temperature was maintained between 600°C-800°C for the gasification of rice husk, bagasse, sawdust and spent coffee seeds. It was found that the air factor, which is the stoichiometric air volume fraction for a unit kilogram of biomass, was the main parameter in gasifier operation. It was concluded that the range of air factor for good operation of a gasifier was 0.2 to 0.4.

Narvaez et al. (1996) experimentally studied the biomass gasification with air in a bubbling fluidized bed of small pilot plant. The operational variables studied included equivalence ratio (from 0.2 to 0.45), bed temperature (750-850°C) and free board temperature (500-600°C), H/C ratio in the feed, use of secondary air (10% of the overall) in the free board and addition (2-5 wt%) of calcined dolomite mixed with the biomass used as the feedstock. Using the tar and gas sampling and analysis methods, the gas composition and tar content in the gas were determined and their variation with the operational parameters were presented. Results indicated that the equivalence ratio (ER) was the most important factor in the biomass gasification with air. It dictated the temperatures of bed and free board, the tar content and composition of gas of the fuel gas. On increasing the ER from 0.2 to 0.45, the heating value decreased by about 2 MJNm<sup>-3</sup> and simultaneously tar content decreased by about 50 wt%. It was noted that increasing the H/C ratio from 1.6 to 2.2, the tar decreased by about 75 wt% while the heating value of the gas increased by about 1 MJNm<sup>-3</sup>. However it was concluded that getting tar contents in the raw gas below 1.0 – 2.0 gNm<sup>-3</sup> was perhaps not possible and

use of secondary cleaning (hot, catalytic bed etc.) was necessary for the elimination of tar below such levels.

Some of the main observations and important results of published works on gasification of biomass with air are presented in the Table 2.5.1. The reactor constructional details and operational conditions used in these studies are summarized in Table 2.5.2.

### 2.5.2 Steam Gasification

In a study of steam gasification of grain dust, Hoveland et al. (1982) found 90% of the gas to be composed of H<sub>2</sub>, CO<sub>2</sub>, and CO with the remaining 10% consisting of CH<sub>4</sub>, C<sub>2</sub>H<sub>4</sub>, and C<sub>2</sub>H<sub>6</sub>. The energy recovery increased linearly from 8 to 55% over a temperature range of 594-760°C.

Van den Aarsen (1982) studied the gasification of beech wood in a pilot-scale fluidized bed and increased the produced gas heating value by injecting steam into the free board zone, taking advantage of the water-gas shift reaction.

Walawender and Clark (1984) studied the fluidized bed gasification of various crop residues. The principal goal of their work was to examine the technical feasibility of a farm-scale gasification system capable of producing an alternative fuel for irrigation pumping and grain drying. A pilot-scale fluidized bed gasifier was used to obtain material balance data and to provide fuel for engine testing with corn stover, sorghum stover and wheat straw. The gasifier performance data for all the three feedstocks exhibited similar trends as functions of temperature; nevertheless, statistically, no significant differences were detected in the produced gas characteristics

Walawender et al. (1985b), steam-gasified  $\alpha$ -cellulose in a bench-scale, fluidized-bed reactor over a temperature range of 600-800°C. The major components of the produced gas were H<sub>2</sub>, CO<sub>2</sub>, CO, and CH<sub>4</sub>; volumetric gas yields of 0.5-1.4 m<sup>3</sup> kg<sup>-1</sup> were observed. The average gas higher heating value was 11.8 MJm<sup>-3</sup>, and the energy recovery as well as the carbon conversion were within the range of 32-90%.

**Table 2.5.1 : Air Gasification of Biomass in Fluidized Beds-Literature Citations**

Investigators (Year)	Biomass	Significant Results	Significant Inferences
Raman et al. (1980)	Feed lot manure	<ul style="list-style-type: none"> <li>• Gas yield and the heating value of the product gas increase with decrease in feed size fraction.</li> <li>• Cellulose content (material make up) of the feed batch appears to be an important parameter.</li> </ul>	<ul style="list-style-type: none"> <li>• The superficial gas velocity and hence the gas residence time did not show a significant influence on the gas composition and its heating value.</li> <li>• As the reactor temperature (Arithmetic mean of bed and free board temperature) increased from 900K to 1000K, the H<sub>2</sub> and CH<sub>4</sub> increased but CO<sub>2</sub> showed a decrease from 40% down to 13%.</li> <li>• The heating value of the gas increased from 12.52 MJNm<sup>-3</sup> to 21.58 MJNm<sup>-3</sup> when the reactor temperature increased from 900 K to 1000 K. The energy recovery increased from 19 to 56% over the temperature range.</li> </ul>
Aarsen van Den et al. (1982)	Rice husk	<ul style="list-style-type: none"> <li>• Temperature control is possible in a fluidized bed reactor.</li> <li>• Inert bed material solves flow problems inside the reactor and also acts as thermal energy fly wheel.</li> <li>• Temperature profile along the height of the reactor indicates an isothermal condition under all circumstances.</li> <li>• Equilibrium conversion of hydrogen, water, carbon dioxide and carbon monoxide is fixed by the homogeneous water gas shift reaction.</li> </ul>	<ul style="list-style-type: none"> <li>• LHV of the gas varied between 4.5 and 6 MJkg<sup>-1</sup>, which makes it suitable to be used as a fuel in internal combustion engines.</li> <li>• Volumetric gas yield increased with temperature but its heating value and concentrations of CO and HC decreased.</li> <li>• Tar content in the product gas decreased with temperature from 6000 mgNm<sup>-3</sup> and 750°C to 800 mgNm<sup>-3</sup> and 940°C. A deeper bed could be used for further reduction of tar.</li> <li>• Carbon conversion efficiency of about 90% and cold gas efficiency of 60 to 67% could be achieved.</li> </ul>
Cherian et al. (1983)	Wood, manure and peat	<ul style="list-style-type: none"> <li>• Tar condensation occurs on cooling the gas, so it is desirable to keep the gas at high temperatures till the point of usage.</li> <li>• Fluidized bed gasifier is suitable for a variety of feedstocks.</li> <li>• Heating value of gas can be enhanced by eliminating N<sub>2</sub> content.</li> </ul>	<ul style="list-style-type: none"> <li>• The yield was of the low-Btu type, the best values obtained ranged from approximately 4.85 to 7.46 MJNm<sup>-3</sup>. Nitrogen was the main component of the gas (over 50% by volume)</li> </ul>

Walawender et al. (1985a)	Corn and sorghum stovers	<ul style="list-style-type: none"> <li>The gas yield, energy recovery and carbon conversion increase with increase in temperature.</li> <li>Increase in temperature decreases the liquid yield.</li> </ul>	<ul style="list-style-type: none"> <li>The compositions of produced gas from the two feedstocks were similar.</li> <li>As the temperature was increased from 730 to 830 K-char yield decreased, CO and CO<sub>2</sub> concentrations decreased increasing H<sub>2</sub> content and produced gas volumetric yield increased from 0.2 to 0.8 m<sup>3</sup> kg<sup>-1</sup>.</li> <li>The HHV of gas attained a maximum of 15.6 MJ m<sup>-3</sup> at 955 K for corn stover and 14.9 MJm<sup>-3</sup> at 960 K for sorghum stover.</li> </ul>
Xu et al. (1985)	Rice husk	<ul style="list-style-type: none"> <li>The bed temperature is controlled by equivalence ratio. It strongly influences the gasification efficiency. Near isothermal conditions can be achieved at different temperatures.</li> <li>Heating value, H<sub>2</sub>/CO ratio and gas yield increase with the temperature.</li> <li>Silica and Potassium oxide in the rice husk ash melt at about 980°C and form a diffusional barrier for further gasification process.</li> <li>Above 900°C, water shift reaction dominates which causes only a shift in H<sub>2</sub> and CO compositions and hence no significant improvement in heating value can be expected.</li> <li>Gasification efficiency exceeds 60%, when the bed temperature is above 700°C.</li> </ul>	<ul style="list-style-type: none"> <li>Sand and ground hull mixture exhibited good fluidization behavior. Sand to husk ratio of 3-7 was found desirable.</li> <li>Superficial velocities of 60 to 75 cms<sup>-1</sup> gave good fluidization and bed expansion.</li> <li>Near maximum efficiency was attained in the temperature range of 700 to 980°C.</li> <li>The gasification rate varied between 2.8 to 4.6 MW<sub>th</sub>m<sup>-2</sup> and the heating value between 5 to 8 MJNm<sup>-3</sup>.</li> <li>The carbon conversion efficiency was found to be 75%.</li> <li>The bed temperature of 700 to 815°C, and equivalence ratio of 0.18 to 0.21, fuel flow rate of 13.6 to 18.2 kghr<sup>-1</sup> and superficial air velocity of 60 to 75 cms<sup>-1</sup> found to be the optimum conditions.</li> </ul>
Flanigan et al (1987)	Rice husk	<ul style="list-style-type: none"> <li>Ground husk has better fluidization quality than whole rice husk, but it requires additional machinery and energy.</li> <li>Gas heating value decreases with temperature beyond 700°C.</li> <li>The rice husk char is only blown out of the bed when it is decreased from its initial size of 5 mm length to 0.4 mm.</li> </ul>	<ul style="list-style-type: none"> <li>For fluidization velocities of 67 to 98 cms<sup>-1</sup> good fluidization quality and bed expansion observed.</li> <li>When the temperature is increased from 500 to 700°C, the heating value of the gas increased from 2.6 to 5.2 MJm<sup>-3</sup>, while the cold gas efficiency and carbon conversion efficiency are increased from 21 to 58% and 55 to 90% respectively.</li> </ul>

		<ul style="list-style-type: none"> <li>• 25 to 30% of the energy content of the rice husk is enough to meet the thermal energy required for gasification in the temperature range of 500 to 700°C</li> <li>• Reaction temperature of rice husk should be controlled below 900°C to avoid ash sintering and agglomeration problems.</li> <li>• Reduction in the gasifier heat loss and recovery of sensible heat from gas can improve the gasifier efficiency to the extent of 10%.</li> </ul>	<ul style="list-style-type: none"> <li>• Thermal energy production rate of 4.4 MWm<sup>-2</sup> has been achieved.</li> <li>• Maximum heating value of the gas was achieved at 700°C.</li> <li>• Surface heat loss from the gasifier was about 10 to 19%.</li> </ul>
Schoeters et al. (1989)	Pine saw dust, Refuse derived fuel	<ul style="list-style-type: none"> <li>• The oxidation reactions occur to a large extent above the sand bed.</li> <li>• Free board temperature is important and a high free board temperature results in higher reaction rates and a shift in the equilibrium value of some gasification reactions.</li> </ul>	<ul style="list-style-type: none"> <li>• The heating value of the gas decreased with increase in the air factor (above 0.4) but the gas yield increased with increase in air factor.</li> <li>• The thermal efficiency was only 50% because of high heat losses and reached maximum air factor between air factor 0.3 to 0.6. At higher values, the thermal efficiency decreased.</li> </ul>
Jiang and Morey. (1992)	Corncobs	<ul style="list-style-type: none"> <li>• Energy yield per unit area is higher for the low temperature runs than that for the high temperature runs, because of lower heating value of the dry producer gas.</li> <li>• Tar measurement is a difficult task because of blockage of sampling lines.</li> <li>• A greater fuel feed rate required at low bed temperature because of the endothermic nature of the self-sustained gasification reactions.</li> </ul>	<ul style="list-style-type: none"> <li>• The sensible heat output rate accounted for 78% of the fuel energy rate at low bed temperature and 91% at high bed temperature</li> </ul>
Hartiniati et al. (1989) and Panaka et al. (1994)	Rice husk	<ul style="list-style-type: none"> <li>• Temperature increase is possible only with higher equivalence ratios, which result in higher gas yield but decreases LHV of gas for the same fuel feed rates.</li> <li>• For a given fuel feed rate, the equivalence ratio is to be increased from 0.30 to 0.48 to increase the gasifier temperature from 721 to 871°C.</li> </ul>	<ul style="list-style-type: none"> <li>• Maximum energy of 12.3 MJ-gas/kg-fuel(daf) was produced at 93 kg h<sup>-1</sup> of fuel feed rate and bed temperature of 785°C. LHV of gas under this condition was 4.1 MJkg<sup>-1</sup>.</li> <li>• Cold gas efficiency varied from 63 to 67%.</li> </ul>

		<ul style="list-style-type: none"> <li>Gas quality varies between 4.1 and 6.3 MJm<sup>-3</sup>, depending upon the bed temperature and equivalence ratio.</li> <li>Concentration of hydrocarbons decreases with increase in gasifier temperature as a result of thermal cracking.</li> </ul>	
Sanchez and Lora (1994)	Rice husk, Saw dust, Sugarcane, bagasse and spent coffee seeds	<ul style="list-style-type: none"> <li>Operation with fine granulometry biomass leads to low efficiency values caused by elutriation.</li> <li>Air factor is the main operational parameter, which defines bed temperature and the reactor efficiency. Common values of the air factor for any gasifier range from 0.2 to 0.4.</li> <li>Low values of efficiency are obtained due to the lack of thermal insulation in the free board zone.</li> <li>Flow constancy and capacity of the feeder to handle fibrous biomass like bagasse are the problems of feeding.</li> </ul>	<ul style="list-style-type: none"> <li>The LHV of the producer gas ranges from 2.7 to 4.3 MJNm<sup>-3</sup>.</li> <li>The cold gas efficiency obtained between 15.5 to 53.9%</li> <li>Gas volume obtained from one Kg of biomass was between 0.8 to 3.1.</li> <li>Volumetric power referred to gas obtained (for 1 m<sup>3</sup> of bed volume) ranged from 1.3 to 2.1 MJm<sup>-3</sup>.</li> </ul>
Narvaez et al. (1996)	Pine saw dust	<ul style="list-style-type: none"> <li>ER is the most important factor in biomass gasification with air, which defines the temperatures of the bed, and of the free board, tar yield and gas composition.</li> <li>H/C ratio is an important factor of quality of raw gas.</li> <li>Feeding near bed bottom is important.</li> </ul>	<ul style="list-style-type: none"> <li>Increase in ER from 0.20 to 0.45, the heating value decreased about 2MJNm<sup>-3</sup> and the tar yield also decreased about 50 wt%.</li> <li>Increasing H/C from 1.6 to 2.2, the tar decreased by about 75 wt% and the heating value increased by about 1 MJNm<sup>-3</sup>.</li> <li>Optimum conditions (Maximum heating value and minimum tar content) are ER around 0.25 –0.30, H/C around 2.2, Bed temperature &gt;800°C, and free board temperature &gt; 600°C.</li> <li>To get raw gas with tar content below 1.0-2.0 gNm<sup>-3</sup> is quite difficult.</li> </ul>
Ergudenler et al (1997)	Wheat straw	<ul style="list-style-type: none"> <li>Equivalence ratio and bed height are important parameters on which bed temperature depends.</li> <li>Effect of fluidization velocity on gas composition is insignificant.</li> </ul>	

Natarajan (1998)	Rice Husk	<ul style="list-style-type: none"> <li>• Rice husk can be gasified in the fluidized bed gasifiers.</li> <li>• The gasification temperature can be easily controlled by adjusting the ER</li> </ul>	<ul style="list-style-type: none"> <li>• Gasification temperature increased from 720 to 950°C when ER was increased from 0.26 to 0.52.</li> <li>• Producer gas of LHV 5 to 5.6 MJNm<sup>-3</sup> was produced in the temperature range of 730 to 840°C</li> <li>• The optimum air flow rate was 1.1 to 1.4 nm<sup>3</sup>kg<sup>-1</sup> of fuel, the average has productivity was 1.5 Nm<sup>3</sup>kg<sup>-1</sup></li> <li>• The maximum thermal power that can be generated by the 150 mm diameter reactor was 2.11 MW<sub>th</sub>m<sup>-2</sup>.</li> <li>• Maximum carbon conversion efficiency was 81.6%.</li> <li>• Cold gas efficiency was more than 60% in the temperature range of 750 to 850°C.</li> <li>• Tar content decreased from 13.4 gNm<sup>-3</sup> to 2.73gNm<sup>-3</sup> when temperature was increased from 700 to 950°C</li> </ul>
Mansaray et al (1999)	Rice husk	<ul style="list-style-type: none"> <li>• The gasifier temperatures increase with increase in fluidization velocity and increase in equivalence ratio.</li> <li>• Tar was not measured because its presence in the gas was insignificant.</li> </ul>	<ul style="list-style-type: none"> <li>• For the fluidization velocities (0.22, 0.28 and 0.33 ms<sup>-1</sup>) and equivalence ratios (0.25, 0.30 and 0.35) the steady state temperature varied from 665 to 830°C.</li> <li>• The ER value of 0.25 appeared to be the optimum with respect to the quality of gas (4% H<sub>2</sub>, 5% hydrocarbons, 15% CO<sub>2</sub>, 20% CO and 57% N<sub>2</sub>).</li> <li>• The higher heating value of gas varied between (3.09 – 5.03 MJ Nm<sup>-3</sup>).</li> <li>• The gas yield and carbon conversion were found to range from 1.30 to 1.98 Nm<sup>3</sup>kg<sup>-1</sup> and 55.0 to 81.0% respectively.</li> </ul>

Note : nm<sup>3</sup> or Nm<sup>-3</sup> indicates the volume or the per volume measured at normal temperature and pressure.



**Table 2.5.2 : Reactor Constructional Details and Operating Conditions in Fluidized Bed Air Gasification of Biomass**

Feeding location	Reactor Constructional Details				Operating Conditions		Reference
	Reactor dia x ht (mm) f.b. dia x ht (mm)	Gas distributor details	Heating arrangement		Temperature Bed Reactor, (°C)	Equivalence ratio	
			Start up	Process			
Top end of reactor	230x 864 410 x 864	Perforated plate 3mm thick made of SS 316, 844 holes of 1.5 mm $\phi$	Propane –air combustion	Radiant jacket surrounding reactor heated by natural gas burner	-x- 527 to 767	0.27 to 0.41	Raman et al. (1980)
Top end of reactor	37 dia x – - x -	-	Electrical furnace	Electrical furnace	400-1000 - x -	-	Sakoda et al. (1981)
- x -	300 x -x -x-	-x-	-	-	750-950	0.27 to 0.34	Aarsen van den (1982)
-x-	300-x -x-	Perforated plate	-x-	-x-	523-907	0.15 to 0.38	Hiler (1982)
-x-	152-x- 2.4	-x-	-x-	-x-	700-815	0.18-0.21	Xu et al (1985)
Top end of reactor	230 x 864 410 x 864	3 mm thick SS 316 perforated plate with 844 holes of 1.5 mm $\phi$	Propane + air combustion	Radiant jacket surrounding reactor heated by natural gas burner	-	-	Walawender et al. (1985).
-x-	150 x 3600	-x-	-x-	-x-	500-757	0.21-0.29	Flanigan et al (1987)
-x-	150 x 3700	-x-	-x-	-x-	500-800	0.26	Bingyan et al (1987)
-x-	400 x 3660	-x-	-x-	-x-	721-871	0.30-0.48	Hartiniati et al (1989)
Top end of reactor	150 x – 300 x – Total height 1000	Perforated Plate -	Two electrical heating blankets of 3 kW each one for reactor and other for free board	Electrical heating	- x - 650-825	0.3-1.0	Schoeters et al. (1989)

Table 2.5.2 (Contd....)

Feeding location	Reactor Constructional Details				Operating Conditions		Reference
	Reactor dia x ht (mm) f.b. dia x ht (mm)	Gas distributor details	Heating arrangement		Temperature Bed Reactor, (°C)	Equivalence ratio	
			Start up	Process			
-	160 x 690 220 x 430 1270 total height	-	Propane + air combustion	Self sustained reactions	647 – 777 - x -	-	Jiang and Morey (1992)
50 mm above the distributor plate	200 x – - x – - 2000 total height	Perforated plate with 2000 holes of 1.3 mm $\phi$	-	-	600 to 800 - x -	0.1 to 0.8	Sanchez and Lora (1994)
Very near distributor plate	60 x – - x -	-	Electrical heating for reactor and for preheating air	Electrical heating	700 to 850	0.2 to 0.4	Narvaez et al. (1996)
200 mm above distributor plate	150 x 1000 250 x 500 1900 Total height	Perforated plate type, 12mm thick with 1.5 mm dia holes	Electrical heating (5 kW) around bed	-	650-950	0.20-0.56	Natarajan (1998)
Under bed in dual-distributor type feeding mechanism	255 x 2305 355 x 395 Total height 2700	Two distributor plates, perforated type with 2 mm dia holes	Propane + air combustion	Self sustained reactions	-	0.2 to 0.4	Ergudenler et al. (1997) Mansaray et al. (1999)

(dia) = diameter; (ht)=height; (fb)=free board; ( $\phi$ )=hole diameter, (-)=not available/not mentioned.

Singh et al. (1986) investigated the steam gasification of cottonwood branches in a fluidized-bed reactor and compared the produced gas characteristics, mentioned earlier, with those for pure cellulose. With the exception of the gas heating value, the energy recovery, carbon conversion and mass yield of gas were found to be lower than those obtained from pure cellulose. Investigations of the effect of steam-to-feed mass ratio on the produced gas characteristics for steam gasification of Siberian elm (Sundar, 1988) have revealed that the influence of this ratio is an important aspect that has to be taken into account.

Boateng et al. (1992) studied experimentally the steam gasification of rice hulls in a laboratory scale fluidized bed reactor. The reactor had an inside diameter 101.6 mm and a height of 550 mm, the upper part of which was 200 mm long with 152.4 mm inside diameter serving as transport disengagement section. The reactor section was heated externally by means of two pairs of cylindrical electrical resistance heaters, each capable of delivering up to 1200 W of power with a maximum sustained operating temperature of 1200°C. The rice hull feed was introduced into the reactor by gravity flow through a vertical feed pipe having an inside diameter of 30 mm. A screw feeder ensured uniform volumetric feed rate. Steam was produced externally. Experiments were conducted for the temperature range 700 to 800°C. The results indicated that a hydrogen-rich gas (above 40% H<sub>2</sub>) was possible to be produced from such a process of steam gasification of rice hulls. The higher heating values of the gas produced from such a process of steam gasification of rice hulls ranged from 12.1 MJm<sup>-3</sup> at 700°C to 11.1 MJm<sup>-3</sup> at 800°C. It was found that, in the temperature range studied, the volumetric gas yield ranged from 0.41 m<sup>3</sup>kg<sup>-1</sup> to 0.7 m<sup>3</sup>kg<sup>-1</sup>. The carbon conversion varied between 31.4 and 45.9%. The majority of the produced gas comprised of CO, CO<sub>2</sub> and H<sub>2</sub>. The gas compositions were similar to those obtained from the fluidized bed steam gasification of crop residues and pure cellulose.

Herguido et al. (1992) studied the effect of the type of the feedstock in fluidized bed gasification at small pilot scale. Steam was the gasification medium and pine sawdust, pine wood chips, cereal straw and thistles were the feedstocks. The gas, tar and char yields, the composition and heating value of the gas produced and the carbon conversion were determined at temperatures between 650°C and 780°C for each material. It was observed that the product distribution varied with the biomass used and the gasification temperature. The differences were very marked for the H<sub>2</sub>, CO and CO<sub>2</sub> contents in the product gas at low temperatures. These differences decreased when the temperature increased to 780°C at which point a gas composition similar for all types of biomass tested was obtained. This was attributed to the equilibrium in the water-gas shift reaction. The attainment of equilibrium of water-gas shift reaction occurred in the free board section of their gasifier. The CH<sub>4</sub> content (at 750°C to 800°C) in the exit gas is 5-7.5 vol%. It was also observed that the size and shape of the biomass had influence on the product distribution. They have remarked that, for the proper operation of the gasifier, good fluidization of the mixture of the inert bed material and biomass was important, i.e. the hydrodynamic factors were more important than the “kinetic” ones.

Rapagna and Latif (1997) carried out steam gasification of ground almond shells in a continuous bench scale, fluidized bed reactor in order to evaluate the effects of particle size and operating temperature on the product yield and distribution. The reactor had an inside diameter of 60 mm with a porous plate gas distributor and was mounted in a electric tube furnace. The gasification of the almond shells was performed at five different temperatures: 600, 650, 700, 750 and 800°C at a constant fuel flow rate of 1gmin<sup>-1</sup> and steam to biomass ratio of 0.8. The results revealed that for smaller particle sizes differences in product yield and distribution practically disappear as the higher temperature was approached, whereas for particles above 1 mm in diameter the yield continued to increase over the entire temperature range, but never reaching that attained by the smaller particle systems. This behaviour was explained as the

significance of extra-and/or intra-particle heat transfer limitations with increasing particle size.

### **2.5.3 Gasification with Steam and Oxygen Mixtures**

Wang and Kinoshita (1992) experimentally analyzed the biomass gasification with steam and oxygen as gasifying agents. Parametric tests were conducted on a bench scale, indirectly heated fluidized bed gasifier that was specially fabricated to study biomass to methanol production. The inside diameter of the gasifier was 89 mm and overall height was 2500 mm with a transport disengagement section of 152 mm inside diameter. A perforated plate type distributor was used at the bottom of the gasifier. Biomass (sawdust) was fed into the gasifier by a calibrated screw feeder that discharged the feedstock 250 mm above the gas distributor. A 10 kW electric heater was used to maintain the internal temperature of the gasifier at a specified level (up to 1100°C). Parametric gasification tests were conducted varying residence time (using nitrogen as a diluent), equivalence ratio, temperature and steam to biomass ratio at approximately atmospheric pressure condition. Actual gas compositions for selected test runs were compared with equilibrium compositions under different gasification conditions. It was observed that there were substantial differences between the actual gas compositions and the theoretically predicted equilibrium compositions. Comparison indicated that longer residence time and higher temperature improved the gasification reactions.

In another work, Gil et al. (1999) studied the effect of the type of gasifying agent on the product distribution in biomass gasification using a bubbling fluidized bed. The three gasifying agents considered were: air (with some moisture), pure steam and steam-oxygen mixtures. They compared the results of their earlier work done in similar gasifiers but with different gasifying agents (Herguido et al., 1992; Narvaez et al., 1996; Gil et al., 1997). The three basic ratios were used for the comparison of the results as follows :

Gasifying agent	Name of ratio used	Symbol
Air	Equivalence ratio	ER
Steam-O <sub>2</sub> mixtures	Gasifying ratio (H <sub>2</sub> O + O <sub>2</sub> )/Biomass	GR
Pure steam	Steam to biomass ratio (H <sub>2</sub> O/Biomass)	SB

They have opined that at least 20 operational parameters concerning the gasifier and feedstock have an influence on the product distribution and gas quality. The following parameters for all the three experimental programs were maintained constant :

Gasifier bed, bed inert material, bed temperature, feed stock, Gas and Tar sampling and analysis.

However, the free board size and the free board temperature varied. The size and temperature of a free board is important because it controls the value of gas residence time. Several reactions like thermal cracking of tar, and CO-shift reactions occur in the free board section.

The following table explains the effect of the gasifying agent on fluidized bed thermal gasification of biomass.

Result/parameter	Gasifying agent and ratio		
	Air ER=0.30, H/C=2.2	Steam-O <sub>2</sub> GR= 0.90, H <sub>2</sub> O/O <sub>2</sub> =3	Steam S/B=0.90
H <sub>2</sub> (vol%, dry basis)	8-10	25-30	53-54
CO (vol%, dry basis)	16-18	43-47	21-22
LHV (MJNm <sup>-3</sup> , dry basis)	4.5-6.5	12.5-13.0	12.7-13.3
Y <sub>gas</sub> (Nm <sup>3</sup> ,dry basis/kg daf)	1.7-2.0	1.0-1.1	1.3-1.4
Tar* content (gNm <sup>-3</sup> )	2-20	4-30	30-80

#### 2.5.4 Modified Fluidized Bed Gasifiers

Prasad and Kuester (1988) utilized the process data from a biomass dual fluidized bed laboratory scale gasification system (throughput rate 10 kgh<sup>-1</sup>) for process

modeling and analysis. The objective of the study was to elucidate the effect of the operational conditions, like temperature, the biomass feedstock composition and the residence time, on the performance of the gasifier. The gasifier comprised of a dual fluidized bed reactor system with connecting circulating solid transfer loops. One fluidized bed was used as a feedstock pyrolyzer while the second bed operated in a combustion mode to heat the circulating solid media. Cellulosic materials were continuously fed to the pyrolyzer and flashed to a synthesis gas consisting of paraffins, olefins, carbon monoxide, hydrogen and carbon dioxide. The gas then passed through a cyclone scrubber system to a compressor. From the compressor, the gas would be distributed to the pyrolyzer and/or to the liquefaction reactor. Recycling the product gas increased the gas residence time while steam as a fluidizing gas decreased the gas residence time.

A linear regression program was used to fit a linear polynomial expression relating the dependent variables with the independent variables, i.e. the temperature and the steam/biomass weight ratio. Models of varying order, with up to 10 parameters, were investigated. The 10-parameter cubic model was chosen to represent the pyrolysis system. The calculated values from this model were compared with the theoretically calculated equilibrium compositions. Studies revealed strong interactions between the temperature and the steam to biomass weight ratio. Comparison of the model predictions and calculated equilibrium product trends indicated that there were two regions of interest. One was a low temperature regime dominated by residence time or reaction rate while the second was at high temperature in which water-gas shift reaction and steam dilution prevailed. At intermediate temperatures, both the phenomena could prevail and the product gas compositions were affected by changes in the temperature and/or the steam flow rates. Equilibrium studies with a number of feedstocks confirmed the experimental observation of the dependence of the product gas compositions on the hydrogen to oxygen ratio (H/O ratio) in the feedstock. The H/O ratio could be utilized

for future modeling studies and for feedstock selection.

Mansaray et al. (1999) conducted an experimental study on the air gasification of rice husk in a dual distributor type fluidized bed gasifier that was developed earlier (Ergudenler et al., 1997) and later modified. The gasifier was of 255 mm inside diameter and 2700 mm total height. The transport disengagement section was 395 mm long with an inside diameter of 355 mm. A dual distributor type feeding arrangement was developed for feeding rice husks. It consisted of the main distributor plate, the secondary distributor plate, the secondary column and the feeding tube. Both the distributor plates were of perforated plate type. The main distributor plate had a circular opening of 75 mm diameter at the center, surrounded by 267 circular holes of 2 mm diameter each. Connected to the main distributor plate at the center was the secondary column of 200 mm length and 75 mm diameter. The secondary distributor plate supported the bed material (alumina granules) within the secondary column. Experiments were conducted varying the fluidization velocity and the equivalence ratio. The steady state temperature varied between 665 and 830°C. The results obtained from this gasification study showed that the reactor temperature, pressure drop, gas composition, gas higher heating value, gas yield and carbon conversion were affected by both the equivalence ratio and the fluidization velocity. The temperature profiles show that the dense bed was essentially isothermal while the temperature decreased with height measured from the distributor plate. The pressure drops in the dense bed as well as in free board regions increased with increasing fluidization velocity and/or decreasing equivalence ratio. The gas yield increased linearly with increasing equivalence ratio but was not significantly sensitive to changes in the fluidization velocity.



---

---

## EXPERIMENTAL

In order to meet the aims and objectives of the present research work, a detailed experimental programme was designed and is described in detail in this chapter.

### 3.1 BIOMASS MATERIALS: COLLECTION AND STORAGE

The biomass materials (residues) were obtained locally and were sun dried before storage. The rice husk was collected from a village rice huller. The rice husk so obtained was sieved and sun-dried. This rice husk was called the *village rick husk* (VRH). Locally this rice husk is available by the name '*kamu*'. This contained, besides crushed outer casing, some quantity of the crushed grain also. The rice husk of basmati paddy was obtained from a local sheller mill and was sieved before drying to clean the dirt particles. This husk was the whole outer case of the basmati rice and will henceforth be called as *mill rice husk (or only as rice husk)* (MRH). The sawdust (SD) was obtained from a local sawmill where normally hard wood was sawn. The sawdust was sieved and the size fraction less than 2 mm size was selected for the study. Bagasse (BG) and pressmud (PM) were procured from RBNS Sugar mills Limited, Laksar (Roorkee). The mill waste bagasse was more powdery than fibrous in nature. The pressmud was in a powdery form as available from the mill. The five-biomass materials used in the present study were thus:

1. Village rice husk (VRH)
2. Mill rice husk (MRH)
3. Sawdust (SD)
4. Bagasse (BG), and
5. Pressmud (PM)

All the biomass materials were stored in airtight plastic containers for further use.

## **3.2 PHYSICO-MECHANICAL CHARACTERISTICS OF BIOMASS MATERIALS**

The physico-mechanical properties of the biomass materials relevant to fluidization namely, bulk density, particle density, particle size, packed bed voidage and angles of repose and slide were determined for the five biomass materials.

### **3.2.1 Bulk Density**

Bulk densities of the biomass materials were determined by the procedure prescribed by ASTM standard method for the bulk density of particulate biomass fuels, E 873-83 (Anon, 1993).

### **3.2.2 Particle Density**

The particle densities of the biomass materials were determined using a pycnometer and light paraffin oil.

### **3.2.3 Particle Size**

The particle sizes of the biomass fractions were determined by conducting sieve analysis, using standard sieves.

### **3.2.4 Packed Bed Voidage**

The values of packed bed voidage (bed porosity) for the biomass materials were calculated from the experimentally determined values of particle density and bulk density and the volume of a cylindrical vessel filled with a known mass of the biomass material.

### **3.2.5 Angle of Repose**

Poured angle of repose for each of the biomass materials was determined by measuring the dimensions of the conical heap formed due to free fall of that biomass residue through a vertically held circular tube. The height and the base diameter of the

heap were measured accurately using a cathetometer. Angle of repose was calculated from the following expression.

$$\theta = \tan^{-1} [ H / (L/2) ],$$

Where,  $\theta$  = angle of repose, degree

H = height of the heap, mm

L = width of the heap, mm

### 3.2.6 Angle of Slide

Angle of slide for each of the biomass materials was measured using a mild steel plate fitted with a protractor for measuring the angle of inclination of the plate. Mild steel plate was chosen because it is often the material of construction of bins and hoppers. The angle of inclination at which the biomass sample just starts sliding down the plate under gravity was taken as the angle of slide (degree).

### 3.2.7 Carrier Solids and their Properties

The biomass materials, in general, are not easily fluidizable when fluidized alone. Carrier solids are the inert materials like sand and bauxite, which are generally used to facilitate the fluidization of powdery biomass materials. The following inert materials were used as the carrier solids to study the fluidization of biomass materials under cold flow atmospheric conditions:

<u>Carrier solid</u>	<u>Size range, <math>\mu\text{m}</math></u>
Silica sand	-500+350
Silica sand	-850+710
Bauxite	-500+420
Bauxite	-850+710

For the fluidized bed gasification experiments only silica sand of the size range - 500+350  $\mu\text{m}$  was used as the carrier solid.

### **Particle density and bulk density**

The particle density ( $\rho_s$ ) of the carrier solids was determined by dropping a known mass of the solid in distilled water contained in a graduated cylinder. The bulk density,  $\rho_b$ , of the carrier solids was determined by filling a 100 ml beaker with the solid and weighing. The average of ten experimental runs has been reported as the value of  $\rho_b$ .

### **3.3 PHYSICO-CHEMICAL AND THERMO-CHEMICAL CHARACTERISTICS OF BIOMASS MATERIALS**

The physicochemical properties, namely volatile matter, ash content, elemental composition and the chemical composition of the ash of biomass residues are necessary to be known for the proper design and operation of a gasifier. The higher and lower heating values, the ash deformation and fusion temperatures and the ash agglomeration characteristics are the thermochemical properties which influence the thermochemical conversion process directly. The process parameters like temperatures, throughput rate etc are to be selected while considering these properties.

A survey of the literature indicated that no standard procedures for the determination of these properties of biomass have yet been evolved. The ASTM standard methods for such solid fuels as coal and coke have been adopted, in the absence of specific standard test procedures. Because of the presence of large quantities of volatiles in the biomass fuels in comparison to those in coal and coke, certain modifications have been suggested by Ebeling and Jenkins, (1985). All these observations have been taken note of in the determination of physico-chemical properties in the present study.

#### **3.3.1 Proximate Analysis**

The ASTM standard method for Proximate Analysis (D-3172-73 through D-3174-82 and D-3175-82 Anon., 1993) was followed. As the biomass samples were

highly volatile, the procedure for sparking fuels was used. A small amount of each biomass was finely ground and a representative sample was then taken for analysis. Each sample was divided into two portions. The first portion of the sample was placed in a silica crucible and its moisture content was determined according to ASTM D 3173-73 (Anon., 1993). After the determination of the moisture content, the sample was heated to 750<sup>0</sup>C in a muffle furnace and maintained at this temperature for 2 hours or more till a constant weight of the residue was obtained. The weight of the residue represented the ash content of the biomass. The second portion of the sample was placed in a crucible and covered with a lid and this was heated in the furnace at 600<sup>0</sup>C for six minutes and thereafter at 950<sup>0</sup>C in the furnace for another six minutes. After cooling the crucible in a dessicator the crucible was weighed. The difference in the weights is due to the loss of volatiles and moisture in the sample. The volatile matter was found by subtracting the corresponding moisture previously determined.

### **3.3.2 Ultimate Analysis**

The ultimate analysis was performed on finely ground and oven-dried biomass samples to determine the weight fractions of carbon, hydrogen, nitrogen and oxygen (by difference). It is well known that the biomass contains negligible amount of sulfur and therefore its determination was not attempted. The weight fractions of carbon, hydrogen and nitrogen were determined using Perkin Elmer CHN Elemental Analyser (Model 2700, available at the Centre of Advanced Study, Chemical Engineering Department, Institute of Technology, Banaras Hindu University, Varanasi, India). The test conditions were: combustion temperature of 920<sup>0</sup>C and reduction temperature of 640<sup>0</sup> C. The ash content was previously determined separately following the standard method. There is no direct method available for the determination of oxygen in biomass fuels and therefore its percentage was estimated by subtracting the sum of carbon, hydrogen, nitrogen, and ash from 100.

### **3.3.3 Heating Values**

The higher heating value of a biomass sample is determined in a standard bomb calorimeter according to ASTM – D 2015 – 17. The biomass samples were ground to 250 $\mu$ m (60 mesh) screen size. One g of each of the powdered biomass samples was pelletised by mixing a little water and then dried. The pellets were burned in the bomb in an atmosphere of oxygen at 30 atmospheric pressure. The higher heating values were determined from the temperature rise of the surrounding water bath and the heat capacity of the system. The lower heating values were then calculated using the relation given by Ebeling and Jenkins(1985).

### **3.3.4 Ash Deformation and Fusion Temperatures**

The ash deformation and fusion temperatures were found using the standard tests for the fusibility of coal and coke ash (ASTM, D- 1857-68) as guidelines.

## **3.4 COLD- FLOW FLUIDIZATION**

### **3.4.1 Experimental Set-Up**

The schematic diagram of the experimental set up used for the study of the fluidization behaviour of the biomass materials is shown in Fig. 3.1. It consisted of a transparent plexiglass column of 76 mm inner diameter, and 1000 mm height with a wall thickness of 5 mm. This column was held perfectly vertical to the ground with suitable clamping arrangements. The transparent wall of the column facilitated visual observation of the phenomenon of fluidization as well as measurement of the bed height. A multi-orifice distributor made of 3 mm thick mild steel plate with 1.5 mm diameter holes drilled in a triangular pitch was fitted to the bottom of the tube to support the fluidizing solids. A stainless steel screen of 200 mesh was spot-welded to the surface of the distributor plate to prevent weeping of the fluidizing solids through the distributor plate holes. A blower capable of supplying 1.5 m<sup>3</sup>min<sup>-1</sup> of air was used to supply the fluidizing air. The air supply system included a gate valve, a calibrated

1. Air blower
2. Air supply pipe line (40 mm dia)
3. By pass line for air (40 mm dia)
4. Flow control gate valve
5. Orifice meter with pressure tapping
6. Colming section
7. Distributor plate assembly
8. Fluidizing column (Plexiglass 76 mm dia x 1000 mm long)
9. Flange with screen

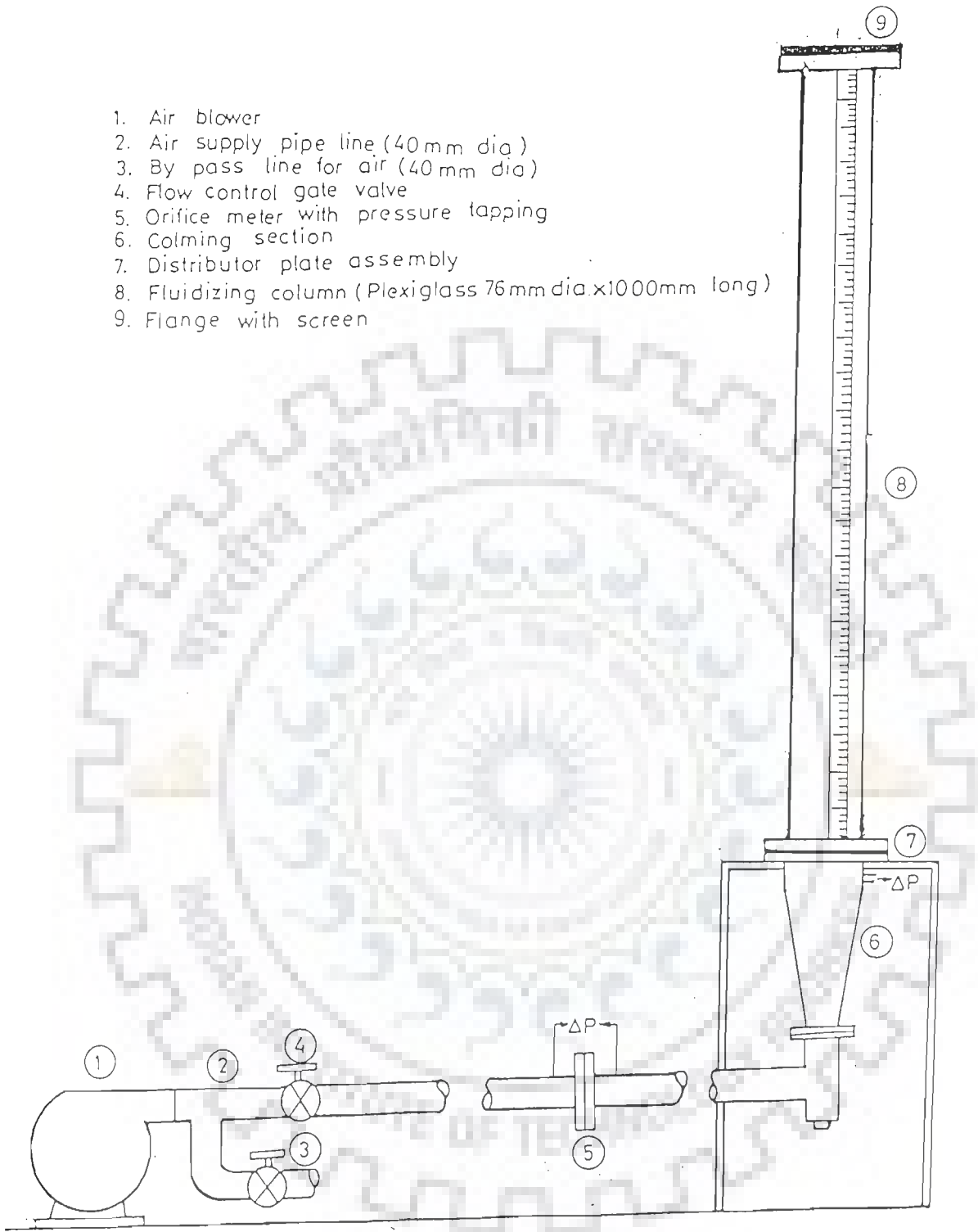


Fig. 3.1 Schematic of the experimental assembly for cold flow fluidization experiments

orifice meter and a calming section. A calibrated orifice plate using an U-tube water manometer was used to determine the flow rate of air to the fluidizing column. The air from orifice meter entered a vertical calming section and then through the distributor plate to the fluidizing column. The calming section was a sufficiently long inverted cone diverging from 40 mm diameter to 76 mm diameter. It was filled with Raschig rings to smoothen the flow so that the air entered the fluidizing column with a flat velocity profile.

The fluidizing solids were fed from the top end of the fluidizing column. The top end of the column could be fitted with a screen of 200 mesh to prevent entrainment of the fluidizing solids during experimentation.

### 3.4.2 Minimum Fluidization Velocity of Carrier Solids

After loading the carrier solid particles into the column, the atmospheric air supplied by the blower was introduced from beneath the distributor plate slowly until the entire bed of the carrier solid was seen vigorously moving and mixing. The airflow was thereafter decreased slowly and finally stopped and the bed was allowed to settle. At this 'condition of minimum consolidation' (Wilhelm and Kwauk, 1944), the height of the bed was measured with the help of a scale attached along the fluidizing column and a cathetometer. This bed height (the height from the distributor plate to the free end surface of the bed charge) could be maintained at different H/D (height to bed diameter) by either adding or removing the solids from the topside of the column.

The pressure drop readings across the bed were noted initially with the bed charge of sand particles of size range (-500 +350 $\mu$ m), for increasing and decreasing the air flow rates. The pressure drop versus superficial air velocity curves thus obtained showed no hysteresis. Therefore, for all the subsequent experiments with all the carrier solids, the fluidization (i.e.  $\Delta P$  versus  $u_s$ ) data were collected while decreasing the superficial air velocity, i.e. by operating the bed from its fluidized state to its fixed bed state.



Minimum fluidization velocities for the different carrier solids were determined from the plots of the pressure drop across the bed versus superficial air velocity. The intersection of a horizontal line for the constant pressure drop during the fluidized state with the inclined straight line for the pressure drop of the fixed bed region yielded the minimum fluidization velocity,  $U_{mf}$ , for a particular carrier solid at a given  $H/D$  ratio.

### **3.4.3 Fluidization of a Biomass When Fluidized Alone**

Attempts were made to fluidize village rice husk, bagasse and sawdust with  $H/D = 1$ . After putting the required quantity of the biomass into the fluidizing column, air was passed slowly increasing its flow rate up to a maximum value, and then it was slowly decreased till all the biomass particles settled back. Visual observation of the bed showed the channeling and bypassing of the air through the bed and the pressure-drop data showed inconsistent results with hysteresis and non-repeatability.

### **3.4.4 Minimum Fluidization Velocity of Mixtures of Carrier Solid and Biomass**

Experimental runs were taken to determine the minimum fluidization velocities for the binary mixture of a biomass and a carrier solid. The carrier solids mentioned earlier were used in these experiments. The experiments were conducted for the mixtures of the carrier solid (one at a time) and the biomass materials (a particular one at a time). The biomass content of the bed mixture (obtained by biomass addition to the bed charge) was varied from 1% to 8% (of the weight of the sand in the bed). The  $H/D$  ratio for the carrier solid in the bed charge was kept unity in all these experiments.

A particular amount of a carrier solid was first loaded into the fluidizing column and its quantity was corrected so that the bed  $H/D=1$  was maintained. The solid charge was thereafter withdrawn, weighed and reloaded in the column. An amount of biomass corresponding to 1% of the weight of this carrier solid was weighed and admixed to the bed charge of the carrier solid. The mixture was then fluidized for sometime usually, for about 5 minutes and the bed pressure drop data were noted while gradually

decreasing the airflow rate in steps. The minimum fluidization velocity could be determined from the plot of bed pressure drop versus superficial air velocity. The procedure was repeated each time after an additional one-weight percent of the biomass was added to the bed charge. The addition of one-weight percent of the biomass material continued until the mixture became 'not fluidizable'.

### **3.5 THERMAL DEGRADATION STUDIES**

The thermal degradation (pyrolysis and gasification) of the biomass materials was studied using the Thermogravimetric and Differential Analysis techniques. The thermal decomposition of each of the biomass material sample was carried out non-isothermally in a Stanton Redcraft Thermoanalyser 780 series available at the Institute Instrumentation Centre. A sample size of 10 mg or less was used for each experimental run. The samples were prepared carefully after crushing and sieving (-500 $\mu\text{m}$  + 350 $\mu\text{m}$ ) so as to obtain homogeneous material properties. The degradation runs were made at two heating rates (20 and 40 $^{\circ}\text{Cmin}^{-1}$  generally and 25 $^{\circ}\text{C min}^{-1}$  in some cases) under an inert atmosphere (flowing nitrogen) for pyrolysis and an oxidizing atmosphere (flowing zero-moisture-free air) for gasification. To study the effect of the flowing nitrogen and/or air on thermal degradation characteristics, certain experimental runs were made at different flow rates for a particular heating rate. The thermogravimetric (TG), differential thermogravimetric (DTG) and differential thermal analysis (DTA) curves obtained for each case were analysed to understand the behaviour of thermal degradation and to determine its kinetics.

### **3.6 EXPERIMENTAL SET UP FOR THE FLUIDIZED BED THERMAL GASIFICATION OF BIOMASS WITH AIR**

A complete fluidized bed thermal gasifier unit was designed, fabricated and installed in the laboratory. The unit incorporated (i) a fluidized bed reactor with a perforated plate type distributor plate, (ii) an air supply unit, (iii) a biomass feeding

unit, (iv) a cyclone, and (v) a product gas after-burner. A schematic diagram of the gasifier unit is shown in Fig.3.2. The details of these are presented hereinafter.

### 3.6.1 The Fluidized Bed Reactor

The main parts of the fluidized bed reactor were the fluidizing column, a transition section (connecting fluidizing column and transport disengagement section), and the transport disengagement section. These are shown in the Fig 3.3. The fluidizing column, which was the main part of the gasifier, was made from a stainless steel pipe AISI 310 of 100 mm inner diameter, 1000 mm length and a wall thickness of 5 mm. The fluidizing column was erected along the vertical axis to the ground with the help of a suitable angled iron - supporting structure. The calming section was fixed to the bottom end of this fluidizing column through flanged joints with a distributor plate in-between. The purpose of the calming section was to make the air enter the fluidizing column with flat velocity profile across its cross section. This calming section was a varying area conical pipe, increasing in diameter from 40 mm to 100 mm. At the end of the conical section, a 100 mm diameter pipe of 150 mm length was also provided for smoothening the flow. A sand loading port of 25 mm diameter was provided at a height of 400 mm above the distributor plate with a leg pipe of 300 mm length and a lid, at an angle of  $45^{\circ}$  upwards. A similar leg pipe of the same dimensions was provided at a height of 300 mm from the distributor plate inclined downwards at an angle of  $45^{\circ}$  with the vertical. This was meant for the withdrawal of the sand, the bed charge and the excess ash as and when required.

A transport disengagement section was mounted co-axially on the fluidizing column. This section was cylindrical in shape with 200 mm internal diameter and 400 mm height and was made from a 5 mm thick mild steel sheet metal. It was connected to the fluidizing column using a transition inverted conical piece (variable area piece), which had 200 mm internal diameter at the top end and 100 mm internal

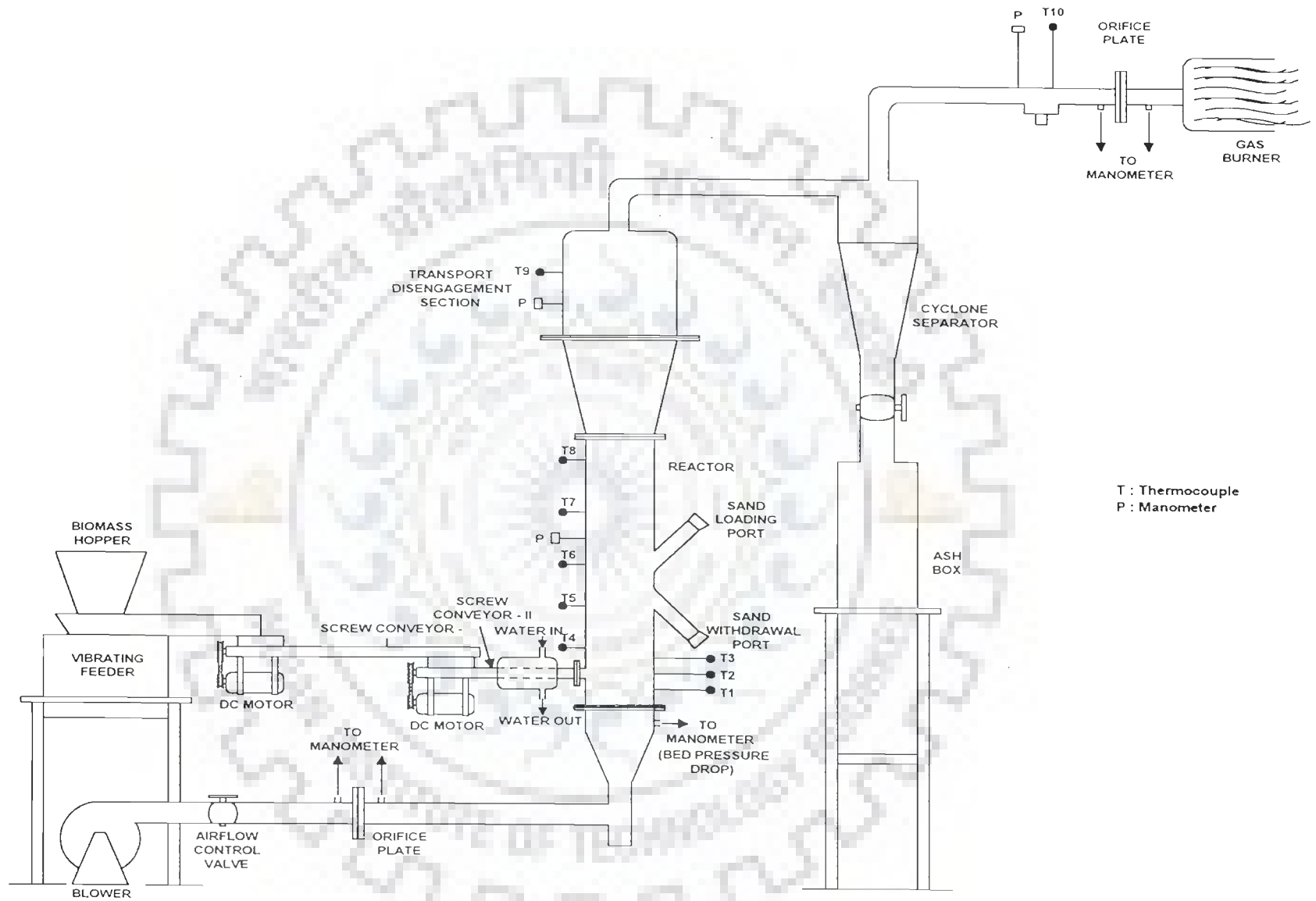


Fig. 3.2 : Schematic Diagram of Fluidized Bed Gasifier Unit

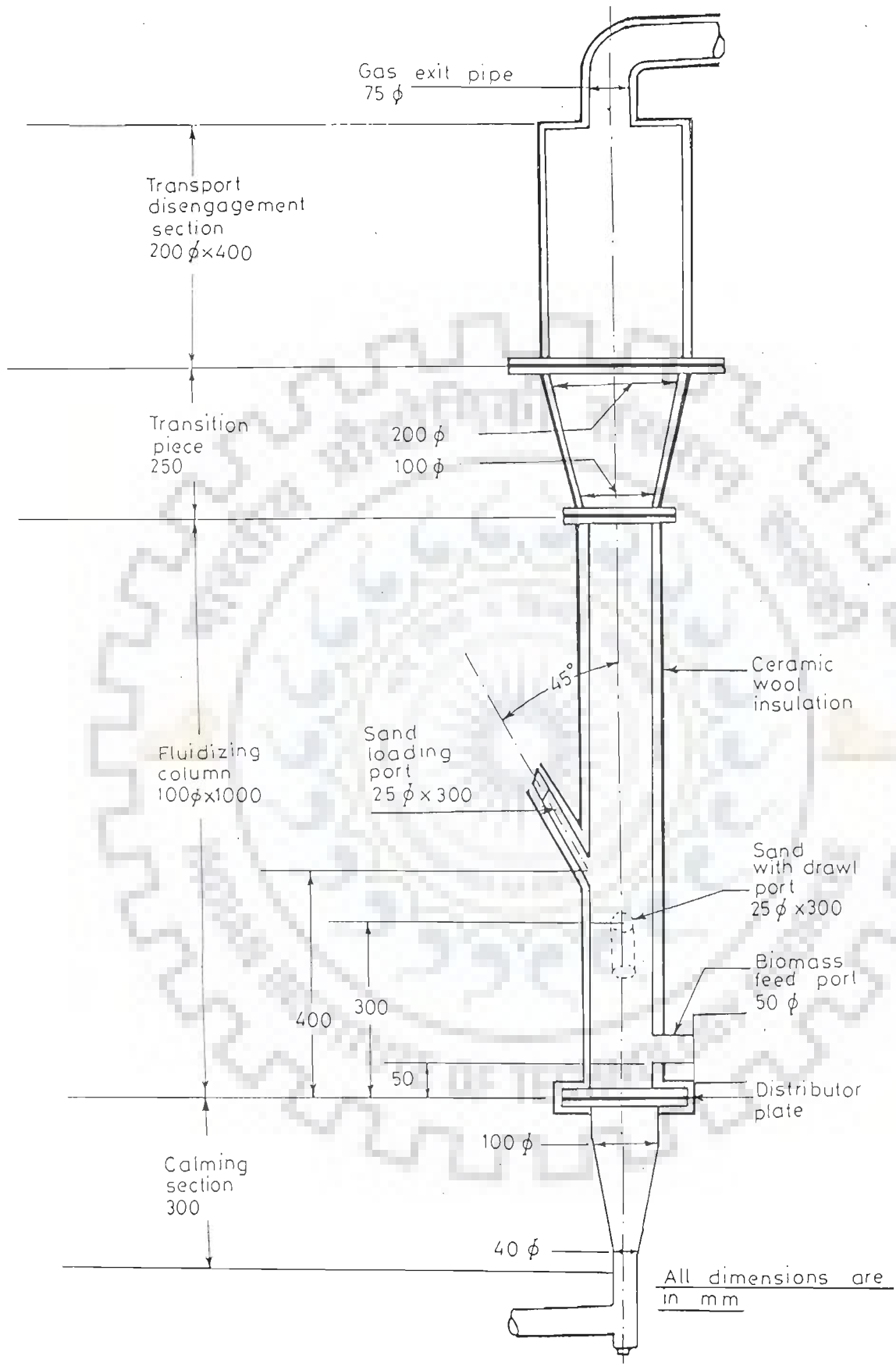


Fig. 3.3 Fluidized bed gasifier : constructional details

diameter at the bottom end, and a length of 250 mm. This transition piece, was also fabricated with a mild steel sheet metal of 5 mm thickness. All the sections were joined with each other using welded standard flanges with high tensile bolts and nuts. The exit gas pipe of 75 mm internal diameter was fixed at the top of the transport disengagement section at its center. This pipe led the gas from the fluidized bed reactor to the cyclone.

A multi-orifice type distributor made of 3mm thick stainless steel plate was fixed to the bottom of the fluidizing column, sandwiched between the flanges of the fluidizing column and that of the calming section. The distributor plate had 654 holes of 1.5 mm diameter drilled in a triangular pitch. A view of the distributor plate is shown in Fig 3.4. A stainless steel mesh of 200  $\mu\text{m}$  sieve size was spot welded to the surface of the distributor plate to prevent the fluidizing solids weeping through its holes. The fluidizing (or the gasifying) air entered the distributor plate from the bottom through the calming section. Heat resistant (Make: Champion, firefly, 20-gauge) gaskets were used at all the flanged joints to make them leak-proof.

Two biomass feed ports were provided in the fluidizing column at the heights of 50 mm and 150 mm above the distributor plate. The discharge end of the auger screw of the smaller screw conveyor remained flush with the inside walls of the fluidizing column through one of the feed ports. The ports were 50 mm in diameter and were just sufficient to accommodate the auger screw, so that while feeding, the fluidized bed charge could hardly escape into the auger housing. The outer casing of the smaller screw conveyor was fixed horizontally to the fluidizing column. The feed material was thus directly discharged into the bed. These ports provided under bed and over bed feeding conditions. After initial trials, it was decided to have only one feeding port at 50 mm height. The other port was closed using a perfect blind flange.

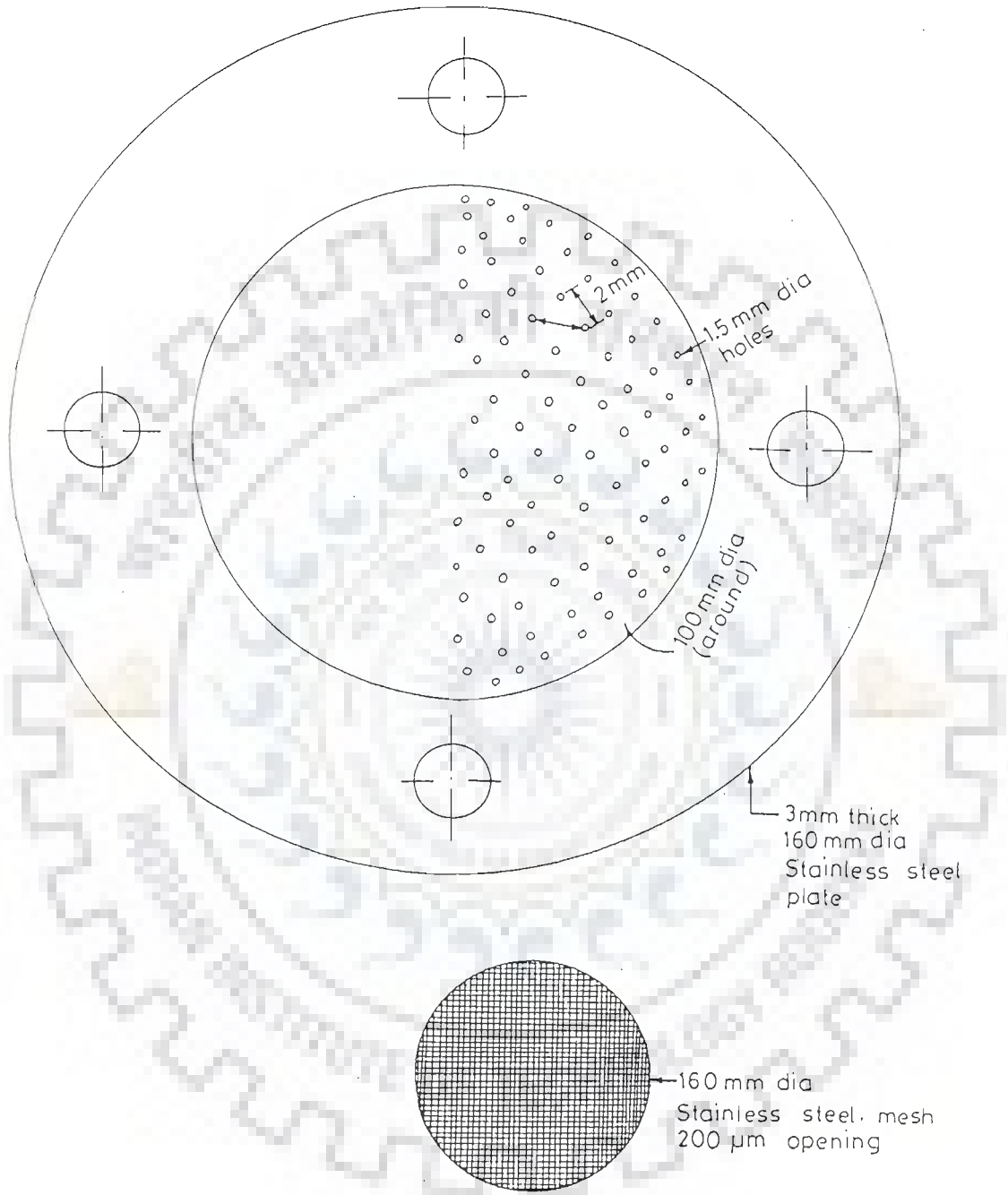


Fig. 3.4 A view of the distributor plate

The fluidizing column was equipped with pressure and temperature measuring probes. For mounting these probes, 12 mm internal diameter threaded sockets were provided at suitable distances measured from the distributor plate. For inserting the thermocouples for measuring the bed temperature, three sockets were provided vertically at a distance of 50 mm from each other. The first socket was provided at 50 mm above the distributor plate. The temperature of the free board section was measured with the thermocouples inserted through sockets welded at the distances of 250, 400, 550, 700, and 850 mm above the distributor plate. Another array of six sockets was provided at an angular distance of  $45^{\circ}$  from the array of thermocouple sockets, and were 150 mm apart from each other; the first being 150 mm from the distributor. The socket at the vertical distance of 450 mm from the distributor plate was connected to a U-tube manometer for pressure measurement. A special, small double-pipe heat exchanger assembly was used to cool the gas entering the U-tube manometer. Water was the cooling medium flowing through the annulus. Two sockets were provided in the transport disengagement section - one for pressure and the other for temperature measurement.

The fluidizing column was covered with 50 mm thick ceramic wool blanket to provide thermal insulation to the column. This blanket could withstand temperatures up to  $1260^{\circ}\text{C}$ . The insulation blanket was covered with a 1 mm thin aluminium sheet to cut down heat losses and also to provide security to the insulation material. The external surfaces of the transport disengagement section, the transition piece and the gas exit pipe were also thermally insulated with the ceramic wool, to minimize the possible heat loss.

### **3.6.2 Air Supply Unit**

The atmospheric air was used as the fluidizing and gasifying agent for the biomass gasification process. Air was supplied continuously by a blower.



(Make: Ralliwolf Ltd., Bombay) which was driven by an AC single-phase motor running at 10000 rpm developing 0.37 kW. The blower was capable of supplying 1.5 m<sup>3</sup> of air per minute. The air passed through a 40 mm diameter metallic pipe to the calming section placed below the distributor plate of the fluidizing column. A flow control gate valve, an air flow measuring orifice meter and its two pressure taps, all at recommended standard distances, were provided in the air flow pipe line. The orifice meter was previously calibrated. An U-tube water manometer was used to measure pressure drop across the orificemeter. The pipe from the blower to the calming section of the fluidizing column was properly clamped to arrest any vibrations and pulsations in the air.

### 3.6.3 The Biomass Feeding Unit

The biomass feeding system comprised of (i) an electrically operated vibrating feeder (Make: Saideep Electricals, Bombay), and (ii) two screw conveyors. The hopper of size 300 mm x 300 mm x 450 mm was mounted on the vibrating feeder. The feed biomass material was discharged from a rectangular slit provided at the bottom of this hopper due to vibrations of the vibrating feeder. This material was further pushed along a chute, mounted and fixed on the vibrating feeder. The vibrating feeder could generate vibrations in a vertical plane as a function of its input DC supply voltage. This DC supply came from a rectifier, which received AC supply through a variac. Therefore the input supply to the rectifier could be controlled precisely by the variac. Accordingly, the DC output of the rectifier and the vibrations of the vibrating feeder could be precisely regulated. Increasing or decreasing the input voltage to the variac could regulate the feedrate of the biomass. The working of the vibrating feeder was of key importance in maintaining the uniform feedrate of biomass to the reactor.

Two screw conveyors, one 600 mm long and the other 400 mm long, of the same auger dimensions were used in further transporting the biomass to the reactor. Some details of the screw conveyors are shown in the Fig. 3.5. The augers had 50 mm diameter

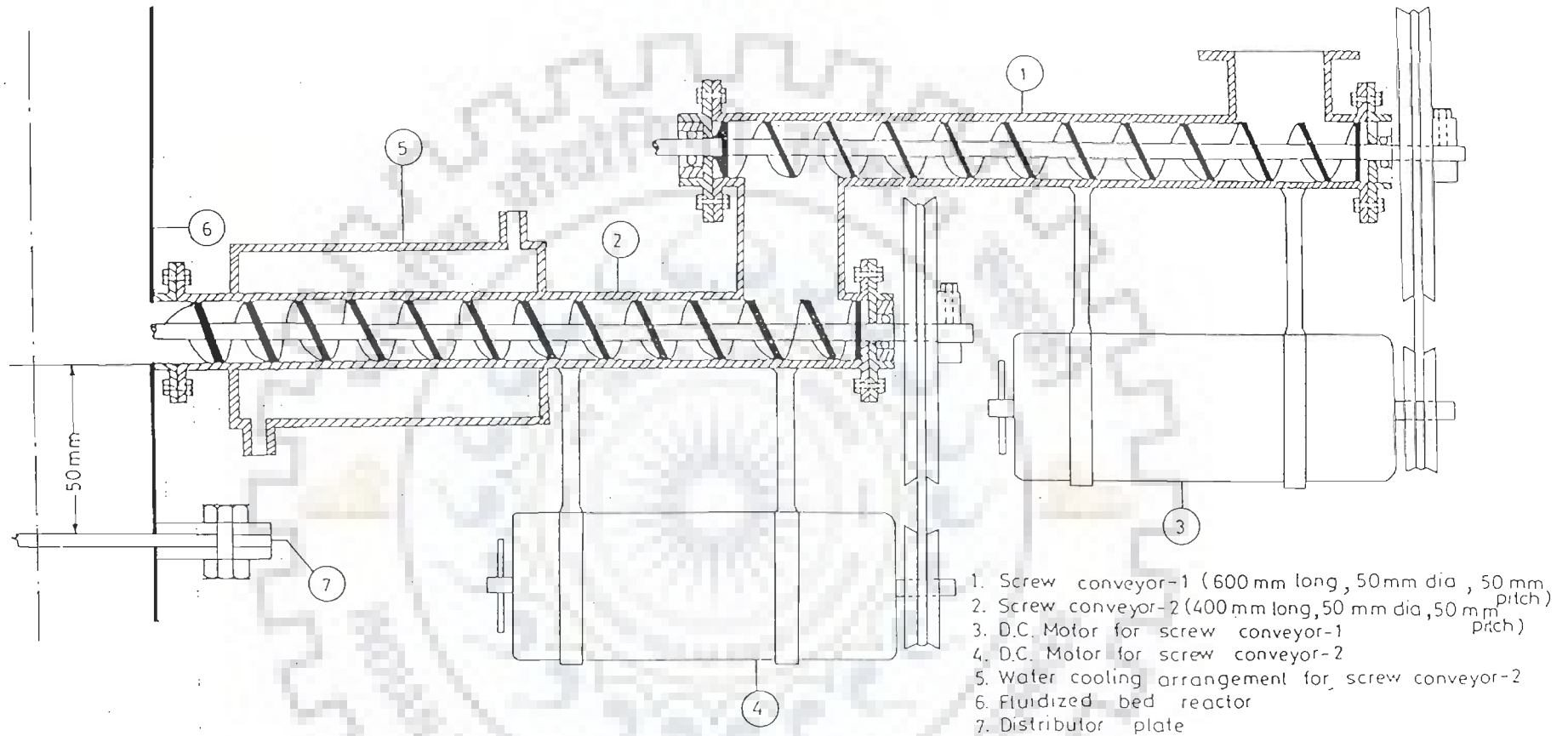


Fig. 3.5 Details of the biomass feeding screw conveyors

flights at 50mm pitch welded on a 15mm diameter solid shaft. The flights of the auger screw were made from 8mm thick mild steel sheet metal. This thickness was so chosen as to withstand the mechanical and thermal stresses developing during the feeding of the biomass to the reactor, especially under hot conditions. The chute at the inlet of the longer screw conveyor discharged the feed material. The longer screw conveyor carried this to a small rectangular duct that connected the two screw conveyors. The feed material descended through it under gravity and entered the smaller screw conveyor. The smaller screw conveyor was connected to the fluidizing column at a suitable height above the distributor plate such that the material was discharged at right angles to the axis of the fluidizing column. The output end of the shaft of the smaller screw conveyor was free like a cantilever so that the biomass entered the bed section of the reactor without any obstacle. The shaft of the longer screw conveyor was supported on either end using gas tight bearings. The smaller screw conveyor was kept at around room temperature by cooling so as to prevent premature pyrolytic reactions taking place in the screw conveyor. This cooling was achieved by water circulation in a shell and tube arrangement, with the tube housing the screw and water being circulated in the shell. Two separate DC motors of 0.18 kW were used for the rotating motion of the two screw conveyors with a pulley and belt arrangement.

The vibrating feeder was calibrated in terms of the input AC voltage to the variac against the mass of biomass collected at the end of the smaller screw conveyor. With the calibration, it was possible to maintain a particular flow rate of the biomass into the fluidized bed gasification reactor. However, the actual amount of the biomass collected in fixed time duration (usually one minute) during each experimental run was taken as the feed rate of biomass. Since the biomass was stored in the hopper mounted on the body of the vibrating feeder, the bulk density of the biomass remained almost invariant during its storage. No bridging or arching was observed in the hopper, which ensured uniform feed flow rate during the experimental runs.

### 3.6.4 Cyclone

A high efficiency cyclone separator was attached to the exit pipe of gas from the fluidized bed reactor to capture the solid particles (dust, ash, char) entrained in the gas stream. The cyclone was made of 5mm thick mild steel sheet metal with a body of 150mm diameter and 300mm height. The cyclone had standard dimensions (Perry and Chilton, 1973). The cyclone dimensions are given in the Fig 3.6.

The cyclone outlet was connected to a horizontal pipe, which incorporated a sampling port and an orifice meter at horizontal recommended distances. The gas outlet pipe had a small pilot burner using liquefied petroleum gas (LPG), which was used to trigger flaring of the gas from the cyclone gas exit pipe.

The cyclone separator together with the gas inlet pipe, gas exit pipe and a part of the ash-collecting pipe were insulated with the ceramic wool blanket.

## 3.7 GASIFICATION MEASUREMENTS

### 3.7.1 Temperature Measurements

K-type thermocouples ingrained at various points along the vertical axis of the fluidized bed reactor and at the sampling port were used in conjunction with a digital temperature indicator to measure temperature. The thermocouples were sheathed in stainless steel tubes of 150 mm length; 8 mm outer diameter and 1.5 mm wall thickness. They had special mounting nuts and sockets made of stainless steel with brass gland packing to avoid gas/air leakage. The mounting nuts facilitated easy mounting and withdrawal of the probes and allowed cleaning of the sensor tips of accumulated dust and tar after an experimental run. The probes were connected to a 24 points selector switch and a digital temperature indicator in series, using heat-resistant glass wool sheathed extension wires. All the thermocouples were calibrated and checked for their accuracy. They were generally found to be correct within  $\pm 5^{\circ}\text{C}$ .

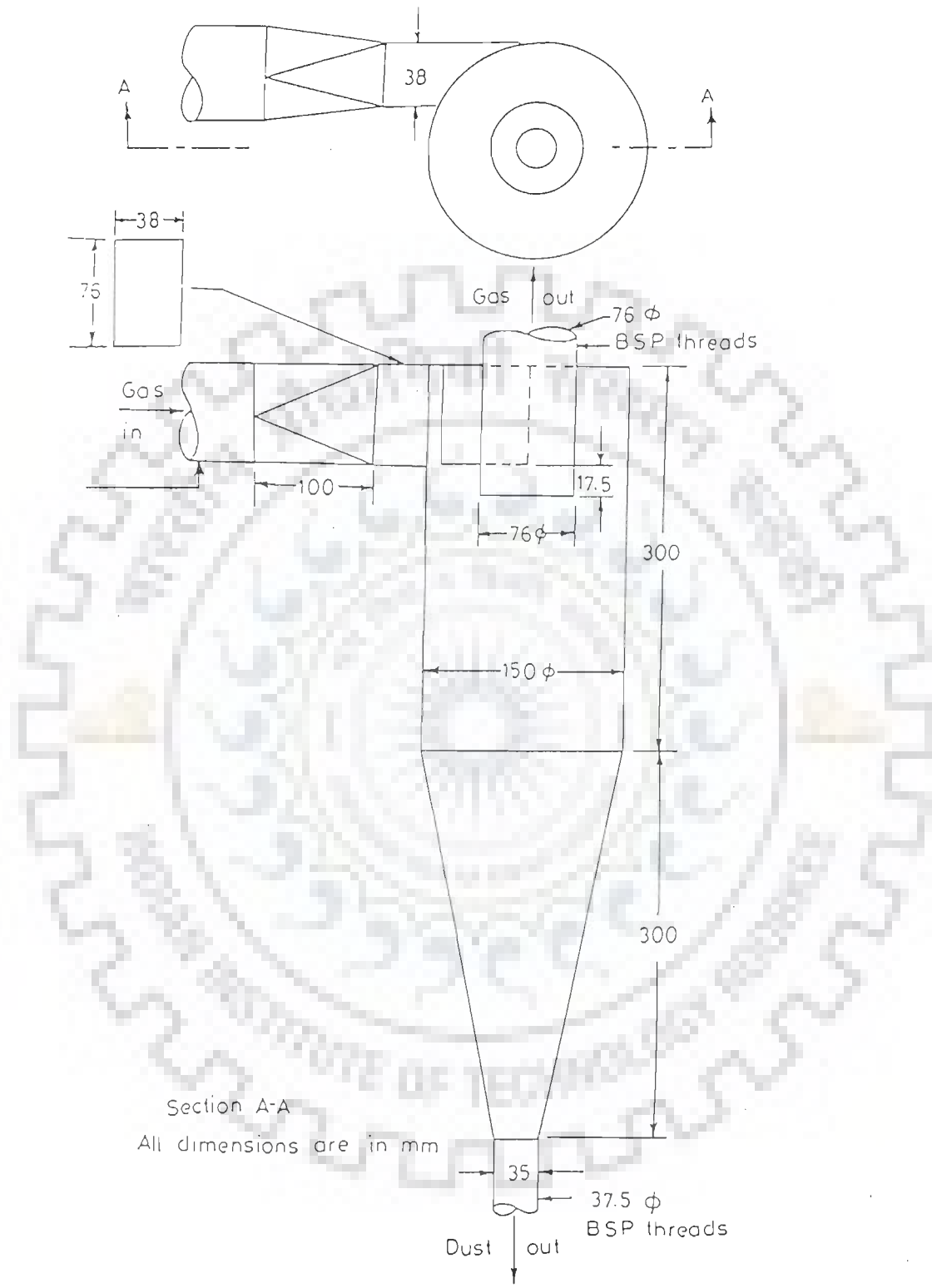


Fig. 3.6 Details of the cyclone

Thermocouples ( $T_1$  to  $T_3$ ) indicated bed temperature while thermocouples ( $T_4$  to  $T_8$ ) indicated temperatures of fluidizing column along its height. Thermocouples ( $T_9$  and  $T_{10}$ ) indicated the temperatures of transport disengagement section and sampling port.

### 3.7.2 Pressure Drop and Flow Rate Measurements

The pressure drops across various points in the fluidized bed gasifier assembly were measured using U-tube manometers with water as the manometric fluid.

The pressure was noted during each experimental run,

- (a) across the orificemeter for air flow rate measurement at the inlet to the calming section.
- (b) across the distributor plate and the bed charge of the fluidized bed gasifier
- (c) at the centre of the fluidizing column
- (d) in the transport disengagement section; and
- (e) across the orificemeter for measuring exit gas flow rate.

Specially fabricated, 15 mm inner diameter and 300 mm long shell and tube heat exchangers were used for cooling the pressure taps along the hot gasifier to enable rubber tubing connection with the manometers. The tubes in these heat exchangers were copper tubes of 6 mm outside diameter and were connected with the manometer limbs. Cooling water was circulated in the shell. The accuracy of the pressure measurement was  $\pm 1$ mm of water. Fig. 3.7 shows the location of thermocouple probes and pressure measuring taps fixed in the gasifier system.

The flow rate of the fluidizing and gasifying medium –air was measured by a calibrated orificemeter. The flow rate of the produced gas was also measured using another calibrated, but similar orificemeter and U tube water manometer. Its details are shown in Fig. 3.8.

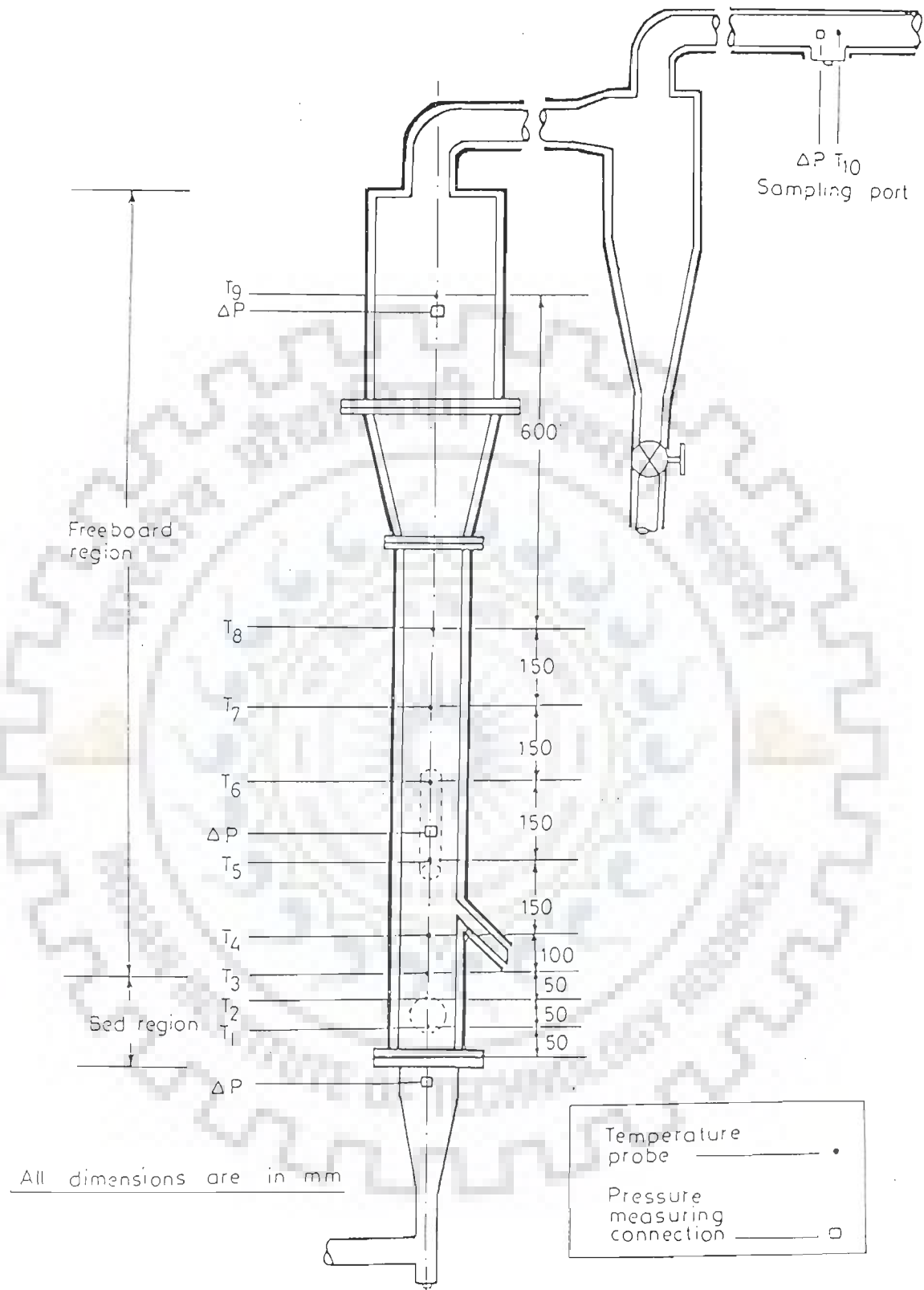


Fig. 3.7 Locations of the thermocouples and the pressure measuring taps in the gasifier system

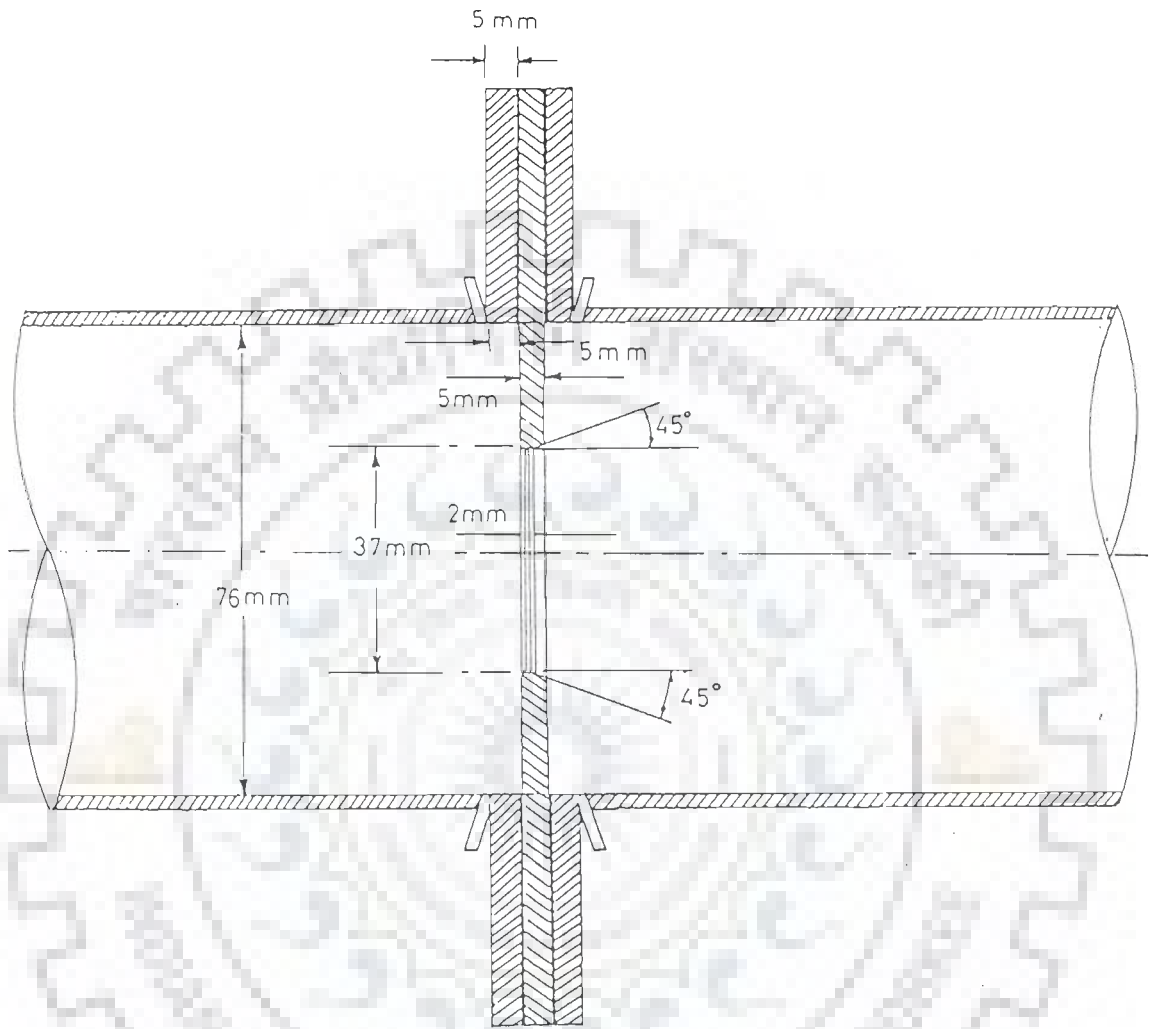


Fig. 3.8 The orifice meter for measuring gas flow



### 3.7.3 Feed Rate of Biomass

The feed rate of biomass was initially set approximately to the desired value using the input voltage control unit of the vibrating feeder. This value was however slightly modified according to the requirements of a particular experimental run so as to obtain the proper quality gas (judged only by its colour and the nature of its flare at the time of actual experimental run). Such value of feed rate that gave the best quality gas for a given equivalence ratio was measured by collecting the actual output of the vibrating feeder at the entry to the longer screw conveyor over one minute duration. Five samples were so collected and the averaged value was taken as the feed rate.

## 3.8 GASIFICATION RUNS

Each experimental run comprised of two different parts namely, the gasifier operation and the sampling and analysis of the gas. The gasifier operation included: start up of the gasifier, steady state operation, and shut down procedures. The gas sampling and analysis included tar sampling and analysis, particulate matter sampling alongwith the compositional analysis of the gas.

The gasification experiments were conducted to evaluate the performance of the fluidized bed biomass gasifier at different equivalence ratios (0.20 to 0.40) and fluidization velocities (0.53 to 0.73  $\text{ms}^{-1}$ ) with VRH and SD as the biomass materials. The amount of actual air needed for the complete combustion of the biomass was first calculated. The stoichiometric air for one kg of village rice husk (VRH) was found to be 4.85 kg where as for the sawdust it was found to be 5.2 kg. The desired value of equivalence ratio could be obtained by suitably adjusting the feed flow and airflow, based on the air requirement for complete combustion. The operational data for the gasification experiments are given in Tables 3.1.1 and 3.1.2 for village rice husk (VRH) and sawdust (SD), respectively. Gasification experiments were performed at four fluidizing air velocities of 0.53, 0.59, 0.68 and 0.73  $\text{ms}^{-1}$  and at five equivalence ratios

**Table 3.1.1 : Village Rice Husk Feed Rates and Air Supply Rates in Fluidized Bed Gasification Experiments**

<b>Airflow Rate (<math>m^3 s^{-1}</math>)</b>	<b>Fluidization Velocity (<math>ms^{-1}</math>)</b>	<b>Village Rice Husk Feed Rate (<math>kgs^{-1}</math>)</b>	<b>Equivalence Ratio <math>\phi</math>, (-)</b>
4.21x 10 <sup>-3</sup>	0.53	4.86x 10 <sup>-3</sup>	0.20
		3.88x 10 <sup>-3</sup>	0.25
		3.19x 10 <sup>-3</sup>	0.30
		2.77x 10 <sup>-3</sup>	0.35
		2.50x 10 <sup>-3</sup>	0.40
4.70 x 10 <sup>-3</sup>	0.59	5.41x 10 <sup>-3</sup>	0.20
		4.38x 10 <sup>-3</sup>	0.25
		3.61x 10 <sup>-3</sup>	0.30
		3.13x 10 <sup>-3</sup>	0.35
		2.77x 10 <sup>-3</sup>	0.40
5.36x 10 <sup>-3</sup>	0.68	6.25x 10 <sup>-3</sup>	0.20
		5.00x 10 <sup>-3</sup>	0.25
		4.16x 10 <sup>-3</sup>	0.30
		3.55x 10 <sup>-3</sup>	0.35
		3.11x 10 <sup>-3</sup>	0.40
5.76x 10 <sup>-3</sup>	0.73	6.66x 10 <sup>-3</sup>	0.20
		5.36x 10 <sup>-3</sup>	0.25
		4.44x 10 <sup>-3</sup>	0.30
		3.83x 10 <sup>-3</sup>	0.35
		3.33x 10 <sup>-3</sup>	0.40

**Table 3.1.2 : Sawdust Feed Rates and Air Supply Rates in the Fluidized Bed Gasification Experiments**

Air Flow Rate ( $\text{m}^3 \text{s}^{-1}$ )	Fluidization Velocity ( $\text{ms}^{-1}$ )	Sawdust Feed Rate ( $\text{kgs}^{-1}$ )	Equivalence Ratio $\phi$ , (-)
$4.21 \times 10^{-3}$	0.53	$4.58 \times 10^{-3}$	0.20
		$3.66 \times 10^{-3}$	0.25
		$3.05 \times 10^{-3}$	0.30
		$2.631 \times 10^{-3}$	0.35
		$2.27 \times 10^{-3}$	0.40
$4.70 \times 10^{-3}$	0.59	$5.13 \times 10^{-3}$	0.20
		$4.08 \times 10^{-3}$	0.25
		$3.38 \times 10^{-3}$	0.30
		$2.91 \times 10^{-3}$	0.35
		$2.55 \times 10^{-3}$	0.40
$5.36 \times 10^{-3}$	0.68	$5.83 \times 10^{-3}$	0.20
		$4.66 \times 10^{-3}$	0.25
		$3.88 \times 10^{-3}$	0.30
		$3.33 \times 10^{-3}$	0.35
		$2.91 \times 10^{-3}$	0.40
$5.76 \times 10^{-3}$	0.73	$6.25 \times 10^{-3}$	0.20
		$5.00 \times 10^{-3}$	0.25
		$4.16 \times 10^{-3}$	0.30
		$3.58 \times 10^{-3}$	0.35
		$3.11 \times 10^{-3}$	0.40

of 0.20, 0.25, 0.30, 0.35 and 0.40 for each fluidizing air velocity. Experimental observations were noted under steady-state condition of gasification at several times-on-stream.

### **3.8.1 Start-Up of the Gasifier**

A predetermined quantity of sand of suitable size as the carrier solid was loaded into the reaction through the loading port. The blower was switched on and the airflow rate control valve was opened slowly to the maximum. After fluidizing the sand for 2-3 minutes the airflow was stopped. The biomass-feeding unit was started and a little amount of biomass was fed. Two side peepholes (12mm diameter sockets provided vertically to the opposite side of the feeder, on the reactor wall slightly above the feeding point and arranged in axial direction) were now opened. Dropping a little amount of kerosene oil and igniting the biomass layer of the bed charge initiated combustion inside the reactor. The auger water-cooling system and the cooling circuits of the manometer connections were immediately turned on. The biomass feeding was continued. The peepholes and the sand loading port were open to atmosphere and the air was sucked downward through the bed in the reverse direction. The temperature of the bed was continuously monitored. After sometime, the peepholes and the sand loading port were closed and air was allowed to flow upward through the bed. This initial combustion of the biomass was continued till the bed temperature was found to be around 600°C. Combustion for 15-20 minutes ensures the heating of the bed and the gasifier assembly.

### **3.8.2 Steady State Operation of the Gasifier**

Once the fluidized bed combustion operation was stable and the bed temperature was found to be about 600°C, the airflow rate and the feed flow rate were adjusted such that a desired value of equivalence ratio was obtained. The peepholes and

the sand loading port were closed properly. Thus the reactor was turned into gasification mode. The bed temperature was found to drop immediately, but could be made stable within  $\pm 20^{\circ}\text{C}$  by the careful manipulation of the airflow and the biomass feed flow while maintaining the same equivalence ratio. This operation was tricky and a complex one as even a very slight variation in the feed flow rate or the airflow rate could turn the process into combustion (indicated by a sharp rise in temperature) or disturb the process (indicated by sharp downfall of the bed temperature). However, once set in, the gasification process continued without trouble. The gas from the cyclone outlet was flared at the exit end of the pipe. To the trained eyes, it was easy to recognize the gas of combustible quality. The stable bed temperature ( $\pm 20^{\circ}\text{C}$ ) was the indication of the attainment of steady state of the process operation. At this stage the dust collector was emptied and reset. All the temperatures and pressures were noted under steady-state operation at several times-on-stream. Gas sampling and tar sampling were also carried out under steady-state condition. At least samplings were done under each steady state condition. The data were processed and the averaged values have been reported. The bed region temperature and the quality of the flare were the gross indicators of the process stability.

### **3.8.3 Shut Down of the Gasifier**

After the sampling of the tar and the gas, and the measurements of temperature and pressure were over, the biomass feeder was switched off and the blower was continued to supply air for some more time, to burn off the residual biomass left in the bed. The dust collector was emptied and the char-ash mixture was consolidated and stored. The reactor cooled down slowly. The unit was completely shut off and the routine cleaning was initiated.

### **3.9 SAMPLING OF GAS**

#### **3.9.1 Gas Sampling Train**

A gas sampling train, as shown in Fig. 3.9, was assembled for the purpose of collection of gas samples during the gasifier operation. A stainless steel tube [10mm internal diameter, 12 mm external diameter and 500 mm long] was wrapped at one end with stainless steel mesh of 300  $\mu\text{m}$  openings to form a shape of the small bulb. The other end of the tube was threaded and connected to another stainless steel tube of the same dimensions using a threaded sleeve. This second tube was water-cooled by double pipe arrangement with water flowing through the annulus. This facilitated the cooling of the hot gas at the time of sampling. The other end of this tube was connected to the suction side of a vacuum pump (0.18 kW) with the help of a good quality rubber hose pipe-via a small cylindrical chamber packed with glass wool. The glass wool-filled chamber worked as a filter to intercept any dust/char, ash and moisture entering the vacuum pump. The whole assembly was leak-tested under pressure before its use for the sampling.

#### **3.9.2 Gas Sampling**

Gas sampling was carried out using the gas sampling train through the sampling port provided in the gas exit pipe located down-stream of the cyclone and upstream of the flow measuring orifice plate. Once the gas temperature at the port reached about 250°C, the sampling was under taken. The stainless steel wire mesh wrapped end of the tube was inserted through the port such that it was positioned midstream of the gas flow. The small annular space between the sampling port and the sampling tube was packed with ceramic wool to avoid the sampled gas being contaminated from the atmospheric air. Water was allowed to flow through the annular cooling circuit and the vacuum pump was switched on. The sampled gas was collected in nylon bags (2 liter capacity) after flushing the bags with the gas by repeated cycles of filling/emptying. Three samples were collected during an experimental run at 5-minute intervals. The nylon bags were tightly clamped and stored at room conditions for analyses.

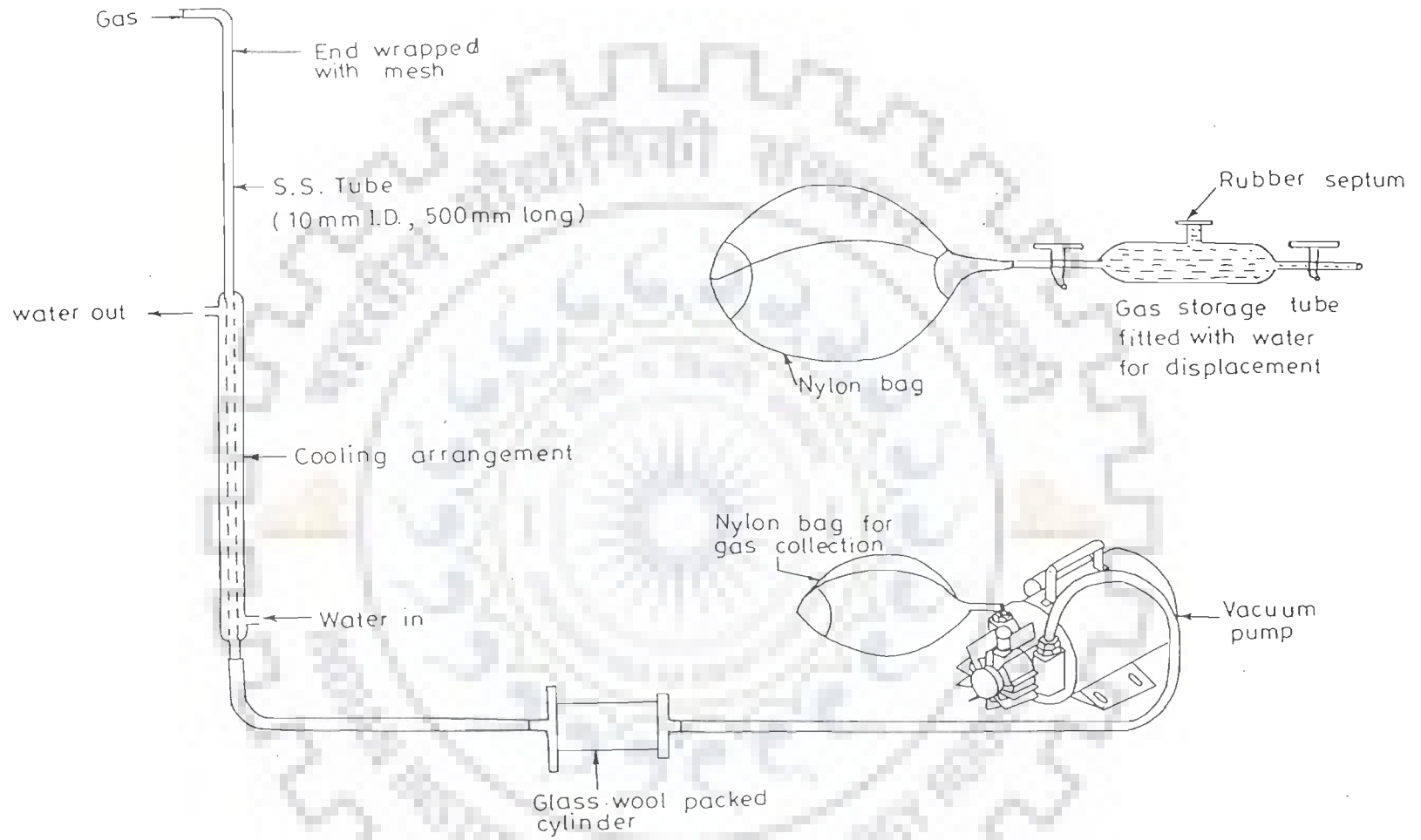


Fig. 3.9 A schematic of the gas sampling train

### 3.9.3 Compositional Analysis of Gas

The gas samples stored at laboratory conditions were analyzed in terms of their composition using a gas chromatograph. Argon was used as a carrier gas with a flow rate of  $30 \text{ ml min}^{-1}$ . A stainless steel column of 3.2 mm diameter and 2437 mm length, packed with molecular sieve 5A, 60/80 mesh and the thermal conductivity detector were used for determining the composition of the gas ( $\text{H}_2$ ,  $\text{O}_2$ ,  $\text{N}_2$ ,  $\text{CH}_4$  and  $\text{CO}$ ). The compositions of  $\text{CO}_2$  and gaseous hydrocarbons ( $\text{C}_2\text{H}_2$  &  $\text{C}_2\text{H}_4$ ) were determined using a stainless steel column of 3.2 mm diameter and 2437 mm length packed with Porapak Q. The temperature conditions maintained were: detector at  $100^\circ\text{C}$ , injector at  $100^\circ\text{C}$  and oven at  $90^\circ\text{C}$ . The gas chromatograph was calibrated using standard calibration mixture.

### 3.10 TAR SAMPLING

#### 3.10.1 Tar Sampling Train

An improvised tar sampling train (Abatzoglou et al. 2000; Neeft, 2000; Hasler, 2000) was assembled for use with the gasifier. It consisted of the following sub units, which were connected serially.

- i. A detachable nozzle made of stainless steel.
- ii. A thimble holder with its casing (housing) and a long stainless steel tube integral with the casing.
- iii. An impinger train consisting of 5 impinger glass bottles connected serially and housed in a thermally insulated cabinet.
- iv. A cabinet housing a negative pressure gauge, a flow control valve and a rotameter, and
- v. A vacuum pump (0.18 kW).

Fig. 3.10 shows the schematic view of the tar sampling train.



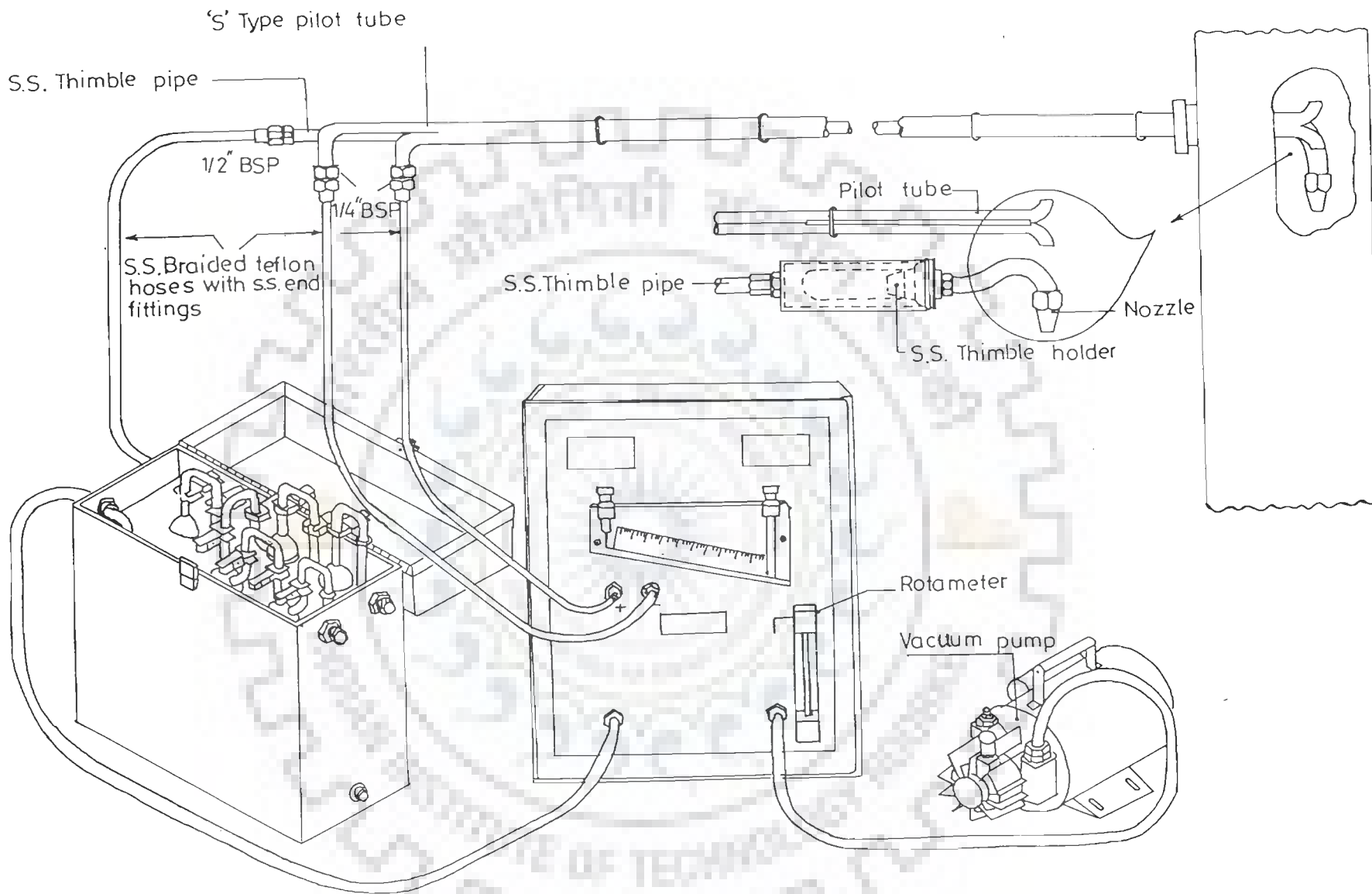


Fig.3.10 A schematic view of the tar sampling train

The detachable nozzle was a 'L' shaped probe made of stainless steel. One end was free to be placed in the gas stream while the other was screwed onto a thimble holder assembly. The thimble holder assembly (details are shown in Fig.3.11) was also made of stainless steel. It consisted of a filter (cartridge) holder and an outer casing. The outer casing could be screwed on the filter holder. The outer casing was integral with a 12 mm internal diameter, 100 mm long stainless steel tube. The free end of this tube was connected to the inlet of the impinger cabinet with the help of a short flexible heat resistant pipe. The impinger cabinet housed five glass impinger bottles of 250ml capacity, all connected in series and cooled by ice surrounding them. The first two bottles contained steel balls, while the third and fourth contained 100ml each of dichloromethane (DCM). The last impinger bottle was left empty and was meant to capture any entrained and carried over droplets of dichloromethane. The exit of the impinger cabinet was connected to a valve that controlled the flow rate, a rotameter to measure the flow rate of the sampled gas and finally to a vacuum pump. No gas was sucked when either the valve was closed or the vacuum pump was not operated. This fact allowed the thimble holder assembly and its steel pipe to undergo preheating to a temperature higher than the tar condensation temperature of 150<sup>0</sup>C, while it was kept in a wait-ready mode for sampling. This preheating was also facilitated by the thermal insulation provided around the thimble housing and its pipe. The thimble holder assembly was kept in vertical position with the help of a specially fabricated tripod stand, so that the nozzle tip was coaxial with the gas outlet pipe, while the sampling was in progress.

### 3.10.2 Tar Sampling

The sampling of tar was carried out under pseudo isokinetic conditions while the gasifier remained operationally stable after the attainment of steady state condition. The procedure adopted as well as the sampling train specifications followed the prescriptions of the draft protocol of Abatzoglou et. al. (2000) and the suggestions of Neef (2000), and Hasler (2000).

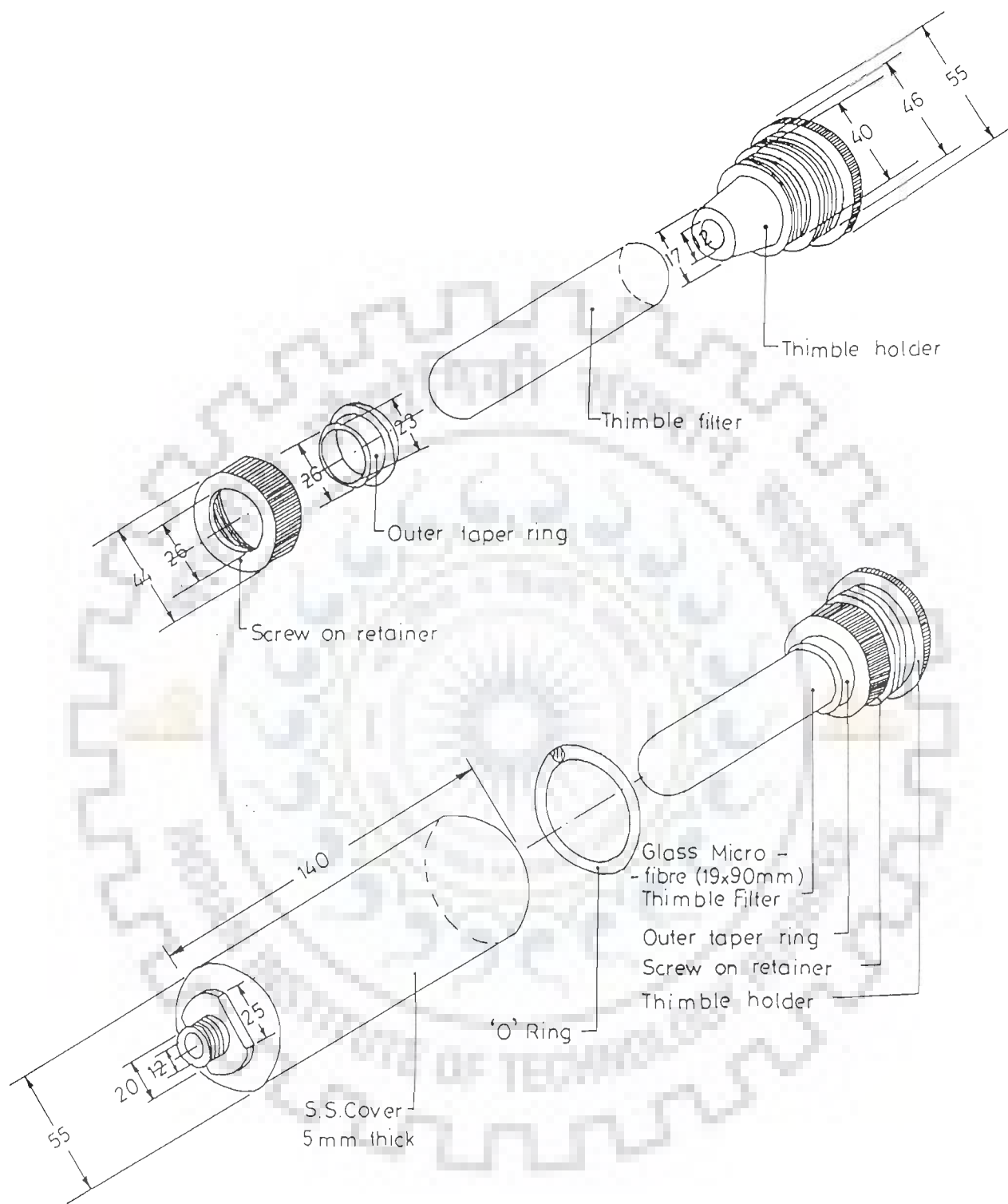


Fig. 3.11 Details of the thimble holder assembly of the tar sampling train

The overall procedure consisted of (1) Pre sampling procedure, (2) Sampling procedure, and (3) Post sampling procedure. The Pre sampling procedure included the (i) preparation of the thimble filter, (ii) establishing isokinetic conditions, and (iii) installation of sampling and Soxhlet's apparatus. A schematic representation of the procedure is shown in the Fig. 3.12.

Glass microfibre thimbles of size 19 mm internal diameter x 90 mm length (Whatman Make) capable of withstanding temperature upto 550<sup>0</sup>C were used. These thimbles had high flow rate and loading capacity. For every experimental run, one fresh thimble was used. Prior to its use for the sampling, the thimble was dried in a constant temperature oven at 105<sup>0</sup>C until constant weight was obtained and then was allowed to acclimatize/cool in a desiccator. It was then weighed accurately to determine its initial weight and was then fitted onto the thimble holder gently inside the thimble housing of the tar sampler.

Once the gasifier attained its steady state operation as that indicated by the different stable temperatures and the stable quality of the flare, the exit gas velocity was measured using a pitot static tube. Based on the velocity of the gas stream, a nozzle of suitable diameter was selected and the isokinetic flow rate at which the gas was to be drawn was decided. The nozzle (detachable) was fitted on the thimble housing and the flow rate was set using the control valve provided in the connection line before the rotameter and the vacuum pump.

After establishing the isokinetic sampling conditions, the thimble filter assembly and its stainless steel pipe were clamped to a tripod stand such that the nozzle was properly placed in the mid of the gas stream and that the thimble holder was held in the vertical position. The free end of the stainless steel pipe was connected to the inlet of the impinger cabinet. The exit of the impinger bottles cabinet was connected to another cabinet housing a suction pressure gauge, a flow control valve and a rotameter. The train was leak-tested before the commencement of the sampling. A Soxhlet's extraction apparatus was also kept ready (Extractor capacity 100 ml, flask capacity, 1000 ml) with 250 ml of dichloromethane filled in its bottom flask.

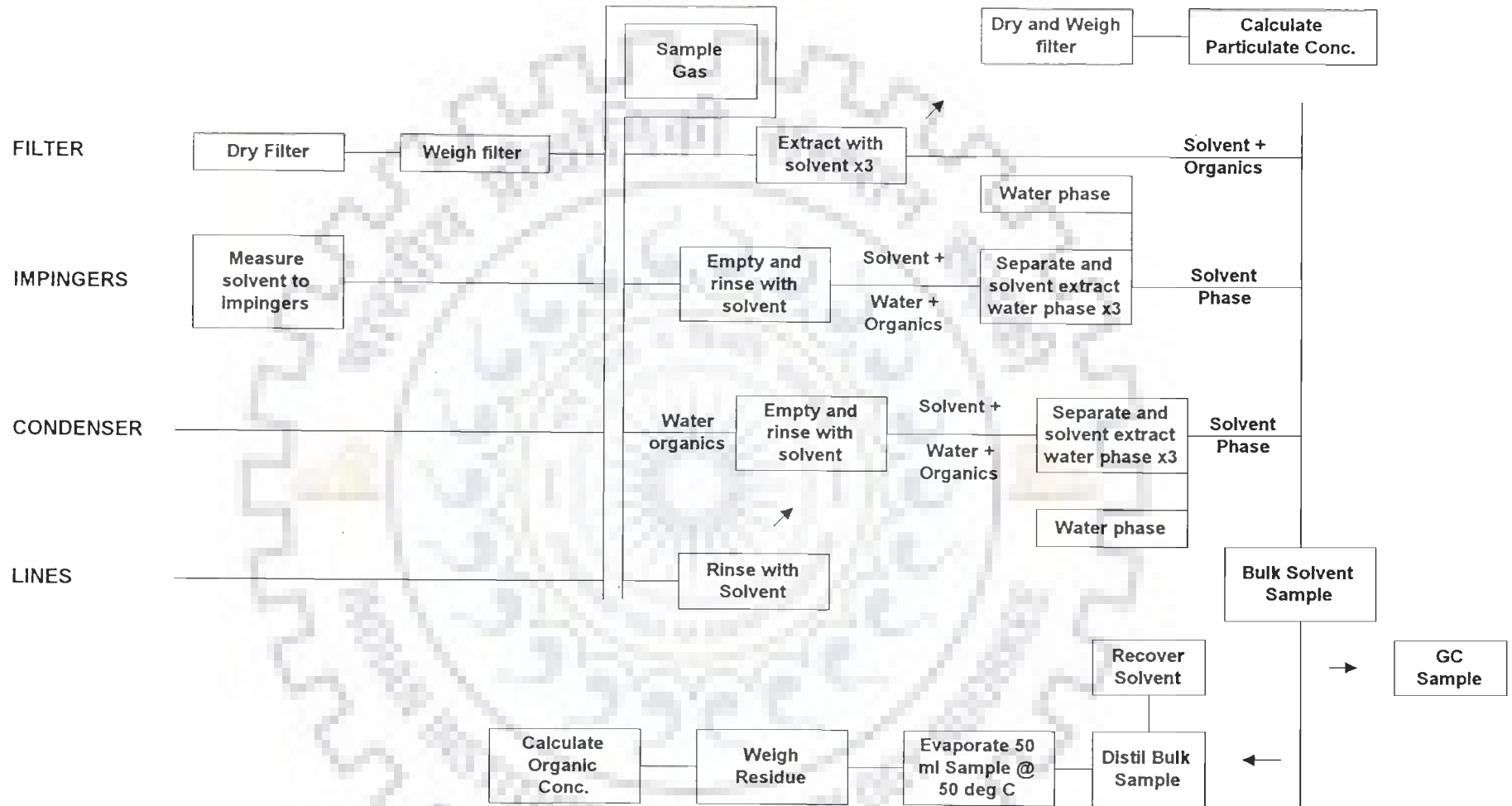


Fig. 3.12 : Schematic for the Protocol [Abatzoglou et al. (2000)]

After the nozzle and the thimble housing got preheated to a temperature of about 160-200<sup>0</sup>C, the vacuum pump was switched on. No gas could enter the nozzle when the vacuum pump was not running. The preheating of the nozzle and the thimble housing took about 10 minutes as cladding with insulation (ceramic wool) minimized the convective heat losses from their surface. The time of the starting of the pump and the suction pressure were noted. The sampling continued for about one hour. This sampling time was sufficient to have sufficient amount of tar trapped in DCM kept in the third and fourth impinger bottles for further analysis. The gas temperatures at the sampling port and at the exit of the rotameter of the sampling train were noted.

After switching off the vacuum pump the sampling was terminated and the nozzle of the sampler was carefully withdrawn from the port. The whole assembly was always held vertical so that the thimble remained vertical to avoid loss of dust particles. The thimble housing was opened and the thimble was carefully taken out and transferred to the Soxhlet's apparatus. Extraction was immediately started to avoid polymerization of sampled tar upon cooling. The temperature of the mantle heater was set at 60<sup>0</sup>C. After three extractions the solvent was totally clear. The thimble was removed and stored in vertical position for the further determination of the particulate matter. The stainless steel pipe of the sampler and the flexible hose used to connect impinger bottles cabinet were rinsed with DCM. This rinsed amount of dichloromethane together with the DCM of the impingers was transferred to a separating funnel to separate carefully the little amount of water associated with it. The Dichloromethane was now carefully transferred to the flask of the Soxhlet's apparatus and continually extracted till a concentrated mixture of the tar and dichloromethane were left in the flask of the Soxhlet's apparatus.

### **3.10.3 Determination of Particulates**

The thimble filter after extraction in Soxhlet's apparatus was dried in a constant temperature oven at 105<sup>0</sup>C for about an hour by keeping it vertical. The dried thimble

filter was then weighed. The difference in the weights of the thimble before and after the sampling run was the amount of the particulates. Together with the amount of producer gas sampled and its temperature, the particulate concentration was calculated in  $\text{mgNm}^{-3}$ .

#### 3.10.4 Gravimetric analysis of tar

The amount of tar was determined by means of solvent distillation and evaporation and the determination of the weight of the organic contaminants.

The thick mixture of tar and dichloromethane was heated at  $60^{\circ}\text{C}$  using a hot water bath. The heating was continued till most of the dichloromethane was distilled off. The residual mixture was then transferred to a semi-circular dish of known weight ( $\pm 0.1$  mg). The dish was kept in a drying cabinet at  $60^{\circ}\text{C}$  to remove all the dichloromethane. The dish was then transferred to a desiccator and allowed to cool down to room temperature. The dish was weighed to  $\pm 0.1$  mg accuracy and the tar amount was calculated. The tar content of the gas was determined from the amount of sampled gas and the tar amount obtained.

---

## RESULTS AND DISCUSSION

### 4.1 FLUIDIZATION BEHAVIOUR OF BIOMASS MATERIALS

In this section, the results of the determination of physico-mechanical properties and cold flow fluidization studies of biomass materials, namely village rice husk, mill rice husk, saw dust, bagasse and press mud have been presented and discussed.

#### 4.1.1 Physico-mechanical Properties of Biomass Materials

The thermochemical processing of a biomass material in a fluidized bed requires *a priori* understanding of its fluidization characteristics (Aznar et al., 1992a). The correct biomass/waste/residue processing/gasification/incineration in a fluidized bed is governed by the hydrodynamic factors and its kinetics (Herguido et al., 1992).

The physico-mechanical properties of biomass materials relevant to their fluidization and bulk solid flow studies are the bulk density, particle density, particle size, packed bed voidage, angle of repose and the angle of slide. In Table 4.1.1(a), such properties for the biomass materials selected for the present study are given. Bulk density of a material is its overall density including inter-particle distance of separation. For biomass fuels, this property should be determined *in situ* for specific applications (Iyer et al., 1997). It is noted that the biomass materials under study have bulk densities lower than  $200 \text{ kgm}^{-3}$ . Bulk density forms the basis of classification of biomass as woody ( $\rho_b > 250 \text{ kgm}^{-3}$ ) and powdery ( $\rho_b < 250 \text{ kgm}^{-3}$ ) biomass (Grover et al., 1989; Sridhar et al., 1996). On the above basis, the biomass materials selected for the present study may be categorized as powdery/non-woody/fine biomass materials. A fluidized bed gasifier can accept low bulk density, fine granularmetry biomass as feedstocks (Schoeters et al., 1989, Gomez et al., 1995). Hence, these can be suitable feedstocks for thermochemical conversion using a fluidized bed gasifier. In a fluidized bed reactor, the



mixing of biomass material is important for uniform temperature distribution. The mixing characteristics are dependent on the bulk density (Hemati et al., 1990). The residence time of a biomass material in a fluidized bed reactor is a factor influenced by its bulk density-lower the bulk density, the lower is the residence time (Bilbao et al., 1988). Bulk density is also an important parameter for consideration in the transportation and storage of biomass materials.

Particle density is the density of a particle including the pores or voids within the individual solids; where as skeletal density or true density is the density of a single particle excluding pores (Cheremissinof, 1984). In Table 4.1.1(a), the particle densities of the selected biomass materials as determined in the laboratory by light paraffin oil pycnometry have been given. This property is scarcely reported in literature; as such the values could not be compared. However, for rice husk, a true particle density value of  $750 \text{ kgm}^{-3}$  has been reported (Govindrao, 1980).

The physical shapes and sizes of the biomass materials are complex. There is no established method, free from ambiguity, to determine the physical sizes of such geometrically irregular shapes as of biomass materials. In the absence of a suitable method, the sizes are generally expressed on the sieve size used for their fractionation. Sen and Ghosh (1992) and Mansaray and Ghaly (1992) have conducted sieve analyses to express the size fractions of rice husk. The values reported in Table 4.1.1(a) were the size fractions of the selected biomass materials adopted for the present study.

The packed bed porosity values for the biomass materials are given in Table 4.1.1(a). For rice husk, Choudhury et al. (1994) have reported a bed voidage value of 0.80. It is to be noted that this value is very sensitive to the degree of packing of the material, and therefore, may vary from one run to another unless a common procedure for loading the material into the experimental container is adopted.

The values of angles of repose and slide for the biomass materials have been given in Table 4.1.1(a). The angle of repose of a biomass material is defined as the

**Table 4.1.1(a) : Physico-mechanical Properties of Biomass Materials**

<b>Properties</b>	<b>Sawdust</b>	<b>Village Rice Husk</b>	<b>Mill Rice Husk</b>	<b>Pressmud</b>	<b>Bagasse</b>
Particle size	-2.032 +0.420 mm	-2.032 +0.420 mm	-2.818+1.00 mm	-1.00 +0.350 mm	-850 +350 $\mu$ m
Particle size in terms of Standard Sieve Size Fraction (ISS)	-40+200	-40+200	-100 + 280	-35 +100	-30 + 85
Bulk density, kgm <sup>-3</sup>	160	150	110	110	75
Particle density, kgm <sup>-3</sup>	1315	1327	1192	1051	961
Packed bed porosity (-)	0.87	0.88	0.90	0.89	0.92
Angle of repose, degree	31	33	29	33	32
Angle of slide, degree	50	52	56	51	53

**Table 4.1.1(b) : Characteristics of Carrier Solids**

<b>Carrier Solid</b>	<b>Size (<math>\mu</math>m)</b>	<b>Standard Sieve Size Fraction (ISS)</b>	<b>Particle Density, <math>\rho_p</math> (kgm<sup>-3</sup>)</b>	<b>Bulk Density, <math>\rho_b</math> (kgm<sup>-3</sup>)</b>	<b>Packed Bed Voidage <math>\epsilon</math>, (-)</b>
Sand -A	-500 + 350	-35+50	2930	1450	0.5069
Sand - B	-850+710	-70+85	2930	1370	0.5324
Bauxite-A	-500 + 420	-40+50	2100	1320	0.3714
Bauxite-B	-850+710	-70+85	2100	1308	0.3771

angle between a line of repose of loose biomass material formed as a heap and a horizontal plane. Its value depends on the magnitude of friction and adhesion between particles and determines the particle mobility. This value is of significance in the design of storage bins and feeding equipment. There are two angles of repose – one is ‘poured angle of repose’ and the other is ‘drained angle of repose’. The poured angle of repose is obtained when a pile of solids is formed and a drained angle of repose is formed when the solids are drained from a bin. In the storage and feeding of biomass materials, the ‘drained angle of repose’ is more important but the difference between the two angles of repose is not appreciable. Since the poured angle of repose is easier to measure, this angle has been measured for all the materials, without vibration of the horizontal support surface. In general, it can be said that the lower the angle of repose is, the freer flowing of the material is attained. The values of angle of repose obtained for the biomass materials used in the present study are found to be lower than that of fine coal (Angle of repose = $36^{\circ}$ , Bulk density= $0.95 \text{ gcm}^{-3}$ ; Cheremissinoff, 1984) and as such do not pose any special problem in their feeding. It may, however, be noted that the angle of repose of a material is very sensitive to its moisture content.

The angle of slide is important in the design of chutes, bins and hoppers. It provides a measure of the relative adhesiveness of a biomass material to a dissimilar surface. The angle depends on the type of particles, the physical and surface properties and the surface configuration. An idea of these angles helps prevent bridging and arching of biomass during feeding in a fluidized bed.

The physico-mechanical and bulk solid flow properties of the carrier solids have also been determined. These are presented in Table 4.1.1(b).

#### **4.1.2 Fluidization Characteristics**

Owing to their peculiar and complex shape, low bulk density ( $<200 \text{ kgm}^{-3}$ ) and poor bin (hopper/bunker) flow characteristics (due to very high angle of repose and

slide), biomass materials exhibit poor gas fluidization characteristics, if fluidized alone. The fluidization of such biomass materials is facilitated by adding and mixing a second solid, called a carrier solid or a fluidizing solid medium, which has good fluidization characteristics. The carrier solid must be chemically inert and thermally stable. Silica sand and alumina have been used frequently in different studies. Here, the fluidization characteristics of carrier solids, namely sand (of two size fractions) and bauxite (of two size fractions) and of their mixtures formed by admixing the two carrier solids or a carrier solid and a biomass material in different mass (or volume) ratios are presented.

To study the possibility of fluidization of a biomass material as a single component bed charge, an experiment was conducted with village rice husk (VRH) as bed material. The ratio of the height of the bed charge to the column diameter (i.e.  $H/D$ ) was kept equal to unity. Village rice husk was selected because it was fluffy, non granular and that there were some reports available about its fluidization (for e.g. Sen and Ghosh, 1992). An attempt was made to fluidize rice husk in the set up described in Section 3.4.1. It was found that the bed pressure drop continuously fluctuated from the beginning of the experiment. At lower superficial air velocities (less than  $52 \text{ cms}^{-1}$ ), the rice husk particles remained interlocked increasing the bed pressure drop. As the air flow rate and hence the superficial air velocity was increased, the air bypassing through vertical channels and passages in the bed mass was observed, leading to the decrease in bed pressure drop. A further increase in the superficial air velocity made the whole aggregated bed lifted up like a piston. Good fluidization was observed at higher air velocities ( $> 52 \text{ cms}^{-1}$ ), although momentarily, till the rice husk particles got aligned themselves vertically providing free channels and air passages through the bedmass. During the fluidization of shallow beds ( $H/D < 1$ ) the rice husk particles were observed to be more like elutriating than fluidizing. Thus it was concluded that the fluidization of the rice husk particles alone as bed material was not possible, and no realistic data for superficial air velocity versus bed pressure drop could be obtained. From these

experimental runs and other reports in literature it was also inferred that a biomass material alone is not fluidizable. This is in agreement with the observations of Aznar et al. (1992a) and Hemati et al. (1990). This observation, however, contradicts the observations of Sen and Ghosh (1992) who could obtain the pressure drop – air velocity data to determine the  $U_{mf}$  for rice husk particles.

Fig. 4.1.1 shows the plot of superficial air velocity,  $U_s$  against the pressure drop,  $\Delta P$  for the packed and fluidized bed of sand particles of size fraction  $-500 + 350 \mu\text{m}$ . The packed bed height to diameter ratio,  $H/D$  was 1. It is seen that for this size fraction the packed bed and the fluidized bed data for increasing and decreasing superficial air velocities show a similar trend with no hysteresis. Similar characteristics were observed for the sand of size fraction,  $-850 + 710 \mu\text{m}$  and bauxite particles of size fractions,  $-500 + 420 \mu\text{m}$  and  $-850 + 710 \mu\text{m}$ . An increase in  $H/D$  ratio increased the pressure drop at any superficial air velocity. No distortion was observed from the normal packed bed and fluidized bed characteristics during the experiments with sand and bauxite particles. A representative plot for sand particles for  $H/D$  ratio varying from 1 to 1.5 is shown Fig. 4.1.2. The use of carrier solids in fluidized bed thermal gasification of biomass materials indicates that a  $H/D$  ratio of 1.0 for carrier solids is the best for facilitating fluidization (Aznar et al. 1992). In view of this, all the experiments were performed at  $H/D$  ratio equal to 1.0 for the carrier solids.

Figure 4.1.3(a) shows the plots of  $\Delta P$  versus  $U_s$  for sand and bauxite particles. It is seen that larger is the size of particles, the lower is the pressure drop at the same  $U_s$ . The minimum fluidization velocity, however, increases with the increase in particle size for the same material. The effect of particle density on the fluidization characteristics of materials having the same size fraction has been shown in Fig. 4.1.3(b). It is found that sand having higher particles density had higher minimum fluidization velocity. Fig. 4.1.4 shows the plot of  $\Delta P$  versus  $U_s$  for sand and bauxite of similar size fractions and their admixture. It is seen that the density difference between

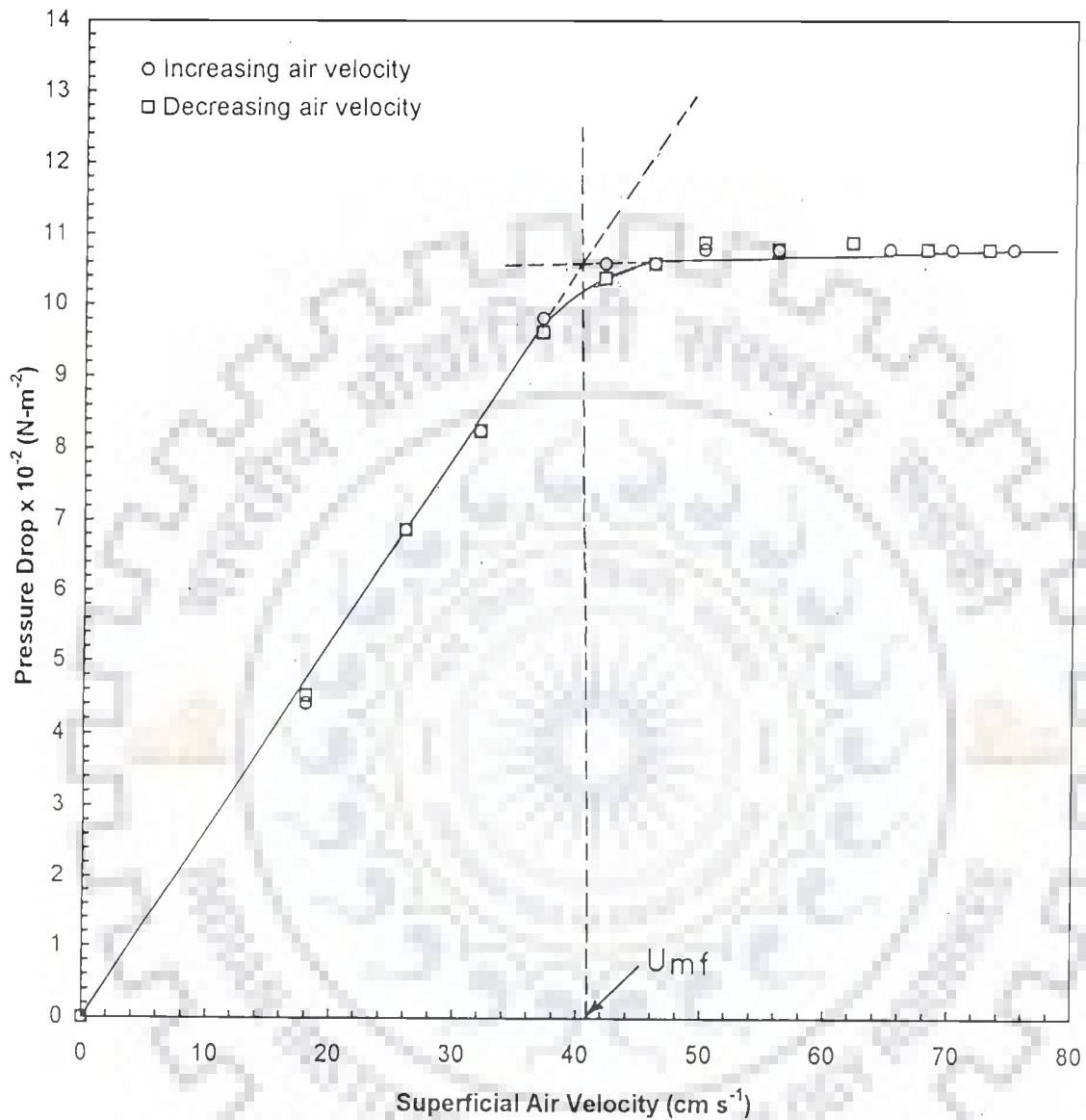


Fig. 4.1.1 : Variation of Pressure Drop with Superficial Air Velocity for Fluidization of Sand ( $d_p = -500 + 350 \mu\text{m}$ )

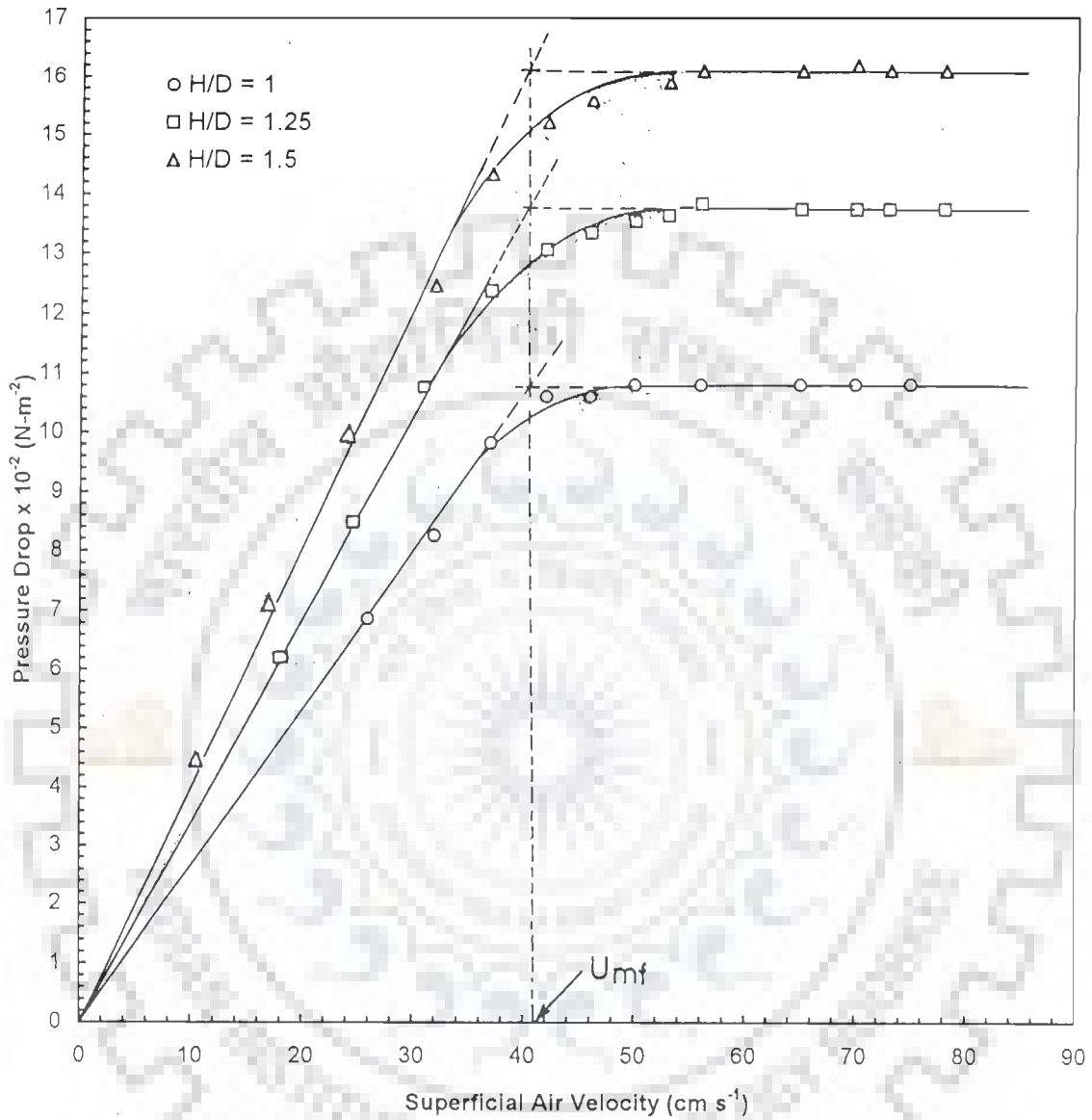


Fig. 4.1.2 : Variation of Pressure Drop with Superficial Air Velocity for Fluidization of Sand ( $d_p = -500 + 350 \mu\text{m}$ ) for Different Bed Height to Diameter Ratios

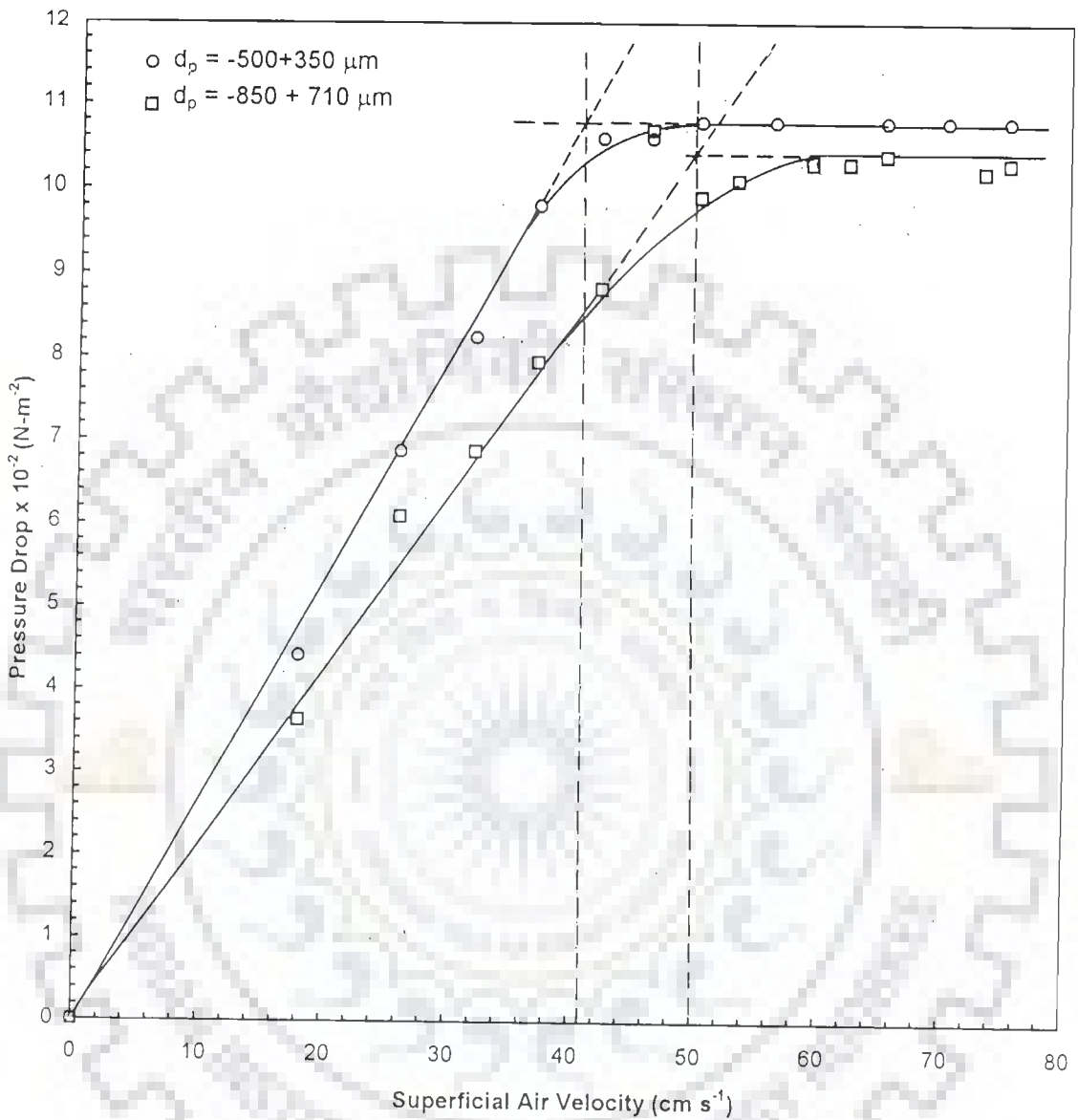


Fig. 4.1.3(a) : Variation of Pressure Drop with Superficial Air Velocity for Fluidization of Sand of Different Particle Sizes

Particle Density =  $2930 \text{ kgm}^{-3}$ ;  $H/D = 1$



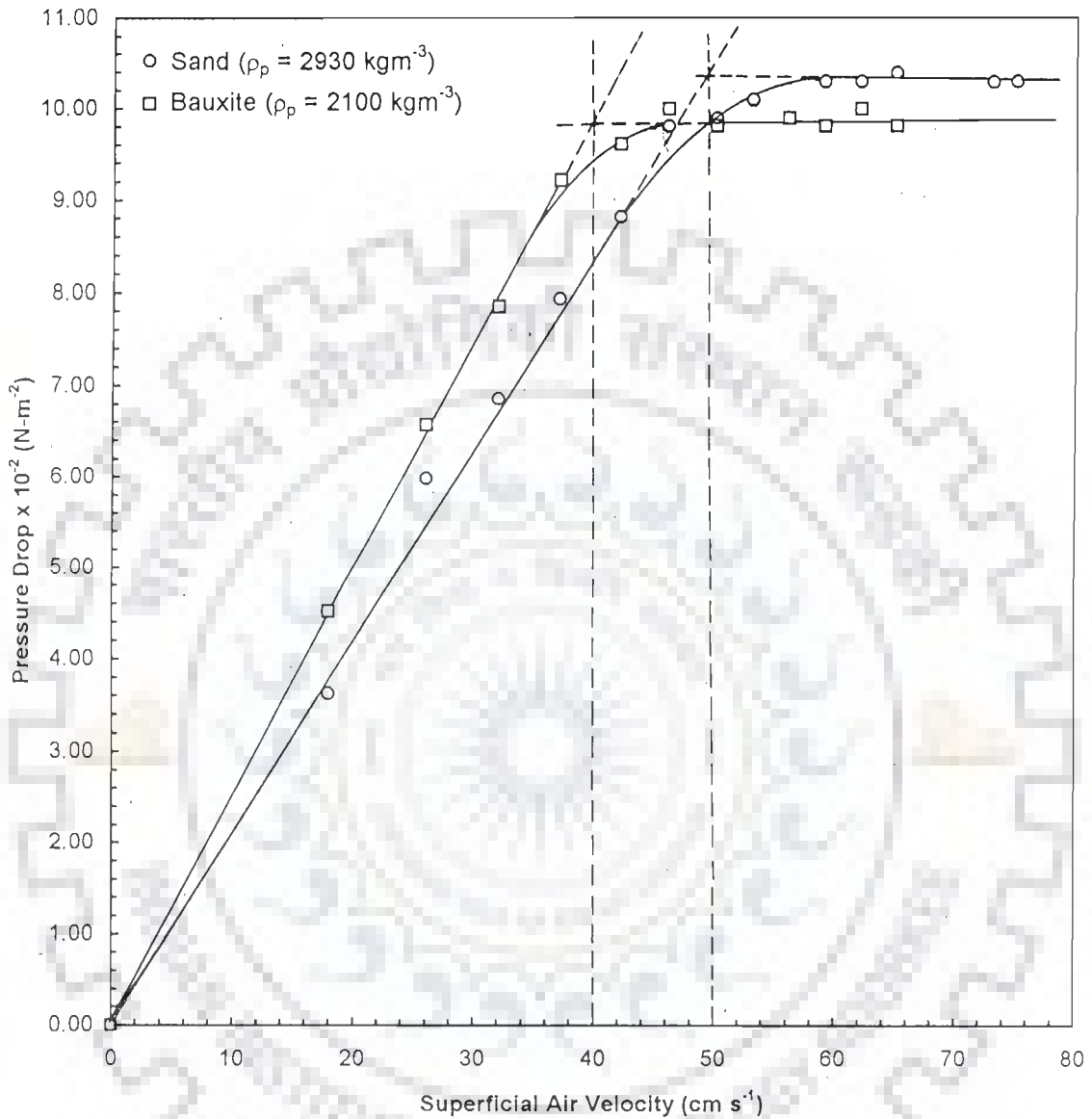
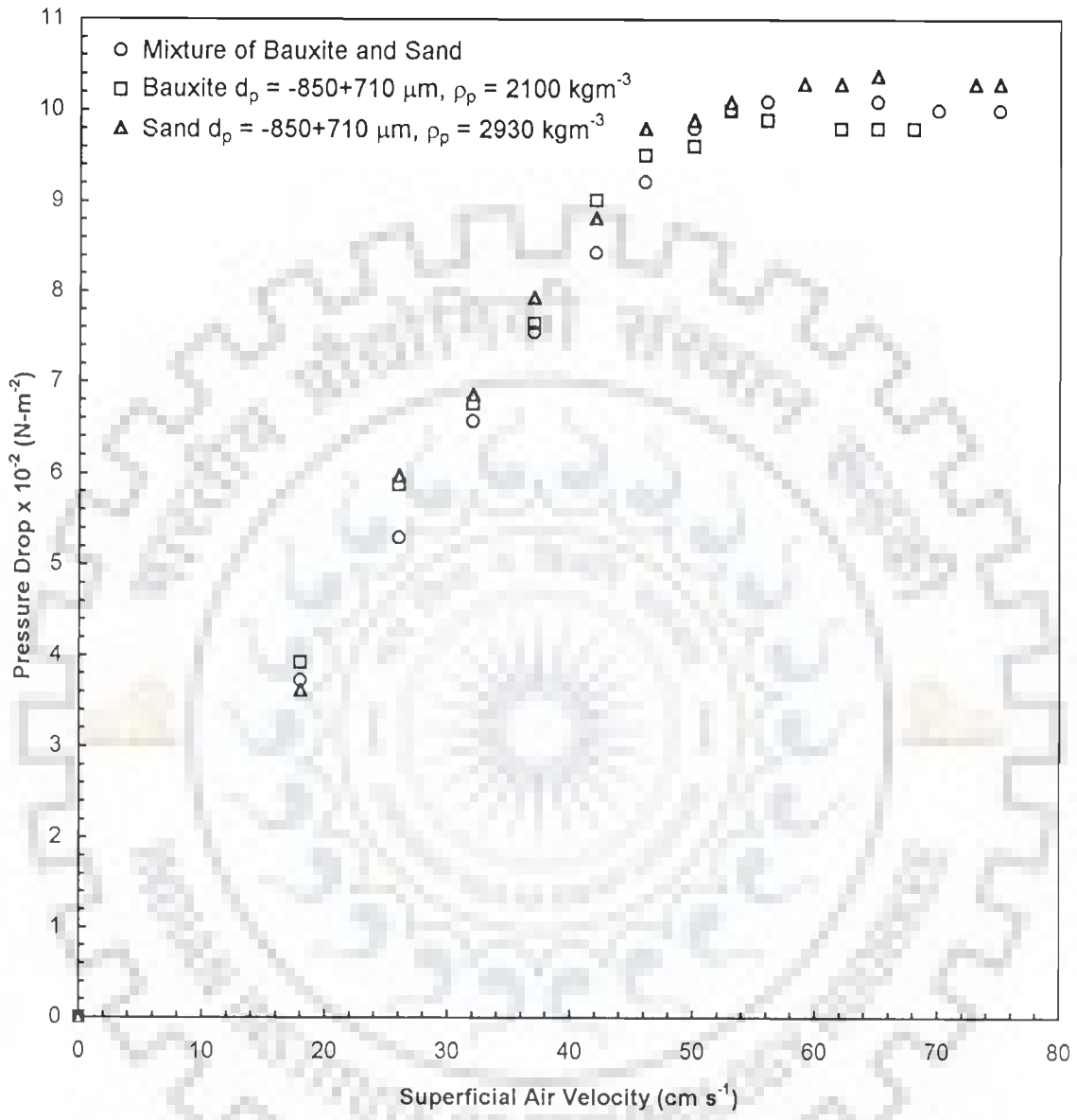


Fig. 4.1.3(b) : Variation of Pressure Drop with Superficial Air Velocity for Fluidization of Carrier Solids of Different Densities but Same Particle Size ( $d_p = -850 + 710 \mu\text{m}$ )



**Fig. 4.1.4 : Variation of Pressure Drop with Superficial Air Velocity for Sand and Bauxite of Same Particle Sizes and Their Mixtures (1:1 Vol., H/D = 1)**

the sand and the bauxite, mixed in 1:1 volume ratio, with H/D ratio maintained at 1.0 does not show any noticeable deviation from the quality of fluidization observed for single components alone. The minimum fluidization velocity, as expected, slightly increased from the values obtained for the individual materials of the same size fraction.

Fig. 4.1.5 shows the pressure drop versus superficial air velocity characteristics for the fluidization of sand admixed with 3 wt% of rice husk. The pressure drop data obtained with increasing as well as with decreasing superficial air velocity (i.e. from fixed bed state to fluidized bed state and *vice versa*) have been plotted. Different patterns are observed for the two cases. Significant hysteresis as a result of the geometrical irregularity in the shape of the village rice husk particles is observed. It is noted that the  $U_{mf}$  value obtained for the case of decreasing superficial air velocity is more than that of the value obtained while increasing the superficial air velocity.

Fig. 4.1.6(a) shows the pressure drop pattern for the mixtures of sand (size  $-500 + 350 \mu\text{m}$ ) and mill rice husk. It is observed that with increase in the percentage content of biomass in the bed mixture, the minimum fluidization velocity of the mixture increases. Beyond a percentage content of 8% (by weight) rice husk in the bed mixture, the fluidization quality goes down as is revealed from the pressure drop-superficial velocity characteristics shown in Fig. 4.1.6 (b). Here, minimum fluidization velocity is the velocity at the point of intersection of the regression line from the origin representing the packed bed pressure drop data, and the horizontal line representing the fluidized bed data. Similar characteristics were observed for the bed of the mixtures of other biomass materials with the sand and bauxite particles. Figs. 4.1.7(a), 4.1.7(b), 4.1.8(a) and 4.1.8(b) represent the variation of the bed pressure drop with superficial air velocity for 1, 4, 8 and 9 wt% of bagasse and pressmud mixed with sand particles.

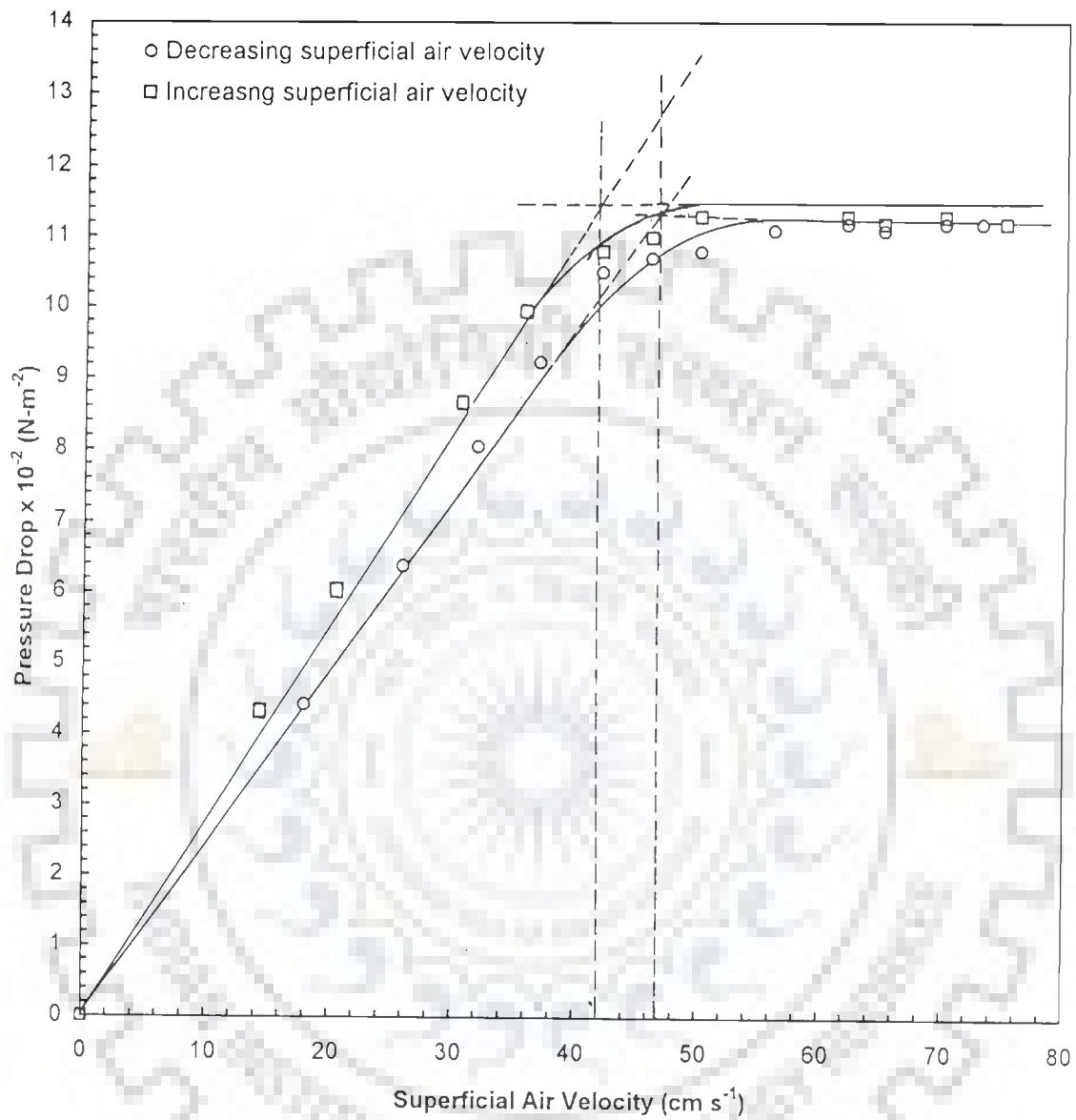
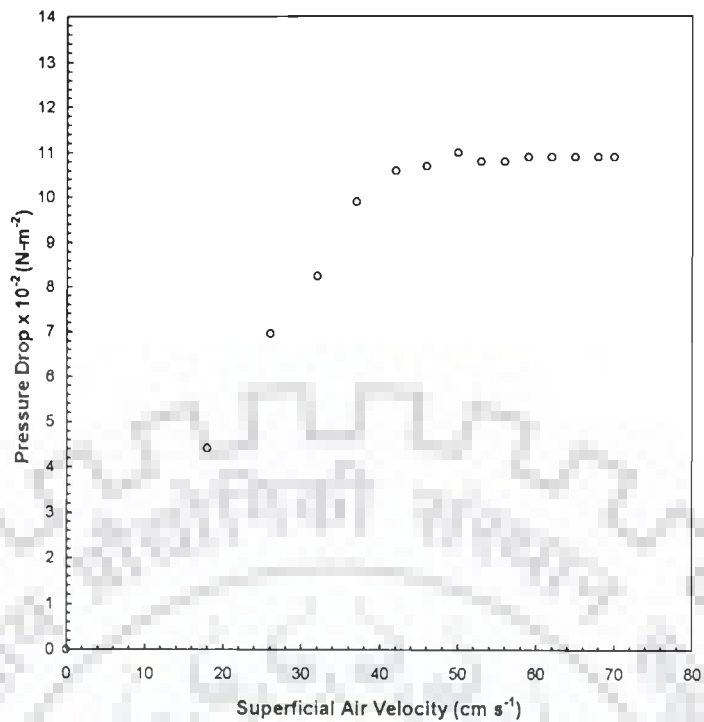
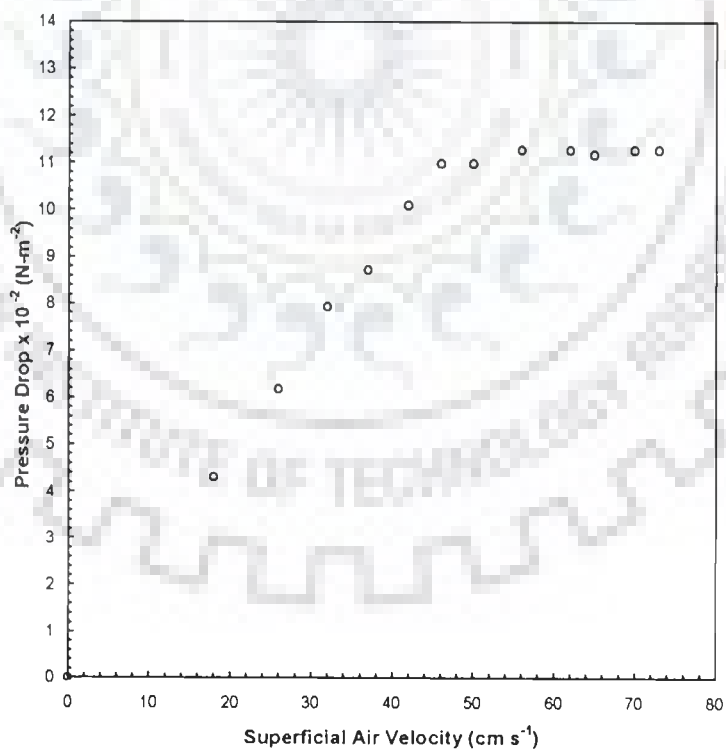


Fig. 4.1.5 : Variation of Pressure Drop with Superficial Air Velocity for Fluidization of Sand and Mill Rice Husk

Sand ( $d_p = -500 + 350 \mu\text{m}$ ) and 3 wt% Rice Husk,  $H/D$  for Sand Bed = 1



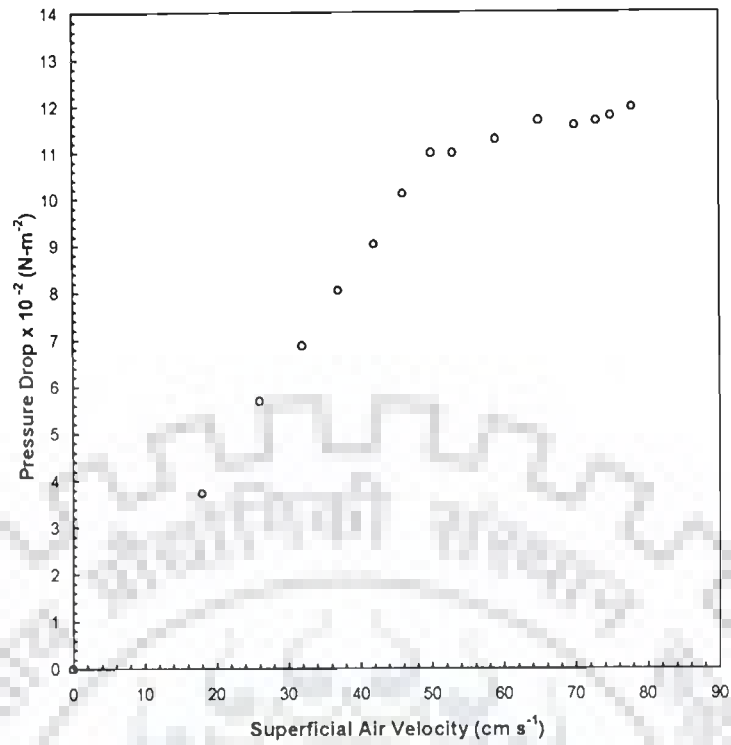
(i) Sand and 1 wt% Mill Rice Husk



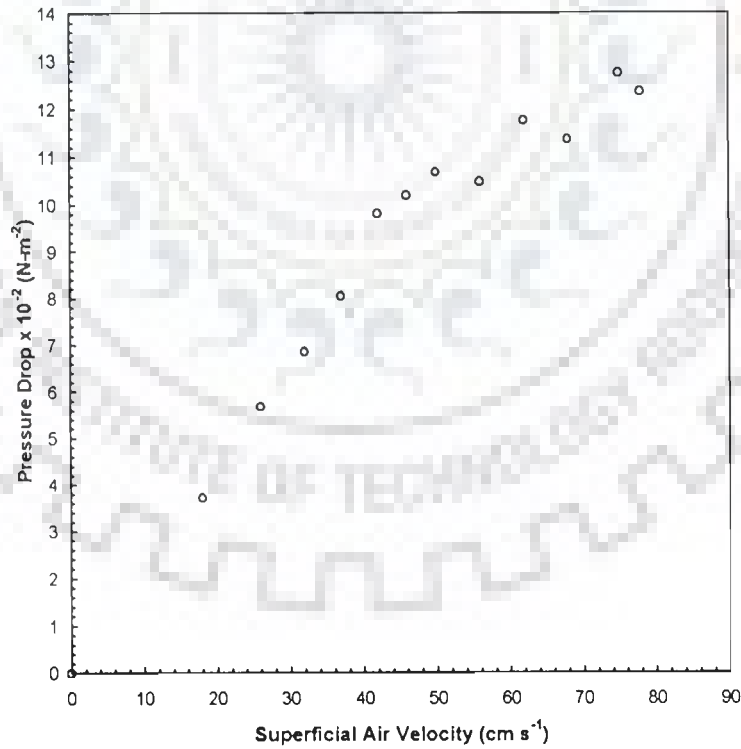
(ii) Sand and 4 wt% Mill Rice Husk

Fig. 4.1.6(a) : Variation of Pressure Drop with Superficial Air Velocity for Fluidization of Sand and Mill Rice Husk Mixture

Sand  $d_p = -500+350 \mu\text{m}$ ;  $H/D = 1$



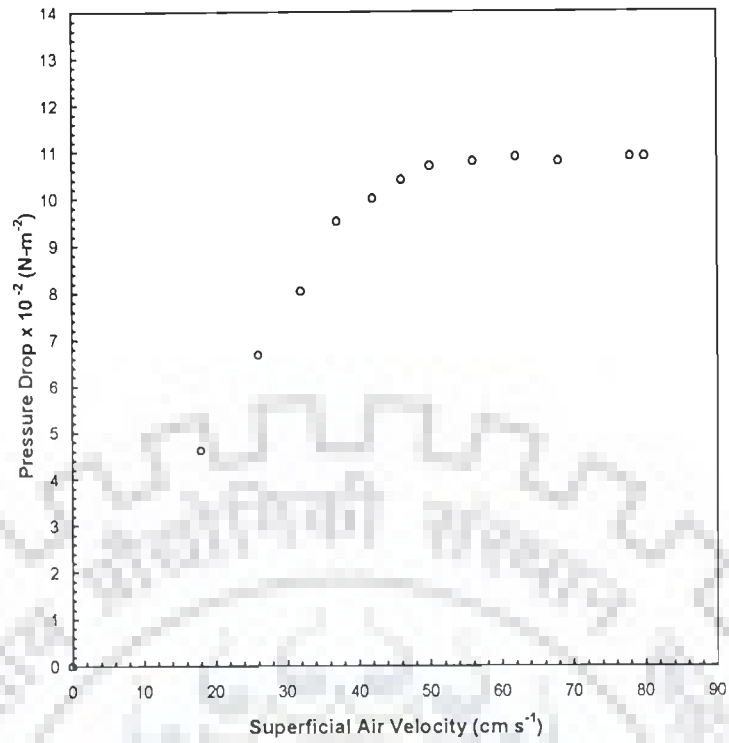
(i) Sand and 8 wt% Mill Rice Husk



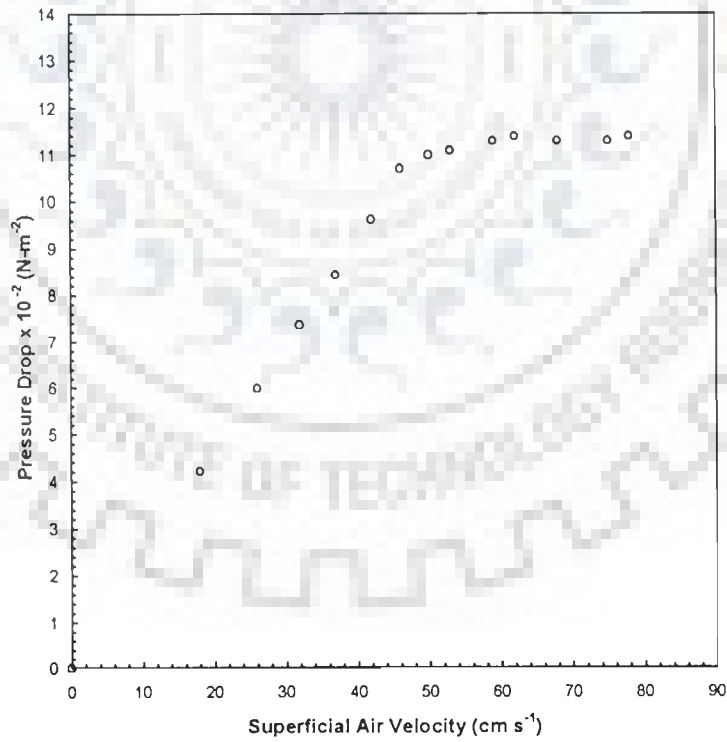
(ii) Sand and 9 wt% Mill Rice Husk

Fig. 4.1.6(b) : Variation of Pressure Drop with Superficial Air Velocity for Fluidization of Sand and Mill Rice Husk Mixture

Sand  $d_p = -500+350 \mu\text{m}$ ;  $H/D$  for Sand Bed = 1



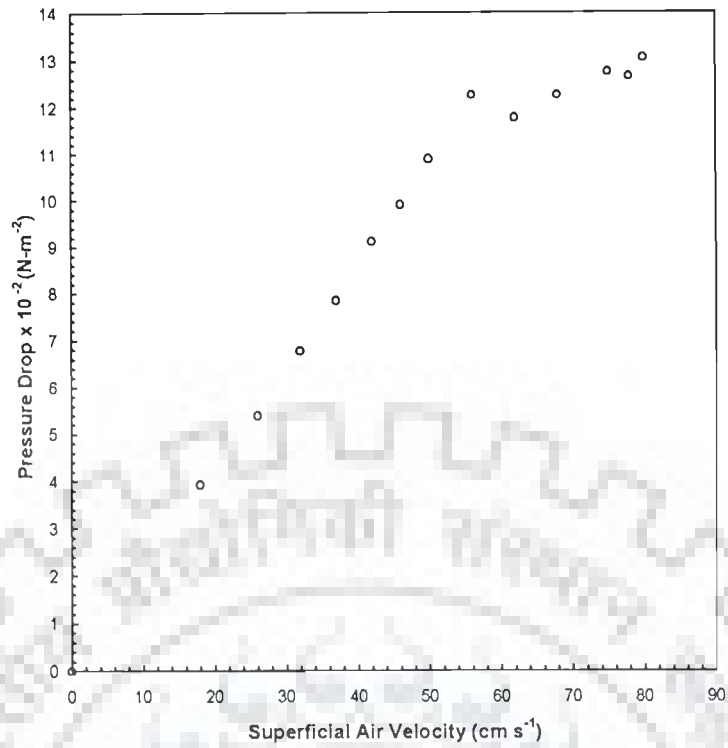
(i) Sand and 1 wt% Bagasse



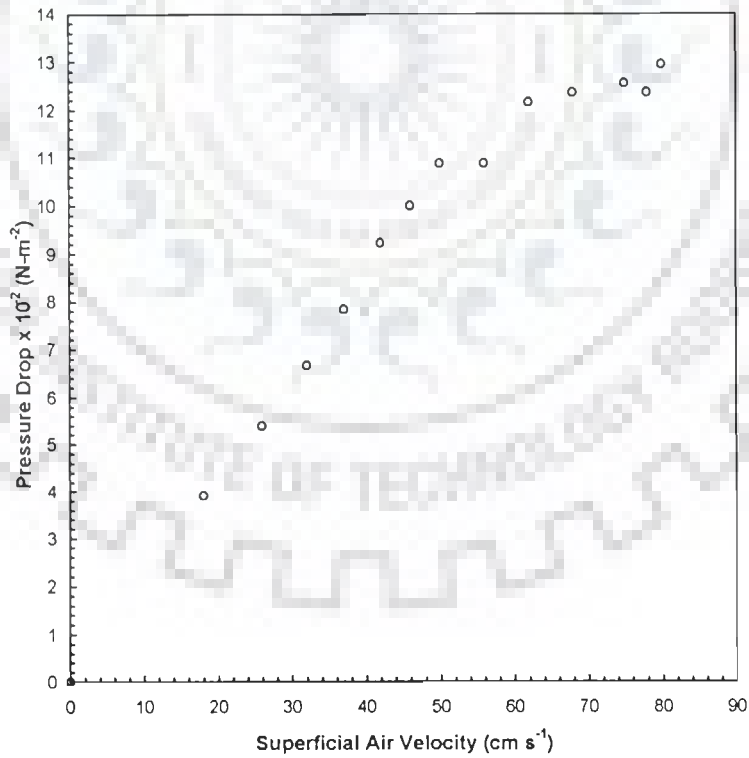
(ii) Sand and 4 wt% Bagasse

Fig. 4.1.7(a) : Variation of Pressure Drop with Superficial Air Velocity for Fluidization of Sand and Bagasse Mixture

Sand  $d_p = -500+350 \mu\text{m}$ ;  $H/D = 1$



(i) Sand and 8 wt% Bagasse

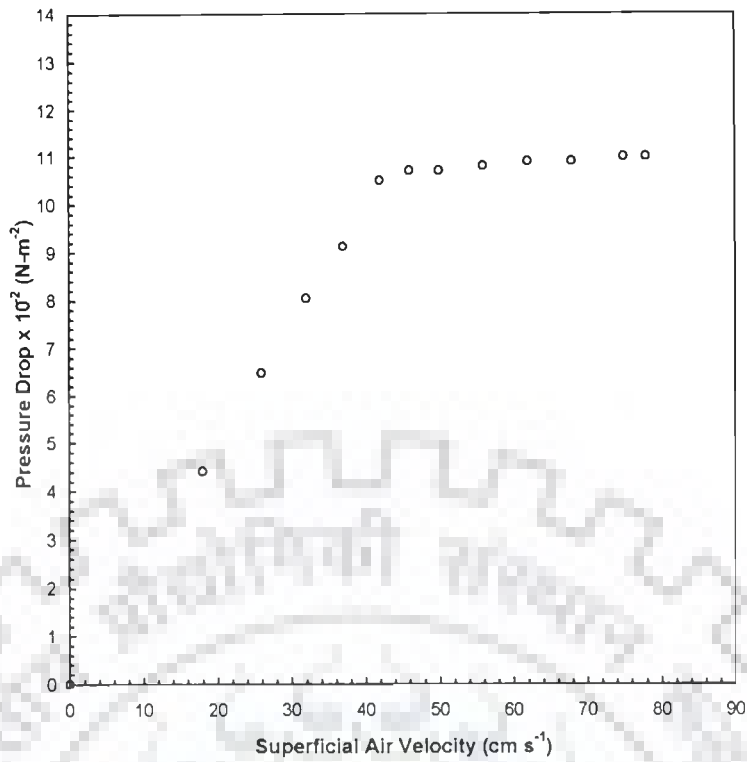


(ii) Sand and 9 wt% Bagasse

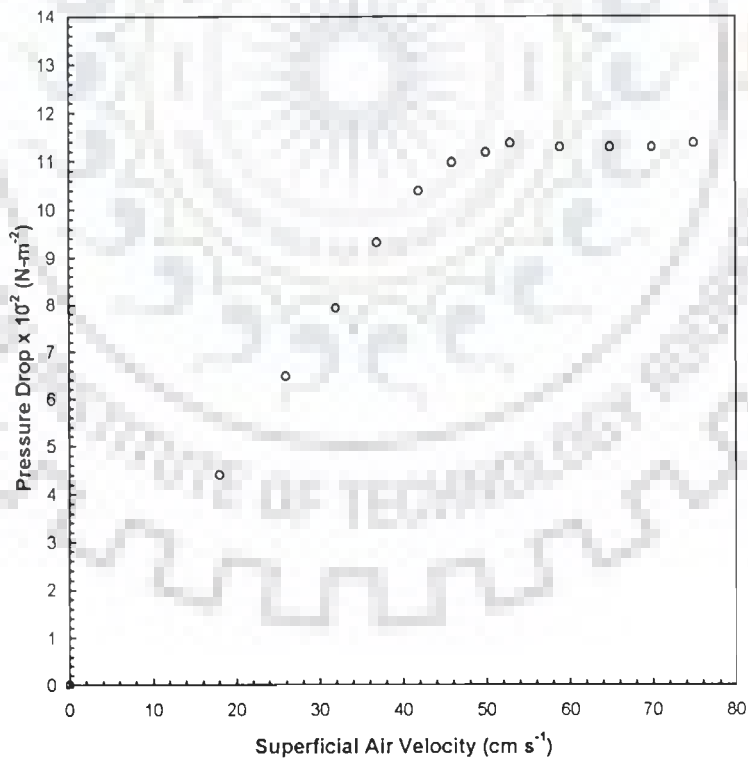
Fig. 4.1.7(b) : Variation of Pressure Drop with Superficial Air Velocity for Fluidization of Sand and Bagasse Mixture

Sand  $d_p = -500+350 \mu\text{m}$ ;  $H/D = 1$





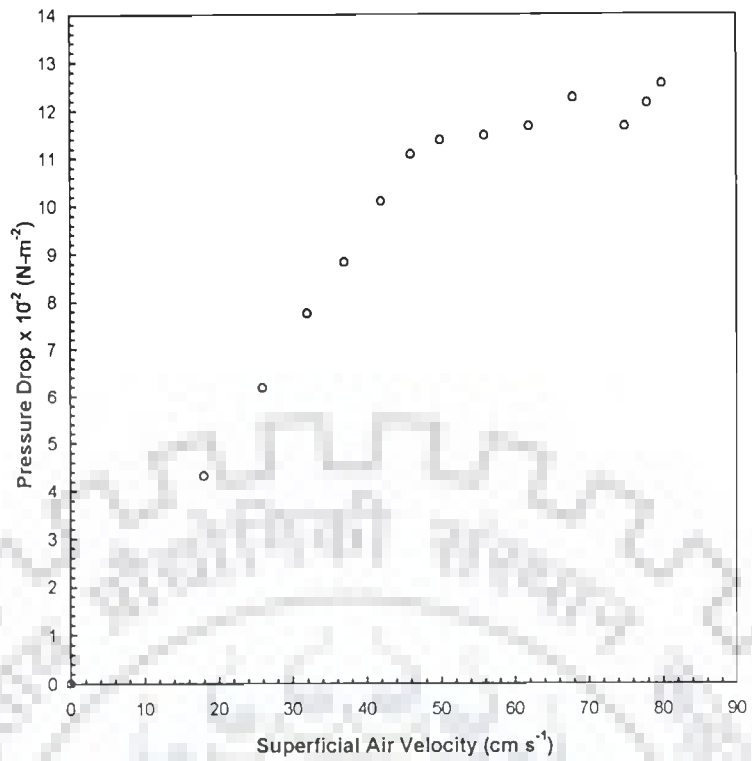
(i) Sand and 1 wt% Pressmud



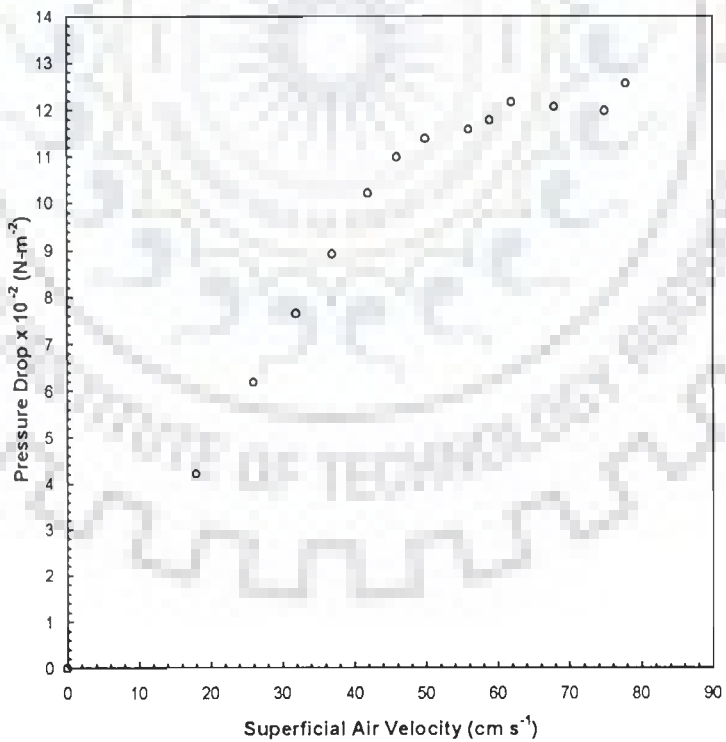
(ii) Sand and 4 wt% Pressmud

Fig. 4.1.8(a) : Variation of Pressure Drop with Superficial Air Velocity for Fluidization of Sand and Pressmud Mixture

Sand  $d_p = -500+350 \mu\text{m}$ ;  $H/D = 1$



(i) Sand and 8 wt% Pressmud



(ii) Sand and 9 wt% Pressmud

Fig. 4.1.8(b) : Variation of Pressure Drop with Superficial Air Velocity for Fluidization of Sand and Pressmud Mixture

Sand  $d_p = -500+350 \mu\text{m}$ ;  $H/D = 1$

From these figures, it is apparent that the fluidization quality started deteriorating as the biomass content of the bed increased beyond 8wt%. Beyond 8wt%, the pressure drop in the fluidized region showed an upward trend rather than a constant pressure drop observed with good quality fluidization.

Chiba et al. (1979) have used mixtures of copper shot, copper powder, and sizes to study the fluidization characteristics. They studied the effect of mixing/segregation state on the relationship between bed pressure drop and superficial gas velocity and defined the states of completely mixed, completely segregated and partial mixing, as well as the characteristics for pure components. Unlike their experiments, the biomass materials used in the present study do not fluidize alone. Further the size range of particles of bagasse, village rice husk and mill rice husk used in the present experiments were much larger than those used by Chiba et al. (1979).

Noda et al. (1986) used the solid-mixtures of sand, glass beads, wood (cubic shape), marten shot, soyabean and rubber (plate-like shape) particles of different sizes and densities ranging from 440 to 7530 kgm<sup>-3</sup>. However, none of the solids used behaved as biomass particles, having peculiar irregular shapes, wide size range of individual component fractions and low densities. Therefore, the characteristics observed by Noda et al., should not be expected to be observed with the sand/bauxite-biomass mixtures. Aznar et al. (1992 a, b) have used two kinds of sands of 4 different size fractions, silica sand of higher density (3600 kgm<sup>-3</sup> as compared to the sands of 2300 and 2700 kgm<sup>-3</sup>) and two size fractions, dolomite of size fraction -630 + 297 μm size, having density of 1200 kgm<sup>-3</sup> and a commercial FCC catalyst of 65 μm size and 1000 kgm<sup>-3</sup> density as fluidizing (carrier) solids and saw dust (-2000 + 100 μm size fraction, average arithmetic mean size of 507 μm), pine wood chips (average size of 2.8x1.6x0.5 cm) and pine straw of -4000 + 200 μm size fraction (with the average

arithmetic means of 874  $\mu\text{m}$ ), a second straw of average size 23x3x1 mm and a third straw of average length of 5 cm. They also used *Cynara Cardumculus* (Thistle) from two energy plantations exhibiting diverse physical aspects, compositions and properties. Type I thistle was ground and contained particles of very diverse sizes and shapes such as thistle splinters, sticks and filaments, of average dimensions-splinters: 1.7x1.0x0.9 cm; sticks: length of 4.00 cm, diameter of 0.6 cm; filaments: 4.5 cm length. Type 2 thistle was of commercial nature having much smaller size and larger proportion of leaves than the thistle type 1 : the conventional size analysis gave the size fraction of  $-30 + 0.20$  mm, with average  $d_p$  of 19 mm. They also used chars obtained from the steam gasification of pine saw dust and chips.

In comparison to these biomass particles used in fluidization experiments, the biomass particles used in the present experiments were of much smaller size fractions.

Aznar et al.(1992 a, b) have used the usual definition of minimum fluidization velocity,  $u_{mf}$  as the velocity at the point of intersection between the horizontal line corresponding to the maximum curve of  $\Delta P-u_s$  and the line of packed bed  $\Delta P-u_s$  passing through the origin (Chiba et al., 1979). They also used a minimum velocity of complete (or maximum) fluidization,  $U_{cf}$  as that velocity at which the entire bed was visually observed to be in motion, irrespective of the condition of the bed and/or particles in the bed. This visual representation has not been related to the pressure drop-superficial velocity data obtained during the experiments. In our view, the conventional wisdom of using  $U_{mf}$ , as defined earlier, may be a better representation of bed fluidization, particularly that obtained during rapid defluidization of the bed. The observations of this kind may then be related to  $\Delta P-u_s$  curve and compared with the results obtained by others. Aznar et al. (1992a) have also observed that H/D ratio between the range  $1 \leq H/D \leq 2$  for the sand-sawdust mixture does not have any effect on  $U_{mf}$ . This

observation is also borne out from the experiments conducted in the present study. As already shown in Fig. 4.1.2,  $H/D$  ratio in the range  $1 \leq H/D \leq 1.5$  for the carrier solids does not show an effect on  $U_{mf}$ . A different trend has been observed for the carrier solid- biomass mixtures; the volume of the bed increasing with each addition of biomass from 1 to 9% (by weight), with the carrier solid  $H/D$  ratio kept at 1.0. In this case, the  $U_{mf}$  increases progressively.

Figs. 4.1.9 to 4.1.13 show the plots of  $U_{mf}$  values for different carrier solid-biomass mixtures, (from 1 to 8 weight % biomass or their corresponding volume %).

It is found that as the biomass percentage in the bed increases (or  $H/D$  ratio of the bed increases)  $U_{mf}$  also increases. Increase in the size fraction of the carrier solid also increases the  $U_{mf}$  values.  $U_{mf}$  values for bauxite-biomass mixtures are lower than that for sand-biomass mixture, for similar size fractions for bauxite and sand. This is due to the lower density of bauxite as compared to that for sand.

As has been pointed out by Aznar et al. (1992a, b), a mathematical extrapolation of the curves shown in Figs. 4.1.9 to 4.1.13 to 100 volume % biomass is neither feasible nor correct, as the biomass percentage higher than 8% does not show proper fluidization characteristics as exemplified by Fig. 4.1.6. Biomass alone cannot be fluidized. Thus, the extrapolation suggested by Bilbao et al. (1987) is not reasonable for the fluidization of binary mixtures of carrier solid-biomass materials.

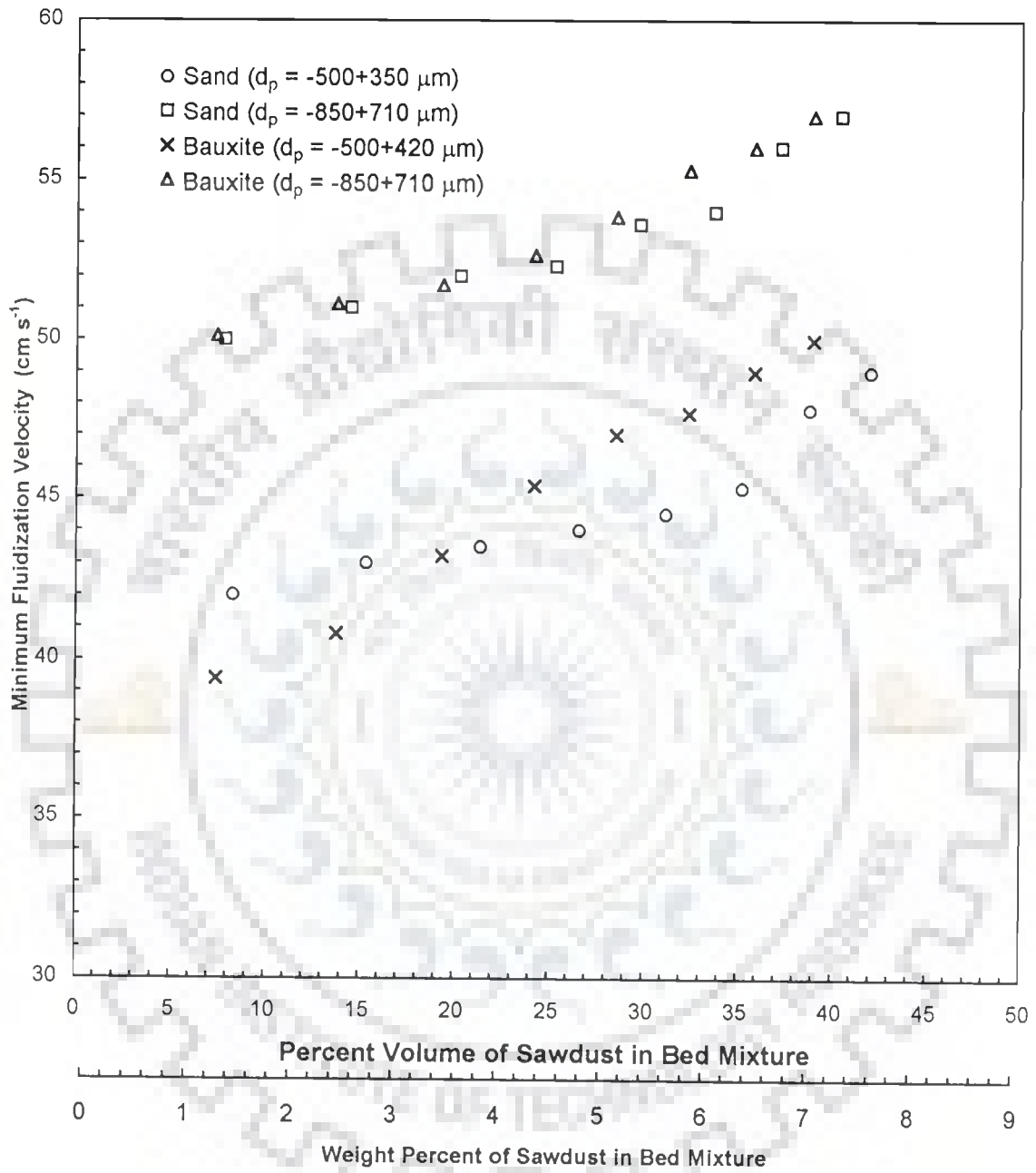


**Fig. 4.1.9 : Variation of Minimum Fluidization Velocity with Percent Volume of Sawdust Content in Bed Mixture**

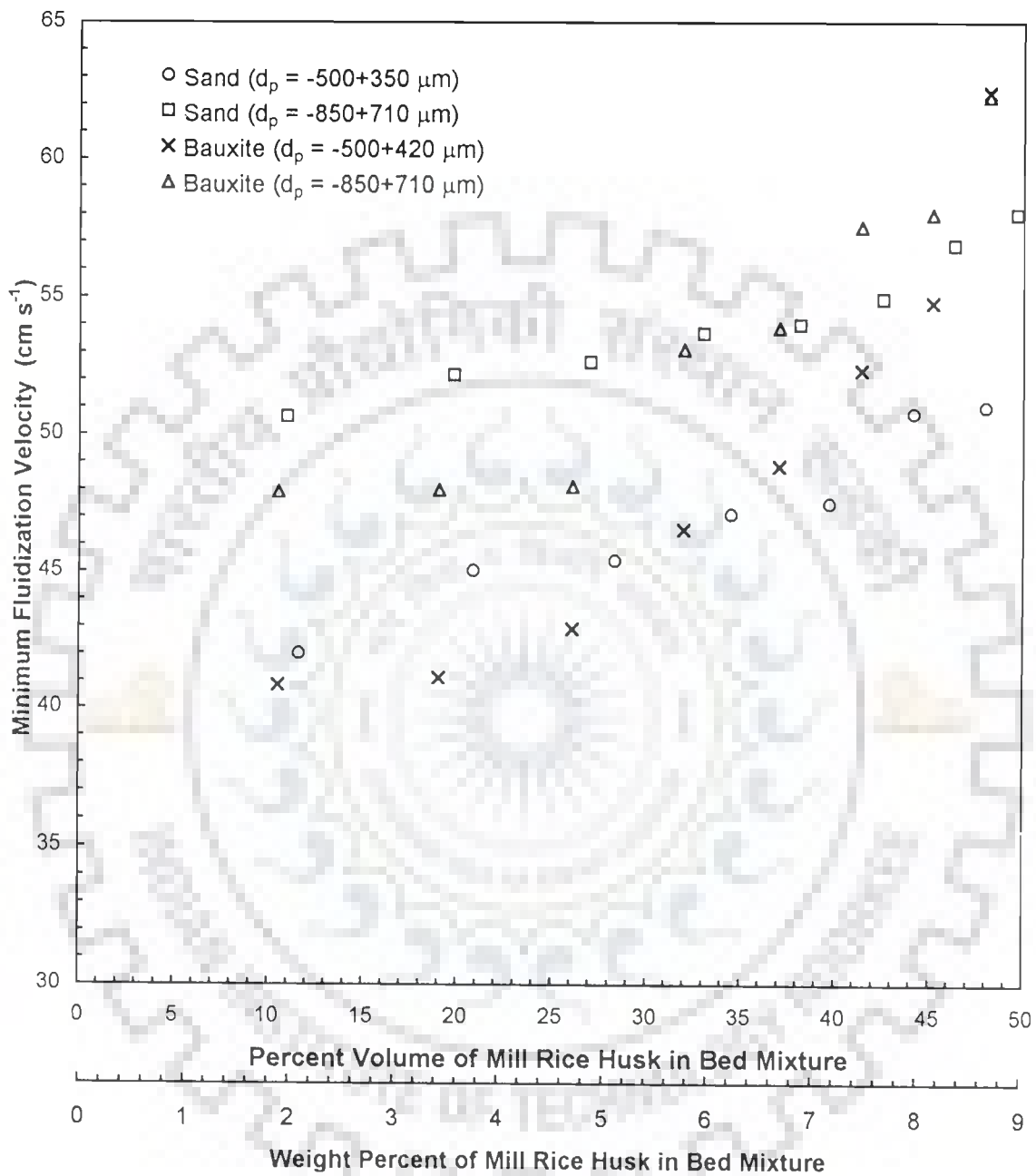


Fig. 4.1.11 : Variation of Minimum Fluidization Velocity with Percent Volume of Mill Rice Husk Content in Bed Mixture

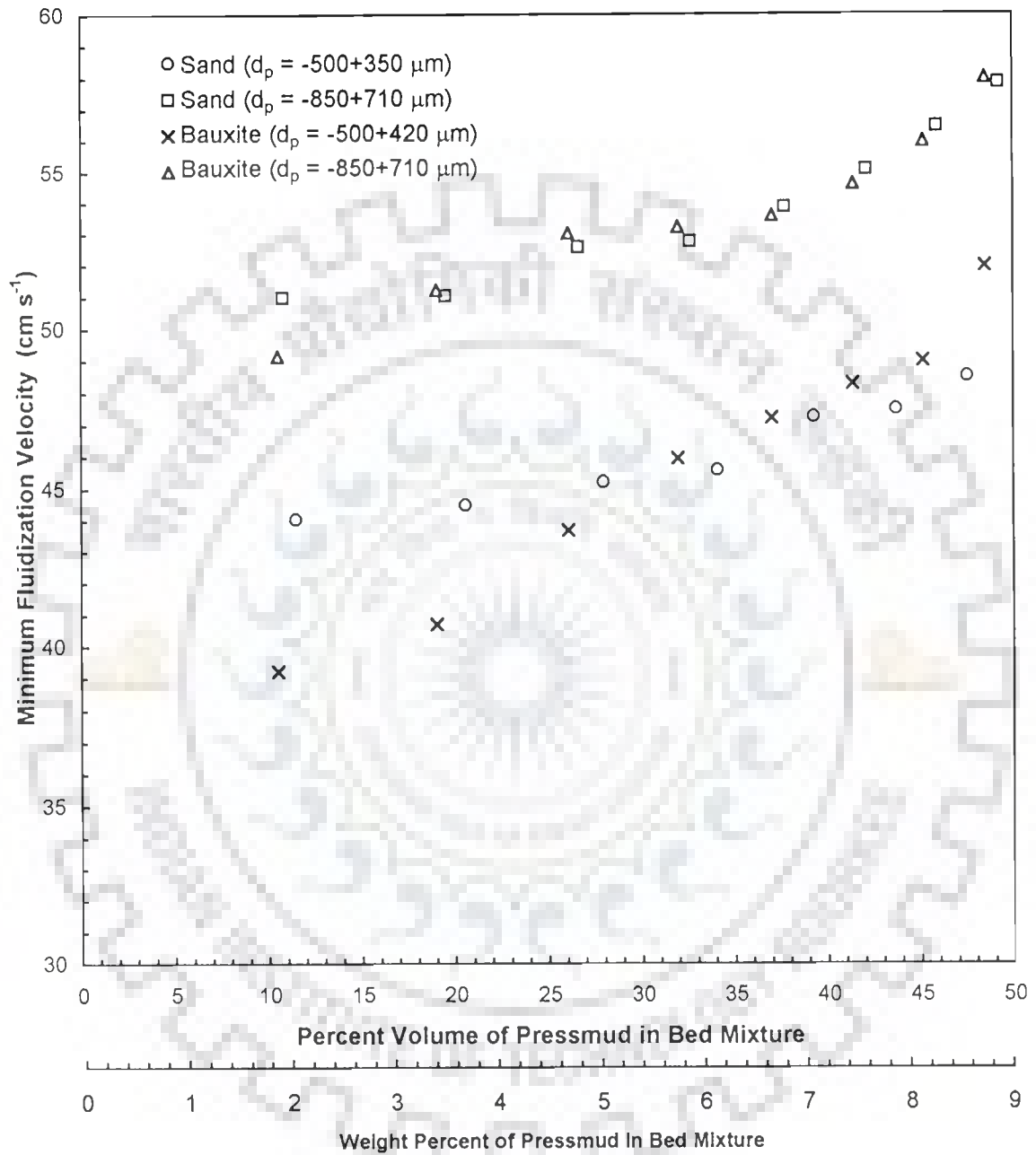
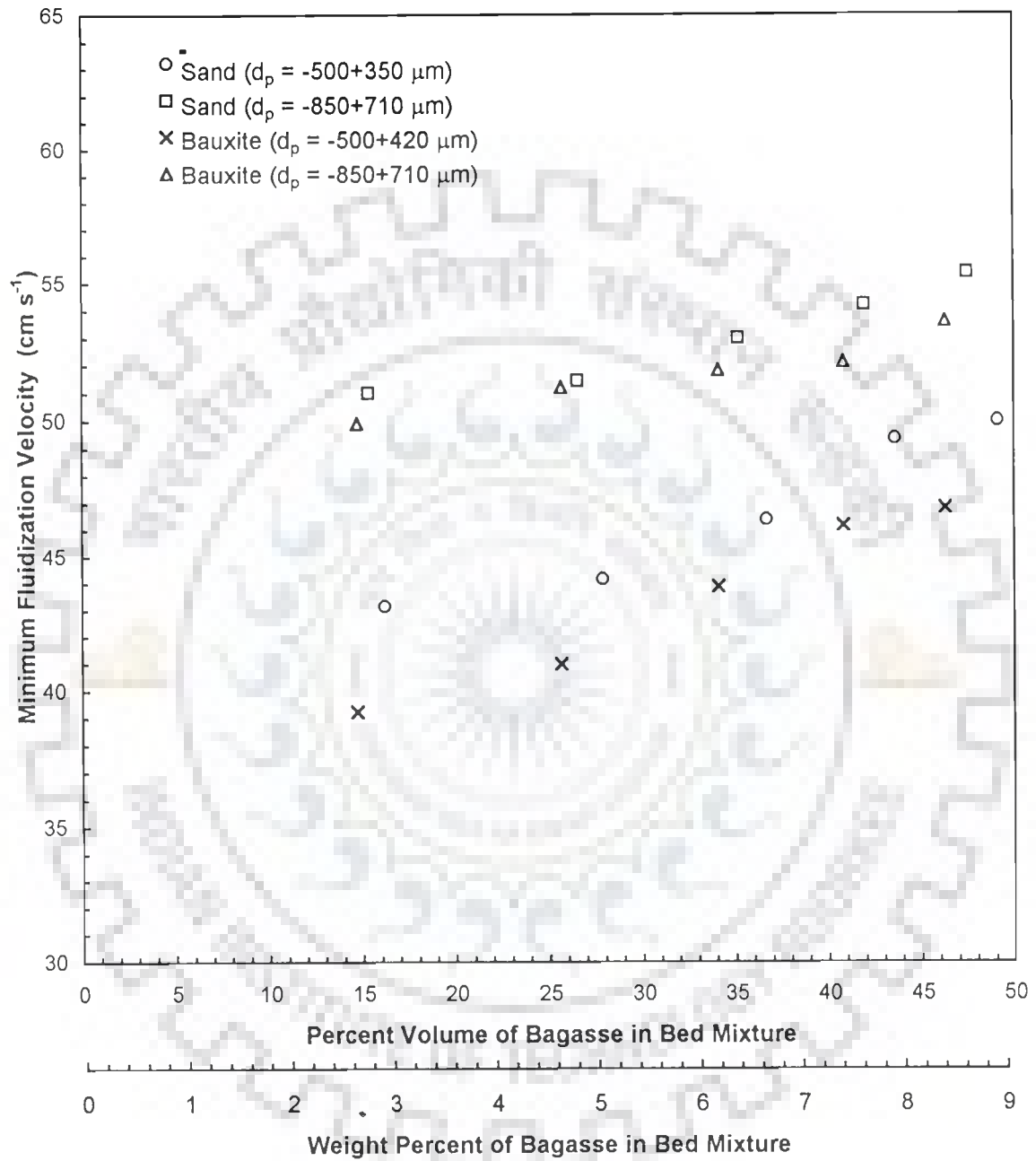


Fig. 4.1.12 : Variation of Minimum Fluidization Velocity with Percent Volume of Pressmud Content in Bed Mixture





**Fig. 4.1.13 : Variation of Minimum Fluidization Velocity with Percent Volume of Bagasse Content in Bed Mixture**

## 4.2 THERMAL DEGRADATION BEHAVIOUR AND KINETICS USING THERMOGRAVIMETRIC ANALYSIS

### 4.2.1 Biomass Materials and Test Conditions

Dynamic Thermogravimetry (TG), Derivative Thermogravimetry (DTG) and Differential Thermal Analysis (DTA) techniques have been used in literature to understand the process of thermal degradation-pyrolysis and oxidation (in the presence of inert or oxidizing atmosphere) of different kinds of materials including biomass. Five biomass materials, namely, village rice husk (VRH), mill rice husk (MRH), sawdust (SD), bagasse (BG) and pressmud (PM) were subjected to TG, DTG and DTA to elicit information regarding their thermal degradation characteristics and to determine kinetics of degradation. Two heating rates, namely,  $20^{\circ}\text{Cmin}^{-1}$  and  $40^{\circ}\text{Cmin}^{-1}$  - under nitrogen and oxygen atmospheres were employed to obtain thermograms, degradation rates and temperature differences due to endothermic and/or exothermic enthalpic transitions or reactions such as dehydration, dissociation or decomposition (pyrolysis), oxidation or other chemical reactions. The characteristic curves from TG, DTG and DTA are shown in Figs. 4.2.1 (a, b) to 4.2.10 (a, b) for the samples under nitrogen and oxidizing air atmospheres. The tests were conducted from the ambient temperature to a final temperature of  $>900^{\circ}\text{C}$ . Higher heating rates (i.e.  $>40^{\circ}\text{Cmin}^{-1}$ ) could not be employed due to limitation of the instrument.

### 4.2.2 Thermal Degradation Characteristics

#### 4.2.2.1 Village Rice Husk (VRH)

The TGA data show that for the village rice husk there is an initial loss of moisture ( $\sim 10\%$ ) from the sample at both the heating rates under nitrogen and air atmospheres. Figs. 4.2.1(a) and 4.2.2(a) showed that the moisture removal continued until  $140^{\circ}\text{C}$ . Higher drying temperature ( $>100^{\circ}\text{C}$ ) is ascribed to the loss of surface tension bound water in the capillaries of the sample material. The second stage of

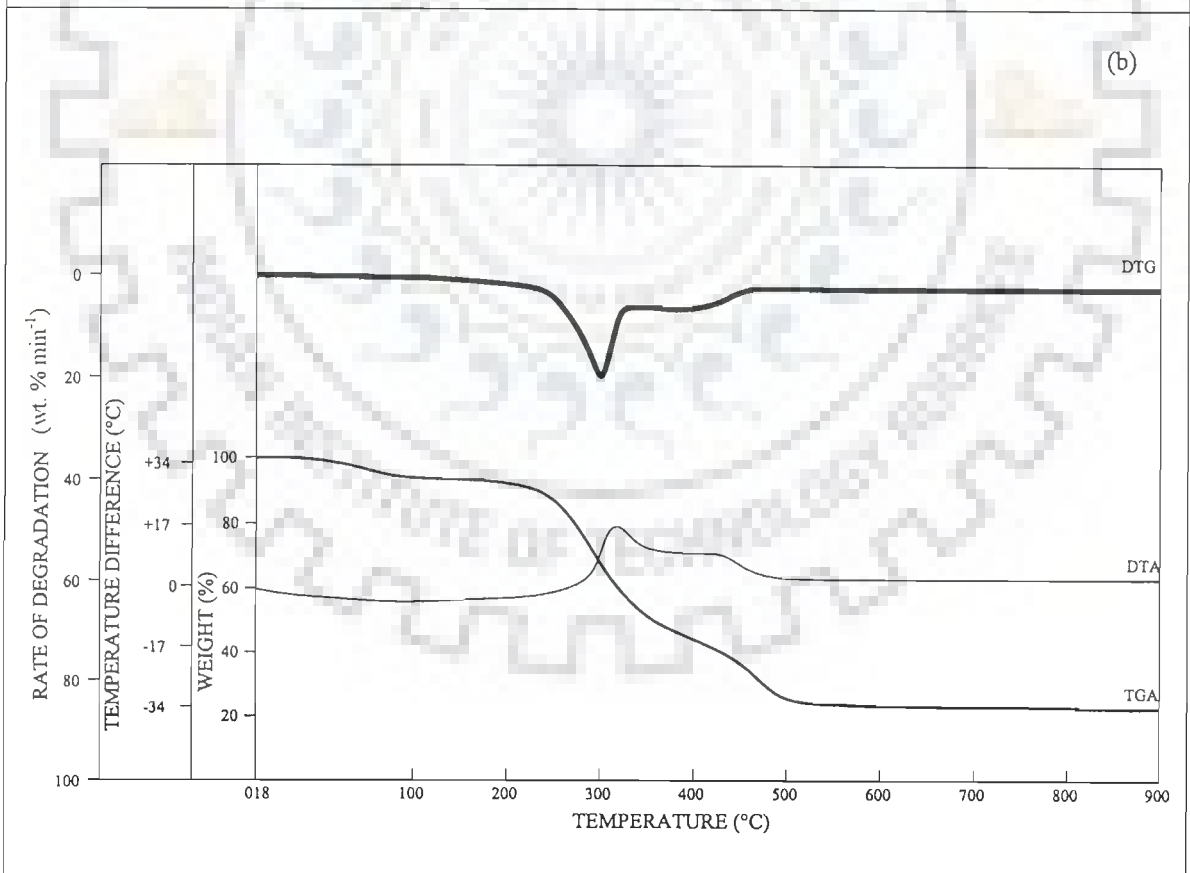
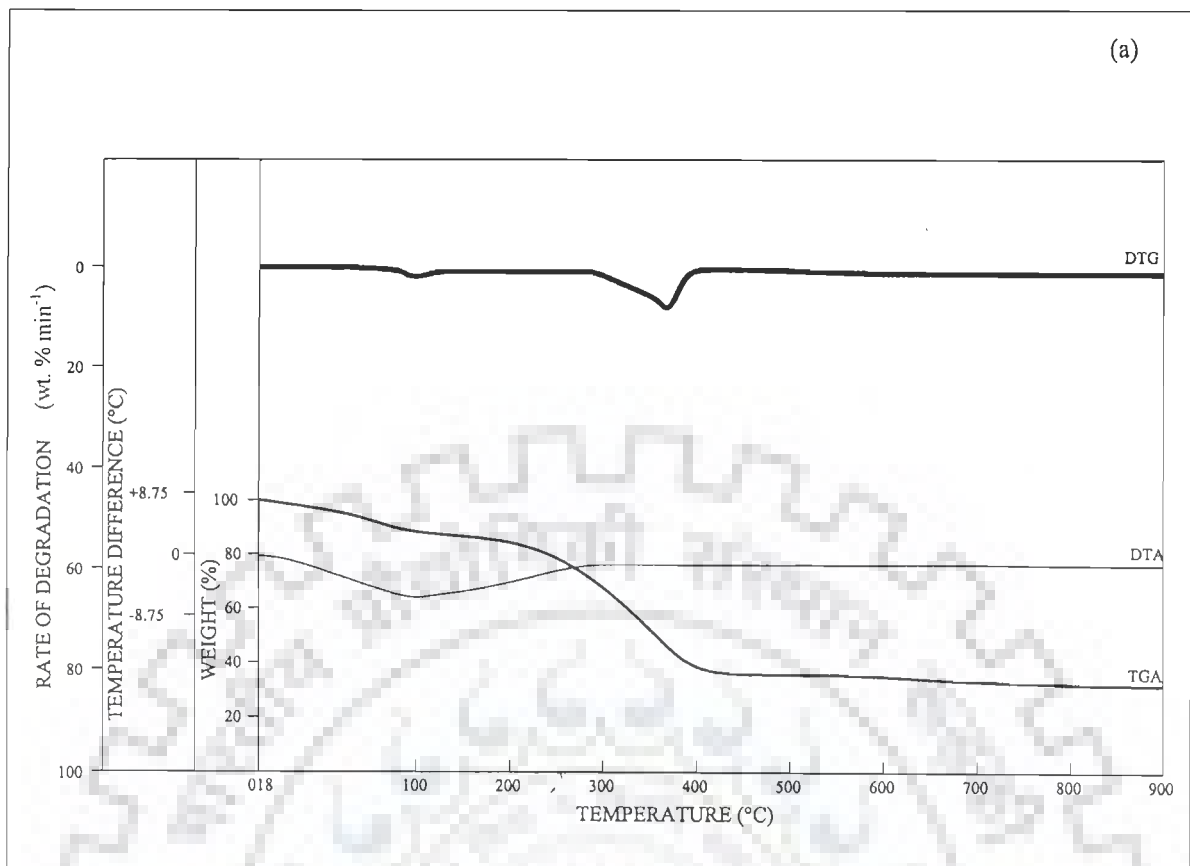


Fig. 4.2.1(a) & (b) : Thermogravimetric and Differential Thermal Analysis of Village Rice Husk in (a) Nitrogen, and (b) Air; Heating Rate = 20°C min<sup>-1</sup>

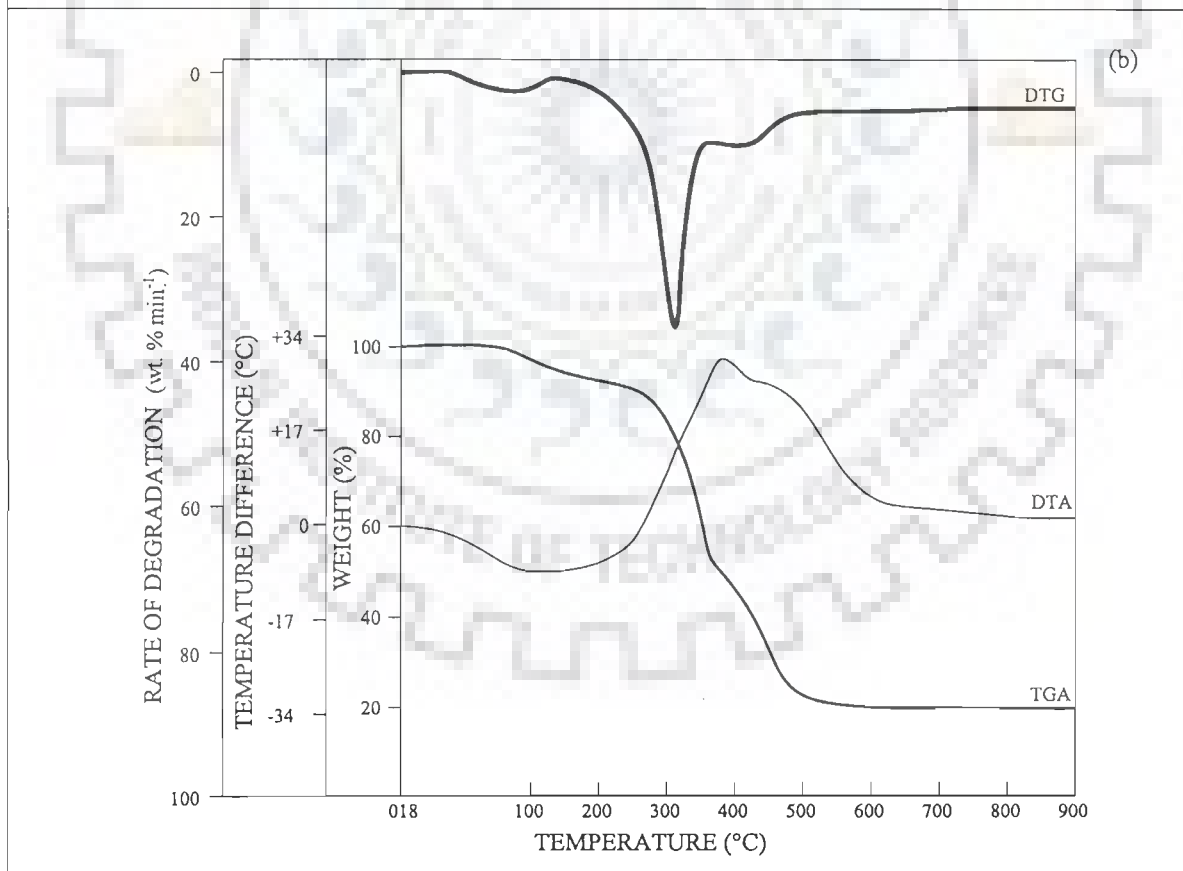
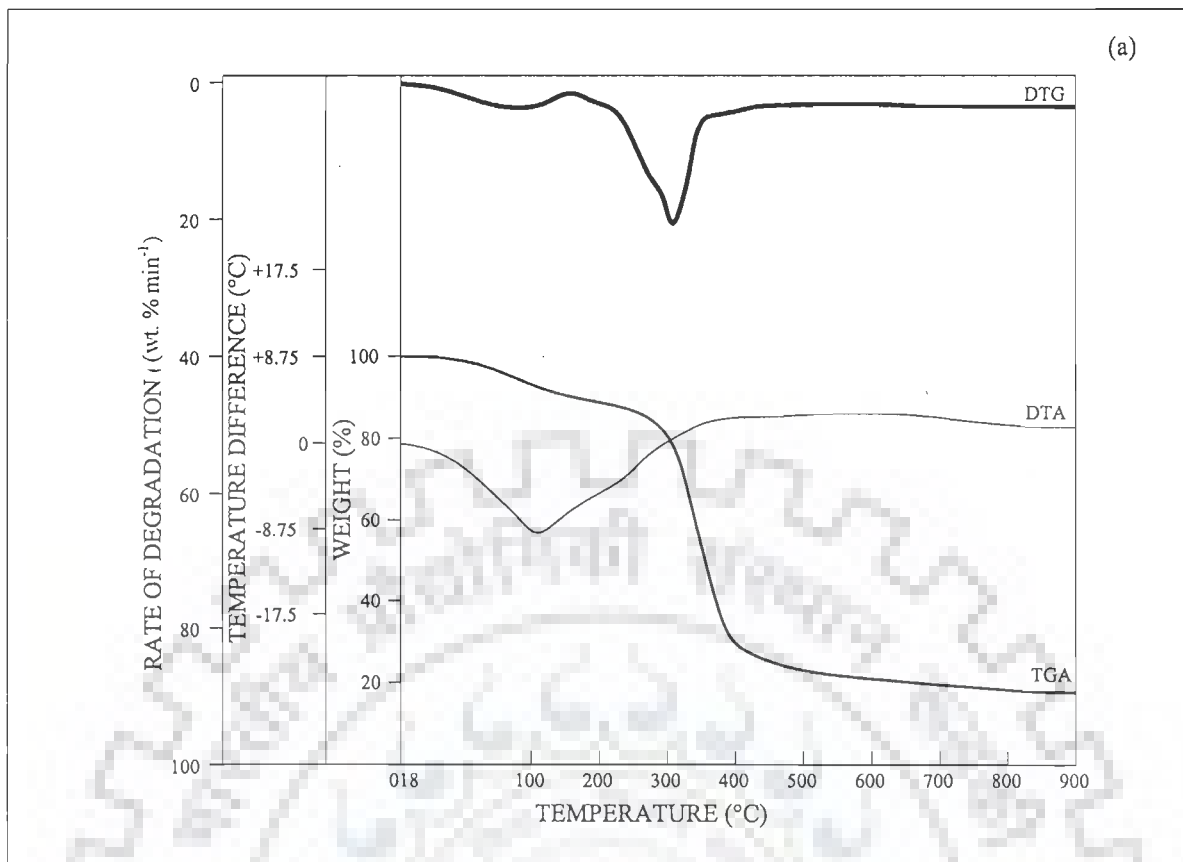


Fig. 4.2.2(a) & (b) : Thermogravimetric and Differential Thermal Analysis of Village Rice Husk in (a) Nitrogen, and (b) Air; Heating Rate = 40°C min<sup>-1</sup>

weight loss, as is evident from both TG and DTG curves, could be due to loss of light volatiles. This stage is seen to exist between 194 and 237°C and may be called the initial thermal degradation stage. Increase in the heating rate from 20 to 40°Cmin<sup>-1</sup> increased the degradation rate and also the total degradation at a given temperature. Increase in heating rate also accelerates the degradation at lower temperature. Early decomposition at ~170°C was obtained with the heating rate of 40°Cmin<sup>-1</sup>. The second stage of degradation followed at a temperature of ~ 240°C and continued up till 290 -300°C. The average degradation rates observed in the third stage were 3.85 and 8.8 wt% min<sup>-1</sup>, respectively for 20 and 40°C min<sup>-1</sup> heating rates. Thereafter rapid degradation started in the third reaction zone (active pyrolysis zone) which continued upto around 390°C for 20°C min<sup>-1</sup> and 409°C for 40°C min<sup>-1</sup> heating rate. In this active pyrolysis zone, a major change in the slopes of the TGA curves for the two heating rates were observed. The total degradation for the two heating rates, were, 35.8 and 41.4%, and the average degradation rates were 8.95% and 18.35%min<sup>-1</sup>, respectively. Finally, a slow degradation zone (the fourth reaction zone) is observed which extends upto 530-548°C for the two heating rates. The total residue obtained at 700°C is around 30%. Thus, the volatile components after pyrolysis are around 70% of the sample mass. The DTG peak temperature of 346°C suggests the temperature at which maximum degradation rate is observed. The DTA peak area tells the enthalpy change during the thermal degradation process. It is found that the drying (dehydration of the sample) is an endothermic process, while pyrolysis may be slightly exothermic in nature. Increase in the heating rate from 20 to 40°C min<sup>-1</sup> showed sharper peaks with larger temperature difference, as seen from Figs. 4.2.1(a) and 4.2.2(a). Change in the atmosphere from nitrogen to air at any heating rate showed sharper peak for the drying process followed by a larger peak area for the exothermic oxidation process. Changes in peak trace slopes indicate that the oxidation of the sample is followed in several

stages – at least three - giving different amounts of heat evolutions corresponding to peak heights and temperature differences. These can be clearly seen in Figs. 4.2.1(a, b) and 4.2.2 (a, b). Thermal degradation characteristics as deduced from these figures are given in Tables 4.2.1 (a, b) and 4.2.2(a, b).

The DTA curve for  $20^{\circ}\text{Cmin}^{-1}$  heating rate under flowing air atmosphere shows the endotherm for the dehydration of the VRH sample coupled with slow evolution of light volatiles ending at  $279^{\circ}\text{C}$ . The exothermic nature is exhibited from  $279^{\circ}\text{C}$  to  $530^{\circ}\text{C}$  with dual exothermic peaks at  $337$  and  $456^{\circ}\text{C}$ . The first exotherm is found to terminate at around  $400^{\circ}\text{C}$ . The first exotherm showed the peak temperature difference of  $19^{\circ}\text{C}$ , while for the second peak temperature difference was  $12.2^{\circ}\text{C}$ .

The DTA curve for  $40^{\circ}\text{C min}^{-1}$  heating rate under oxidizing air atmosphere is similar to  $20^{\circ}\text{Cmin}^{-1}$  heating rate curve. The exothermicity is exhibited between  $279$  and  $563^{\circ}\text{C}$  with dual exothermic peaks- the first peak at  $385^{\circ}\text{C}$  and the second at  $460^{\circ}\text{C}$ . The peak exothermic temperature differences were  $31.3$  and  $25.8^{\circ}\text{C}$ , respectively. Higher heating rate enhances heat evolution resulting in larger temperature difference.

#### **4.2.2.2 Mill Rice Husk (MRH)**

The mill rice husk TG, DTG and DTA curves under flowing nitrogen and air atmospheres at the two heating rates,  $25$  and  $40^{\circ}\text{C min}^{-1}$  are shown in Figs. 4.2.3(a, b) and 4.2.4(a, b), respectively. The thermal degradation characteristics are shown in Tables 4.2.1 (a, b) and 4.2.2 (a, b) for flowing nitrogen and air atmospheres, respectively.

In may be seen from Figs. 4.2.3 and 4.2.4 that the dehydration of the sample of MRH starts at around ambient temperature and continues until  $120^{\circ}\text{C}$ . The initiation of evolution of light volatiles starts at around  $190^{\circ}\text{C}$  and continues upto  $\sim 310^{\circ}\text{C}$  under

**Table 4.2.1(a) : Thermal Degradation in the Initial Degradation Zone**  
(Nitrogen: 50 mlmin<sup>-1</sup>)

Biomass	Heating Rate (°C min <sup>-1</sup> )	Moisture Removed (%)	Degradation Temperature (°C)			Total Degradation (wt%)	Degradation Rate, (wt% min <sup>-1</sup> )	
			Initial	Final	Maxm.		Avg.	Maxm
VRH	20	10.0	194	239	239	3.6	3.85	6.2
	40	10.0	170	237	237	4.5	1.60	3.0
MRH	25	8.0	190	300	300	5.6	3.4	6.9
	40	8.0	192	310	310	3.1	14.0	29.0

**Table 4.2.1(b) : Thermal Degradation in the Second Reaction Zone**  
(Nitrogen: 50 mlmin<sup>-1</sup>)

Biomass	Heating Rate (°C min <sup>-1</sup> )	Degradation Temperature (°C)			Total Degradation (wt%)	Degradation Rate, (wt% min <sup>-1</sup> )	
		Initial	Final	Maxm.		Avg.	Maxm.
VRH	20	239	300	300	6.2	3.9	6.2
	40	237	290	290	2.2	8.8	14.6
MRH	25	300	395	353	39.5	19.7	37.5
	40	310	432	360	48.7	31.6	59.7

**Table 4.2.1(c) : Thermal Degradation in the Third Reaction Zone**  
(Nitrogen : 50 mlmin<sup>-1</sup>)

Biomass	Heating Rate (°C min <sup>-1</sup> )	Degradation Temperature (°C)			Total Degradation (wt%)	Degradation Rate, (wt% min <sup>-1</sup> )		Residue at 700°C (wt%)
		Initial	Final	Maxm.		Avg.	Maxm.	
VRH	20	300	390	346	35.8	7.0	11.7	
	40	290	409	346	41.4	13.6	23.1	
MRH	25	395	584	-	11.2	0.08	1.7	34.6
	40	438	700	-	8.8	3.2	6.2	32.5

**Table 4.2.1(d) : Thermal Degradation in the Fourth Reaction Zone**  
(Nitrogen : 50 mlmin<sup>-1</sup>)

Biomass	Heating Rate (°C min <sup>-1</sup> )	Degradation Temperature (°C)			Total Degradation (wt%)	Degradation Rate, (wt% min <sup>-1</sup> )		Residue at 700°C (wt%)
		Initial	Final	Maxm.		Avg.	Maxm.	
VRH	20	390	530	-	8.6	0.07	1.55	30.1
	40	409	548	-	9.7	1.60	3.10	29.6

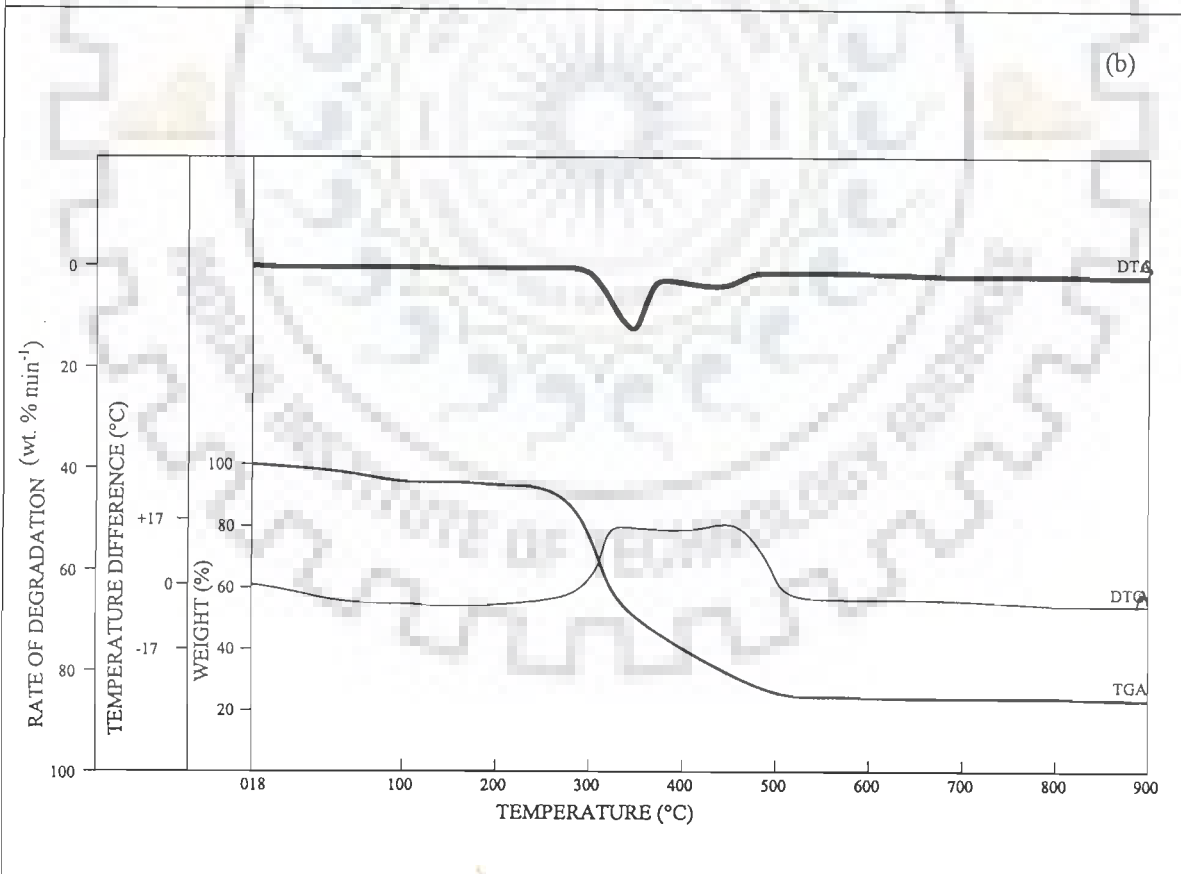
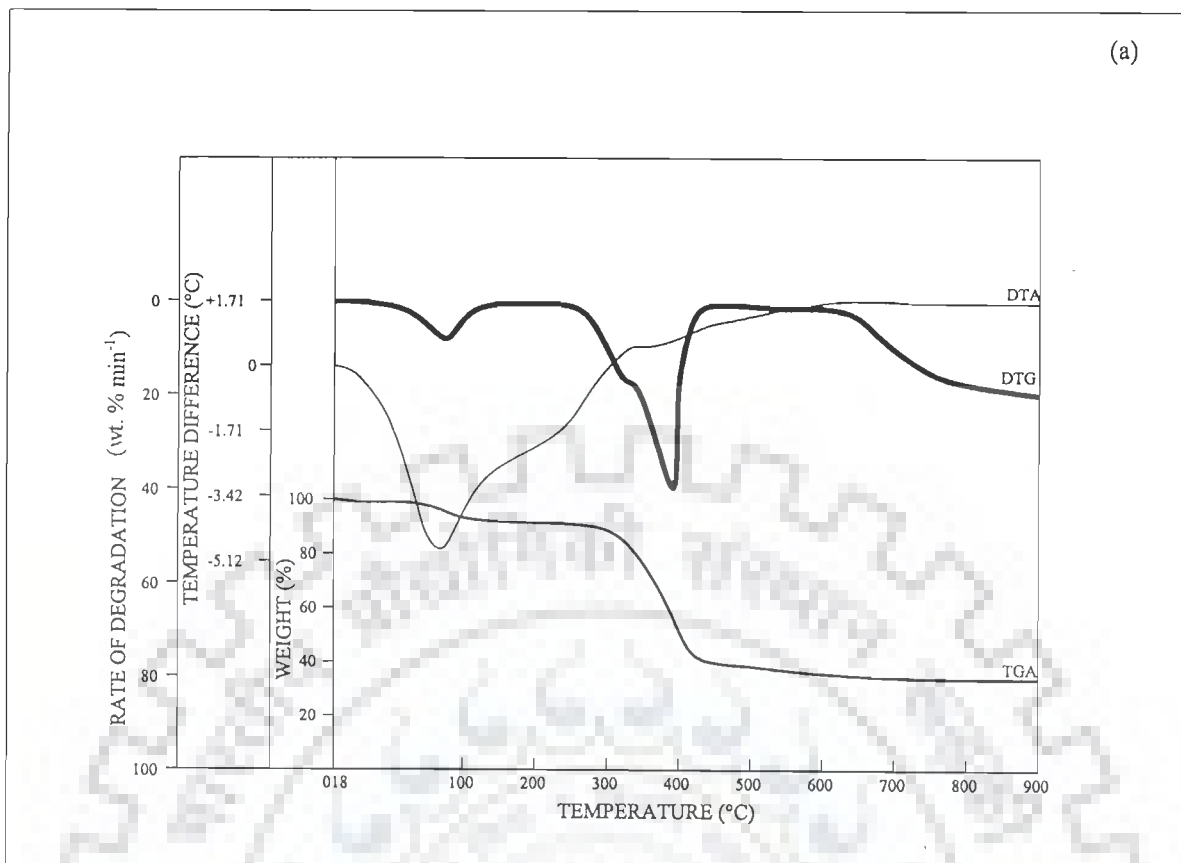


Fig. 4.2.3(a) & (b) : Thermogravimetric and Differential Thermal Analysis of Mill Rice Husk in (a) Nitrogen, and (b) Air; Heating Rate = 20°C min<sup>-1</sup>



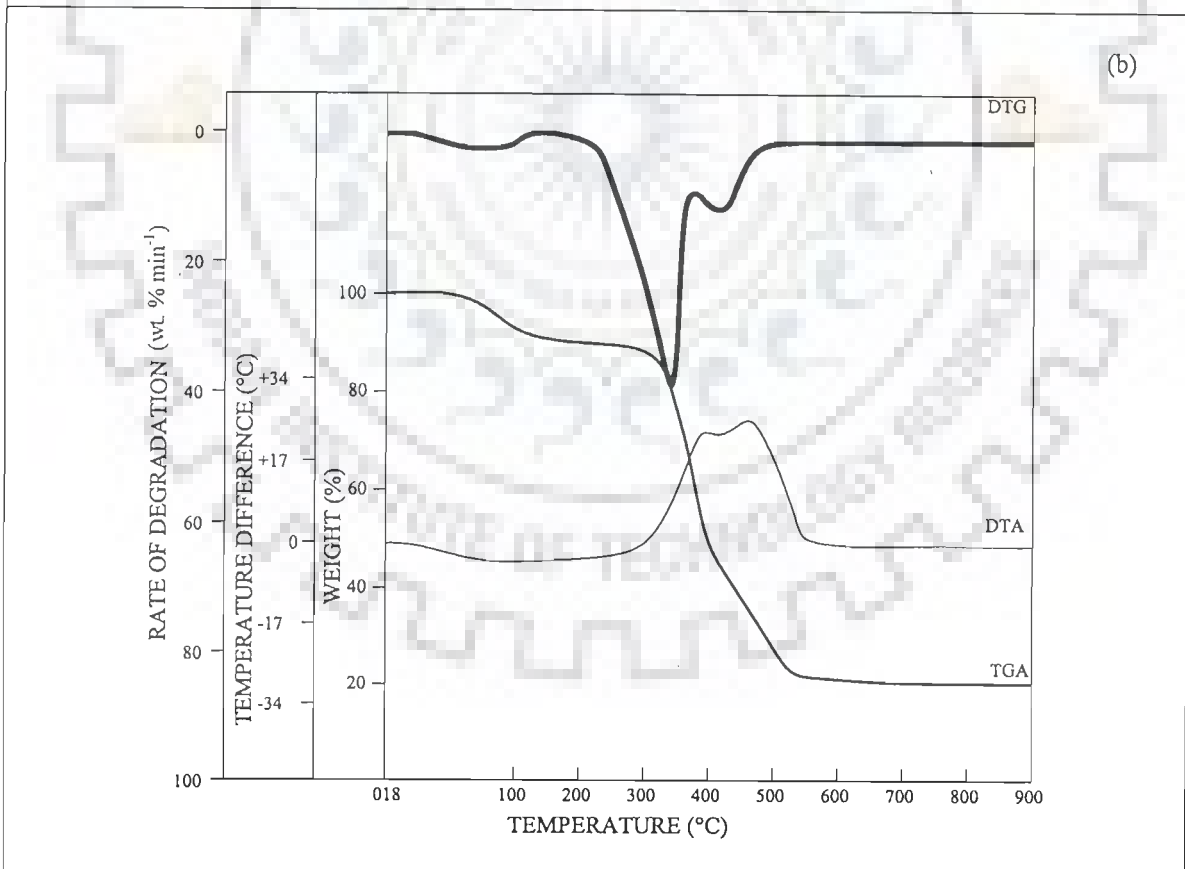
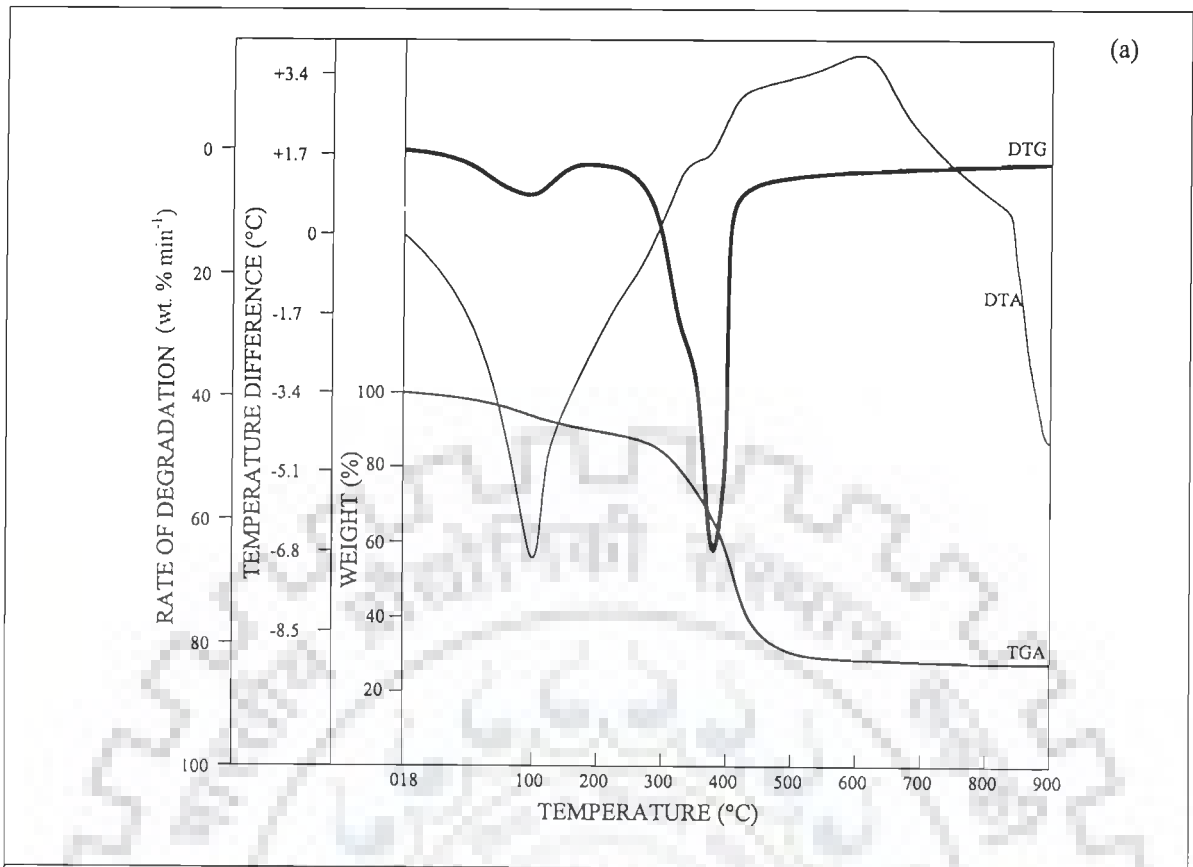


Fig. 4.2.4(a) & (b) : Thermogravimetric and Differential Thermal Analysis of Mill Rice Husk in (a) Nitrogen, and (b) Air; Heating Rate =  $40^{\circ}\text{C min}^{-1}$

**Table 4.2.2(a) : Thermal Degradation in the First Reaction Zone  
(Air: 50 mlmin<sup>-1</sup>)\***

Biomass	Heating Rate (°C min <sup>-1</sup> )	Moisture Removed (%)	Degradation Temperature (°C)			Total Degradation (wt%)	Degradation Rate, (wt% min <sup>-1</sup> )	
			Initial	Final	Maxm.		Avg.	Maxm.
VRH	20	8.8	258	350	300	37.2	8.5	17.5
	40	8.0	258	385	300	40.9	19.7	39.5
MRH	20	5.1	258	360	325	36.37	6.4	14.9
	40	6.1	258	428	335	47.50	18.5	37.0

\* For 40°C min<sup>-1</sup> heating rate, air flow rate was 60 mlmin<sup>-1</sup> for MRH

**Table 4.2.2(b) : Thermal Degradation in Second Reaction Zone (Air:50mlmin<sup>-1</sup>)\***

Biomass	Heating Rate (°Cmin <sup>-1</sup> )	Degradation Temperature (°C)			Total Degradation (wt%)	Degradation Rate, (wt% min <sup>-1</sup> )		Residue at 700°C (wt%)
		Initial	Final	Maxm.		Avg.	Maxm.	
VRH	20	350	530	428	30.2	2.0	3.9	16.0
	40	385	548	475	26.6	3.2	6.5	15.6
MRH	20	360	521	456	35.8	3.3	5.0	22.7
	40	443	628	480	23.9	5.4	10.8	15.0

\* For 40°C min<sup>-1</sup> heating rate, air flow rate was 60 mlmin<sup>-1</sup> for MRH

nitrogen atmosphere. The second degradation zone starts at around 310°C and continues upto 395°C for 25°C min<sup>-1</sup> heating rate and 432°C for 40°Cmin<sup>-1</sup> heating rate. This is the active pyrolysis zone giving 39.5 and 48.7% degradation at 25°C min<sup>-1</sup> and 40°Cmin<sup>-1</sup>, respectively. The maximum degradation rate of 37.5 and 59.7% min<sup>-1</sup> are obtained for the two respective heating rates at around 360°C. The third stage of degradation at 25°C min<sup>-1</sup> heating rate continued uptill 584°C while at 40°Cmin<sup>-1</sup> it continued uptill 700°C. The residue at 700°C were 34.6 and 32.5% for the two respective heating rates. With flowing air, at 40°C min<sup>-1</sup>, heating rate, the degradation starts at ~ 258°C and continues upto ~428°C, with the maximum degradation temperature being 335°C. Total degradation in the first pyrolysis zone is found to be insignificant, much lower than those observed for village rice husk. The degradation data are listed in Tables 4.2.1(a-d) and 4.2.2 (a, b).

The DTA curves for the two heating rates under nitrogen atmosphere showed dehydration endotherm followed by three distinct, but low exothermic peaks with a maximum ~4°C temperature difference. The DTA curve under oxidizing atmosphere (flowing air, 60 mlmin<sup>-1</sup>) showed endothermic degradation (pyrolysis) followed by dual peak exotherms with a maximum temperature difference of 28.7°C. Slight endothermicity is again manifested beyond ~ 575 °C. DTA curves at 40°Cmin<sup>-1</sup> heating rate at different air flow rates (20, 40 and 60 mlmin<sup>-1</sup>) showed that with the increasing air flow rates, exothermic process temperature difference decreases slightly (from 30.6 °C at 20 mlmin<sup>-1</sup> to 28.7°C at 60 ml min<sup>-1</sup>). The DTA curves also showed that the increase in air flow rate reduces the exothermic peak area with the reaction completing at lower temperatures. TG curves showed that the total degradation increases at higher air flow rates, although only marginally.

The small endothermic peaks observed at around 100°C on the DTA curves under nitrogen and air atmospheres were due to evaporation of water from the sample.

The two exothermic peaks represented the two successive oxidation reactions taking place during the thermal decomposition of the mill rice husk samples. The two overlapping reactions took place between 290 and 521°C at 20°C min<sup>-1</sup> heating rate and between 258 and 575°C at 40°C min<sup>-1</sup> heating rate. The first exothermic reaction started at temperature over 290°C and reached its peak value at 360°C for 20°C min<sup>-1</sup> heating rate. At 40°C min<sup>-1</sup>, the peak temperature was observed at 409°C. The temperature difference due to the exothermic reaction was around 12.2 and 25.5°C for the two heating rates, respectively. The second exothermic reaction started at temperatures around 409 and 440°C- around 40°C higher than the temperature at which the first reaction peaks were observed. The peak temperatures in the second reaction zone were found at around 453 and 521°C for the two heating rates of 20 and 40°C min<sup>-1</sup>, respectively. The temperature difference due to exothermic reaction in the second reaction zone was marginally higher than that observed for the first reaction zone (28.7 to 25.5°C) for 40°C min<sup>-1</sup> whereas they were found to be almost same ~12.3°C for 20°C min<sup>-1</sup> heating rate.

#### 4.2.2.3 Sawdust

Figs. 4.2.5(a) and 4.2.6(a) show the TG, DTG and DTA curves for sawdust under nitrogen purging condition for the two heating rates of 20 and 40°C min<sup>-1</sup>. Thermograms and the DTG curves showed that there were five clearly distinct reaction zones, although the first and the fifth reaction zones were much slower than the second active pyrolysis zone. Dehydration is found to start from the ambient temperature due to physical drying and thermal evaporation of moisture. The first degradation zone starts at around 175°C and continues upto around 287°C giving 5.6% total degradation. The maximum degradation rate was observed to be 12.3 wt%min<sup>-1</sup> the maximum degradation rate increased to 29.2 wt%min<sup>-1</sup> at T<sub>max</sub> = 269°C for 20°Cmin<sup>-1</sup> heating rate.

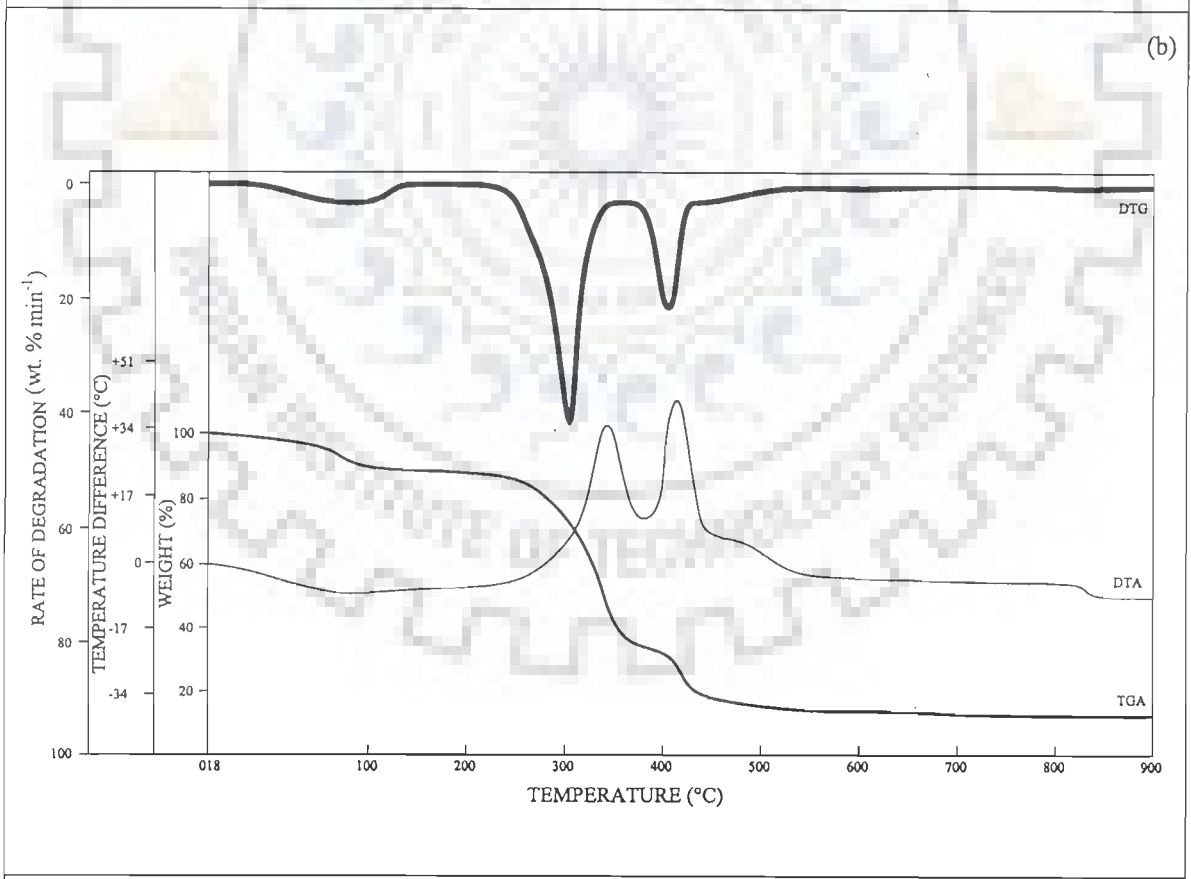
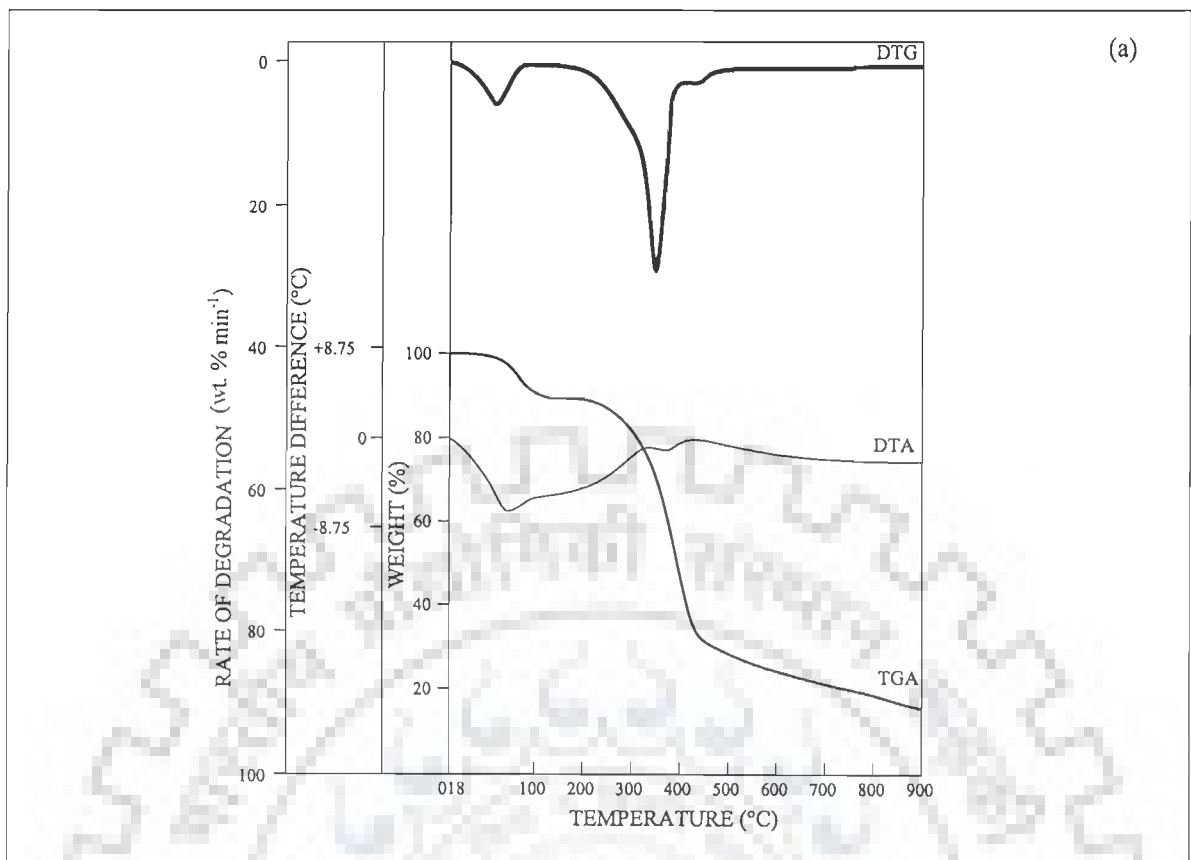


Fig. 4.2.5(a) & (b) : Thermogravimetric and Differential Thermal Analysis of Sawdust in (a) Nitrogen, and (b) Air; Heating Rate =  $20^{\circ}\text{C min}^{-1}$

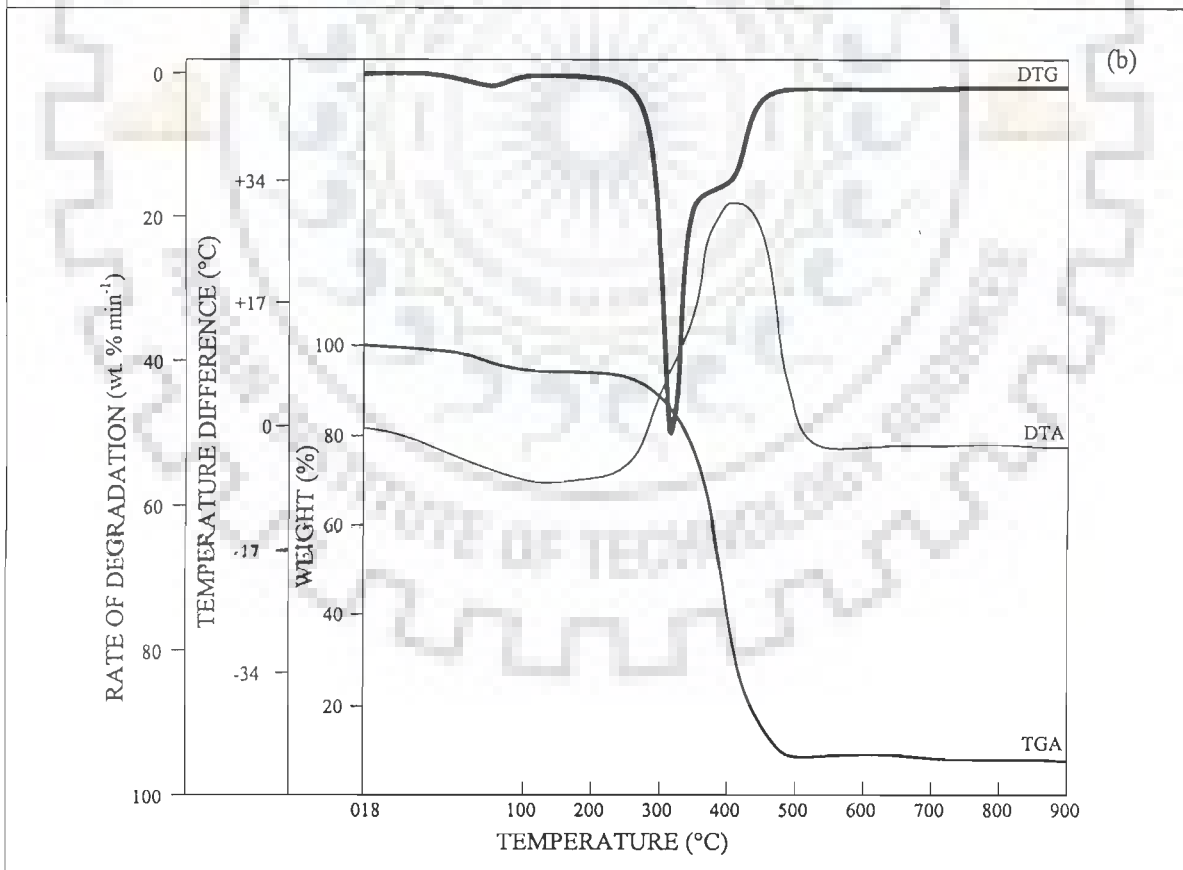
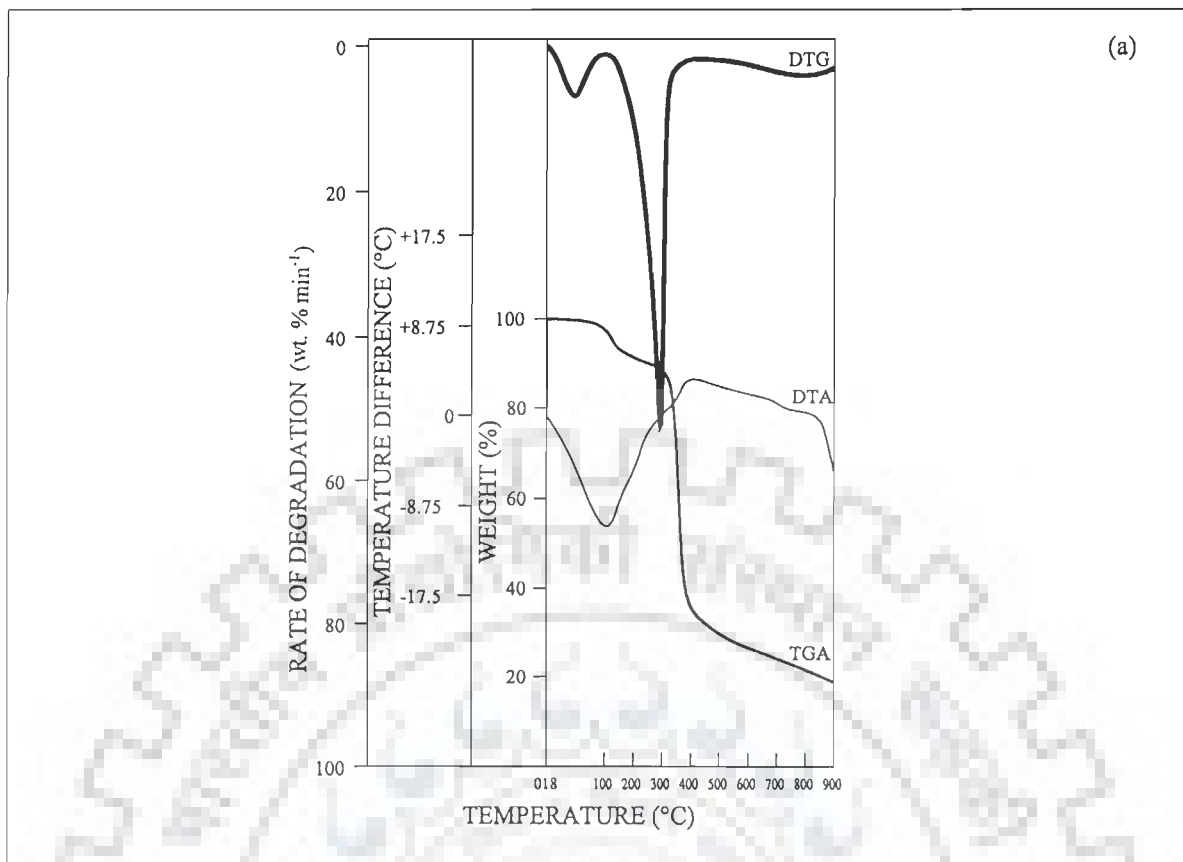


Fig. 4.2.6(a) & (b) : Thermogravimetric and Differential Thermal Analysis of Sawdust in (a) Nitrogen, and (b) Air; Heating Rate =  $40^{\circ}\text{C min}^{-1}$

With increase in the heating rate to  $40^{\circ}\text{C min}^{-1}$  at  $T_{\text{max}} = 269^{\circ}\text{C}$ , the total degradation in this reaction zone, however, decreased from 5.6% to 2%. In the second degradation (active pyrolysis) zone, the degradation started at  $290^{\circ}\text{C}$  and continued upto  $460^{\circ}\text{C}$  giving a total degradation of 60% at  $20^{\circ}\text{C min}^{-1}$  heating rate. Increase in the heating rate to  $40^{\circ}\text{C min}^{-1}$  initiated the degradation at a lower temperature of  $258^{\circ}\text{C}$  and the degradation continued upto  $456^{\circ}\text{C}$ . Total degradation in this reaction zone at  $40^{\circ}\text{C min}^{-1}$  heating rate was  $\sim 56.25\%$ . Maximum degradation rate was found to be 29.7 and 56.9%, respectively for the two heating rates, 20 and  $40^{\circ}\text{C min}^{-1}$ . The third degradation zone, a very slow degradation zone, lasted upto  $700^{\circ}\text{C}$  giving a total degradation of 16.25% for  $20^{\circ}\text{C min}^{-1}$  and 8.75% for  $40^{\circ}\text{C min}^{-1}$  heating rate, respectively. Slower heating rate, however, is able to degrade the sawdust more than at higher heating rate, as is evident from the Table 4.2.3(b). This decrease may be attributed to encrustation outside the particle surface offering larger temperature difference between the particle center and the outside surface as also offering larger diffusional resistance to release of volatiles from the interior surface. The third reaction zone is slower as is evident from the TG and DTG curves. The degradation data under nitrogen atmosphere are listed in Table 4.2.3(a, b).

Change from the nitrogen atmosphere to air atmosphere changes the degradation characteristics. The contrasting characteristics can be observed from the Figs. 4.2.5(a) and (b) and 4.2.6(a) and (b). After the drying, slow pyrolysis starts followed by gasification and combustion. For  $20^{\circ}\text{C min}^{-1}$  heating rate, the first reaction (devolatilization) zone is found to start at  $\sim 210^{\circ}\text{C}$  and end at  $\sim 295^{\circ}\text{C}$ . For  $40^{\circ}\text{C min}^{-1}$  heating rate, the first devolatilization zone started at  $\sim 150^{\circ}\text{C}$  and ended at  $\sim 300^{\circ}\text{C}$ .  $\text{min}^{-1}$ . In this zone the total degradation is found to be 9.25% at  $20^{\circ}\text{C min}^{-1}$  and 2.4% for  $40^{\circ}\text{C min}^{-1}$  heating rate. Moisture removal at  $40^{\circ}\text{C min}^{-1}$  was found to be 5.6%. The maximum degradation rate is observed to be 16.4 and  $20.9 \text{ wt}\% \text{min}^{-1}$ ,

**Table 4.2.3(a) : Thermal Degradation of Sawdust in the First Reaction Zone  
(Nitrogen : 50 mlmin<sup>-1</sup>)**

Heating Rate (°C min <sup>-1</sup> )	Water evolved (wt%)	Degradation Temperature (°C)			Total Degradation (wt%)	Degradation Rate, (wt% min <sup>-1</sup> )	
		Initial	Final	Maxm.		Avg.	Maxm.
20	10.0	175	290	269	6.25	6.2	12.3
40	8.1	133	290	195	2.50	14.7	29.2

**Table 4.2.3(b) : Thermal Degradation of Sawdust in the Second and Third  
Reaction Zones  
(Nitrogen : 50 mlmin<sup>-1</sup>)**

Reaction Zone	Heating Rate (°C min <sup>-1</sup> )	Degradation Temperature (°C)			Total Degradation (wt%)	Degradation Rate, (wt% min <sup>-1</sup> )		Residue at 700°C (wt%)
		Initial	Final	Maxm.		Avg.	Maxm.	
II	20	290	409	341	60.00	14.0	29.7	-
	40	258	456	310	56.25	28.7	56.9	-
III	20	409	700	-	16.25	-	-	17.5
	40	456	700	-	8.75	-	-	25.0

**Table 4.2.4(a) : Thermal Degradation of Sawdust in the First Reaction Zone  
(Air : 50 mlmin<sup>-1</sup>)**

Heating Rate (°C min <sup>-1</sup> )	Water evolved (wt%)	Degradation Temperature (°C)			Total Degradation (wt%)	Degradation Rate, (wt% min <sup>-1</sup> )	
		Initial	Final	Maxm.		Avg.	Maxm.
20	10	215	295	295	9.25	8.2	16.4
40	5.6	204	290	-	2.40	10.4	20.9

**Table 4.2.4(b) : Thermal Degradation of Sawdust  
(Air: 50 mlmin<sup>-1</sup>)**

Reaction Zone	Heating Rate (°C min <sup>-1</sup> )	Degradation Temperature (°C)			Total Degradation (wt%)	Degradation Rate, (wt% min <sup>-1</sup> )		Residue (wt%)
		Initial	Final	Maxm.		Avg.	Maxm.	
II	20	295	370	325	40.75	31.5	46.6	-
	40	290	380	320	52.00	36.3	51.6	-
III	20	370	438	403	16.4	13.2	28.5	-
	40	380	489	433	31.2	5.5	10.50	6.4
IV	20	438	512	-	12.45	2.25	5.5	10.5



respectively at 20 and 40°C min<sup>-1</sup> heating rates. The second reaction zone starts at ~ 290°C and lasts uptill 380°C. Total degradation in this zone is found to be much larger : ~ 40.75% at 20°C min<sup>-1</sup> and ~ 52% at 40°C min<sup>-1</sup> heating rate. The maximum degradation rate in this zone was found to be 46.6 and 51.6 wt% min<sup>-1</sup> at 20 and 40°Cmin<sup>-1</sup> heating rates, respectively. The third degradation zone starts at around 380°C and continued upto 438°C for 20°Cmin<sup>-1</sup>. For 40°Cmin<sup>-1</sup> heating rate, the third degradation zone started at 380°C and continued upto 489°C. Total degradations observed in this zone were 16.4 and 31.2% for 20 and 40°C min<sup>-1</sup>, respectively. The maximum degradation rate for 40°Cmin<sup>-1</sup> was 10.5 wt%min<sup>-1</sup> at ~433°C. At 20°Cmin<sup>-1</sup> heating rate, the degradation is found to continue at a slower rate upto 512°C from 438°C with a total degradation of 12.45% in this zone. After that, the oxidation is extremely slow with final residue being 10.5 and 6.4%, respectively for 20 and 40°C min<sup>-1</sup> heating rates at 700°C. The DTA curves for the two heating rates under nitrogen atmosphere show endothermic nature of dehydration followed by pyrolysis. Under oxidizing atmosphere (flowing air, 50mlmin<sup>-1</sup>) at 20°C min<sup>-1</sup> heating rate, dehydration followed by the first reaction zone show endothermicity, with a maximum temperature difference of 7.4°C during dehydration. The second and third reaction zones show dual exotherm peaks at temperature differences of 30.8 and 37.2°C, respectively.

The DTA curves under flowing air atmosphere show sharp dual peak exotherms starting at ~ 290°C and terminating at ~500°C for 20°C min<sup>-1</sup> heating rate. The dehydration followed by devolatilization of lighter volatiles showed endothermicity, with a maximum temperature difference of 7.4°C for the dehydration process. The first exothermic peak is found at 370°C which terminates at ~390°C. The second exothermic peak is found at ~428°C and terminates at ~ 440°C. The second exotherm is followed by a third slower exotherm with its peak at ~456°C. These three exothermic degradations are also manifested at TG and DTG curves. The second

exothermic degradation step is found to be short but sharp, whereas the third exothermic process seemed to represent a longer but very slow linear degradation.

The DTA curve for  $40^{\circ}\text{C min}^{-1}$  under air atmosphere showed only dual peak exothermicity in contrast to three peaks for  $20^{\circ}\text{C min}^{-1}$  heating rate. Unlike the fully developed sharp peaks separated from each other, the higher heating rate amalgamated the exothermic degradation processes. The exothermicity starts at  $300^{\circ}\text{C}$  and ends at  $515^{\circ}\text{C}$ . The first exothermic peak was observed at  $400^{\circ}\text{C}$  showing a temperature difference of  $45.2^{\circ}\text{C}$ . The second peak was found at  $433^{\circ}\text{C}$  with a temperature difference of  $39.6^{\circ}\text{C}$ . In contrast, the temperature differences at the two peaks observed for  $20^{\circ}\text{C min}^{-1}$  heating rate, were respectively,  $30.8$  and  $37.2^{\circ}\text{C}$ . Thus, while the maximum heat evolution is delayed at  $20^{\circ}\text{C min}^{-1}$  heating rate, the increase in the heating rate to  $40^{\circ}\text{C min}^{-1}$  accelerated the degradation process with the maximum heat evolution observed at a lower temperature.

#### 4.2.2.4 Bagasse

The thermal degradation characteristics of bagasse under flowing nitrogen and air atmospheres, as obtained by TG, DTG and DTA are shown in Figs.4.2.7(a, b) and 4.2.8(a, b) for the two heating rates  $20^{\circ}\text{C}$  and  $40^{\circ}\text{C min}^{-1}$ , respectively. Under nitrogen atmosphere, moisture removal is observed to occur upto  $152^{\circ}\text{C}$ , followed by the removal of light volatiles upto  $300^{\circ}\text{C}$  at  $20^{\circ}\text{Cmin}^{-1}$  heating rate (Fig. 4.2.7(a)). In this volatile evolution zone, total weight loss is found to be  $10.6\%$  with the average and maximum degradation rates of  $6.4\%$  and  $12.8\%$ , respectively. This initial zone is followed by the active pyrolysis (second degradation) zone from  $300^{\circ}\text{C}$  to  $390^{\circ}\text{C}$ , showing very fast degradation. Total degradation in this zone is found as  $52.2\%$  with the maximum degradation rate of  $22.5 \text{ wt}\%\text{min}^{-1}$  at  $T_{\text{max}}=363^{\circ}\text{C}$ . The subsequent degradation is found to proceed slowly which continued beyond  $900^{\circ}\text{C}$ . The

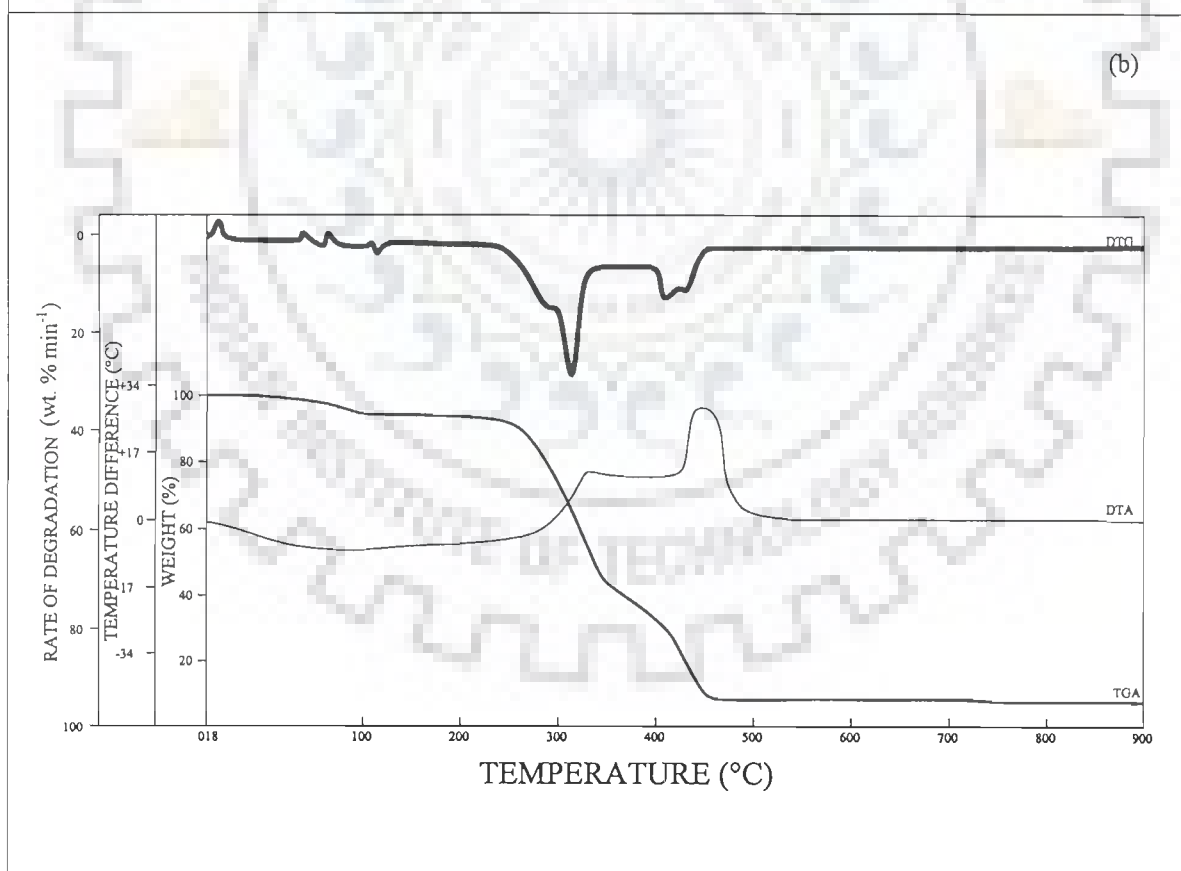
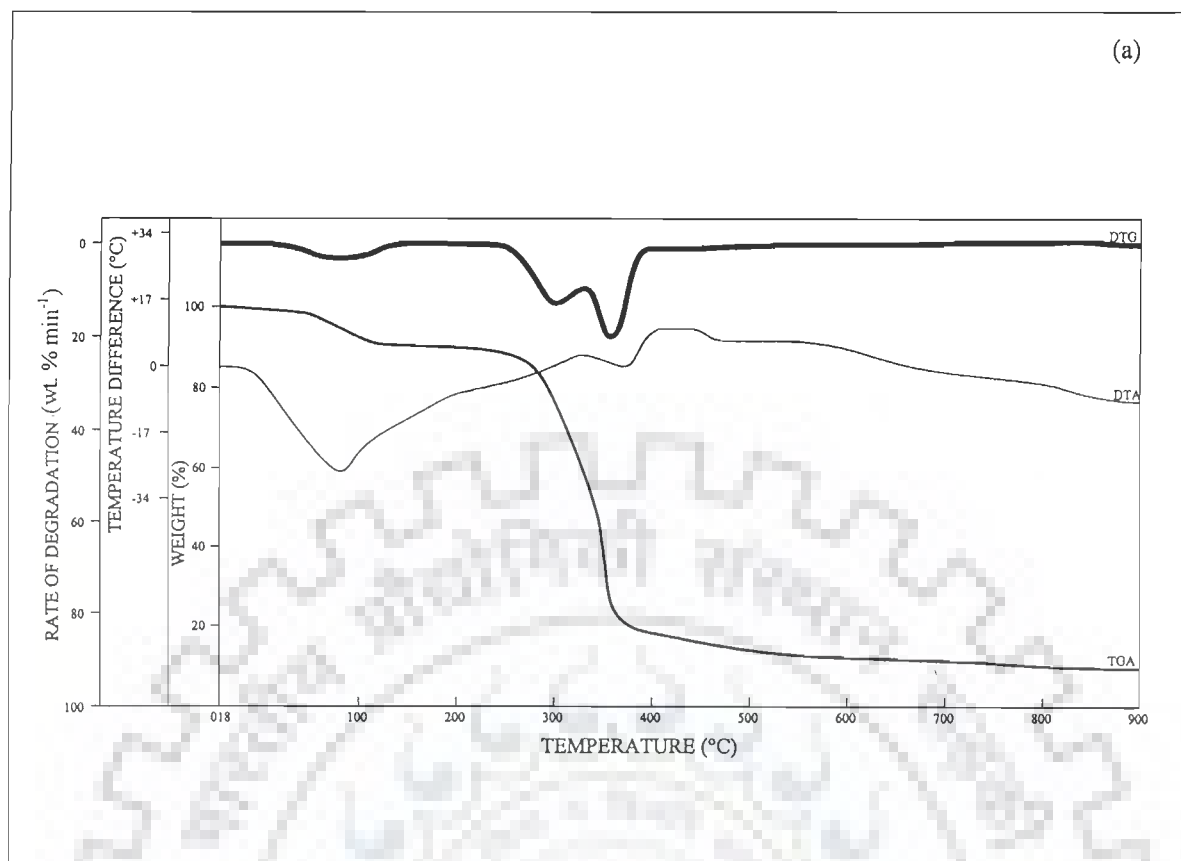


Fig. 4.2.7(a) & (b) : Thermogravimetric and Differential Thermal Analysis of Bagasse in (a) Nitrogen, and (b) Air; Heating Rate = 20°C min<sup>-1</sup>

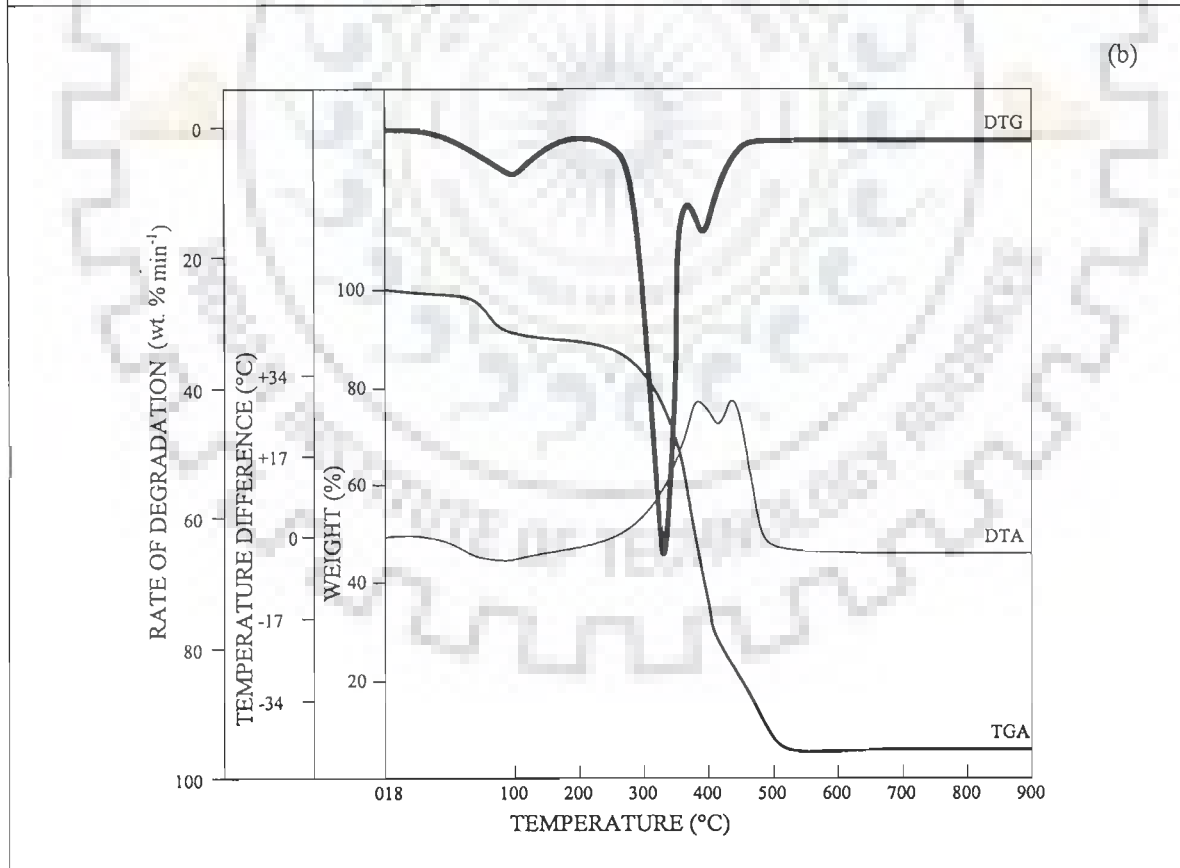
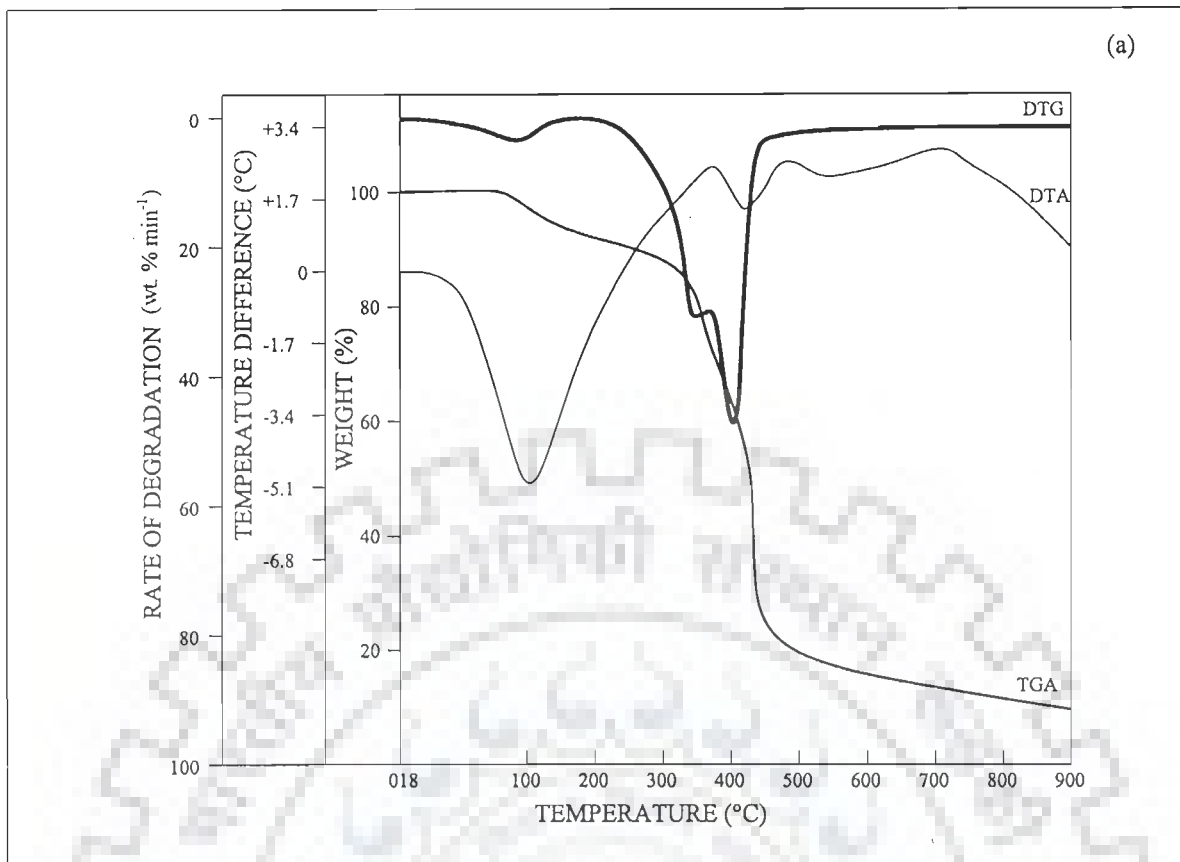


Fig. 4.2.8(a) & (b) : Thermogravimetric and Differential Thermal Analysis of Bagasse in (a) Nitrogen, and (b) Air; Heating Rate = 40°C min<sup>-1</sup>

degradation upto 700°C in this zone was found to be ~ 12% and the residue at 700°C was 18.6%.

At 40°C min<sup>-1</sup> heating rate, [Fig. 4.2.8(a)] the evolution of volatiles started at 195°C and continued upto 315°C, with a total weight loss of 10.25%. The maximum degradation rate was found to be 29.4% at 302°C. This degradation rate was found to be more than twice of the rate obtained at 20°C min<sup>-1</sup> heating rate. This zone was followed by the active pyrolysis zone upto 419°C, giving a total degradation of 61.5% with the maximum degradation rate of 49.6% min<sup>-1</sup> at T<sub>max</sub> = 360°C. The degradation in this zone occurs in very short time ~ 2.8 min, and the rate of degradation is more than two times of that observed at 20°C min<sup>-1</sup> heating rate. The degradation continued beyond 900°C, although very slowly. Upto 700°C, the total degradation was found to be 9.7%; the residue at 700°C being 11.5% of the original sample weight.

DTA curves at the two heating rates under flowing nitrogen atmosphere suggested that the endothermicity of dehydration was followed by exothermic reactions. The three peak exotherms showed the sequence of initial volatiles evolution followed by the active pyrolysis and slower degradation. The thermal degradation data are presented in Tables 4.2.5 (a, b).

Thermal degradation characteristics in flowing air atmosphere showed contrasting behaviour with the characteristics observed in nitrogen atmosphere. The characteristic curves under oxidizing air are shown in Figs. 4.2.7(b) and 4.2.8(b) for 20 and 40°Cmin<sup>-1</sup> heating rates, respectively. The data obtained from these figures are presented in Tables 4.2.6(a) and 4.2.6(b). Dehydration continued upto around 200°C. Thereafter, the first-phase of degradation started and continued upto 300°C. During this initial degradation, total degradation obtained was ~ 8%. The maximum degradation rates were found to be 12.8 and 36.9 wt%min<sup>-1</sup>, respectively at 20 and 40°C min<sup>-1</sup> heating rates. This initial zone was followed by a fast degradation zone

**Table 4.2.5(a) : Thermal Degradation of Bagasse in the First Reaction Zone**  
(Nitrogen : 50 mlmin<sup>-1</sup>)

Heating Rate (°C min <sup>-1</sup> )	Water evolved (wt%)	Degradation Temperature (°C)			Total Degradation (wt%)	Degradation Rate, (wt% min <sup>-1</sup> )	
		Initial	Final	Maxm.		Avg.	Maxm.
20	7.0	169	300	300	10.7	6.4	12.8
40	7.0	195	315	302	10.25	14.7	29.4

**Table 4.2.5(b) : Thermal Degradation of Bagasse**  
(Nitrogen : 50 mlmin<sup>-1</sup>)

Reaction Zone	Heating Rate (°C min <sup>-1</sup> )	Degradation Temperature (°C)			Total Degradation (wt%)	Degradation Rate, (wt% min <sup>-1</sup> )		Residue (wt%)
		Initial	Final	Maxm.		Avg.	Maxm.	
II	20	300	390	363	52.2	11.7	22.5	-
	40	315	419	370	61.5	26.3	49.6	-
III	20	390	700	-	12.0	-	-	18.6
	40	419	700	-	9.7	-	-	11.5

**Table 4.2.6 (a) : Thermal Degradation of Bagasse in the First Reaction Zone**  
(Air: 50 mlmin<sup>-1</sup>)

Heating Rate (°C min <sup>-1</sup> )	Moisture Removed (%)	Degradation Temperature (°C)			Total Degradation (wt%)	Degradation Rate, (wt% min <sup>-1</sup> )	
		Initial	Final	Maxm.		Avg.	Maxm.
20	8.00	248	300	300	8.00	6.4	12.8
40	8.25	181	300	-	8.25	18.4	36.9

**Table 4.2.6(b) : Thermal Degradation of Bagasse (Air: 50 mlmin<sup>-1</sup>)**

Reaction Zone	Heating Rate (°C min <sup>-1</sup> )	Degradation Temperature (°C)			Total Degradation (wt%)	Degradation Rate, (wt% min <sup>-1</sup> )		Residue (wt%)
		Initial	Final	Maxm.		Avg.	Maxm.	
II	20	300	338	326	27.9	15.6	28.4	-
	40	300	360	326	35.0	55.3	64.6	-
III	20	338	356	-	19.9	3.5	3.5	-
	40	360	399	-	20.6	18.8	-	-
IV	20	356	438	428	17.0	8.3	11.4	
	40	399	466	419	17.5	9.1	16.9	
V	20	438	499	445	18.2	6.8	9.9	2.0
	40	466	575	-	11.3	-	-	2.0

from 300°C to 338°C, with a total degradation of 27.9% and 35% with the maximum degradation rates of 28.4 and 64.6% min<sup>-1</sup> at 20 and 40°C min<sup>-1</sup> heating rates, respectively. T<sub>max</sub> was found to be ~ 326°C. This zone coincided with the first of the dual peak exotherms obtained from DTA. The second zone was followed by a sharper but a smaller duration of degradation continuing upto 356°C and 399°C for the two heating rates, respectively. In this zone the degradation was around 20% at both heating rates. This zone was further followed by an exothermic reaction giving 17% and 17.5% total degradation at 20 and 40°C min<sup>-1</sup> heating rate, respectively. The fifth zone was the culmination of the degradation process showing a total degradation of 18.2% and 11.3%, respectively for the two heating rates. It was found that the total residue left after this zone was only around 2%.

The DTA data deduced from the DTA curves are given below :

**DTA Data**

Heating Rate (°C min <sup>-1</sup> )	Exothermic Peaks			
	First Peak		Second Peak	
	T	ΔT	T	ΔT
	(°C)		(°C)	
20	355	14.4	447	30.3
40	390	31.1	440	31.6

**Note :** T = Peak Temperature °C, ΔT = Temperature difference due to exothermic reactions.

The dual exothermic peaks as observed from DTA curves represented two successive reactions taking place during the thermal decomposition of bagasse samples. The two reactions overlapped each other and took place between 290 and 499°C at 20°Cmin<sup>-1</sup> and between 258 and 535°C at 40°C min<sup>-1</sup> heating rate.

The second exothermic reactions started at temperatures ~ 30°C and 56°C higher than the first exothermic reaction peaks at 20 and 40°C min<sup>-1</sup> heating rates, respectively. While the temperature differences for the two peaks at 20°C min<sup>-1</sup> heating

rate were close to each other, the temperature difference at the second peak was more than two times that observed at the first peak for  $40^{\circ}\text{Cmin}^{-1}$  heating rate.

#### 4.2.2.5 Pressmud

The thermal degradation characteristics of pressmud under flowing nitrogen and air are given in Figs. 4.2.9 and 4.2.10, for 20 and  $40^{\circ}\text{Cmin}^{-1}$  heating rate, respectively. Pressmud loses moisture (~8%) followed by volatile evolution and thermal degradation under nitrogen atmosphere [Figs. 4.2.9(a) and 4.2.10(a)]. The first degradation started at  $145^{\circ}\text{C}$  and ended at  $310^{\circ}\text{C}$ , with the maximum degradation rate of  $6.2 \text{ wt}\%\text{min}^{-1}$  at  $T_{\text{max}} = 265^{\circ}\text{C}$  at  $25^{\circ}\text{C min}^{-1}$  heating rate. Total degradation in this phase was found to be 5.6%. With  $40^{\circ}\text{C min}^{-1}$  heating rate, the degradation started at  $169^{\circ}\text{C}$  and ended at  $279^{\circ}\text{C}$ . Total degradation at this heating rate was only 3%, with the maximum degradation rate of  $7.7 \text{ wt}\%\text{min}^{-1}$ . This phase was followed by the second and faster degradation phase which continued upto  $409\text{-}419^{\circ}\text{C}$ . The total degradation, maximum degradation rate and the temperature at which this occurs, for 25 and  $40^{\circ}\text{C min}^{-1}$  heating rates, were respectively, 16.7%,  $9.7 \text{ wt}\%\text{min}^{-1}$ ,  $341^{\circ}\text{C}$ , and 16.1%,  $14.0 \text{ wt}\%\text{min}^{-1}$  and  $360^{\circ}\text{C}$ . This phase was followed by the at least two other phases, one very short phase of degradation occurring at  $642^{\circ}\text{C}$  and  $772^{\circ}\text{C}$  (peak temperatures) for 25 and  $40^{\circ}\text{C min}^{-1}$  heating rates, respectively. Before this short phase the rate of degradation was found to be almost constant. For calculation purposes, the total degradation from the end of the second reaction zone to  $850^{\circ}\text{C}$  has been taken to be occurring as if in one single zone. The total degradations so calculated were, respectively 20.5% and 19.9% for the two heating rates, as seen from Table 4.2.6(b). Under nitrogen atmosphere, pressmud degradation is incomplete even at  $900^{\circ}\text{C}$ , and the residues obtained at  $850^{\circ}\text{C}$  were, respectively, 49.1 and 52.8% for 25 and  $40^{\circ}\text{C min}^{-1}$  heating rates. DTG and DTA curves also characterize the degradation. It is found that unlike VRH and MRH, pressmud pyrolysis shows exothermic-endothermic reaction characteristics, with large exothermicity at higher heating rate.



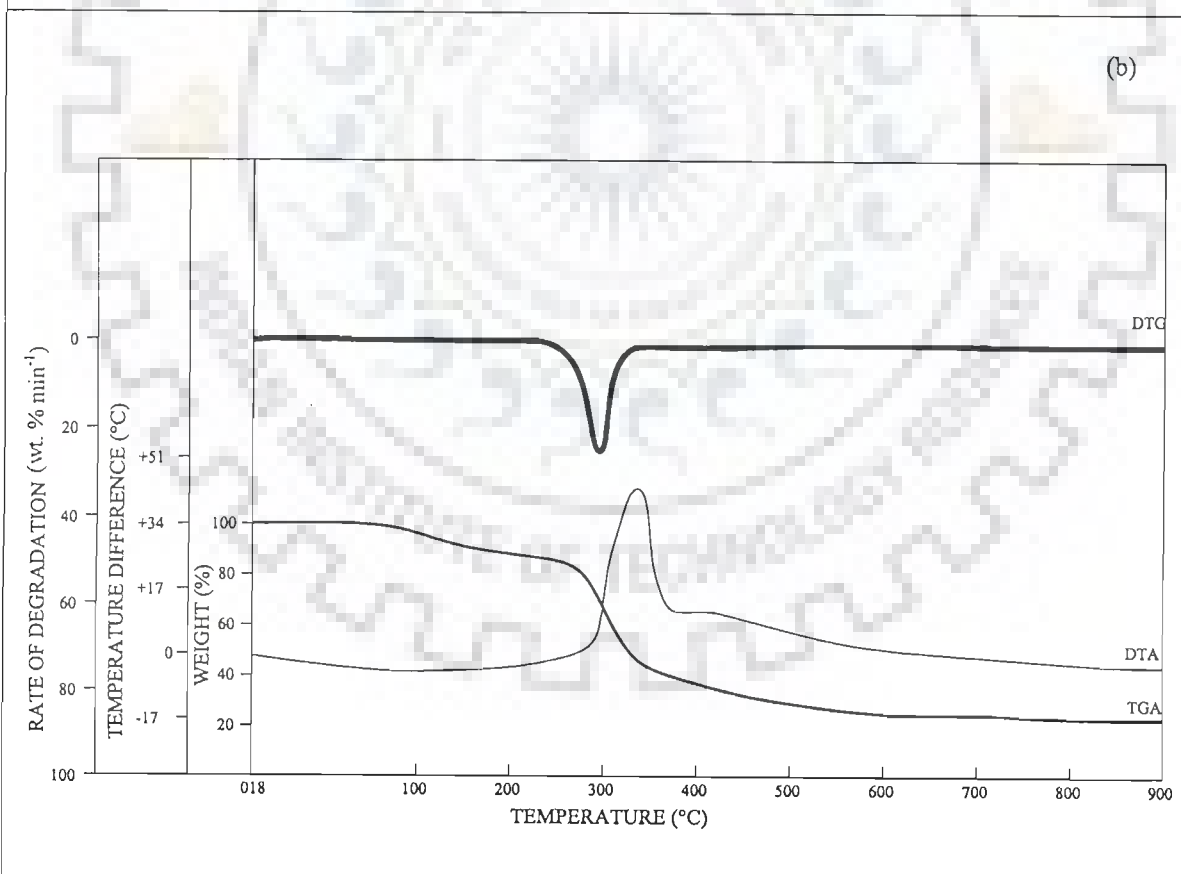
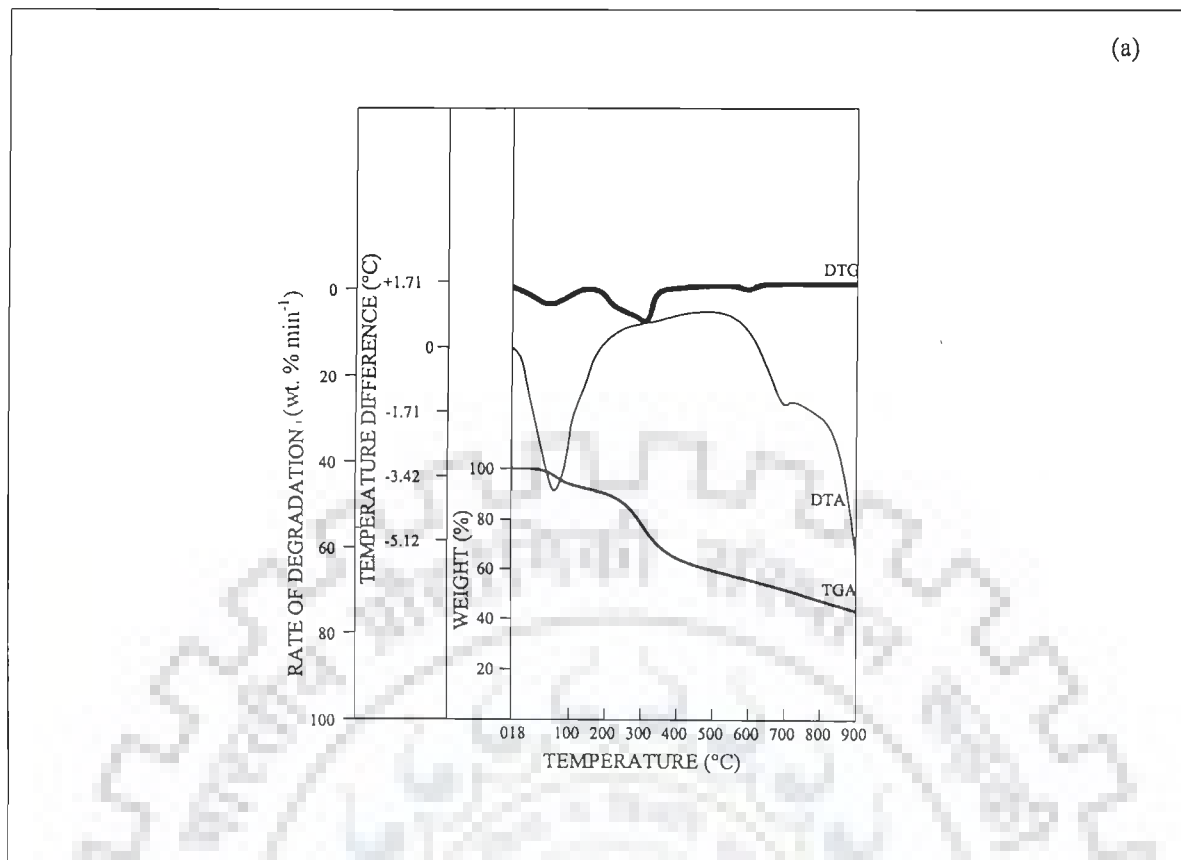


Fig. 4.2.9(a) & (b) : Thermogravimetric and Differential Thermal Analysis of Pressmud in (a) Nitrogen, Heating Rate = 25°Cmin<sup>-1</sup> (b) Air, Heating Rate = 20°Cmin<sup>-1</sup>.

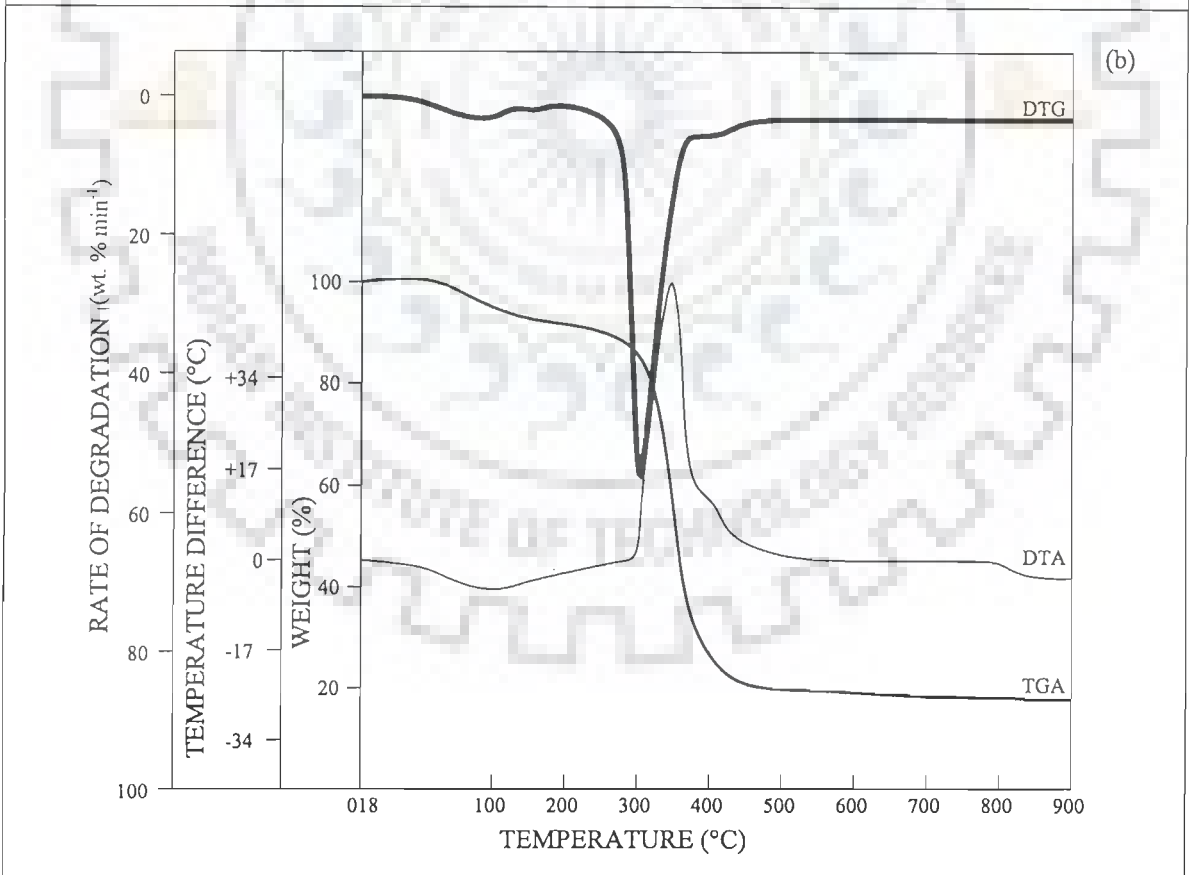
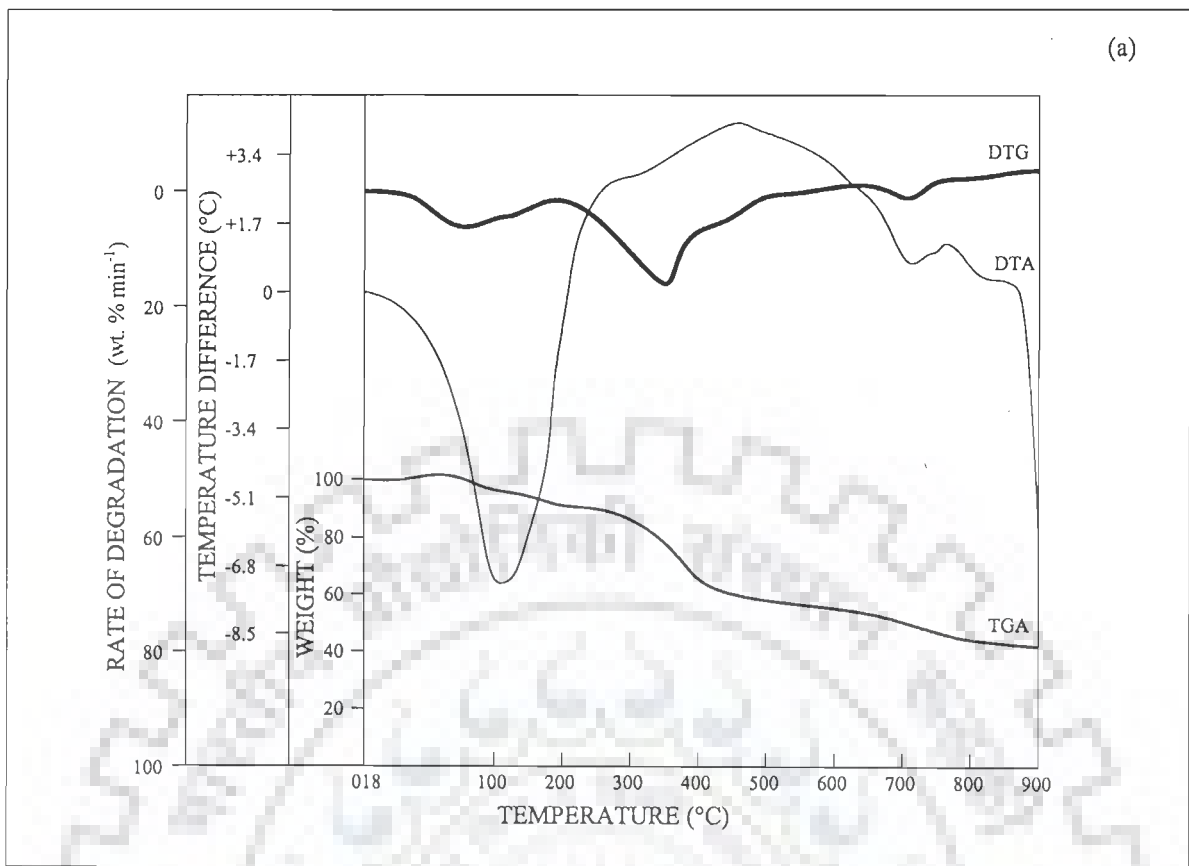


Fig. 4.2.10(a) & (b) : Thermogravimetric and Differential Thermal Analysis of Pressmud in (a) Nitrogen, and (b) Air; Heating Rate = 40°C min<sup>-1</sup>

Changing the atmosphere from flowing nitrogen to flowing air at  $60 \text{ ml min}^{-1}$  catapults the degradation characteristics in contrast to pyrolysis. DTG and DTA curves exemplify the acceleration in degradation rate and the heat evolution due to exothermic reactions at different temperatures [Figs. 4.2.9(b) and 4.2.10(b)]. The first phase of degradation is slow giving a total degradation of 16.3 and 9.3% at  $20$  and  $40^\circ\text{C min}^{-1}$  heating rates, respectively. This phase is seen to start at  $169^\circ\text{C}$  ending at  $320^\circ\text{C}$  for  $20^\circ\text{C min}^{-1}$  heating rate. For  $40^\circ\text{C min}^{-1}$  heating rate, this phase started at  $133^\circ\text{C}$  and ended at  $304^\circ\text{C}$ . A small kink is seen during this phase in both DTG and DTA curves. The second phase showed very fast degradation ending at  $362$  and  $385^\circ\text{C}$  for  $20$  and  $40^\circ\text{C min}^{-1}$  heating rates, respectively. The maximum degradation rate was found to be  $78.3 \text{ wt\%min}^{-1}$  at  $304^\circ\text{C}$  at  $40^\circ\text{C min}^{-1}$ . During this reaction zone, total degradation was found to be 24.4% at  $20^\circ\text{C min}^{-1}$  and 46.9% at  $40^\circ\text{C min}^{-1}$ . Last phase of degradation was found to be very slow. Taking the degradation upto  $700^\circ\text{C}$  as if a single reaction zone, total degradations were found to be 16.7 and 18.5% and the residue obtained were 34.1 and 16.5% at  $700^\circ\text{C}$  for  $20$  and  $40^\circ\text{C min}^{-1}$  heating rates, respectively.

It is, thus, very clear that the oxidation helps achieve much larger over all degradation in flowing air atmosphere with the remaining residue being only 34.1 and 16.5% of the original sample in comparison to 49.1 and 52.8% with nitrogen at  $20$  and  $40^\circ\text{Cmin}^{-1}$  heating rates, respectively. The degradation data are presented in Tables 4.2.7 and 4.2.8.

The DTA curves obtained under oxidizing atmosphere at  $20^\circ\text{C min}^{-1}$  heating rate showed that the exothermic oxidation of pressmud started at  $370^\circ\text{C}$  and ended at  $530^\circ\text{C}$ . Dual peak exotherms were observed, with the first exotherm peak starting at  $341^\circ\text{C}$  and terminating at  $\sim 370^\circ\text{C}$ . The temperature difference was  $\sim 47^\circ\text{C}$ . The second peak was observed at  $\sim 400^\circ\text{C}$  giving a temperature difference of  $\sim 9.5^\circ\text{C}$ . Beyond  $530^\circ\text{C}$ , the degradation was found to be endothermic in nature.

Table 4.2.7(a) : Initial Thermal Degradation of Pressmud  
(Nitrogen: 50 mlmin<sup>-1</sup>)

Heating Rate (°C min <sup>-1</sup> )	Moisture Removed (%)	Degradation Temperature (°C)			Total Degradation (wt%)	Degradation Rate, (wt% min <sup>-1</sup> )	
		Initial	Final	Maxm.		Avg.	Maxm.
25	8.1	145	310	265	5.6	-	6.2
40	8.1	169	279	279	3.0	-	7.7

Table 4.2.7(b) : Thermal Degradation of Pressmud  
(Nitrogen: 50 mlmin<sup>-1</sup>)

Reaction Zone	Heating Rate (°C min <sup>-1</sup> )	Degradation Temperature (°C)			Total Degradation (wt%)	Degradation Rate, (wt% min <sup>-1</sup> )		Residue at 850°C (wt%)
		Initial	Final	Maxm.		Avg.	Maxm.	
II	25	310	409	341	16.7	7.0	9.7	-
	40	279	419	360	16.1	9.3	14.0	-
III	25	409	850	-	20.5	-	2.0	49.1
	40	419	850	-	19.9	2.8	3.8	52.8

Table 4.2.8(a) : Initial Thermal Degradation of Pressmud  
(Air : 50 mlmin<sup>-1</sup>)

Heating Rate (°C min <sup>-1</sup> )	Moisture Removed (%)	Degradation Temperature (°C)			Total Degradation (wt%)	Degradation Rate, (wt% min <sup>-1</sup> )	
		Initial	Final	Maxm.		Avg.	Maxm.
20	4.8	169	320	290	16.9	15.5	26.4
40	8.2	133	304	-	9.3	-	-

Table 4.2.8(b) : Thermal Degradation of Pressmud  
(Air : 50 mlmin<sup>-1</sup>)

Reaction Zone	Heating Rate (°C min <sup>-1</sup> )	Degradation Temperature (°C)			Total Degradation (wt%)	Degradation Rate, (wt% min <sup>-1</sup> )		Residue at 700°C (wt%)
		Initial	Final	Maxm.		Avg.	Maxm.	
II	20	300	362	290	24.4	5.7	90.0	-
	40	304	385	304	46.9	-	78.3	-
III	20	362	700	400	16.7	1.0	1.9	34.1
	40	385	700	-	18.5	-	-	16.5

For  $40^{\circ}\text{C min}^{-1}$  heating rate, the DTA curve showed similar characteristics as for  $20^{\circ}\text{C min}^{-1}$ . The exothermic oxidation was found to start at  $258^{\circ}\text{C}$  and end at  $568^{\circ}\text{C}$ . Dual peak exotherms were observed with overlapping. The first exothermic peak was observed at  $390^{\circ}\text{C}$  giving a temperature difference of  $\sim 48.8^{\circ}\text{C}$ . The second peak was found at  $\sim 477^{\circ}\text{C}$  showing a temperature difference of  $13.3^{\circ}\text{C}$ . Beyond  $568^{\circ}\text{C}$ , the degradation was found to be almost negligible.

### **4.3 KINETICS OF BIOMASS THERMAL DECOMPOSITION**

#### **4.3.1 Integral and Differential Methods for the Use of Thermogravimetry**

Dynamic thermogravimetry has been widely used during the last four decades to study the kinetics of thermal decomposition/degradation reactions for inorganic and organic chemicals, coal, biomass materials and petroleum products. The advantages and disadvantages of using non-isothermal thermogravimetry have been discussed in the classical texts on thermal methods of analysis (Wendlandt, 1974; Charsley and Warrington, 1992). Several methods of kinetic analysis and reaction mechanisms have been proposed for biomass degradation using thermogravimetry. For a one step irreversible reaction model, differential and integral methods have been suggested for the determination of kinetic parameters, namely, the order of reaction, the specific reaction rate constant and its dependence on temperature using Arrhenius equation. The frequency factor or pre-exponential factor,  $k_0$ , has either been used as a constant (as used by most of the investigators) or as a function of temperature (like in collision theory) as defined by Gaur and Reed (1994) and later used by Sharma and Rao (1999). In the present work, Arrhenius equation has been used to represent the variation of the specific reaction rate constant with temperature. Thermogravimetric data have been analysed using the integral methods of Coats and Redfern (1964), Horowitz and Metzger (1963), Piloyan and Novikova (1967), Reich and Stivala (1982) and Agarwal and Sivasubramanian (1987), and the differential method of Freeman and Carroll

(1958) to determine kinetic parameters for the thermal degradation of five biomass materials, namely village rice husk (VRH), mill rice husk (MRH), saw dust (SD), bagasse (BG) and press mud (PM).

Coats and Redfern (1964) and Freeman and Carroll (1958) methods have been used very widely. In the Coats and Redfern method, the integrand  $\int \exp(-E/RT)dT$  of equation 2.4.5 is approximated by

$$\int_0^T \exp(-E/RT)dT = \frac{RT^2}{E} \left(1 - \frac{2RT}{E}\right) \exp(-E/RT) \quad (4.3.1)$$

Agarwal and Sivasubramanian (1987) proposed an improvement over the Coats and Redfern approximation, so that the approximation showed minimum deviation from the exact numerical integral over a wide range of E values. Their approximation is given as :

$$\int_0^T \exp(-E/RT)dT = \frac{RT^2}{E} \left[ \frac{1 - 2(RT/E)}{1 - 5(RT/E)^2} \right] \exp(-E/RT) \quad (4.3.2)$$

In order to avoid poor parameter estimation due to improper scaling, the reparameterization recommended by Chen and Aris (1992) has been used for the determination of best fit values of n, k<sub>0</sub> and E :

$$\alpha_1 = -\frac{E}{10^3 R}; \alpha_2 = \ln \frac{k_0 R}{\beta E} b; x = \frac{10^3}{T} \quad (4.3.3)$$

where b = 1-2 RT/E; for Coats and Redfern approximation

$$= \frac{1 - 2(RT/E)}{1 - 5(RT/E)^2}; \text{ for Agarwal and Sivasubramanian approximation} \quad (4.3.4)$$

Thus, the integral equation for the determination of kinetic parameters with either of the above approximations is manipulated with the rescaled parameters as

$$y = a_1 x + a_2 \quad (4.3.5)$$

where  $y = \ln \left\{ \frac{1 - (1-x)^{1-n}}{(1-n)T^2} \right\}$  n ≠ 1

$$= \ln \left[ -\ln(1-x)/T^2 \right] n = 1 \quad (4.3.6)$$

= experimentally determined conversion (decomposition) function.

The second term  $a_2$  of Eq. (4.3.5) is found to be almost invariant with time or temperature and therefore could be taken as a constant. Then a plot of  $y$  against  $x$  should yield the value of  $a_1$  (or  $E$ ) and  $a_2$  (or  $k_0$ ) for an assumed value of  $n$  used in the determination of  $y$  in Eq. (4.3.6). The best fit values of  $a_1$  and  $a_2$  are obtained by using least squares technique i.e. the minimization of the squares of the differences between the experimental and predicted values of  $y$  for a given  $n$ , i.e.

$$F = \sum_{j=1}^{nn} (y_{j,\text{exp}} - y_{j,\text{pred}})^2$$

$$= \sum_{j=1}^{nn} (y_{j,\text{exp}} - a_1 x - a_2)^2$$

That value of  $n$  which gives the highest (or closest to 1.0) value of  $R^2$  (regression coefficient) for the best fit of the experimental data plotted as Eq. 4.3.5 is chosen for the determination of  $a_1$  and  $a_2$ . From this value of  $a_1$  and  $a_2$ , the activation energy,  $E$  and the pre-exponential factor,  $k_0$  have been determined.

In the following the results obtained for the kinetics of pyrolysis and oxidation degradation are presented.

#### 4.3.2 Kinetics of Pyrolysis

The biomass materials are normally composed of cellulose, hemicellulose, lignin and other complex compounds. Due to complexity of their composition, the pyrolysis of individual components is generally not attempted. Several researchers have described the products, mechanisms and rates of degradation of cellulose, hemicellulose, lignin and whole biomass and the role of a complex sequence of competing solid-and vapour-phase pyrolysis pathways (Antal, 1985; Ramaih, 1970; Antal and Varhegyi, 1995; Ahuja et al., 1996).

In the range of heating rates employed (i.e. 20 and 40°Cmin<sup>-1</sup>), and the size of the samples (<10 mg) the thermogravimetric analysis, usually evidences a distinct DTG peak resulting from the decomposition of cellulose and a lower temperature peak

associated with hemicellulose pyrolysis. In some of the biomass samples, a broad peak is observed due to merging of the two peaks (Antal and Varhegyi, 1995). In the DTG curves obtained with the biomass samples, similar trends were observed, excepting for pressmud. Pressmud is not exactly a biomass of flora origin, but an industrial waste originating from the clarification of sugar cane juice and syrup during the manufacture of cane sugar. The observation that no peak attributed to lignin decomposition is obtained under any circumstance is found to be true for the four biomass used in the present study. Alves and Figueiredo (1988), Koufopoulos et al. (1989), Font et al. (1991), Varhegyi et al. (1989, 1994), and Teng et al. (1997) have all used summative kinetic analysis using individual volatile product evolution model. Global kinetics are of interest in modeling solid hydrocarbons decomposition in many applications in which the representation of full hydrocarbon degradation process makes no sense (Milosavljevic and Suuberg, 1995). Global kinetics are looked to be offering a clue to the key mechanistic steps in the overall biomass degradation process (Teng et al., 1997). In this model it is assumed that the hemicellulose and cellulose components of whole biomass decompose independently of one another, following a simple; single step, first order irreversible reaction. Antal and Varhegyi (1995) have examined the experimental evidences available to pronounce that the cellulose pyrolysis is not affected by the presence of hemicellulose and lignin. If the sample size is small (usually less than 10 mg) and the size of the particles in the sample is also small, as the case for the present study, then the heat and mass transfer effects could be neglected during the thermal degradation.

Based on the above analysis, the experimental data of TG, DTG and DTA analyses have been examined. In the present analysis, the pyrolysis of whole biomass (i.e. VRH, MRH, SD and BG) and pressmud (PM) samples have been divided into different temperature (time or reaction) zones and the kinetic parameters have been determined using the integral and differential methods of analysis. Agarwal and Sivasubramanian's approximation with the integral method has also been employed for



the full range of volatile evolution. This simple model is applicable in the present study as the pyrolysis volatiles have been continuously purged with the flowing nitrogen. Thus, the residence time of the volatiles, to have any appreciable interaction with the solid/solid char, is very very short. The results of the kinetic analysis are presented in Tables 4.3.1 – 4.3.5.

#### 4.3.2.1 Village Rice Husk

As seen from Fig. 4.2.1(a) and 4.2.2(a), the pyrolysis TG and DTG curves show three distinct regions of weight loss, excluding the initial moisture loss peak. The first zone of weightloss is between ~ 195 and 300°C and 170-290°C for 20 and 40°C min<sup>-1</sup>, heating rates, respectively, and could be seen as the zone of light volatiles evolution. The second and third zones represent the pyrolysis zones of hemicellulose, cellulose. Lignin degradation takes place, perhaps, throughout the temperature range (Evans and Milne 1987a, b; Varhegyi et al., 1989 and Antal and Varhegyi, 1995). It may be seen that the fourth zone is a very slow decomposition zone over a large temperature range. Shafizadeh et al. (1977) have shown that hemicellulose represented by xylan decomposes between 250 and 320°C, cellulose decomposes between 250 and 360°C and lignin decomposes gradually between 180 and 500°C. Thus, between 180 and 320°C all the three decompose and degrade, while between 320°C and 360°C, cellulose and lignin decompose simultaneously.

As the hemicellulosic and cellulosic decomposition loss account for around 60-70% of the total weight loss, it has been thought to determine the lower-temperature range degradation (pyrolysis) kinetics using the above-mentioned methods. The kinetic parameters are reported in Table 4.3.1(a, b). Village rice husk has slightly lower fixed carbon and slightly higher ash content but slightly higher hydrogen than those for mill rice husk obtained from mechanized mills. It is also found to have lower heating value and lower ash deformation temperature than mill rice husk. The pyrolysis kinetic

Table 4.3.1 (a) : Kinetic Parameters for Village Rice Husk Pyrolysis from Thermogravimetric Analysis.  
(Nitrogen : 50 mlmin<sup>-1</sup>), Heating Rate : 20°C min<sup>-1</sup>

Temp. Zone (°C)	Method of Analysis					
	Coats & Redfern	Agarwal & Sivasubramanian	Piloyan & Novikova	Reich & Stivala	Horowitz & Metzger	Freeman & Carroll
194-300	n = 1.0 E=84.3 k <sub>o</sub> = 8.2x10 <sup>7</sup> R <sup>2</sup> =0.9983	n = 1.0 E=84.3 k <sub>o</sub> = 8.08x10 <sup>7</sup> R <sup>2</sup> =0.9983	- E=69.62 k <sub>o</sub> = 1.675x10 <sup>5</sup>	n = 2.00 E=61.61 k <sub>o</sub> = 1.68x10 <sup>5</sup>	n = 2.50 E=25.52 k <sub>o</sub> = 4.11x10 <sup>3</sup>	n = 2.21 E=225.60 k <sub>o</sub> = 6.143x10 <sup>4</sup>
300-390	n = 2.25 E=169.52 k <sub>o</sub> = 2.65x10 <sup>4</sup> R <sup>2</sup> =0.9114	n = 2.25 E=169.52 k <sub>o</sub> = 2.64x10 <sup>14</sup> R <sup>2</sup> =0.9114	- E=74.49 k <sub>o</sub> = 1.792x10 <sup>5</sup>	n = 0.75 E=113.41 k <sub>o</sub> = 6.92x10 <sup>4</sup>	n = 2.50 E=39.23 k <sub>o</sub> = 1.43x10 <sup>5</sup>	n = 0.66 E=11.29 k <sub>o</sub> = 1.68x10 <sup>4</sup>
390-530	n = 1.25 E=127.55 k <sub>o</sub> = 1.25x10 <sup>9</sup> R <sup>2</sup> =0.9932	n = 1.25 E=127.55 k <sub>o</sub> = 1.24x10 <sup>9</sup> R <sup>2</sup> =0.9932	- E=98.70 k <sub>o</sub> = 2.37x10 <sup>5</sup>	n = 0.33 E=134.70 k <sub>o</sub> = 2.99x10 <sup>5</sup>	-	n = 0.54 E=93.61 k <sub>o</sub> = 4.26x10 <sup>5</sup>
194-530	-	n = 1.25 E=62.60 k <sub>o</sub> = 6.25x10 <sup>4</sup> R <sup>2</sup> =0.9956 For n = 1.00 E=53.78 k <sub>o</sub> = 7.63x10 <sup>3</sup> R <sup>2</sup> =0.9778	-	-	-	-

Note : E is in kJmol<sup>-1</sup>; k<sub>o</sub> is in min<sup>-1</sup>.

**Table 4.3.1 (b) : Kinetic Parameters for Village Rice Husk Pyrolysis from Thermogravimetric Analysis.**  
 (Nitrogen : 50 mlmin<sup>-1</sup>), Heating Rate : 40°C min<sup>-1</sup>

Temp. Zone (°C)	Method of Analysis					
	Coats & Redfern	Agarwal & Sivasubramanian	Piloyan & Novikova	Reich & Stivala	Horowitz & Metzger	Freeman & Carroll
170-290	n = 1.0 E=85.83 k <sub>o</sub> = 2.95x10 <sup>8</sup> R <sup>2</sup> =0.9731	n = 1.0 E=85.83 k <sub>o</sub> = 2.93x10 <sup>8</sup> R <sup>2</sup> =0.9731	- E=70.37 k <sub>o</sub> = 3.39x10 <sup>5</sup>	n = 0.00 E=44.25 k <sub>o</sub> = 2.3x10 <sup>5</sup>	n = 0.95 E=27.29 k <sub>o</sub> = 4.85x10 <sup>4</sup>	n = 0.78 E=2.54 k <sub>o</sub> = 3.33x10 <sup>5</sup>
290-409	n = 1.00 E=111.57 k <sub>o</sub> = 1.90x10 <sup>9</sup> R <sup>2</sup> =0.9955	n = 1.00 E=111.57 k <sub>o</sub> = 1.88x10 <sup>9</sup> R <sup>2</sup> =0.9955	- E=75.39 k <sub>o</sub> = 3.63x10 <sup>5</sup>	n = 0.25 E=103.997 k <sub>o</sub> = 4.15x10 <sup>5</sup>	n = 1.00 E=33.214 k <sub>o</sub> = 5.21x10 <sup>4</sup>	n = 2.53 E=298.63 k <sub>o</sub> = 1.86x10 <sup>7</sup>
409-548	n = 2.50 E=167.83 k <sub>o</sub> = 2.67x10 <sup>12</sup> R <sup>2</sup> =0.9632	n = 2.50 E=167.83 k <sub>o</sub> = 2.65x10 <sup>12</sup> R <sup>2</sup> =0.9632	- E=96.56 k <sub>o</sub> = 4.65x10 <sup>5</sup>	n = 0.50 E=171.10 k <sub>o</sub> = 5.34x10 <sup>5</sup>	-	n = 0.52 E=20.85 k <sub>o</sub> = 8.18x10 <sup>4</sup>
170-548	-	n = 1.75 E=70.14 k <sub>o</sub> = 5.79x10 <sup>5</sup> R <sup>2</sup> =0.9982 n = 1.00 E=56.85 k <sub>o</sub> = 2.26x10 <sup>4</sup> R <sup>2</sup> =0.9739	-	-	-	-

Note : E is in kJmol<sup>-1</sup>; k<sub>o</sub> is in min<sup>-1</sup>.

parameters as determined by using Agarwal and Sivasubramanian (1987) and Coats and Redfern (1964) methods yield similar results for activation energy. For different reaction zones, the values of  $E$  and  $k_0$  indicate their dependence on the order of reaction. Reich and Stivala (1982) and Horowitz and Metzger (1963) methods show the best fit results with second order and/or 2.5 order of reaction, respectively. The values of activation energy obtained by these methods are much lower in comparison to those obtained by Agarwal and Sivasubramanian method.

The heating rate does affect the best fit order of reaction which influences the values of activation energy and the frequency factor. For 20 and 40°C min<sup>-1</sup> heating rates, the order of reaction for the Agarwal and Sivasubramanian method are different for each reaction zone. For the entire range of temperature also, the order of reaction and consequently  $E$  are found to be different. However, it should be noted that the regression coefficient values are found to be very high ( $R^2 > 0.90$ ) even for range of order of reaction ( $n$ ) values. Taking first order of reaction (i.e.  $n=1$ ) for the entire degradation for comparison purposes, it is found that the value of  $E$  are comparable for the two heating rates, although  $k_0$  values are significantly different.

#### 4.3.2.2 Mill Rice Husk (MRH)

Similar to the pyrolysis characteristics of village rice husk, mill rice husk also shows TG and DTG curves for pyrolysis as shown in Fig. 4.2.3(a) and 4.2.4(a), although the first zone of devolatilization as found in VRH is not evident. Tables 4.3.2 (a, b) show the kinetic parameters for mill rice husk pyrolysis at two heating rates of 25°Cmin<sup>-1</sup> and 40°Cmin<sup>-1</sup> in the temperature range shown by the sharp sloped but straighter portion of the S-shaped TG curve. Using the best fit of the experimental data, the values of  $n$ ,  $E$  and the frequency factor are given for all the methods. Due to regression analysis for obtaining the optimized values with the highest regression coefficient values, the order of reaction is found to vary a great deal, from  $n=0$  (zero-order) to  $n = 2.50$ . The order of reaction is found to have profound effect on the values of  $E$  and  $k_0$ .

**Table 4.3.2 (a) : Kinetic Parameters for Mill Rice Husk Pyrolysis from Thermogravimetric Analysis.**  
(Nitrogen : 50 mlmin<sup>-1</sup>), Heating Rate : 25°C min<sup>-1</sup>

Temp. Zone (°C)	Method of Analysis					
	Coats & Redfern	Agarwal & Sivasubramanian	Piloyan & Novikova	Reich & Stivala	Horowitz & Metzger	Freeman & Carroll
190-300	n = 1.00 E=85.4 k <sub>o</sub> = 5.32x10 <sup>7</sup> R <sup>2</sup> =0.9820	n = 1.00 E=85.4 k <sub>o</sub> = 5.2x10 <sup>7</sup> R <sup>2</sup> =0.9820	- E=74.26 k <sub>o</sub> = 1.79x10 <sup>5</sup>	n = 0.00 E=48.03 k <sub>o</sub> = 1.24x10 <sup>5</sup>	n = 2.00 E=25.38 k <sub>o</sub> = 4.45x10 <sup>3</sup>	n = 0.21 E=73.05 k <sub>o</sub> = 2.38x10 <sup>5</sup>
300-295	n = 2.00 E=178.28 k <sub>o</sub> = 8.38x10 <sup>14</sup> R <sup>2</sup> =0.9803	n = 2.00 E=178.28 k <sub>o</sub> = 8.34x10 <sup>14</sup> R <sup>2</sup> =0.9803	- E=75.75 k <sub>o</sub> = 1.82x10 <sup>5</sup>	n = 0.95 E=346.68 k <sub>o</sub> = 1.095x10 <sup>5</sup>	n = 2.50 E=45.75 k <sub>o</sub> = 1.13x10 <sup>6</sup>	n = 1.19 E=144.45 k <sub>o</sub> = 1.205x10 <sup>6</sup>
395-584	n = 2.50 E=149.56 k <sub>o</sub> = 6.87x10 <sup>10</sup>	n = 2.50 E=149.56 k <sub>o</sub> = 6.82x10 <sup>10</sup>	- E=96.53 k <sub>o</sub> = 2.31x10 <sup>5</sup>	n = 0.95 E=269.61 k <sub>o</sub> = 7.59x10 <sup>4</sup>	-	n = 0.49 E=81.47 k <sub>o</sub> = 3.55x10 <sup>5</sup>
190-584	--	n = 2.25 E=98.86 k <sub>o</sub> = 1.2x10 <sup>8</sup> R <sup>2</sup> =0.9913 For n= 1.25 E=68.54 k <sub>o</sub> = 1.19x10 <sup>5</sup> R <sup>2</sup> =0.9560 for n= 1.00 E=62.51 k <sub>o</sub> = 2.94x10 <sup>4</sup> R <sup>2</sup> =0.9358	-	-	-	-

Note : E is in kJmol<sup>-1</sup>; k<sub>o</sub> is in min<sup>-1</sup>.

**Table 4.3.2 (b) : Kinetic Parameters for Mill Rice Husk Pyrolysis from Thermogravimetric Analysis  
(Nitrogen : 50 mlmin<sup>-1</sup>), Heating Rate : 40°C min<sup>-1</sup>**

Temp. Zone (°C)	Method of Analysis					
	Coats & Redfern	Agarwal & Sivasubramanian	Piloyan & Novikova	Reich & Stivala	Horowitz & Metzger	Freeman & Carroll
192-310	n = 1.00 E=80.278 k <sub>o</sub> = 3.22x10 <sup>7</sup> R <sup>2</sup> =0.9719	n = 1.00 E=80.278 k <sub>o</sub> = 3.19x10 <sup>7</sup> R <sup>2</sup> =0.9719	- E=76.058 k <sub>o</sub> = 3.66x10 <sup>5</sup>	n = 0.33 E=74.25 k <sub>o</sub> = 2.497x10 <sup>5</sup>	n = 0.30 E=26.08 k <sub>o</sub> = 2.62x10 <sup>4</sup>	n = 0.77 E=34.46 k <sub>o</sub> = 4.275x10 <sup>5</sup>
310-438	n = 3.00 E=185.21 k <sub>o</sub> = 3.24x10 <sup>15</sup>	n = 3.00 E=185.21 k <sub>o</sub> = 3.225x10 <sup>15</sup>	- E=77.40 k <sub>o</sub> = 3.72x10 <sup>5</sup>	n = 0.33 E=169.76 k <sub>o</sub> = 5.743x10 <sup>5</sup>	n = 3.00 E=52.41 k <sub>o</sub> = 1.51x10 <sup>9</sup>	n = 0.59 E=108.20 k <sub>o</sub> = 1.015x10 <sup>6</sup>
338-700	n = 3.00 E=187.06 k <sub>o</sub> = 1.26x10 <sup>13</sup>	n = 3.00 E=187.06 k <sub>o</sub> = 1.26x10 <sup>13</sup>	- E=101.00 k <sub>o</sub> = 4.859x10 <sup>5</sup>	n = 0.33 E=148.80 k <sub>o</sub> = 5.08x10 <sup>5</sup>	-	n = 0.03 E=54.83 k <sub>o</sub> = 3.015x10 <sup>5</sup>
192-700	--	n = 2.50 E=106.605 k <sub>o</sub> = 5.76x10 <sup>8</sup> R <sup>2</sup> =0.9983 For n = 1.00 E=60.92 k <sub>o</sub> = 3.05x10 <sup>5</sup> R <sup>2</sup> =0.9439	-	-	-	-

Note : E is in kJmol<sup>-1</sup>; k<sub>o</sub> is in min<sup>-1</sup>.

Williams and Besler (1993) have divided the thermal pyrolysis thermograms of rice husk in to two temperature ranges based on DTG peaks. For  $20^{\circ}\text{Cmin}^{-1}$  heating rate, they defined the ranges as  $275\text{-}345^{\circ}\text{C}$  and  $345\text{-}410^{\circ}\text{C}$ , whereas for  $40^{\circ}\text{Cmin}^{-1}$  heating rate, the temperature ranges were  $270\text{-}365^{\circ}\text{C}$  and  $365\text{-}425^{\circ}\text{C}$ . For these two ranges separately as also for the overall temperature range assuming the first order of pyrolysis reaction, they have reported E and pre-exponential factor values. Their values of E and  $k_0$  for  $20^{\circ}\text{Cmin}^{-1}$  heating rate are, respectively  $105.3\text{ kJmol}^{-1}$  and  $8.4 \times 10^5\text{ min}^{-1}$ , and for  $40^{\circ}\text{Cmin}^{-1}$  heating rate, the corresponding values are  $85\text{ kJmol}^{-1}$  and  $4 \times 10^4\text{ min}^{-1}$ . The values of E and  $k_0$  obtained from the present studies for first order reaction rate for the overall temperature range and using Agarwal and Sivasubramanian integral approximation are, respectively,  $62.51\text{ kJmol}^{-1}$  and  $2.94 \times 10^4\text{ min}^{-1}$ , for  $20^{\circ}\text{C min}^{-1}$  heating rate, and  $60.92\text{ kJ mol}^{-1}$  and  $3.059 \times 10^5\text{ min}^{-1}$   $40^{\circ}\text{Cmin}^{-1}$  heating rate. The best fit values of E and  $k_0$ , were however different. Using second order reaction and Coats and Redfern method, Singamsetti and Rao (2000) reported E values of  $89.4$  and  $89.8\text{ kJmol}^{-1}$  for  $25$  and  $50^{\circ}\text{Cmin}^{-1}$  heating rates, respectively, for the lower temperature range of  $225\text{-}350^{\circ}\text{C}$ . The corresponding  $k_0$  values were  $5.04 \times 10^{11}$  and  $8.79 \times 10^{11}\text{ min}^{-1}$  at the two heating rates. Iyer et al. (1997) reported a value of  $E=82.48\text{ kJ mol}^{-1}$  in the temperature range of  $220\text{-}350^{\circ}\text{C}$ . Coats and Redfern integral technique with first order reaction has been used in the determination of activation value.

In the present study, for the first zone of  $190\text{-}300^{\circ}\text{C}$  for  $20^{\circ}\text{Cmin}^{-1}$  and  $190\text{-}310^{\circ}\text{C}$  for  $40^{\circ}\text{Cmin}^{-1}$  heating rate, the Coats and Redfern method gave the values of E as  $85.40\text{ kJmol}^{-1}$  and  $80.28\text{ kJmol}^{-1}$  for the first order reaction. Thus, the values of E obtained are in agreement with those reported by Iyer et al.(1997). The results obtained from the present study show the optimum values of n, E and  $k_0$  for the two heating rates, i.e.  $20$  and  $40^{\circ}\text{C min}^{-1}$ , respectively, as  $n=2.25$ ,  $E=98.86\text{ kJmol}^{-1}$  and  $k_0 = 1.2 \times 10^8\text{ min}^{-1}$ ; and  $n=2.50$ ,  $E=106.605\text{ kJmol}^{-1}$  and  $k_0 = 5.76 \times 10^8\text{ min}^{-1}$ . For  $n=1.0$ ,

the values of  $E_0$  obtained are 62.51 and 60.92  $\text{kJmol}^{-1}$  at 20 and  $40^\circ\text{Cmin}^{-1}$ , respectively. These values are slightly higher than those obtained for village rice husk.

The variation in kinetic parameters obtained by different workers reflect the variation in the sample compositions, instrumental reliabilities, accuracies in the weightloss determination and the use of different equations. It is, however, noteworthy that simple single step irreversible reaction mechanism correlates the experimental data for the entire degradation range satisfactorily. This is a significant result which simplifies the design of pyrolysis reactor.

#### 4.3.2.3 Sawdust

The kinetic parameters as determined by various methods for the two heating rates, i.e. 20 and  $40^\circ\text{Cmin}^{-1}$  are given in Tables 4.3.3(a) and 4.3.3(b). The TGA and DTG curves showed [Figs. 4.2.5(a) and 4.2.6(a)] that the sawdust devolatilization occurs in two distinct zones, followed by a third slow degradation zone. Because of the three-step nature of pyrolysis, it is necessary to use different kinetic parameters in different temperature zones to accurately describe the thermal decomposition characteristics. The kinetic parameters of all the reaction zones as also for the entire temperature range upto  $700^\circ\text{C}$  are given in Tables 4.3.3 (a, b) for the two heating rates, i.e. 20 and  $40^\circ\text{Cmin}^{-1}$ . The values of activation energy,  $E$  had different values for different methods; the order of reaction also varied. Using the integral method of analysis, the Agarwal and Sivasubramanian (1987) approximation and that of Coats and Redfern (1964) gave similar results for  $E$  and  $n$ , while  $k_0$  values are different. The values of  $E$  and  $k_0$  were obtained by varying  $n$  and using the multiple liner regression analysis method. For the integral method of analysis, it was thought to use the Agarwal and Sivasubramanian method for the entire temperature range as well. For  $20^\circ\text{Cmin}^{-1}$  heating rate, the best fit value of  $n = 1.75$ , activation energy was found to be 58.65  $\text{kJmol}^{-1}$  with  $R^2 = 0.9894$ ; whereas for  $n = 1.0$ ,  $E = 42.52 \text{ kJmol}^{-1}$  with  $R^2 = 0.9610$ . It is



**Table 4.3.3 (a) Kinetic Parameters for Sawdust Pyrolysis from Thermogravimetric Analysis  
(Nitrogen : 50 mlmin<sup>-1</sup>), Heating Rate : 20°C min<sup>-1</sup>**

Temp. Zone (°C)	Method of Analysis					
	Coats & Redfern	Agarwal & Sivasubramanian	Piloyan & Novikova	Reich & Stivala	Horowitz & Metzger	Freeman & Carroll
175-290	n = 0.00 E=41.28 k <sub>o</sub> = 2.01x10 <sup>3</sup> R <sup>2</sup> =0.9412	n = 0.00 E=41.28 k <sub>o</sub> = 1.89x10 <sup>3</sup> R <sup>2</sup> =0.9412	- E=72.77 k <sub>o</sub> = 1.750	n = 0.50 E=50.96 k <sub>o</sub> = 6.29x10 <sup>4</sup>	n = 0.00 E=13.28 k <sub>o</sub> = 1.05x10 <sup>2</sup>	n = 0.86 E=100.25 k <sub>o</sub> = 1.09x10 <sup>5</sup>
290-409	n = 2.50 E=135.82 k <sub>o</sub> = 1.318x10 <sup>11</sup> R <sup>2</sup> =0.9609	n = 2.50 E=135.82 k <sub>o</sub> = 1.308x10 <sup>11</sup> R <sup>2</sup> =0.9609	- E=75.39 k <sub>o</sub> = 1.81x10 <sup>5</sup>	n = 0.50 E=50.86 k <sub>o</sub> = 6.29x10 <sup>4</sup>	n = 2.50 E=37.44 k <sub>o</sub> = 9.15x10 <sup>4</sup>	n = 0.07 E=149.43 k <sub>o</sub> = 4.067x10 <sup>5</sup>
409-700	n = 2.50 E=107.29 k <sub>o</sub> = 1.176x10 <sup>7</sup>	n = 2.50 E=107.29 k <sub>o</sub> = 1.159x10 <sup>7</sup>	- E=105.301 k <sub>o</sub> = 2.53x10 <sup>5</sup>	n = 0.75 E=256.10 k <sub>o</sub> = 4.82x10 <sup>5</sup>	-	n = 1.00 E=2.416 k <sub>o</sub> = 1.071x10 <sup>5</sup>
175-700	--	n = 1.75 E=58.65 k <sub>o</sub> = 1.5x10 <sup>4</sup> R <sup>2</sup> =0.9894 for n = 1.00 E=42.52 k <sub>o</sub> = 3.11x10 <sup>2</sup> R <sup>2</sup> =0.9610	-	-	-	-

Note : E is in kJmol<sup>-1</sup>; k<sub>o</sub> is in min<sup>-1</sup>.

Table 4.3.3 (b) : Kinetic Parameters for Sawdust Pyrolysis from Thermogravimetric Analysis.  
(Nitrogen : 50 mlmin<sup>-1</sup>), Heating Rate : 40°C min<sup>-1</sup>

Temp. Zone (°C)	Method of Analysis					
	Coats & Redfern	Agarwal & Sivasubramanian	Piloyan & Novikova	Reich & Stivala	Horowitz & Metzger	Freeman & Carroll
133-290	n = 0.00 E=13.38 k <sub>0</sub> = 5.56 R <sup>2</sup> =0.9188	n = 0.00 E=13.38 k <sub>0</sub> = 3.06 R <sup>2</sup> =0.9188	- E=72.31 k <sub>0</sub> = 3.48x10 <sup>5</sup>	n = 0.00 E=9.92 k <sub>0</sub> = 8.476x10 <sup>3</sup>	n = 0.00 E=3.613 k <sub>0</sub> = 3.29	n = 0.89 E=28.19 k <sub>0</sub> = 4.03x10 <sup>5</sup>
290-456	n = 0.25 E=69.66 k <sub>0</sub> = 1.26x10 <sup>5</sup> R <sup>2</sup> =0.9972	n = 0.25 E=69.66 k <sub>0</sub> = 1.22x10 <sup>5</sup> R <sup>2</sup> =0.9972	- E=79.90 k <sub>0</sub> = 3.84x10 <sup>5</sup>	n = 0.25 E=94.65 k <sub>0</sub> = 4.07x10 <sup>5</sup>	n = 0.25 E=33.86 k <sub>0</sub> = 1.15x10 <sup>5</sup>	n = 0.34 E=88.12 k <sub>0</sub> =3.33x10 <sup>5</sup>
456-700	n = 1.25 E=76.39 k <sub>0</sub> = 2.55x10 <sup>4</sup>	n = 1.25 E=76.39 k <sub>0</sub> = 2.44x10 <sup>4</sup>	- E=119.36 k <sub>0</sub> = 5.74x10 <sup>5</sup>	n = 0.25 E=67.65 k <sub>0</sub> = 2.98x10 <sup>5</sup>	-	-
133-700	--	n = 0.50 E=42.87 k <sub>0</sub> = 5.81x10 <sup>2</sup> R <sup>2</sup> =0.9881 For n= 1.00 E=47.47 k <sub>0</sub> = 1.82x10 <sup>3</sup> R <sup>2</sup> =0.9808	-	-	-	-

Note : E is in kJmol<sup>-1</sup>; k<sub>0</sub> is in min<sup>-1</sup>.

thus clear that with increase in  $n$ ,  $E$  increased with corresponding values for  $k_0$ . For  $40^\circ\text{Cmin}^{-1}$ , with  $n = 1.0$ ,  $E$  was found to be  $47.47 \text{ kJmol}^{-1}$  with  $R^2 = 0.9808$ . The best fit value was obtained at  $n = 0.50$  with  $E = 42.87 \text{ kJmol}^{-1}$  and  $k_0 = 5.81 \times 10^2 \text{ min}^{-1}$  and  $R^2 = 0.9881$ . It is also clear that the heating rate had an influence on the activation energy for the overall reaction as well as the reaction in different temperature zones.

#### 4.3.2.4 Bagasse

Figs. 4.2.7(a) and 4.2.8(a) exhibit the TGA, DTG and DTA characteristics of cane bagasse pyrolysis at  $20$  and  $40^\circ\text{Cmin}^{-1}$  heating rates. DTG and TGA curves clearly showed that the pyrolysis occurred in two clear temperature zones of devolatilization followed by the char degradation in the third zone. The two pyrolysis zones of devolatilization, i.e.  $169\text{-}300^\circ\text{C}$  and  $300\text{-}390^\circ\text{C}$  have been subjected to kinetic analysis following the methods described earlier. It is again found that the values of activation energy as obtained by the best-fit results of the methods employed differ greatly from one another. For zero order pyrolysis in the first reaction zone, the value of  $E$  varied from  $26.68$  to  $193.92 \text{ kJmol}^{-1}$ , with Horowitz and Metzger method giving the lowest value, for  $20^\circ\text{C min}^{-1}$  heating rate. For  $40^\circ\text{C min}^{-1}$  heating rate, the  $E$  values varied from  $19.0$  to  $49.51 \text{ kJmol}^{-1}$  for zeroth order reaction. Again, Horowitz and Metzger method gave the lowest value. For the second reaction zone of  $300\text{-}390^\circ\text{C}$  (for  $20^\circ\text{C min}^{-1}$  heating rate) and  $315\text{-}419^\circ\text{C}$  (for  $40^\circ\text{C min}^{-1}$  heating rate), the values of  $n$  varied from one method to another, as also the order of reaction. For the integral method of analysis, Coats and Redfern, and Agarwal and Sivasubramanian methods gave the order of reaction as  $2.50$  and  $2.00$  and  $E = 177.68$  and  $141.93 \text{ kJmol}^{-1}$  for  $20$  and  $40^\circ\text{C min}^{-1}$  heating rates, respectively. For second order reaction, the values of  $E$  were respectively,  $164.45$  and  $141.93 \text{ kJmol}^{-1}$  and  $k_0$  values were  $7.255 \times 10^{13}$  and  $5.71 \times 10^{11} \text{ min}^{-1}$ , respectively. The overall values for the degradation upto  $700^\circ\text{C}$  were  $n = 2.25$ ,  $E = 89.48 \text{ kJmol}^{-1}$  and  $k_0 = 2.03 \times 10^7 \text{ min}^{-1}$  for  $20^\circ\text{C min}^{-1}$  and  $n=2.00$ ,

**Table 4.3.4 (a) : Kinetic Parameters for Bagasse Pyrolysis from Thermogravimetric Analysis.**  
 (Nitrogen : 50 mlmin<sup>-1</sup>), Heating Rate : 20°C min<sup>-1</sup>

Temp. Zone (°C)	Method of Analysis					
	Coats & Redfern	Agarwal & Sivasubramanian	Piloyan & Novikova	Reich & Stivala	Horowitz & Metzger	Freeman & Carroll
169-300	n = 0.00 E=74.27 k <sub>o</sub> = 3.751x10 <sup>6</sup> R <sup>2</sup> =0.9903	n = 0.00 E=74.27 k <sub>o</sub> = 3.684x10 <sup>6</sup> R <sup>2</sup> =0.9903	- E=71.295 k <sub>o</sub> = 1.715x10 <sup>5</sup>	n = 0.00 E=47.45 k <sub>o</sub> = 1.20x10 <sup>5</sup>	n = 0.00 E=26.68 k <sub>o</sub> = 2.7x10 <sup>4</sup>	n = 0.64 E=193.92 k <sub>o</sub> = 2.54x10 <sup>5</sup>
300-390	n = 2.50 E=177.68 k <sub>o</sub> = 1.211x10 <sup>15</sup> R <sup>2</sup> =0.9706	n = 2.50 E=177.68 k <sub>o</sub> = 1.206x10 <sup>5</sup> R <sup>2</sup> =0.9706	- E=72.530 k <sub>o</sub> = 1.745x10 <sup>5</sup>	n = 0.50 E=427.375 k <sub>o</sub> = 8.913x10 <sup>5</sup>	-	n = 0.40 E=4.671 k <sub>o</sub> = 1.775x10 <sup>4</sup>
390-700	n = 2.50 E=77.108 k <sub>o</sub> = 1.873x10 <sup>5</sup> R <sup>2</sup> = 0.9757	n = 2.50 E=77.108 k <sub>o</sub> = 1.873x10 <sup>5</sup> R <sup>2</sup> = 0.9757	- E=98.19 k <sub>o</sub> = 2.362x10 <sup>5</sup>	n = 0.95 E=227.656 k <sub>o</sub> = 9.255x10 <sup>4</sup>	-	n = 1.08 E=81.94 k <sub>o</sub> = 7.495x10 <sup>4</sup>
169-700	--	n = 2.25 E=89.48 k <sub>o</sub> = 2.03 x10 <sup>7</sup> R <sup>2</sup> =0.9812	-	-	-	-

Note : E is in kJmol<sup>-1</sup>; k<sub>o</sub> is in min<sup>-1</sup>.

**Table 4.3.4 (b) : Kinetic Parameters for Bagasse Pyrolysis from Thermogravimetric Analysis.**  
(Nitrogen : 50 mlmin<sup>-1</sup>), Heating Rate : 40°C min<sup>-1</sup>

Temp. Zone (°C)	Method of Analysis					
	Coats & Redfern	Agarwal & Sivasubramanian	Piloyan & Novikova	Reich & Stivala	Horowitz & Metzger	Freeman & Carroll
195-315	n = 0.00 E=49.51 k <sub>o</sub> = 1.93x10 <sup>4</sup> R <sup>2</sup> =0.9949	n = 0.00 E=49.51 k <sub>o</sub> = 1.854x10 <sup>4</sup> R <sup>2</sup> =0.9949	- E=73.19 k <sub>o</sub> = 3.52x10 <sup>5</sup>	n = 0.00 E=34.80 k <sub>o</sub> = 1.92x10 <sup>5</sup>	n = 0.00 E=19.00 k <sub>o</sub> = 1.22x10 <sup>3</sup>	n = 1.67 E=167.12 k <sub>o</sub> = 1.57x10 <sup>5</sup>
315-419	n = 2.00 E=141.93 k <sub>o</sub> = 5.71x10 <sup>11</sup> R <sup>2</sup> =0.9725	n = 2.00 E=141.93 k <sub>o</sub> = 5.67x10 <sup>11</sup> R <sup>2</sup> =0.9725	- E=73.90 k <sub>o</sub> = 3.65x10 <sup>5</sup>	n = 0.95 E=399.10 k <sub>o</sub> = 4.18x10 <sup>5</sup>	n = 2.00 E=43.39 k <sub>o</sub> = 5.092x10 <sup>5</sup>	n = 0.08 E=109.72 k <sub>o</sub> = 6.19x10 <sup>5</sup>
419-700	n = 2.50 E=103.29 k <sub>o</sub> = 1.43x10 <sup>7</sup> R <sup>2</sup> = 0.9708	n = 2.50 E=103.29 k <sub>o</sub> = 1.40x10 <sup>7</sup> R <sup>2</sup> = 0.9708	- E=106.89 k <sub>o</sub> = 5.14x10 <sup>5</sup>	n = 0.95 E=202.84 k <sub>o</sub> = 1.79x10 <sup>5</sup>	-	n = 0.12 E=56.97 k <sub>o</sub> = 3.63x10 <sup>5</sup>
195-700	-	n = 2.00 E=72.30 k <sub>o</sub> = 5.81 x10 <sup>5</sup> R <sup>2</sup> =0.9868	-	-	-	-

Note : E is in kJmol<sup>-1</sup>; k<sub>o</sub> is in min<sup>-1</sup>.

$E = 72.3 \text{ kJmol}^{-1}$  and  $k_0 = 5.8 \times 10^5 \text{ min}^{-1}$  for  $40^\circ\text{C min}^{-1}$  heating rate. At  $n = 2.00$  for  $20^\circ\text{C min}^{-1}$  heating rate, the values of  $E$  and  $k_0$  were, respectively,  $82.81 \text{ kJmol}^{-1}$  and  $4.28 \times 10^6 \text{ min}^{-1}$ . These data again confirm that an increase in the heating rate decreased the activation energy needed for the degradation to proceed.

Antal and Varhegyi (1995) have reported the activation energy values for cellulose in bagasse pyrolysis at  $10$  and  $20^\circ\text{C min}^{-1}$  heating rate. Nassar (1985) has reported these values at  $5^\circ\text{C min}^{-1}$  heating rate with helium as the purge gas. Antal and Varhegyi reported  $215$  and  $225 \text{ kJmol}^{-1}$  as activation energies for sugar cane bagasse and IEA-NIST standard sugar cane bagasse cellulose decomposition, respectively. Nassar's values are  $118$  and  $69.1 \text{ kJmol}^{-1}$  for activation energy below  $350^\circ\text{C}$  and above  $350^\circ\text{C}$  degradation respectively. Iyer et al. (1997) reported a value of  $E=53.2 \text{ kJmol}^{-1}$  for the pyrolysis in  $226\text{-}370^\circ\text{C}$  temperature range. The values of activation energy reported in the present study are much higher than that reported by Iyer et al. (1997) as also reported by Nassar (1985), although the temperature ranges used are different. However, it is apparent that a single irreversible reaction was able to relate the TGA data for the overall pyrolysis of bagasse.

#### 4.3.2.5 Pressmud

As already discussed earlier, pressmud is an industrial waste obtained from the sugar mills. Pyrolytic behaviour of pressmud is not akin to what has been witnessed for the biomass samples. Pressmud showed a number of reaction zones, but the pyrolysis characteristics have been divided in three reaction zones for  $25$  and  $40^\circ\text{C min}^{-1}$  heating rates. (Figs. 4.2.9 a and 4.2.10a). The kinetic parameters were determined for each reaction zone separately by using the methods described earlier. The integral method using Coats and Redfern, and Agarwal and Sivasubramanian approximations give same results for activation energy at any value of  $n$ , but the pre-exponential factor values differ slightly. The best fit value of  $n$  is chosen to record the values of  $E$  and  $k_0$ . The results of kinetic parameters are shown in Tables 4.3.5 (a, b) for  $25$  and  $40^\circ\text{C min}^{-1}$  heating rates.

**Table 4.3.5 (a) : Kinetic Parameters for Pressmud Pyrolysis from Thermogravimetric Analysis.**  
 (Nitrogen : 50 mlmin<sup>-1</sup>), Heating Rate : 25°C min<sup>-1</sup>

Temp. Zone (°C)	Method of Analysis					
	Coats & Redfern	Agarwal & Sivasubramanian	Piloyan & Novikova	Reich & Stivala	Horowitz & Metzger	Freeman & Carroll
145-310	n = 2.50 E=47.14 k <sub>o</sub> = 8.59x10 <sup>3</sup> R <sup>2</sup> =0.9646	n = 2.50 E=47.14 k <sub>o</sub> =8.29x10 <sup>3</sup> R <sup>2</sup> =0.9646	- E=75.12 k <sub>o</sub> =2.26x10 <sup>5</sup>	n = 0.90 E=44.43 k <sub>o</sub> = 2.04x10 <sup>4</sup>	n = 2.50 E=7.91 k <sub>o</sub> = 2.670	n = 0.23 E=46.41 k <sub>o</sub> = 1.99x10 <sup>5</sup>
310-409	n = 1.50 E=105.88 k <sub>o</sub> = 3.05x10 <sup>8</sup> R <sup>2</sup> =0.9695	n = 1.50 E=105.88 k <sub>o</sub> = 3.01x10 <sup>8</sup> R <sup>2</sup> =0.9695	- E=82.33 k <sub>o</sub> =2.48x10 <sup>5</sup>	n = 0.25 E=107.02 k <sub>o</sub> = 2.69x10 <sup>5</sup>	n = 1.50 E=24.22 k <sub>o</sub> = 9.51x10 <sup>2</sup>	n = 0.28 E=34.94 k <sub>o</sub> = 9.74x10 <sup>4</sup>
409-850	n = 2.50 E=58.90 k <sub>o</sub> =2.08x10 <sup>3</sup> R <sup>2</sup> = 0.9103	n = 2.50 E=58.90 k <sub>o</sub> = 1.95x10 <sup>3</sup> R <sup>2</sup> = 0.9103	- E=118.68 k <sub>o</sub> =3.57x10 <sup>5</sup>	n = 0.50 E=55.37 k <sub>o</sub> = 1.03x10 <sup>5</sup>	-	n = 3.38 E=82.05 k <sub>o</sub> = 9.48x10 <sup>3</sup>
145-850	-	n = 1.25 E=27.84 k <sub>o</sub> =3.21 x10 <sup>1</sup> R <sup>2</sup> =0.9916	-	-	-	-

Note : E is in kJmol<sup>-1</sup>; k<sub>o</sub> is in min<sup>-1</sup>.

**Table 4.3.5 (b) : Kinetic Parameters for Pressmud Pyrolysis from Thermogravimetric Analysis.**  
(Nitrogen : 50 mlmin<sup>-1</sup>), Heating Rate : 40°C min<sup>-1</sup>

Temp. Zone (°C)	Method of Analysis					
	Coats & Redfern	Agarwal & Sivasubramanian	Piloyan & Novikova	Reich & Stivala	Horowitz & Metzger	Freeman & Carroll
169-279	n = 2.50 E=72.25 k <sub>o</sub> = 56.95x10 <sup>6</sup> R <sup>2</sup> =0.9341	n = 2.50 E=72.25 k <sub>o</sub> = 5.84x10 <sup>6</sup> R <sup>2</sup> =0.9341	- E=74.50 k <sub>o</sub> = 3.58x10 <sup>5</sup>	n = 0.50 E=69.65 k <sub>o</sub> = 2.08x10 <sup>5</sup>	n = 2.50 E=12.34 k <sub>o</sub> = 3.39x10 <sup>1</sup>	n = 0.31 E=59.33 k <sub>o</sub> = 2.34x10 <sup>5</sup>
279-419	n = 2.50 E=121.66 k <sub>o</sub> = 1.71x10 <sup>10</sup> R <sup>2</sup> =0.9851	n = 2.50 E=121.66 k <sub>o</sub> =1.69x10 <sup>10</sup> R <sup>2</sup> =0.9851	- E=81.38 k <sub>o</sub> = 3.92x10 <sup>5</sup>	n = 0.50 E=223.90 k <sub>o</sub> = 7.08x10 <sup>5</sup>	n = 2.50 E=34.59 k <sub>o</sub> = 2.92x10 <sup>4</sup>	n = 0.37 E=29.08 k <sub>o</sub> = 2.56x10 <sup>5</sup>
419-850	n = 2.50 E=62.82 k <sub>o</sub> = 5.12x10 <sup>3</sup> R <sup>2</sup> = 0.9143	n = 2.50 E=62.82 k <sub>o</sub> = 5.43x10 <sup>3</sup> R <sup>2</sup> = 0.9143	- E=112.92 k <sub>o</sub> = 5.43x10 <sup>5</sup>	n = 0.25 E=89.68 k <sub>o</sub> =3.86x10 <sup>5</sup>	-	n = 0.93 E=12.05 k <sub>o</sub> = 2.09x10 <sup>2</sup>
169-850	-	n = 2.50 E=33.44 k <sub>o</sub> = 9.51 x10 <sup>1</sup> R <sup>2</sup> =0.9542 n = 1.25 E=24.91 k <sub>o</sub> = 1.06 x10 <sup>1</sup>	-	-	-	-

Note : E is in kJmol<sup>-1</sup>; k<sub>o</sub> is in min<sup>-1</sup>.



It is found that the differential method of Freeman and Carroll gave the lowest value of  $n$ , whereas Horowitz and Metzger and the integral approximations of Agarwal and Sivasubramanian, and Coats and Redfern gave the highest value of  $n$  for the first two reaction zones for  $25^{\circ}\text{C min}^{-1}$  heating rate. Reich and Stivala method gave a value of  $n = 0.90$  and  $0.25$  for the first two reaction zones for  $25^{\circ}\text{C min}^{-1}$  heating rate. But the values of  $E$  obtained by integral approximation methods and the methods of Reich and Stivala and Freeman and Carroll were similar, i.e.  $\sim 45 \text{ kJ mol}^{-1}$  for the first reaction zone. The Piloyan and Novikova method yielded the highest value of activation energy,  $E = 75.12 \text{ kJ mol}^{-1}$ , whereas the Horowitz and Metzger method gave the lowest value of  $E = 7.91 \text{ kJ mol}^{-1}$ . For the second reaction zone, the values of  $E$  obtained from the integral approximation methods and that of Reich and Stivala gave similar values :  $E \approx 106 \text{ kJ mol}^{-1}$ , whereas the values obtained by Horowitz and Metzger and Freeman and Carroll methods were low. As before, Piloyan and Novikova method gave a value of  $E = 82.33 \text{ kJ mol}^{-1}$  which is in between the values reported by other methods.

Using the Agarwal and Sivasubramanian's method of integral approximation, the best fit value of  $E$  and  $k_0$  were obtained at  $n = 1.25$  for the overall degradation rate. As usual, the values of  $E$  and  $k_0$  varied as the value of  $n$  was changed.

Similar results were obtained for  $40^{\circ}\text{C min}^{-1}$  heating rate. However, the values of  $n$ ,  $E$  and  $k_0$  were consistently different for the best fit of experimental value of the conversion function. For the overall degradation, the optimum values were obtained at  $n = 1.25$  for  $25^{\circ}\text{C min}^{-1}$  and  $n = 2.50$  for  $40^{\circ}\text{C min}^{-1}$  heating rates. Comparison of  $E$  values at  $n = 1.25$  showed that at higher heating rate of  $40^{\circ}\text{C min}^{-1}$ , lower value of  $E$  was obtained. At  $n = 1.25$ ,  $E = 27.84 \text{ kJ mol}^{-1}$  and  $k_0 = 3.21 \times 10^7 \text{ min}^{-1}$  for  $25^{\circ}\text{C min}^{-1}$  heating rate, whereas for  $40^{\circ}\text{C min}^{-1}$  heating rate, at  $n = 1.25$ ,  $E = 24.91 \text{ kJ mol}^{-1}$  and  $k_0 = 1.06 \times 10^1 \text{ min}^{-1}$ .

The kinetic parameters determined in this study were only global values resulting from a complex kinetic system with multiple simultaneous reactions. These could be used in the design of pyrolysis reactors.

### 4.3.3 Kinetics of Thermal Degradation in Oxidizing (Air) Atmosphere

The kinetic parameters for thermal degradation of the four biomass samples and that of press mud were determined using the same methods as described earlier for pyrolysis. The simple single step irreversible reaction was assumed to represent the complex oxidation characteristics of the samples. This representation was applied to each reaction temperature zone observed during the degradation history of the samples from TGA, DTG and DTA curves.

#### 4.3.3.1 Village Rice Husk and Mill Rice Husk

As discussed by DiBlasi and Branca (1999) thermogravimetric data allows only global degradation characteristics to be defined. While most of the investigators have discussed the kinetics of biomass degradation in air as a single step reaction, many have used multi-reaction mechanisms. DiBlasi and Branca (1999) used a multi step reaction model consisting of two-step devolatilization followed by a combustion step. Jain et al. (1999) used a single step model and used Bining and Jenkins (1992) and Agarwal Sivasubramanian (1987), and the Coats and Redfern (1964) model for determining kinetic parameters at 10 and 100°Cmin<sup>-1</sup> heating rates under air and air-Nitrogen atmospheres in different temperature ranges during thermal degradation as recorded by TG trace. Mansaray and Ghaly (1999) determined the kinetic parameters from TGA data using the rate expression given by Wendlandt (1974) and linearization of the Arrhenius equation for rice husks in air. They used four different varieties of rice husk.

The present work is based on the single- irreversible reaction model for each reaction (temperature zone) and the kinetic parameters were determined using different methods and equations as discussed earlier under section on pyrolysis. As seen from Figs. 4.2.1(a, b), 4.2.2 (a, b), 4.3.3(a, b) and 4.2.4 (a, b) the TG, DTG and DTA traces indicate that the thermal degradation of rice husks (both VRH and MRH) occurs in three reaction (temperature) zones – the first is probably the devolatilization the second

**Table 4.3.6 (a) : Kinetic Parameters for Village Rice Husk Thermal Degradation from TGA /DTG Data  
(Air : 50 mlmin<sup>-1</sup>), Heating Rate : 20°C min<sup>-1</sup>**

Temp. Zone (°C)	Method of Analysis					
	Coats & Redfern	Agarwal & Sivasubramanian	Piloyan & Novikova	Reich & Stivala	Horowitz & Metzger	Freeman & Carroll
192-258	n = 2.00 E=386.826 k <sub>o</sub> = 8.684x10 <sup>39</sup> R <sup>2</sup> =0.9990	n = 2.00 E=386.826 k <sub>o</sub> = 8.679x10 <sup>39</sup> R <sup>2</sup> =0.9990	- E=66.227 k <sub>o</sub> = 1.665x10 <sup>5</sup>	n = 0.50 E=282.132 k <sub>o</sub> = 3.588x10 <sup>5</sup>	-	n = 0.68 E=169.306 k <sub>o</sub> = 2.145x10 <sup>5</sup>
258-350	n = 2.50 E=173.469 k <sub>o</sub> = 3.799x10 <sup>15</sup> R <sup>2</sup> =0.9810	n = 2.50 E=173.469 k <sub>o</sub> = 3.785x10 <sup>5</sup> R <sup>2</sup> =0.9810	- E=69.886 k <sub>o</sub> = 1.681x10 <sup>5</sup>	n = 0.25 E=188.948 k <sub>o</sub> = 3.607x10 <sup>5</sup>	n = 2.50 E=43.872 k <sub>o</sub> = 1.109x10 <sup>7</sup>	n = 0.47 E=22.437 k <sub>o</sub> = 1.122x10 <sup>5</sup>
350-530	n = 2.50 E=101.382 k <sub>o</sub> = 2.407x10 <sup>7</sup> R <sup>2</sup> = 0.9632	n = 2.50 E=101.382 k <sub>o</sub> = 2.371x10 <sup>7</sup> R <sup>2</sup> = 0.9632	- E=84.655 k <sub>o</sub> = 2.036x10 <sup>5</sup>	n = 0.67 E=104.241 k <sub>o</sub> = 9.331x10 <sup>4</sup>	n = 2.50 E=36.610 k <sub>o</sub> = 3.068x10 <sup>3</sup>	n = 0.37 E=53.055 k <sub>o</sub> = 1.027x10 <sup>5</sup>
192-530	-	n = 2.50 E=73.492 k <sub>o</sub> = 8.044 x10 <sup>5</sup> R <sup>2</sup> =0.9916  For n=1.00 E=50.751 k <sub>o</sub> = 1.746 x10 <sup>4</sup> R <sup>2</sup> =0.9721	-	-	-	-

Note : E is in kJmol<sup>-1</sup>; k<sub>o</sub> is in min<sup>-1</sup>.

Table 4.3.6 (b) : Kinetic Parameters for Village Rice Husk Thermal Degradation from TGA /DTG Data  
(Air : 50 mlmin<sup>-1</sup>), Heating Rate : 40°C min<sup>-1</sup>

Temp. Zone (°C)	Method of Analysis					
	Coats & Redfern	Agarwal & Sivasubramanian	Piloyan & Novikova	Reich & Stivala	Horowitz & Metzger	Freeman & Carroll
258-385	n = 1.00 E=108.978 k <sub>o</sub> = 2.332x10 <sup>9</sup> R <sup>2</sup> =0.9944	n = 1.00 E=108.978 k <sub>o</sub> = 2.308x10 <sup>9</sup> R <sup>2</sup> =0.9944	- E=73.624 k <sub>o</sub> = 3.542x10 <sup>5</sup>	n = 0.95 E=492.469 k <sub>o</sub> = 8.951x10 <sup>5</sup>	n = 2.50 E=27.538 k <sub>o</sub> = 1.994x10 <sup>4</sup>	n = 0.73 E=1.129 k <sub>o</sub> = 2.721x10 <sup>4</sup>
385-548	n = 1.00 E=85.363 k <sub>o</sub> = 6.829x10 <sup>5</sup> R <sup>2</sup> =0.9929	n = 1.00 E=85.363 k <sub>o</sub> = 6.656x10 <sup>5</sup> R <sup>2</sup> =0.9929	- E=91.829 k <sub>o</sub> = 4.418x10 <sup>5</sup>	n = 0.75 E=258.898 k <sub>o</sub> = 7.117x10 <sup>5</sup>	n = 2.50 E=41.957 k <sub>o</sub> = 7.989x10 <sup>3</sup>	n = 0.43 E=57.703 k <sub>o</sub> =4.986x10 <sup>5</sup>
258-548	-	n = 2.50 E=69.503 k <sub>o</sub> = 3.859x10 <sup>5</sup> R <sup>2</sup> = 0.8548  For n =1.00 E=35.894 k <sub>o</sub> = 1.854 x10 <sup>2</sup> R <sup>2</sup> =0.7747	-	-	-	-

Note : E is in kJmol<sup>-1</sup>; k<sub>o</sub> is in min<sup>-1</sup>.

the combustion and third gasification. The second and third steps show fast weight loss with the second step showing largest rate of weight loss with time and temperature. Based on this three-step nature of the thermograms, the kinetic parameters for the zones have been determined separately. Thermal degradation characteristics of rice husks in oxidizing atmosphere were also reported by Jain et al. (1999) and Mansaray and Ghaly (1999). However, the first zone of Jain et al. (1999) and that of Mansaray and Ghaly (1999) starts from the point of devolatilization which is very slow and goes until the transition point of fast devolatilization/combustion is obtained. In the present analysis, the slow devolatilization zone where the weight loss is very small, has been separated from the later faster weight loss zone. Thus, the first reaction zone of Jain et al. and Mansaray and Ghaly represent the first and second reaction zones of the present analysis. The values reported here are the ones giving the best regression fit of the equations with the TG data. The transition point for the three zones has been defined on the basis of the natural break in the slope of the TG curve. The transition points for the second and third zones were found to correspond to the first peak temperature of the DTA exotherm and the terminal point of the first peak of the DTG curve. The termination of the second zone has been taken as the point of break in the slope of the TG curve, which corresponds, to the end of the second peak of the DTG rate of degradation curve and also the second exotherm of the DTA curve.

The values of  $n$ ,  $E$  and  $k_0$  for VRH and MRH as obtained by using different methods of analysis are given in Tables 4.3.6(a, b) and 4.3.7(a, b).

The kinetic parameters were determined for each zone separately as well as the entire temperature (degradation) range. The Horowitz and Metzger method gave the least values of activation energy. The Freeman and Carroll method and the Piloyan and Novikova method also give much lower values as compared to Coats and Redfern or agarwal and Sivasubramanian and Reich and Stivala methods. It may, however, be noted that the Reich and Stivala method yielded comparable values with those obtained by the

**Table 4.3.7 (a) : Kinetic Parameters for Mill Rice Husk Thermal Degradation from TGA /DTG Data  
(Air : 50 mlmin<sup>-1</sup>), Heating Rate : 20°C min<sup>-1</sup>**

Temp. Zone (°C)	Method of Analysis					
	Coats & Redfern	Agarwal & Sivasubramanian	Piloyan & Novikova	Reich & Stivala	Horowitz & Metzger	Freeman & Carroll
258-360	n = 0.75 E=107.325 k <sub>o</sub> = 1.216x10 <sup>9</sup> R <sup>2</sup> =0.9961	n = 0.75 E=107.325 k <sub>o</sub> = 1.204x10 <sup>9</sup> R <sup>2</sup> =0.9961	- E=71.924 k <sub>o</sub> = 1.730x10 <sup>5</sup>	n = 0.00 E=62.434 k <sub>o</sub> = 1.607x10 <sup>5</sup>	n = 2.50 E=34.504 k <sub>o</sub> =5.996x10 <sup>4</sup>	n = 10.03 E=1033.061 k <sub>o</sub> = 5.698x10 <sup>10</sup>
360-521	n = 1.50 E=104.239 k <sub>o</sub> = 2.311x10 <sup>7</sup> R <sup>2</sup> =0.9951	n = 1.50 E=104.239 k <sub>o</sub> = 2.275x10 <sup>7</sup> R <sup>2</sup> =0.9951	- E=87.588 k <sub>o</sub> = 2.107x10 <sup>5</sup>	n = 0.75 E=285.444 k <sub>o</sub> = 4.772x10 <sup>5</sup>	n = 2.50 E=43.763 k <sub>o</sub> = 1.134x10 <sup>4</sup>	n = 2.87 E=219.574 k <sub>o</sub> =9.723x10 <sup>6</sup>
258-521	-	n = 2.00 E=77.981 k <sub>o</sub> = 1.026x10 <sup>6</sup> R <sup>2</sup> = 0.9862  For n =1.00 E=52.959 k <sub>o</sub> = 3.781 x10 <sup>3</sup> R <sup>2</sup> =0.9552	-	-	-	-

Note : E is in kJmol<sup>-1</sup>; k<sub>o</sub> is in min<sup>-1</sup>.

**Table 4.3.7 (b) : Kinetic Parameters for Mill Rice Husk Thermal Degradation from TGA /DTG Data  
(Air : 60 mlmin<sup>-1</sup>), Heating Rate : 40°C min<sup>-1</sup>**

Temp. Zone (°C)	Method of Analysis					
	Coats & Redfern	Agarwal & Sivasubramanian	Piloyan & Novikova	Reich & Stivala	Horowitz & Metzger	Freeman & Carroll
258-428	n = 1.25 E=107.623 k <sub>o</sub> = 7.644x10 <sup>8</sup> R <sup>2</sup> =0.9994	n = 1.25 E=107.623 k <sub>o</sub> = 7.555x10 <sup>8</sup> R <sup>2</sup> =0.9994	- E=77.032 k <sub>o</sub> = 3.706x10 <sup>5</sup>	n = 0.75 E=348.657 k <sub>o</sub> = 1.496x10 <sup>6</sup>	n = 2.50 E=34.792 k <sub>o</sub> = 3.798x10 <sup>4</sup>	n = 0.68 E=0.854 k <sub>o</sub> = 2.893x10 <sup>4</sup>
428-628	n = 1.25 E=128.949 k <sub>o</sub> = 5.2020x10 <sup>8</sup> R <sup>2</sup> =0.9546	n = 1.25 E=128.949 k <sub>o</sub> = 4.960x10 <sup>8</sup> R <sup>2</sup> =0.9546	- E=94.170 k <sub>o</sub> = 4.531x10 <sup>5</sup>	n = 0.95 E=438.344 k <sub>o</sub> = 3.979x10 <sup>5</sup>	n = 2.50 E=55.153 k <sub>o</sub> = 2.513x10 <sup>5</sup>	n = 0.80 E=200.642 k <sub>o</sub> =2.254x10 <sup>6</sup>
258-628	-	n = 2.50 E=78.585 k <sub>o</sub> = 1.419x10 <sup>6</sup> R <sup>2</sup> = 0.9798  For n=1.00 E=42.392 k <sub>o</sub> = 6.346 x10 <sup>2</sup> R <sup>2</sup> =0.8920	-	-	-	-

Note : E is in kJmol<sup>-1</sup>; k<sub>o</sub> is in min<sup>-1</sup>.

Agarwal and Sivasubramanian or Coats and Redfern method for  $20^{\circ}\text{Cmin}^{-1}$  heating rate. No correspondence was, however, found for  $40^{\circ}\text{C min}^{-1}$  data. The values of  $n$  obtained from Coats and Redfern or Agarwal and Sivasubramanian methods were the same, as were the values for activation energy. Due to slight change in the approximations used by two groups of researchers, the frequency factor (or pre-exponential factor) values differed slightly. As the values of  $E$  depend very heavily on  $n$  when integral method is used, the best-fit values of  $E$  obtained for  $20$  and  $40^{\circ}\text{C min}^{-1}$  were found to be very different. The overall kinetic parameters were surprisingly similar for both the heating rates. The values of  $E$  obtained by Mansaray and Ghaly (1999) are much lower ( $37\text{-}55 \text{ kJmol}^{-1}$ ) with  $n$  taking values between  $1.21$  and  $1.64$  for the first reaction zone ( $<320^{\circ}\text{C}$ ) while for the second reaction zone, these values were  $E \sim 18.0 - 21.0 \text{ kJmol}^{-1}$  and  $n \sim 0.40\text{-}0.55$ . Jain et al. (1999) reported that at  $10^{\circ}\text{C min}^{-1}$  heating rate, the activation energy values increased with the increase in  $n$ . In the similar temperature range ( $260\text{-}310^{\circ}\text{C}$  of Jain et al. 1999 and  $258\text{-}350^{\circ}\text{C}$  in the present study), the values of  $E$  at  $n = 2.50$  were found to be  $466.0 \text{ kJmol}^{-1}$  and  $173.47 \text{ kJmol}^{-1}$  by Jain et al. (1999) and the present study (for village rice husk). Wide discrepancy in the  $E$  values observed at same  $n$  value is not explainable, particularly when the rice husks do not have very significant physico-chemical characteristics and elemental composition. However, it is to be noted that the entire temperature (degradation) range could be correlated satisfactorily by a single-step reaction by using the integral method with the approximation of Agarwal and Sivasubramanian (1987). The best fit value of  $n$  varied from  $2.0$  to  $2.50$ ,  $E$  values varied from  $69.5$  to  $78.6 \text{ kJmol}^{-1}$  and the pre-exponential factor varied from  $3.86 \times 10^5$  to  $1.42 \times 10^6 \text{ min}^{-1}$ . Di Blasi and Branca (1999) divided the rice husk degradation in air in three temperature zones :  $190\text{-}350^{\circ}\text{C}$ ;  $350\text{-}383^{\circ}\text{C}$  and  $383\text{-}587^{\circ}\text{C}$ . The  $E$  values for these zones were found to be  $E = 73.04, 87.10$  and  $80.06 \text{ kJmol}^{-1}$ , respectively and  $n = 1.659$  for the third zone. The values of  $k_0$  for the three



zones were, respectively,  $3.74 \times 10^6$ ,  $2.9 \times 10^6$  and  $7.56 \times 10^6 \text{ min}^{-1}$ . The E values obtained for the entire degradation range in the present study are in the similar range as those of DiBlasi and Branca.

#### 4.3.3.2 Sawdust

Figs. 4.2.5 (b) and 4.2.6(b) show the data for thermal degradation of sawdust in air for the two heating rates, viz.  $20$  and  $40^\circ\text{C min}^{-1}$ . The thermogravimetric and DTG curves clearly show two distinct temperature (or degradation zones) with the transition point demarcated by the first exotherm peak temperature on DTA curve. From the TGA curve for  $40^\circ\text{C min}^{-1}$  heating rate, it is observed that the rate of weight loss beyond the dehydration zone, is slow upto certain temperature, after which the rate becomes very fast. In view of this, the first degradation zone has been divided in two zones, the first one being that of light volatiles evolution followed by a very fast degradation zone, which is the second degradation zone. The third degradation zone started from the first transition point. The termination of the third zone was taken as the end of the second DTG peak. The TGA, DTG and DTA curves for  $20^\circ\text{C min}^{-1}$  heating rate indicated several degradation zones, unlike those of  $40^\circ\text{C min}^{-1}$  heating rate. Slower heating rate might have affected the degradation characteristics. Unlike  $40^\circ\text{C min}^{-1}$  curves, four clearly distinct peaks with base line deviations between the second and third peaks on DTG and DTA curves are discerned. In view of this, the entire degradation zone has been divided in five zones.

The kinetic parameters as determined by using different methods are listed in Tables 4.3.8(a, b), for the two heating rates. As has been the case for the rice husk, the values of n for the best fit values of E and  $k_0$  are different for different zones and different for various methods. However, it may be noted that the entire degradation zone for each heating rate could be easily fitted by the integral method with the approximations of Agarwal and Sivasubramanian (1987). For the same order

**Table 4.3.8 (a) : Kinetic Parameters for Sawdust Thermal Degradation from TGA /DTG Data  
(Air : 50 mlmin<sup>-1</sup>), Heating Rate : 20°C min<sup>-1</sup>**

Temp. Zone (°C)	Method of Analysis					
	Coats & Redfern	Agarwal & Sivasubramanian	Piloyan & Novikova	Reich & Stivala	Horowitz & Metzger	Freeman & Carroll
215-295	n = 0.00 E=53.900 k <sub>o</sub> = 3.368x10 <sup>4</sup> R <sup>2</sup> =0.9632	n = 0.00 E=53.90 k <sub>o</sub> = 3.253x10 <sup>4</sup> R <sup>2</sup> =0.9632	- E=71.450 k <sub>o</sub> = 1.719x10 <sup>5</sup>	n = 0.00 E=35.851 k <sub>o</sub> = 9.698x10 <sup>4</sup>	n = 0.00 E=19.663 k <sub>o</sub> = 9.966x10 <sup>2</sup>	n = 0.80 E=30.862 k <sub>o</sub> = 2.013x10 <sup>5</sup>
295-370	n = 2.00 E=249.238 k <sub>o</sub> = 4.805x10 <sup>21</sup> R <sup>2</sup> =0.9731	n = 2.00 E=249.238 k <sub>o</sub> = 4.795x10 <sup>21</sup> R <sup>2</sup> =0.9731	- E=73.042 k <sub>o</sub> = 1.757x10 <sup>5</sup>	n = 0.50 E=250.261 k <sub>o</sub> = 4.423x10 <sup>5</sup>	E=46.535 k <sub>o</sub> = 7.991x10 <sup>6</sup>	n = 0.88 E=175.390 k <sub>o</sub> =1.062x10 <sup>6</sup>
370-390	n = 2.00 E=1250.559 k <sub>o</sub> = 7.814x10 <sup>100</sup>	n = 2.00 E=1250.559 k <sub>o</sub> = 7.813x10 <sup>100</sup>	- E=81.378 k <sub>o</sub> = 1.958x10 <sup>5</sup>	n = 0.50 E=1167.508 k <sub>o</sub> = 1.524x10 <sup>6</sup>	-	n = 0.28 E=36.30 k <sub>o</sub> = 8.128x10 <sup>4</sup>
390-438	n = 2.00 E=361.966 k <sub>o</sub> = 8.212x10 <sup>27</sup> R <sup>2</sup> =0.9671	n = 2.00 E=361.966 k <sub>o</sub> = 8.202x10 <sup>27</sup> R <sup>2</sup> =0.9671	- E=86.313 k <sub>o</sub> = 2.076x10 <sup>5</sup>	n = 0.75 E=394.717 k <sub>o</sub> = 2.733x10 <sup>5</sup>	n=2.00 E=70.461 k <sub>o</sub> = 3.545x10 <sup>8</sup>	n = 0.08 E=93.870 k <sub>o</sub> =2.286x10 <sup>5</sup>
438-512	n = 2.50 E=588.417 k <sub>o</sub> = 1.334x10 <sup>43</sup> R <sup>2</sup> =0.8855	n = 2.50 E=588.417 k <sub>o</sub> = 1.33x10 <sup>43</sup> R <sup>2</sup> =0.8855	- E=85.917 k <sub>o</sub> = 2.067x10 <sup>5</sup>	n = 0.95 E=464.428 k <sub>o</sub> = 8.508x10 <sup>4</sup>	-	n = 0.28 E=79.259 k <sub>o</sub> = 1.613x10 <sup>5</sup>
215-512	-	n = 2.25 E=86.675 k <sub>o</sub> = 1,082x10 <sup>7</sup> R <sup>2</sup> =0.9894  For n =1.00 E=65.246 k <sub>o</sub> = 6.502 x10 <sup>4</sup> R <sup>2</sup> =0.9689	-	-	-	-

Note : E is in kJmol<sup>-1</sup>; k<sub>o</sub> is in min<sup>-1</sup>.

**Table 4.3.8 (b) : Kinetic Parameters for Sawdust Thermal Degradation from TGA /DTG Data  
(Air : 50 mlmin<sup>-1</sup>), Heating Rate : 40°C min<sup>-1</sup>**

Temp. Zone (°C)	Method of Analysis					
	Coats & Redfern	Agarwal & Sivasubramanian	Piloyan & Novikova	Reich & Stivala	Horowitz & Metzger	Freeman & Carroll
198-290	n = 0.00 E=145.726 k <sub>o</sub> = 8.89x10 <sup>13</sup> R <sup>2</sup> =0.9743	n = 0.00 E=145.726 k <sub>o</sub> = 8.846x10 <sup>13</sup> R <sup>2</sup> =0.9743	- E=76.876 k <sub>o</sub> = 3.699x10 <sup>5</sup>	n = 0.00 E=91.017 k <sub>o</sub> = 4.25x10 <sup>5</sup>	-	n = 0.01 E=128.180 k <sub>o</sub> = 6.576x10 <sup>5</sup>
290-380	n = 1.25 E=173.077 k <sub>o</sub> = 4.523x10 <sup>14</sup> R <sup>2</sup> =0.9986	n = 1.25 E=173.077 k <sub>o</sub> = 4.504x10 <sup>14</sup> R <sup>2</sup> =0.9986	- E=73.327 k <sub>o</sub> = 3.528x10 <sup>5</sup>	n = 0.00 E=166.785 k <sub>o</sub> = 9.708x10 <sup>5</sup>	n=1.25 E=38.927 k <sub>o</sub> = 4.090x10 <sup>6</sup>	n = 4.87 E=621.137 k <sub>o</sub> =2.329x10 <sup>4</sup>
380-490	n = 2.00 E=200.218 k <sub>o</sub> = 1.786x10 <sup>15</sup> R <sup>2</sup> =0.9787	n = 2.00 E=200.218 k <sub>o</sub> = 1.779x10 <sup>15</sup> R <sup>2</sup> =0.9787	- E=82.598 k <sub>o</sub> = 3.974x10 <sup>5</sup>	n = 0.50 E=193.508 k <sub>o</sub> = 5.797x10 <sup>5</sup>	n = 2.00 E=68.230 k <sub>o</sub> = 7.453x10 <sup>7</sup>	n = 1.18 E=209.308 k <sub>o</sub> = 3.424x10 <sup>6</sup>
198-490	-	n = 2.25 E=132.899 k <sub>o</sub> = 1.145x10 <sup>11</sup> R <sup>2</sup> =0.9974  For n=1.00 E=118.201 k <sub>o</sub> = 4.056 x10 <sup>9</sup> R <sup>2</sup> =0.9928	-	-	-	-

Note : E is in kJmol<sup>-1</sup>; k<sub>o</sub> is in min<sup>-1</sup>.

of reaction  $n=2.25$  for the entire degradation zone,  $E$  values were 86.67 and 132.90  $\text{kJmol}^{-1}$ , and  $k_0$  values were  $1.08 \times 10^7$  and  $1.14 \times 10^{11} \text{ min}^{-1}$ , for 20 and  $40^\circ\text{C min}^{-1}$  heating rate, respectively.

#### 4.3.3.3 Bagasse

The thermograms, derivative thermograms and differential thermal analysis thermograms for bagasse indicate [Figs. 4.2.7(b) and 4.2.8(b)] that there are three clearly distinct zones of degradation in the presence of air; each zone identified from the natural break in the slope of TGA curve alongwith the peaks of DTG and the endotherm-exotherm characteristics of DTA curves. As the heating rate was changed from 20 to  $40^\circ\text{Cmin}^{-1}$ , the peaks became sharper. In all, five zones have been identified and the kinetic parameters have been determined for each of these zones by using the methods as discussed earlier. It may be seen that the value of  $n$ ,  $E$  and  $k_0$  differed from one method to another Table 4.3.9 (a, b). As discussed previously, the values obtained by the integral method of analysis with either Coats and Redfern approximation or the Agarwal and Sivasubramanian approximation have been taken as the reference. The overall temperature range data have been used for the determination of kinetic parameters. For  $n = 2.50$ , the values of  $E$  and  $k_0$  were found to be  $118.34 \text{ kJmol}^{-1}$  and  $k_0 = 5.46 \times 10^9 \text{ min}^{-1}$  for  $20^\circ\text{Cmin}^{-1}$ , and for  $n = 1.25$ ,  $E = 62.46 \text{ kJmol}^{-1}$  and  $k_0 = 5.097 \times 10^4 \text{ min}^{-1}$  for  $40^\circ\text{Cmin}^{-1}$  heating rate. The regression coefficients were good enough for engineering design purposes. For  $20^\circ\text{Cmin}^{-1}$  heating rate, for  $n = 1.25$ , the value of  $E$  and  $k_0$  were found to be  $79.93 \text{ kJmol}^{-1}$  and  $1.1 \times 10^6 \text{ min}^{-1}$ , respectively, with  $R^2 = 0.8615$ .

It may be noted that the over all range used for  $20^\circ\text{Cmin}^{-1}$  heating rate was from 248 to  $495^\circ\text{C}$ , whereas for  $40^\circ\text{Cmin}^{-1}$  heating rate, the overall range was  $181\text{-}575^\circ\text{C}$ . Because of the larger temperature range, the values of  $E$  and  $k_0$  for  $40^\circ\text{Cmin}^{-1}$  heating rate have been found to be lower than those obtained for  $20^\circ\text{Cmin}^{-1}$ .

**Table 4.3.9 (a) : Kinetic Parameters for Bagasse Thermal Degradation from TGA /DTG Data  
(Air : 50 mlmin<sup>-1</sup>), Heating Rate : 20°C min<sup>-1</sup>**

Temp. Zone (°C)	Method of Analysis					
	Coats & Redfern	Agarwal & Sivasubramanian	Piloyan & Novikova	Reich & Stivala	Horowitz & Metzger	Freeman & Carroll
248-300	n = 1.50 E=255.380 k <sub>o</sub> = 1.233x10 <sup>24</sup> R <sup>2</sup> =0.9793	n = 1.50 E=255.380 k <sub>o</sub> = 1.231x10 <sup>24</sup> R <sup>2</sup> =0.9793	- E=72.012 k <sub>o</sub> =1.732x10 <sup>5</sup>	n = 0.00 E=159.154 k <sub>o</sub> = 3.915x10 <sup>5</sup>	n = 1.50 E=53.325 k <sub>o</sub> = 8.141x10 <sup>8</sup>	n = 0.27 E=26.897 k <sub>o</sub> = 1.061x10 <sup>5</sup>
300-338	n = 1.50 E=250.570 k <sub>o</sub> = 1.471x10 <sup>22</sup> R <sup>2</sup> =0.9839	n = 1.50 E=250.570 k <sub>o</sub> = 1.469x10 <sup>22</sup> R <sup>2</sup> =0.9839	- E=71.591 k <sub>o</sub> = 1.722x10 <sup>5</sup>	n = 0.00 E=161.094 k <sub>o</sub> = 4.160x10 <sup>5</sup>	n=1.50 E=52.336 k <sub>o</sub> = 8.537x10 <sup>7</sup>	n = 1.57 E=256.184 k <sub>o</sub> =3.057x10 <sup>6</sup>
338-356	n = 1.00 E=662.514 k <sub>o</sub> = 8.825x10 <sup>55</sup> R <sup>2</sup> =0.9905	n = 1.00 E=662.514 k <sub>o</sub> = 8.822x10 <sup>55</sup> R <sup>2</sup> =0.9905	- E=73.951 k <sub>o</sub> = 1.779x10 <sup>5</sup>	n = 0.00 E=496.198 k <sub>o</sub> = 1.256x10 <sup>6</sup>	-	n = 2.30 E=1065.637 k <sub>o</sub> = 2.590x10 <sup>7</sup>
356-438	n = 1.50 E=131.688 k <sub>o</sub> = 1.462x10 <sup>10</sup> R <sup>2</sup> =0.9939	n = 1.50 E=131.688 k <sub>o</sub> = 1.450x10 <sup>10</sup> R <sup>2</sup> =0.9939	- E=94.256 k <sub>o</sub> = 2.267x10 <sup>5</sup>	n = 0.00 E=80.760 k <sub>o</sub> = 2.194x10 <sup>5</sup>	n=1.50 E=43.716 k <sub>o</sub> = 3.68x10 <sup>4</sup>	n = 0.65 E=62.982 k <sub>o</sub> =9.025x10 <sup>4</sup>
438-499	n = 2.50 E=540.792 k <sub>o</sub> =4.632x10 <sup>38</sup> R <sup>2</sup> =0.9943	n = 2.50 E=540.792 k <sub>o</sub> =4.629x10 <sup>38</sup> R <sup>2</sup> =0.9943	- E=85.288 k <sub>o</sub> = 2.052x10 <sup>5</sup>	n = 0.00 E=205.249 k <sub>o</sub> = 4.82x10 <sup>5</sup>	n = 2.50 E=191.933 k <sub>o</sub> = 1.716x10 <sup>22</sup>	n = 2.30 E=1065.632 k <sub>o</sub> = 2.590x10 <sup>7</sup>
248-499	-	n = 2.50 E=118.339 k <sub>o</sub> = 5.462x10 <sup>9</sup> R <sup>2</sup> =0.9763  For n=1.00 E=73.916 k <sub>o</sub> = 2.843 x10 <sup>5</sup> R <sup>2</sup> =0.8255	-	-	-	-

Note : E is in kJmol<sup>-1</sup>; k<sub>o</sub> is in min<sup>-1</sup>.

Table 4.3.9 (b) : Kinetic Parameters for Bagasse Thermal Degradation from TGA /DTG Data  
(Air : 50 mlmin<sup>-1</sup>), Heating Rate : 40°C min<sup>-1</sup>

Temp. Zone (°C)	Method of Analysis					
	Coats & Redfern	Agarwal & Sivasubramanian	Piloyan & Novikova	Reich & Stivala	Horowitz & Metzger	Freeman & Carroll
181-300	n = 0.00 E=39.430 k <sub>o</sub> = 2.078x10 <sup>3</sup> R <sup>2</sup> =0.8296	n = 0.00 E=39.430 k <sub>o</sub> = 1.145x10 <sup>3</sup> R <sup>2</sup> =0.8296	- E=74.391 k <sub>o</sub> =3.579x10 <sup>5</sup>	n = 0.95 E=54.997 k <sub>o</sub> = 1.710x10 <sup>3</sup>	-	n = 0.29 E=54.701 k <sub>o</sub> =3.991x10 <sup>5</sup>
300-360	n = 0.50 E=164.162 k <sub>o</sub> = 1.204x10 <sup>14</sup> R <sup>2</sup> =0.9803	n = 0.50 E=164.162 k <sub>o</sub> = 1.982x10 <sup>14</sup> R <sup>2</sup> =0.9803	- E=73.645 k <sub>o</sub> =3.543x10 <sup>5</sup>	n = 0.33 E=164.936 k <sub>o</sub> = 5.223x10 <sup>5</sup>	n=2.50 E=51.408 k <sub>o</sub> = 8.728x10 <sup>7</sup>	n = 0.30 E=83.394 k <sub>o</sub> =3.265x10 <sup>5</sup>
360-399	n = 1.50 E=418.949 k <sub>o</sub> = 1.625x10 <sup>34</sup> R <sup>2</sup> =0.9947	n = 1.50 E=418.949 k <sub>o</sub> = 1.624x10 <sup>34</sup> R <sup>2</sup> =0.9947	- E=77.082 k <sub>o</sub> = 3.709x10 <sup>5</sup>	n = 0.95 E=1970.337 k <sub>o</sub> = 4.136x10 <sup>6</sup>	-	n = 0.01 E=12.201 k <sub>o</sub> = 7.095x10 <sup>4</sup>
399-466	n = 1.25 E=178.248 k <sub>o</sub> = 2.629x10 <sup>13</sup> R <sup>2</sup> =0.9745	n = 1.25 E=178.248 k <sub>o</sub> = 2.615x10 <sup>13</sup> R <sup>2</sup> =0.9745	- E=84.368 k <sub>o</sub> = 4.059x10 <sup>5</sup>	n = 0.25 E=154.240 k <sub>o</sub> = 6.176x10 <sup>5</sup>	n=2.50 E=58.096 k <sub>o</sub> = 6.047x10 <sup>6</sup>	n = 0.02 E=45.513 k <sub>o</sub> =2.668x10 <sup>5</sup>
466-575	n = 2.50 E=506.872 k <sub>o</sub> =4.853x10 <sup>35</sup> R <sup>2</sup> =0.9548	n = 2.50 E=506.972 k <sub>o</sub> =4.850x10 <sup>35</sup> R <sup>2</sup> =0.9548	- E=89.130 k <sub>o</sub> = 4.288x10 <sup>5</sup>	n = 0.95 E=638.099 k <sub>o</sub> = 3.654x10 <sup>5</sup>	-	n = 0.62 E=123.126 k <sub>o</sub> = 3.456x10 <sup>5</sup>
181-575	-	n = 1.25 E=62.459 k <sub>o</sub> = 5.097x10 <sup>4</sup> R <sup>2</sup> =0.9677  For n=1.00 E=57.733 k <sub>o</sub> = 1.642 x10 <sup>4</sup> R <sup>2</sup> =0.9675	-	-	-	-

Note : E is in kJmol<sup>-1</sup>; k<sub>o</sub> is in min<sup>-1</sup>.

Nassar (1985) has reported DTG and TGA thermograms for bagasse under oxidizing (air) atmosphere at  $5^{\circ}\text{Cmin}^{-1}$  heating rate. Their thermograms also showed similar characteristics as observed in the present study. However, he has divided the whole degradation range in two parts with the transition temperature as  $360^{\circ}\text{C}$ . For pseudo first order degradation characteristics, they reported E values  $\sim 140 \text{ kJmol}^{-1}$  for the first zone ( $<360^{\circ}\text{C}$ ) and  $\sim 77 \text{ kJmol}^{-1}$  for the second zone ( $>360^{\circ}\text{C}$ ). In comparison to the values of Nassar (1985), the values of activation energies from the present investigation were found to be lower.

#### 4.3.3.4 Pressmud

Although pressmud is an industrial waste from the sugar mills, the thermal degradation characteristics in air (oxidizing) atmosphere are well described by a single sharp peak followed by a weak slow peak in both the DTG and DTA [Figs. 4.2.9(b) and 4.2.10(b)] curves. Kinetic parameters have been determined for a slow degradation first zone followed by the fast devolatilization second zone and a slower devolatilization and combustion zone. As discussed earlier with other biomass materials, the values of activation energy and pre-exponential factor are found to vary with n. The values reported in Table 4.3.10(a, b) are the best-fit values for that value of n which gave the highest regression coefficient  $R^2$  (nearest to 1.0). It is found that the integral method with the approximation of Coats and Redfern and Agarwal and Sivasubramanian gave same values of E for a particular n, although  $k_0$  values were different.

The kinetic parameters for the entire range of degradation temperature at the two heating rates indicated that the order or reaction  $n=2.50$  for the best-fit of the experimental data for  $20^{\circ}\text{Cmin}^{-1}$  heating rate and  $n = 1.75$  for  $40^{\circ}\text{Cmin}^{-1}$  heating rate. For  $n = 1.75$  with similar regression coefficient for  $40^{\circ}\text{Cmin}^{-1}$  heating rate, the E values for 20 and  $40^{\circ}\text{Cmin}^{-1}$  heating rates were, respectively, 69.15 and  $57.41 \text{ kJmol}^{-1}$ . The corresponding  $k_0$  values were  $2.41 \times 10^5$  and  $3.27 \times 10^4 \text{ min}^{-1}$  with  $R^2$  being 0.9608 and 0.9640, respectively. It may thus be seen that although, the kinetic parameters for each reaction zone may be obtained, the parameters obtained for the entire reaction zone are also satisfactory for engineering design of gasifiers.

**Table 4.3.10 (a) : Kinetic Parameters for Pressmud Thermal Degradation from TGA /DTG Data  
(Air : 50 mlmin<sup>-1</sup>), Heating Rate : 20°C min<sup>-1</sup>**

Temp. Zone (°C)	Method of Analysis					
	Coats & Redfern	Agarwal & Sivasubramanian	Piloyan & Novikova	Reich & Stivala	Horowitz & Metzger	Freeman & Carroll
169-320	n = 1.25 E=105.794 k <sub>o</sub> = 4.228x10 <sup>9</sup> R <sup>2</sup> =0.9864	n = 1.25 E=105.794 k <sub>o</sub> = 4.189x10 <sup>9</sup> R <sup>2</sup> =0.9864	- E=70.740 k <sub>o</sub> =1.702x10 <sup>5</sup>	n = 0.25 E=100.893 k <sub>o</sub> = 1.903x10 <sup>5</sup>	n = 1.25 E=25.709 k <sub>o</sub> = 1.030x10 <sup>4</sup>	n = 0.72 E=137.466 k <sub>o</sub> =1.690x10 <sup>5</sup>
320-362	n = 0.75 E=232.142 k <sub>o</sub> = 4.242x10 <sup>19</sup> R <sup>2</sup> =0.9917	n = 0.75 E=232.142 k <sub>o</sub> = 4.232x10 <sup>19</sup> R <sup>2</sup> =0.9917	- E=74.115 k <sub>o</sub> =1.783x10 <sup>5</sup>	n = 0.00 E=245.724 k <sub>o</sub> = 7.105x10 <sup>5</sup>	-	n = 0.06 E=256.55 k <sub>o</sub> =5.974x10 <sup>5</sup>
362-700	n = 1.75 E=62.278 k <sub>o</sub> =1.488x10 <sup>4</sup> R <sup>2</sup> =0.9859	n = 1.75 E=62.278 k <sub>o</sub> = 1.410x10 <sup>4</sup> R <sup>2</sup> =0.9859	- E=99.382 k <sub>o</sub> = 2.391x10 <sup>5</sup>	n = 0.25 E=67.708 k <sub>o</sub> =1.585x10 <sup>5</sup>	n = 1.75 E=21.475 k <sub>o</sub> = 1.144	n = 4.91 E=60.103 k <sub>o</sub> = 1.236x10 <sup>3</sup>
169-700	-	n = 2.50 E=88.921 k <sub>o</sub> = 2.266x10 <sup>7</sup> R <sup>2</sup> =0.9935  For n=1.00 E=53.025 k <sub>o</sub> = 5.573 x10 <sup>3</sup> R <sup>2</sup> =0.8821	-	-	-	-

Note : E is in kJmol<sup>-1</sup>; k<sub>o</sub> is in min<sup>-1</sup>.



**Table 4.3.10 (b) : Kinetic Parameters for Pressmud Thermal Degradation from TGA /DTG Data  
(Air : 50 mlmin<sup>-1</sup>), Heating Rate : 40°C min<sup>-1</sup>**

Temp. Zone (°C)	Method of Analysis					
	Coats & Redfern	Agarwal & Sivasubramanian	Piloyan & Novikova	Reich & Stivala	Horowitz & Metzger	Freeman & Carroll
133-304	n = 0.00 E=21.706 k <sub>o</sub> =3.563x10 <sup>1</sup> R <sup>2</sup> =0.9756	n = 0.00 E=21.706 k <sub>o</sub> = 2.852x10 <sup>1</sup> R <sup>2</sup> =0.9756	- E=72.564 k <sub>o</sub> =3.491x10 <sup>5</sup>	n = 0.50 E=21.194 k <sub>o</sub> = 5.910x10 <sup>4</sup>	-	n = 5.81 E=210.427 k <sub>o</sub> =3.125x10 <sup>3</sup>
340-385	n = 1.00 E=164.649 k <sub>o</sub> = 6.829x10 <sup>13</sup> R <sup>2</sup> =0.9977	n = 1.00 E=164.649 k <sub>o</sub> = 6.795x10 <sup>13</sup> R <sup>2</sup> =0.9977	- E=75.854 k <sub>o</sub> =3.649x10 <sup>5</sup>	n = 0.25 E=193.302 k <sub>o</sub> = 9.269x10 <sup>5</sup>	n = 2.50 E=38.175 k <sub>o</sub> = 1.565x10 <sup>6</sup>	n = 0.57 E=128.499 k <sub>o</sub> =1.168x10 <sup>6</sup>
385-700	n = 2.50 E=105.536 k <sub>o</sub> =8.806x10 <sup>7</sup> R <sup>2</sup> =0.9512	n = 2.50 E=105.536 k <sub>o</sub> = 8.662x10 <sup>7</sup> R <sup>2</sup> =0.9512	- E=100.213 k <sub>o</sub> = 4.821x10 <sup>5</sup>	n = 0.95 E=77.859 k <sub>o</sub> =3.594x10 <sup>4</sup>	-	n = 0.42 E=61.231 k <sub>o</sub> = 5.159x10 <sup>5</sup>
133-700	-	n = 1.75 E=57.413 k <sub>o</sub> = 3.270x10 <sup>4</sup> R <sup>2</sup> =0.9640  For n = 1.00 E=39.913 k <sub>o</sub> = 5.141 x10 <sup>2</sup> R <sup>2</sup> =0.9259	-	-	-	-

**Note :** E is in kJmol<sup>-1</sup>; k<sub>o</sub> is in min<sup>-1</sup>.

#### **4.4 FLUIDIZED BED GASIFICATION OF VILLAGE RICE HUSK AND SAW DUST**

In this section, the results of the determination of physico-chemical and thermochemical properties of the biomass materials, namely village rice husk, mill rice husk, sawdust, bagasse and pressmud have been presented and discussed. Of the five-biomass materials, sawdust and village rice husk were employed for the fluidized bed gasification experiments at different equivalence ratios and fluidization velocities.

##### **4.4.1 Physico Chemical Properties of the Biomass**

###### **4.4.1.1 Proximate Analysis**

The results of the proximate analysis of the biomass materials are given in Table 4.4.1(a). The average volatile matter, fixed carbon, and ash content of the five biomass materials ranged from 76% (for sawdust) to 53.9% (for bagasse), 35% (for bagasse) to 13.8% (village rice husk) and 20% (for village rice husk and pressmud) to 3.6% (sawdust), respectively. It is seen that sawdust and village rice husk have high volatile matter as compared to coal available in India (20-30%, Iyer et al. 1997) and therefore are readily amenable to gasification yielding considerably less residue. Compared to coal, less amount of heat is required for the reactions due to high volatile matter content which makes them possible to be gasified at lower temperatures (Schiefelbein, 1989, Mukunda and Paul, 1994). Hence the biomass materials selected for study are potentially useful fuels for gasification. The volatile matter of biomass fuels is important because it characterizes the possibility and to some extent magnitude of tar formation in a thermochemical conversion system. The volatiles released in the temperature range of 320 to 500°C are termed as 'Potential Tar Forming Volatiles' (PTFV) (Iyer et al., 1997). The volatiles burn as gaseous products in the flame but fixed carbon does not produce a flame and burns slowly (Strehler, 1985).

Ash is an undesirable component of any fuel. It contributes to the overall weight and reduces the heating values of the material. More ash implies that more fuel needs to be combusted to heat the inert material, thus lowering the heating value of the fuel gas (Faaiz et al., 1997).

The ash content of the sawdust and the village rice husk are on the higher side. Rice husk is known to contain high ash and has been classified as a high ash content biomass (Grover, 1996). The present sample of sawdust was from a local saw mill where a variety of forest wood is normally sawn. The values of ash content for the village rice husk and sawdust are comparable with the values of ash content of rice husk and sawdust compiled by Iyer et al. (1997).

#### **4.4.1.2 Ultimate Analysis**

The results of the ultimate analyses of the biomass materials are presented in Table 4.4.1(b). This analysis is necessary to determine the theoretical air requirement for complete combustion of the biomass and to determine the equivalence ratio. The results indicate that the major elemental constituents of the biomass materials are carbon, hydrogen and oxygen. It is seen that the weight fraction of carbon varied from 37.40% (for rice husk) to 44.50% (for pressmud), hydrogen varied from 5.26% (for bagasse) to 6.18% (for sawdust) and oxygen varied from 28.80% (for pressmud) to 45.67% (for sawdust).

The measured values of these components are in the ranges reported by Iyer et al. (1997). The low content of nitrogen offer environmentally more desirable fuel properties. The sulphur and chlorine contents are very low in biomass materials in general; they have not been determined and reported for the present biomass materials here. From the ultimate analysis, it can be said that, although the biomass exists in different physical shapes, chemically they are similar to each other. This is in contrast to the structure of coal which is basically formed by biomass. Different types of coals are physically same but chemically differ greatly.

**Table 4.4.1 (a) : Proximate Analysis of Biomass Materials (% dry basis)**

Biomass Materials	Volatile Matter (%)	Fixed Carbon (%)	Ash (%)	Moisture Content % wet basis
Sawdust	76	20.4	3.6	12.4
Village rice husk	66.2	13.8	20.0	12.0
Mill rice husk	66.1	14.7	19.2	11.8
Pressmud	54.0	26.0	20.0	9.5
Bagasse	53.9	35.0	11.1	10.2

**Table 4.4.1(b) : Ultimate Analysis (%) dry basis)**

Biomass Materials	Carbon	Hydrogen	Nitrogen	Oxygen (by difference)	Ash
Sawdust	43.94	6.18	0.61	45.67	3.60
Village rice husk	37.43	6.01	1.32	35.24	20.00
Mill rice husk	37.40	5.54	0.34	37.52	19.20
Pressmud	44.50	5.60	1.10	28.80	20.00
Bagasse	44.10	5.26	1.00	38.54	11.10

**Table 4.4.2(a) : Heating Value of Biomass Materials**

Biomass Materials	Higher Heating Value (MJkg <sup>-1</sup> )	Lower Heating Value (MJkg <sup>-1</sup> )
Sawdust	18.2	15.66
Village rice husk	14.90	12.84
Mill rice husk	15.80	13.67
Pressmud	13.60	11.98
Bagasse	16.85	15.12

**Table 4.4.2(b) : Ash Deformation and Fusion Temperatures**

Biomass Materials	Temperature, (°C)	
	Deformation	Fusion
Sawdust	1350	>1400
Village rice husk	1250	1400
Mill rice husk	1400	1450
Pressmud	1300	1350
Bagasse	1200	1350

## 4.4.2 Thermochemical Properties of the Biomass

### 4.4.2.1 Heating values

The higher and lower heating values for the biomass materials are presented in Table 4.4.2(a). The lower heating values of the biomass have been calculated using the formula given by Ebeling and Jenkins (1985).

$$\text{LHV} = (1 - \text{MC}) \left[ \text{HHV} - Y \left( \frac{\text{MC}}{1 - \text{MC}} \right) + \frac{18H}{200} \right] \quad (4.4.1)$$

Where

MC = moisture content of fuel on wet basis (decimal)

Y = latent heat of vaporization for water, ( $\text{MJkg}^{-1}$ ), and

H = hydrogen content of the fuel on weight basis (decimal)

It is seen from the Table 4.4.2(a) that the lower heating values range from  $11.98 \text{ MJ kg}^{-1}$  (for press mud) to  $15.66 \text{ MJ kg}^{-1}$  (for saw dust). The village rice husk has a heating value of  $12.84 \text{ MJ kg}^{-1}$ . It can be easily seen that as the ash content decreases the heating value of the biomass increases. Weight for weight, the selected biomass materials have energy values more than half of the energy content of average coal found in India ( $\approx 20.00 \text{ MJ kg}^{-1}$ ) and are, therefore, important potential sources of energy.

### 4.4.2.2 Ash deformation and fusion temperatures

The behaviours of ash from the biomass materials at high temperatures were determined by conducting ash deformation and fusion tests. The tests were conducted only in oxidizing (air) atmosphere. The results have been presented in Table 4.4.2(b). The values obtained are in the same range of values as reported by Iyer et al. (1997) for some biomass materials.

It can be seen that the temperatures of ash deformation and fusion of all the biomass materials studied are higher than the normal operational temperature range of a

fluidized bed gasifier (650-850°C). Kaupp (1984) has reported that the softening and melting temperatures of biomass materials are significantly reduced by the presence of large amounts of low melting temperature mineral oxides such as  $K_2O$  and  $Na_2O$  in the ash.

#### 4.4.3 Biomass Gasification in the Fluidized Bed

Gasification experiments were performed at four fluidizing velocities, 0.53, 0.59, 0.68 and 0.73  $ms^{-1}$  and at five equivalence ratios, 0.20, 0.25, 0.30, 0.35 and 0.40. The measurements of temperature in the bed, free board, disengagement section and at the sampling port, and sampling of the gas, tar and particulates were done at different times-on-stream under steady state conditions. Under steady-state conditions, insignificant variations in the values for temperature, gas composition, tar content and particulates content were observed. The values reported in the tables and the figures are the averaged values of the several readings/analyses at different times-on-stream.

##### 4.4.3.1 Gasifier temperature

The average temperatures recorded along the fluidized gasifier bed (T1-T4), free board (T5-T8), transport disengagement section (TDS) (T9) and the sampling port (T10) are given in Tables 4.4.3(a) and 4.4.3(b) for village rice husk (VRH) and sawdust (SD), respectively. The temperatures reported here are the averaged values of three readings. These temperatures are plotted in Figs. 4.4.1 (a-d) and 4.4.2 (a-d) for VRH and SD, respectively, for different equivalence ratios (ER=0.2, 0.25, 0.3, 0.35 and 0.40) at each of the fluidization velocities (0.53, 0.59, 0.68 and 0.73  $ms^{-1}$ ). It is found that the temperature in the bed varied from around 650°C to 850°C and then decreased to around 650°C. In the free board region, from 500 mm to 1400 mm above the distributor plate, the temperature varied from 650°C to 580°C. The disengagement section temperature varied from 465 to 505°C.

**Table 4.4.3(a) : Temperature Measurements in the Fluidized Bed Gasification Experiments**  
 (Each Average of 3 readings) (°C)  
 Feed Stock : Village Rice Husk

Fluidization Velocity (m/s)	Eq. Ratio $\phi$	Bed				Free Board				TDS	Sampling Port	Average Bed Temperature	Average Free Board Temperature	Average Reactor Temperature
		T <sub>1</sub>	T <sub>2</sub>	T <sub>3</sub>	T <sub>4</sub>	T <sub>5</sub>	T <sub>6</sub>	T <sub>7</sub>	T <sub>8</sub>	T <sub>9</sub>	T <sub>10</sub>			
0.53	0.20	650	667	673	710	695	670	611	540	465	315	675	596	635
	0.25	659	688	702	740	717	677	618	545	471	322	697	605	651
	0.30	668	710	731	770	742	685	625	551	478	330	719	616	667
	0.35	674	722	755	795	755	687	626	555	479	334	736	620	678
	0.40	680	735	780	820	768	690	629	560	480	336	753	625	689
0.59	0.20	655	680	705	741	708	675	615	547	463	313	695	601	648
	0.25	666	702	724	760	730	686	624	554	470	321	713	612	662
	0.30	677	724	743	780	756	697	635	562	477	329	731	625	678
	0.35	682	734	770	804	766	701	637	565	481	333	741	630	688
	0.40	687	745	797	831	777	705	640	568	485	338	765	635	700
0.68	0.20	661	690	711	750	722	680	619	545	466	315	703	606	654
	0.25	673	711	734	772	743	692	629	556	475	325	722	619	670
	0.30	685	733	755	795	765	705	640	567	486	336	742	632	687
	0.35	690	744	780	816	776	709	641	568	488	338	757	636	696
	0.40	695	756	805	840	788	714	643	570	490	340	774	641	707
0.73	0.20	669	701	707	760	734	687	623	550	472	320	709	613	661
	0.25	680	724	734	785	757	698	634	561	484	332	730	626	678
	0.30	691	748	761	810	780	710	645	572	496	345	752	640	696
	0.35	697	756	784	831	788	716	651	576	500	350	767	646	706
	0.40	703	765	807	853	797	720	657	580	505	355	782	651	716

**Table 4.4.3(b) : Temperature Measurements in the Fluidized Bed Gasification Experiments**  
 (Each Average of 3 readings) (°C)  
 Feed Stock : Sawdust

Fluidization Velocity (m/s)	Eq. Ratio $\phi$	Bed				Free Board				TDS	Sampling Port	Average Bed Temperature	Average Free Board Temperature	Average Reactor Temperature
		T <sub>1</sub>	T <sub>2</sub>	T <sub>3</sub>	T <sub>4</sub>	T <sub>5</sub>	T <sub>6</sub>	T <sub>7</sub>	T <sub>8</sub>	T <sub>9</sub>	T <sub>10</sub>			
0.53	0.20	655	670	680	716	695	672	615	550	465	350	680	599	635
	0.25	660	691	712	746	720	694	635	560	486	368	702	619	656
	0.30	670	715	740	777	745	716	655	590	510	390	725	643	679
	0.35	674	723	751	803	757	728	670	608	525	407	733	658	693
	0.40	678	740	786	830	770	740	685	626	540	425	758	672	710
0.59	0.20	656	684	711	745	724	695	635	570	485	365	699	622	656
	0.25	662	709	721	766	740	710	652	588	505	386	715	639	672
	0.30	682	730	749	787	756	725	670	611	526	410	737	657	692
	0.35	683	733	783	812	769	738	680	617	532	413	753	667	705
	0.40	687	751	805	837	782	751	690	625	540	427	770	677	718
0.68	0.20	660	695	715	760	740	700	645	583	495	380	708	632	665
	0.25	664	717	729	781	756	717	660	597	510	391	723	648	681
	0.30	686	740	761	803	772	735	675	615	525	405	747	664	701
	0.35	692	743	769	826	783	747	687	626	537	416	757	676	712
	0.40	695	763	812	850	795	760	700	640	550	431	780	689	729
0.73	0.20	669	710	722	768	750	715	655	595	510	390	717	645	677
	0.25	675	731	741	792	767	732	672	609	525	401	735	661	693
	0.30	691	760	767	817	785	750	690	625	542	425	759	678	714
	0.35	694	767	780	838	795	758	700	636	553	430	770	688	724
	0.40	705	775	825	860	805	765	710	650	568	440	791	699	740



The average temperature in the bed varied between 675 to 782°C for village rice husk gasification and 680 to 791°C for sawdust gasification depending upon the operating conditions, i.e. the fluidization velocity and the equivalence ratio. At any fluidization velocity the average bed temperature varied by about 100-110°C. The temperature variation in a downdraft gasifier is, however, very large, e.g. 300-450°C (Sharma, 1988, Mansaray et al., 1999). Downdraft and updraft gasifiers normally experience the hot spots at different points due to stagnation of particles. However, the fluidized bed gasifier does not experience this problem, except at low equivalence ratio, when bridging of the biomass occurs in the bed. The bed temperature variation observed in the present study is in contrast with those observed by different investigators (Boateng et al., 1992; Narvaez et al., 1996) in fluidized bed gasifiers using different biomass. These investigators have reported uniform temperature in the bed, which was heated externally. In the present study, no external heating of the bed is done and the air enters the bed under ambient conditions. The drying and pyrolysis (devolatilization) processes are endothermic while gasification is an exothermic process. The biomass is also fed directly into the bed. Due to this the temperature shows an increasing trend upto 200 mm above the distributor plate and thereafter decreases linearly. The linear variation continues uptill the free board region. The average free board temperature in the present experiments varied between 596°C to 651°C for the VRH and 599 to 699°C for the SD for the full range of equivalence ratio and the fluidization velocity. Maintenance of high free board temperature facilitates higher reaction rates and a shift in the equilibrium value of some gasification reactions, e.g. the homogeneous water gas shift reaction (Schoeters et al., 1989):



Schoeters et al. (1989) have shown the effect of free board temperature on the equilibrium constant for wood shavings and refuse derived fuel (RDF), and in turn on

the high heating value of the produced gas. Since the above reaction is exothermic, the high heating value decreases as the free board temperature increases.

The average free board temperatures are around 79 to 131°C and 81 to 92°C lower than the average bed temperatures for VRH and SD, respectively, for the fluidizing velocities and equivalence ratios employed in the experiments. The lower temperatures in TDS and at the sampling port may be due to endothermic reactions and/or heat losses to the outside environment.

As can be seen, the temperature at any point along the gasifier increases as the equivalence ratio is increased. Similarly, with increase in the fluidization velocity, the temperatures increase. This increase in temperature is due to increase in the rate of exothermic reactions due to larger availability of oxygen per unit mass of the biomass. Increase in fluidization velocity also increased the mixing, which resulted in the increased rate of exothermic reactions thus releasing higher energy.

The lower and upper temperature limits in the biomass gasifier are dictated by the conditions of complete carbon conversion and the ash deformation (and fusion) temperatures. As seen from Table 4.4.2(b), the ash deformation and fusion temperatures are, 1250 and 1400°C for VRH and 1350 and >1400°C for SD, respectively. The temperatures recorded along the gasifier indicated that the higher limit of temperature could nowhere reach. The lower temperature mainly depends upon the elemental composition of the biomass and the equivalence ratio (and/or fluidization velocity). For rice husk, Xu et al. (1985) have suggested this temperature to be 700°C for an ER of 0.2, and that it decreases from 700°C with the increase in ER. Below this temperature, part of the carbon in the biomass remains unconverted/unburnt and accumulates in the reactor, resulting in lower gasifier efficiencies and lower concentration of fuel gases in the produced gas.

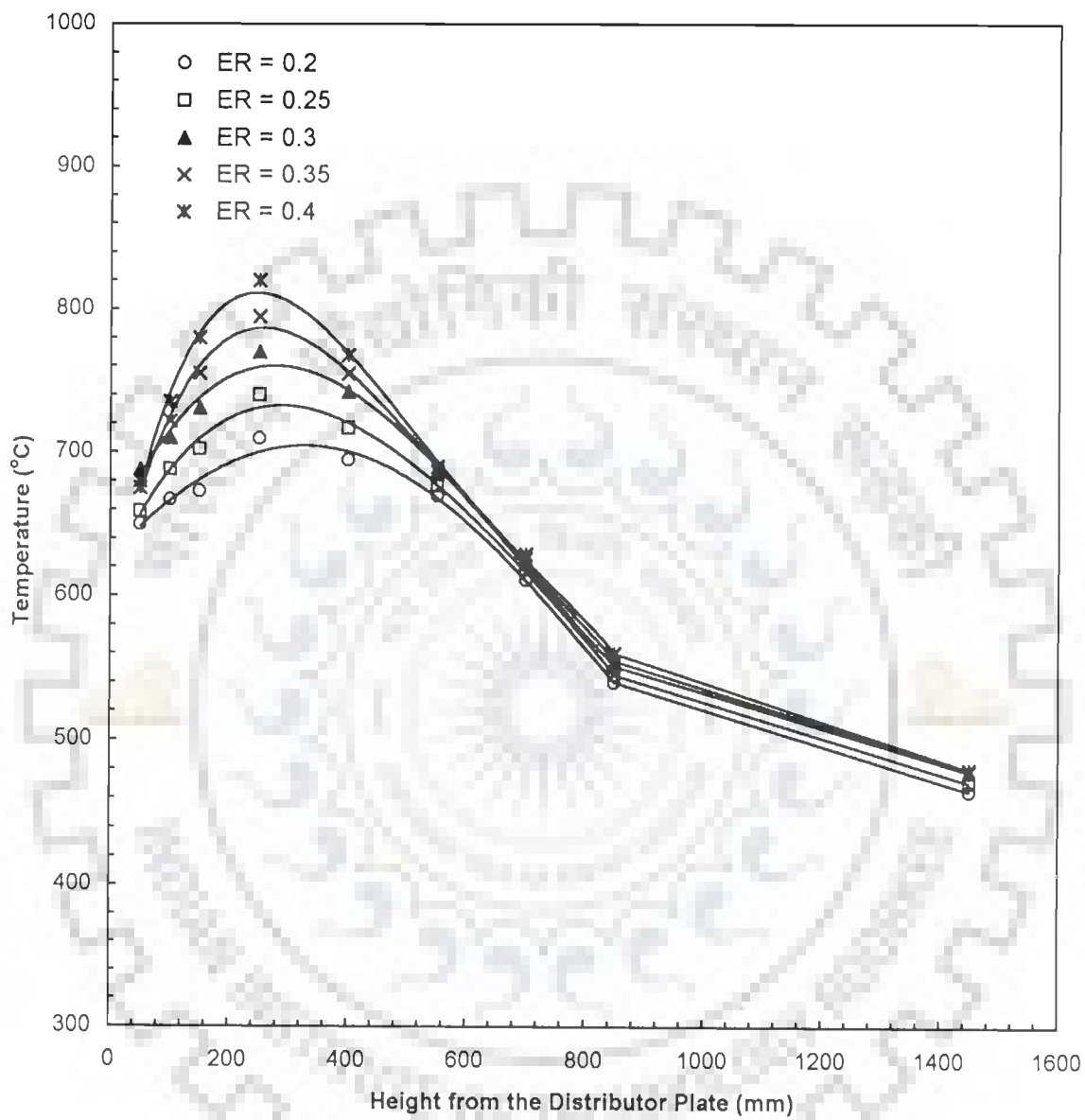


**Fig. 4.4.1(a) : Temperature Profile of the Fluidized Bed Gasifier**

**Feed Stock : Village Rice Husk**

Fluidization Air Velocity =  $0.53 \text{ ms}^{-1}$

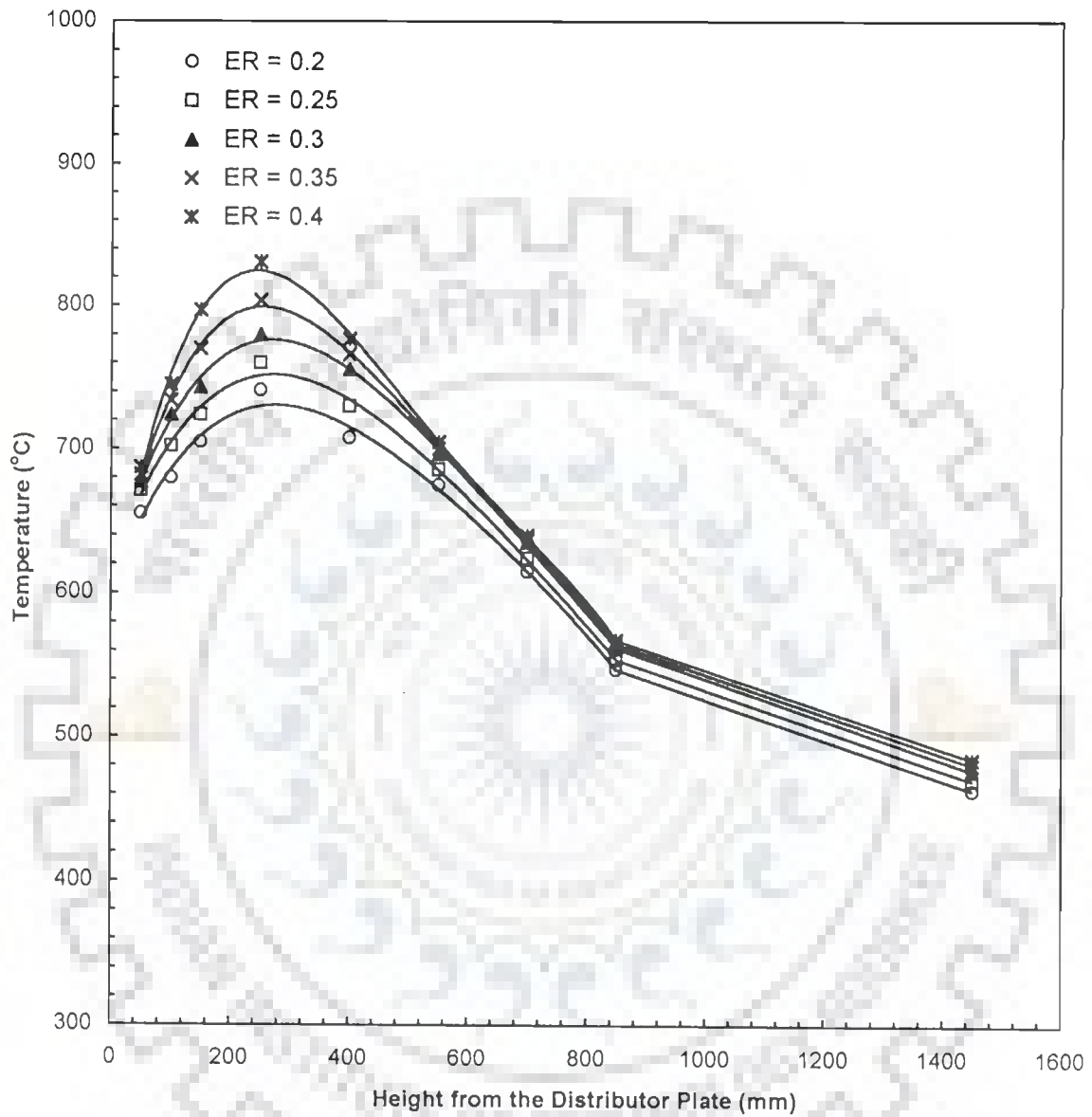


**Fig. 4.4.1(b) : Temperature Profile of the Fluidized Bed Gasifier**

**Feed Stock : Village Rice Husk**

Fluidization Air Velocity =  $0.59 \text{ ms}^{-1}$

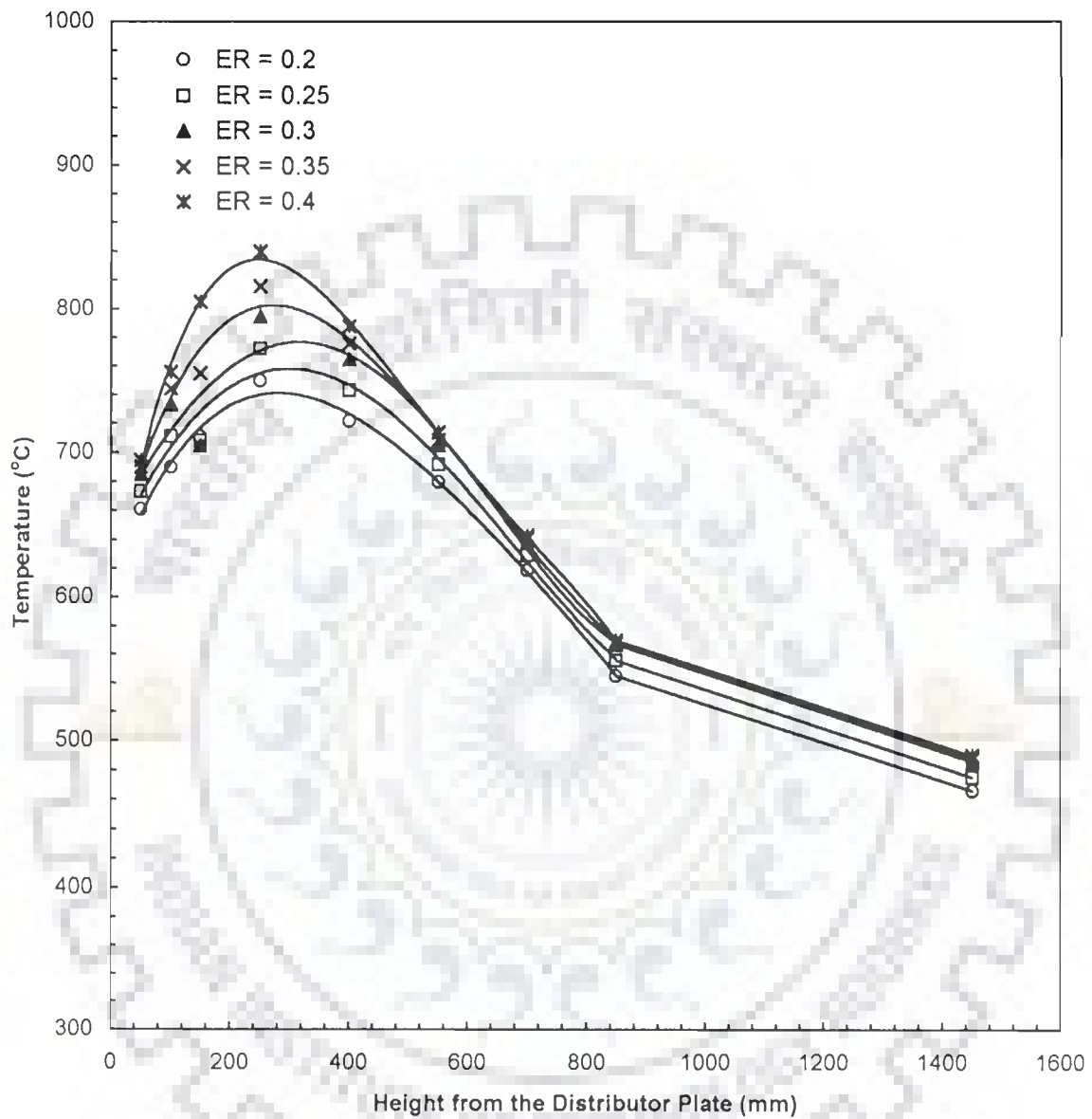


**Fig. 4.4.1(c) : Temperature Profile of the Fluidized Bed Gasifier**

**Feed Stock : Village Rice Husk**

Fluidization Air Velocity =  $0.68 \text{ ms}^{-1}$

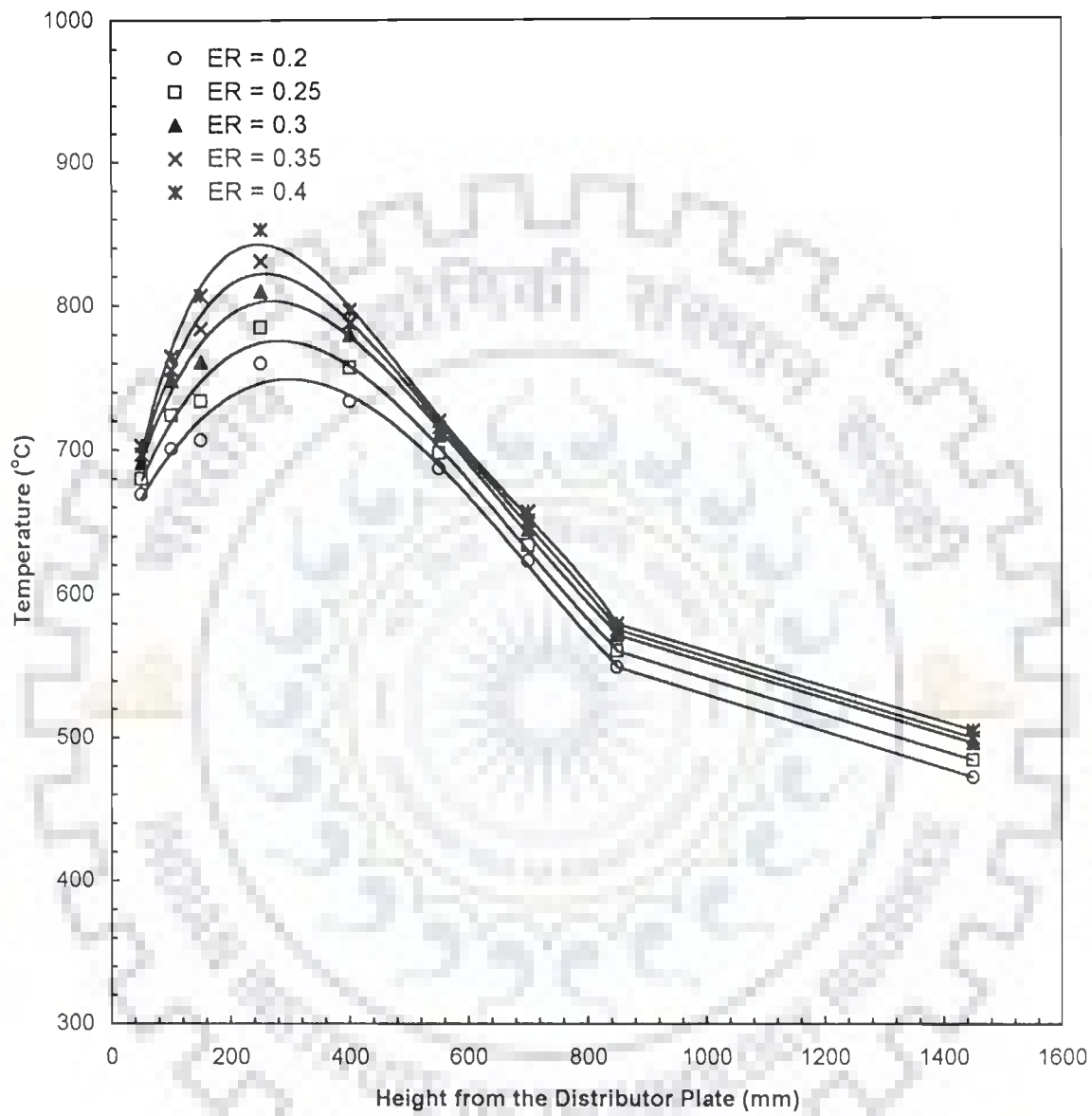


**Fig. 4.4.1(d) : Temperature Profile of the Fluidized Bed Gasifier**

**Feed Stock : Village Rice Husk**

Fluidization Air Velocity =  $0.73 \text{ ms}^{-1}$

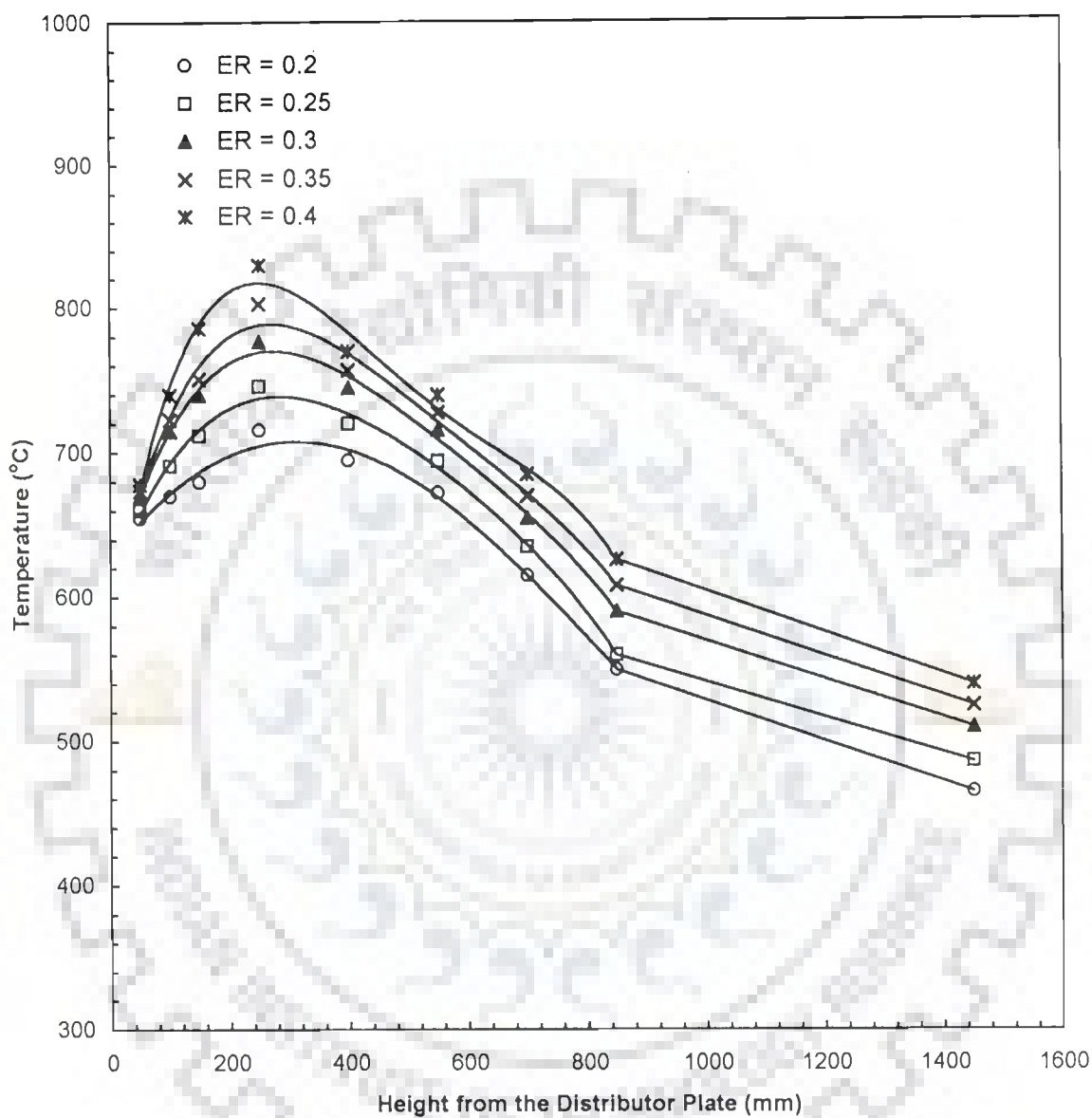


**Fig. 4.4.2(a) : Temperature Profile of the Fluidized Bed Gasifier**

**Feed Stock : Sawdust**

Fluidization Air Velocity =  $0.53 \text{ ms}^{-1}$

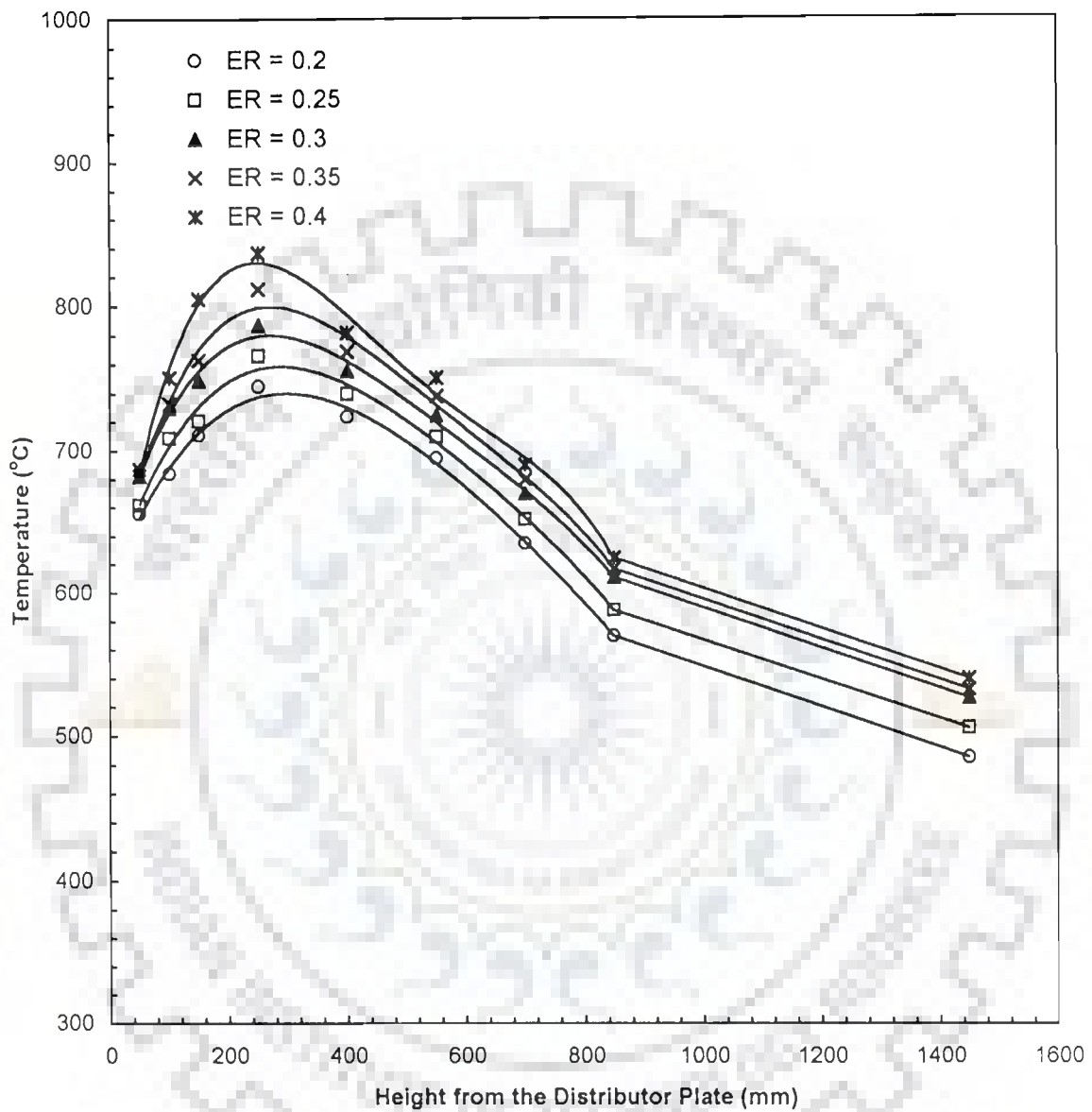


**Fig. 4.4.2(b) : Temperature Profile of the Fluidized Bed Gasifier**

**Feed Stock : Sawdust**

Fluidization Air Velocity =  $0.59 \text{ ms}^{-1}$



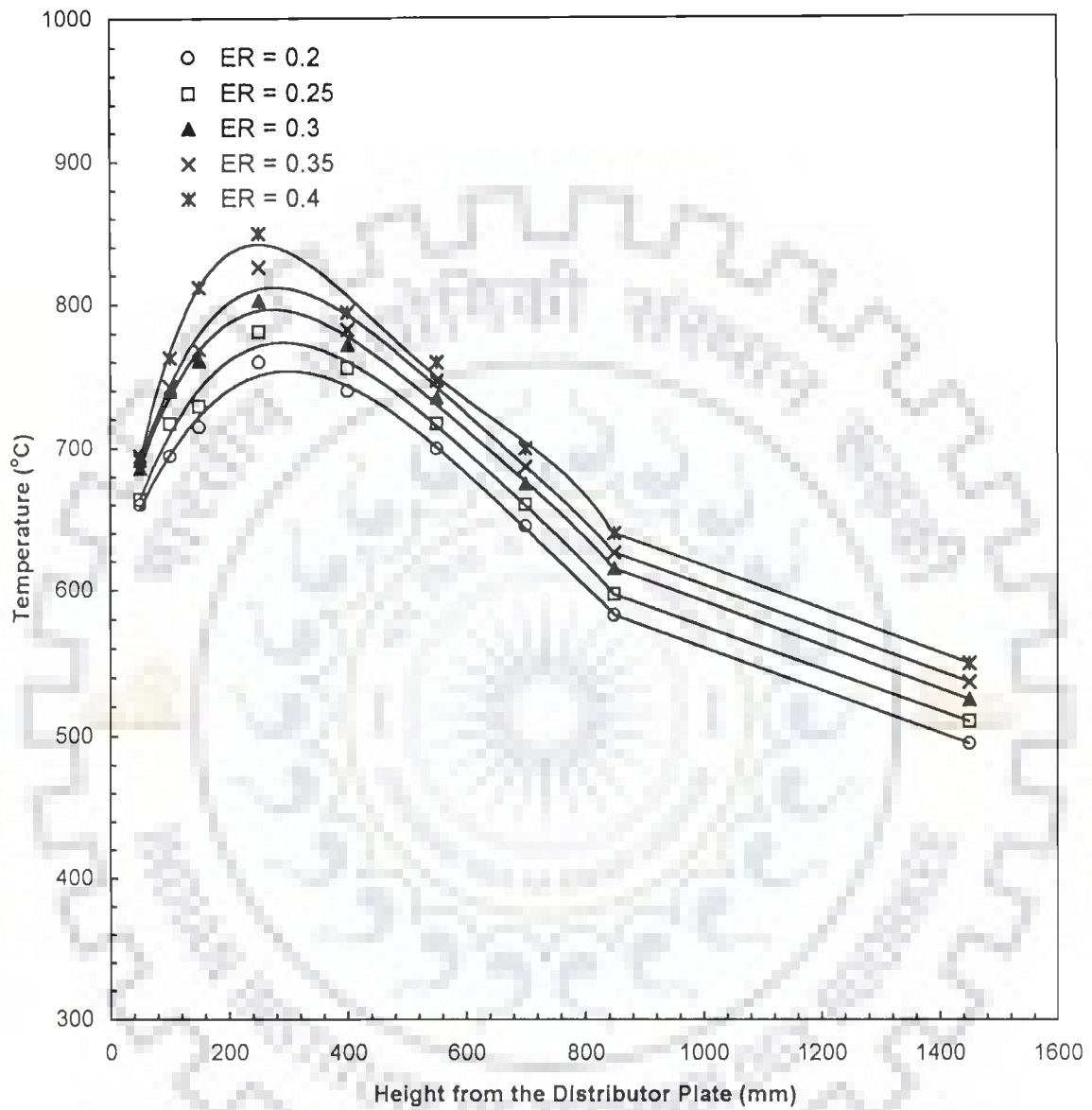
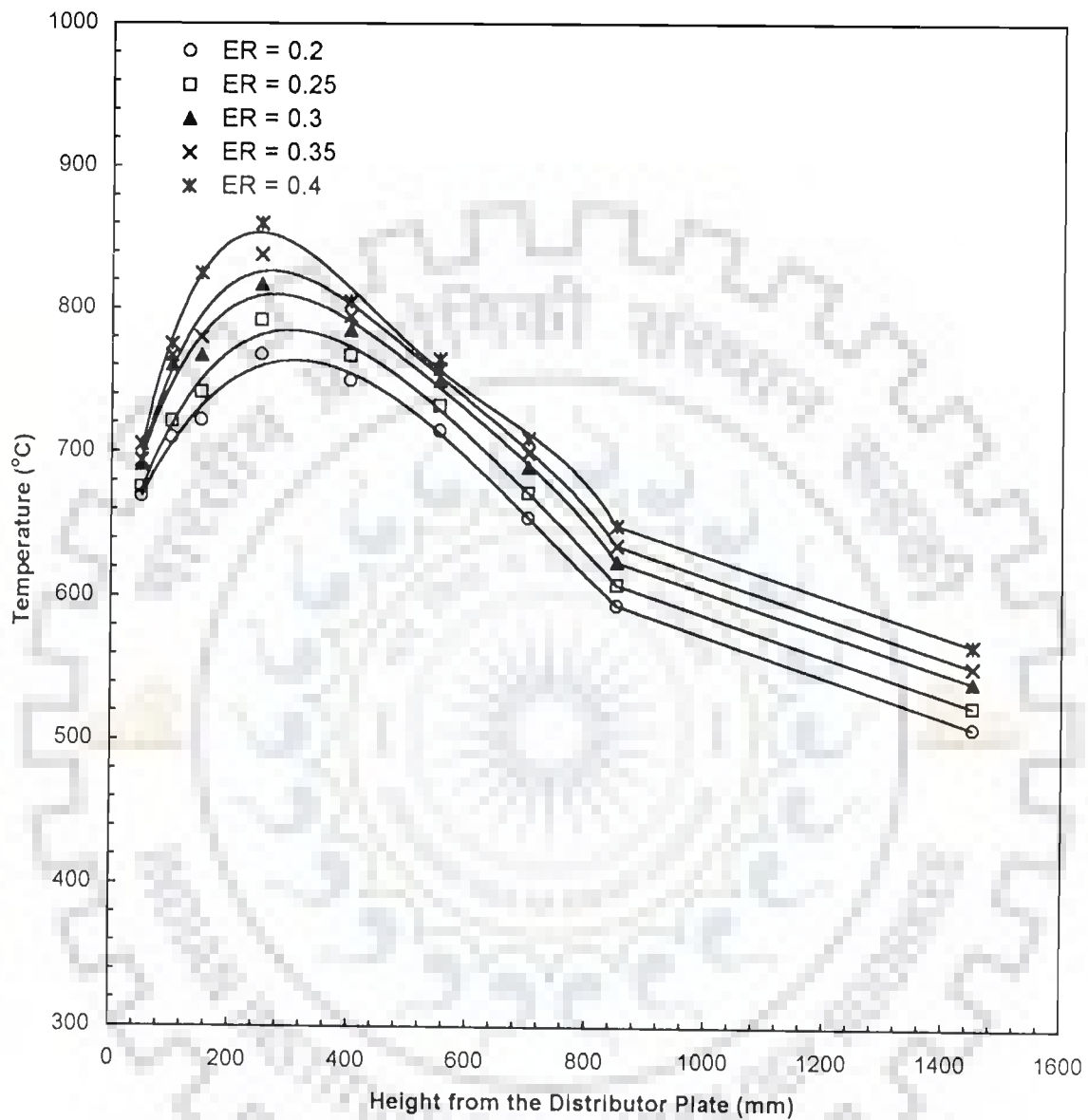


Fig. 4.4.2(c) : Temperature Profile of the Fluidized Bed Gasifier

Feed Stock : Sawdust

Fluidization Air Velocity =  $0.68 \text{ ms}^{-1}$



**Fig. 4.4.2(d) : Temperature Profile of the Fluidized Bed Gasifier**

**Feed Stock : Sawdust**

Fluidization Air Velocity =  $0.73 \text{ ms}^{-1}$

#### 4.4.3.2 Gas Composition

The average composition of the gas produced from village rice husk (VRH) and sawdust (SD) is given in Tables 4.4.4(a) and 4.4.4(b), respectively. These are also plotted in Figs. 4.4.3 (a-d) and 4.4.4 (a-d) for VRH and SD, respectively. From the tables, it is found that among the fuel gases, CO had the highest concentration (11.2-19.4% for VRH and 12.8 to 19.9% for SD, on dry basis by volume), followed by hydrogen (2.7-2.8% for VRH; 3.1 – 4.3 % for SD), methane (1.5-2.3% for VRH; 2.0-2.7% for SD). The other fuel gases,  $C_2H_m$  are found in much lower quantity (0.5-0.9% for VRH; 0.3-0.7% for SD).  $CO_2$  was found to vary between 14.1 to 17.4% for VRH and 13.2 to 17.2% for SD.

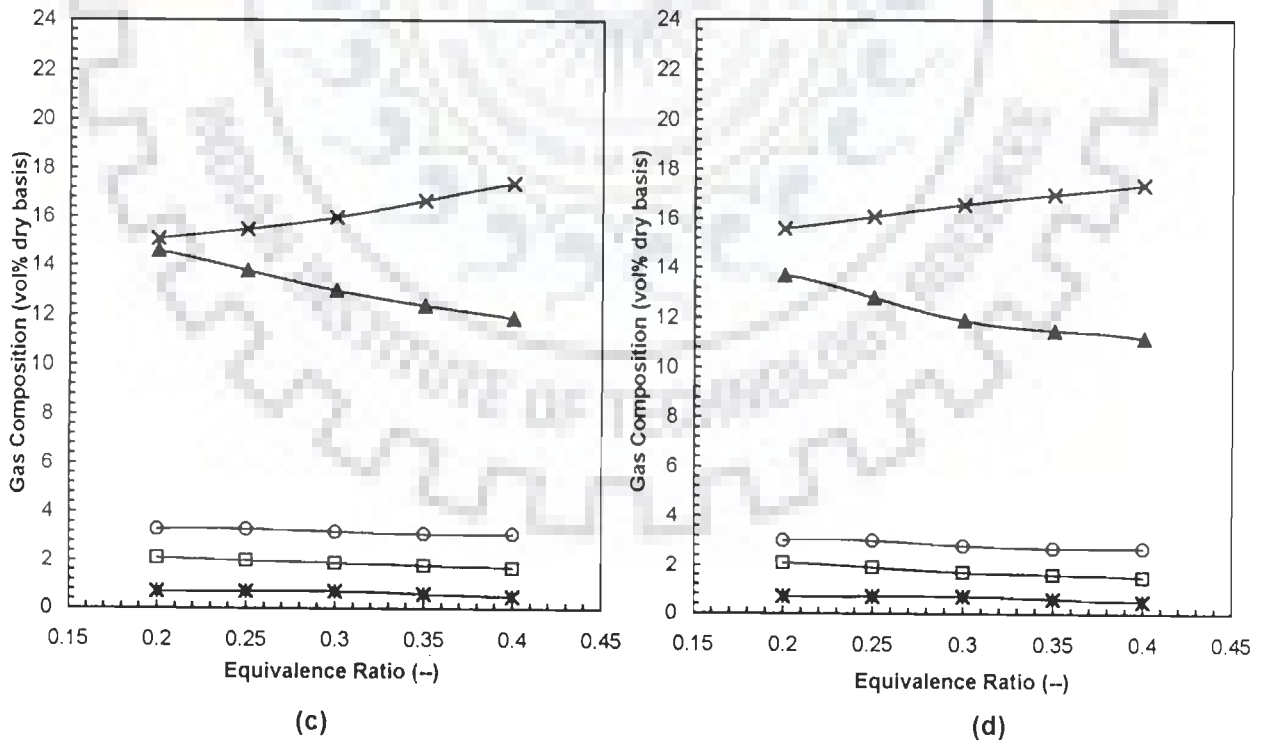
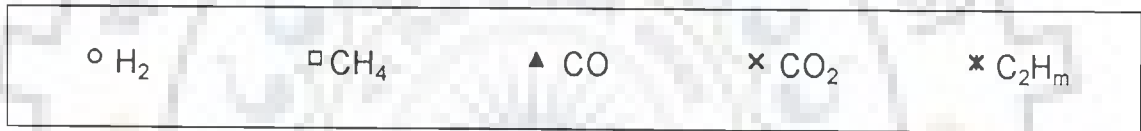
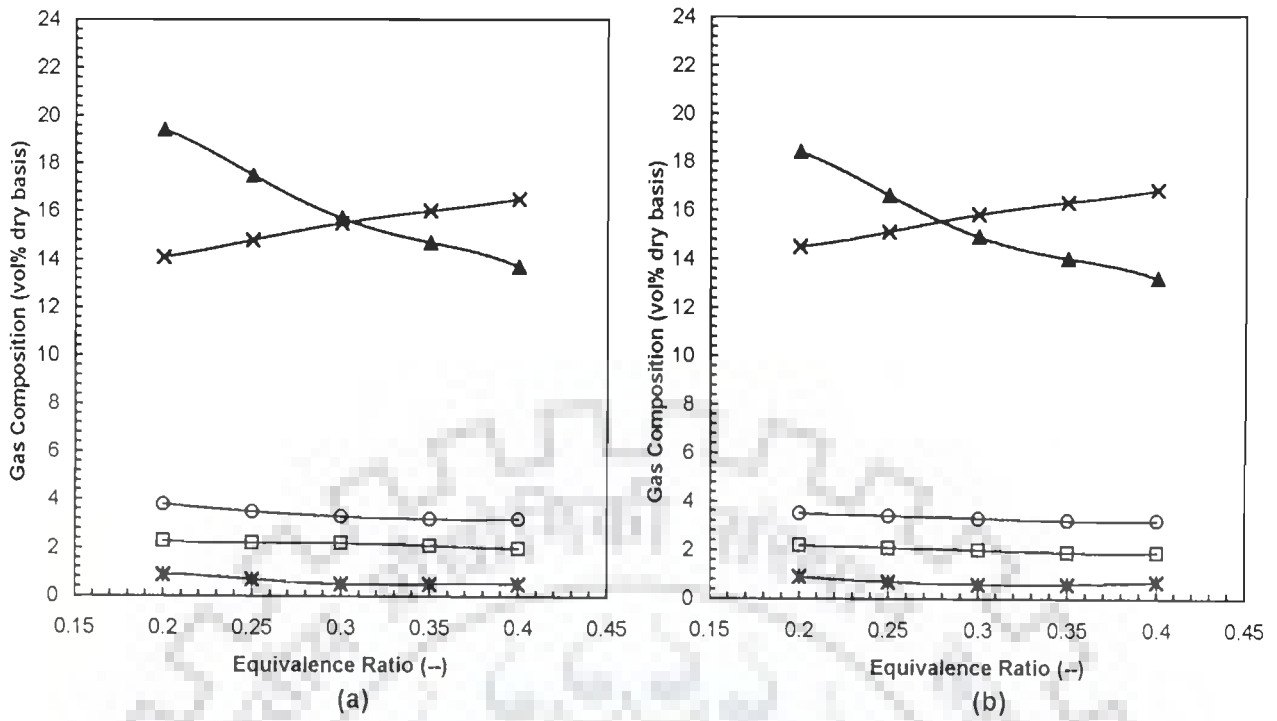
Figs. 4.4.3 and 4.4.4 show the variation in composition of fuel gases and  $CO_2$  with the equivalence ratio (ER) for different fluidization velocities. The general trends of the compositional variation for VRH and SD are found to be similar for all the gases. It is noted that as the ER increased,  $CO_2$  concentration also increased, whereas the concentrations of fuel gases, viz., CO,  $H_2$ ,  $CH_4$  and  $C_2H_m$  decreased. The decrease in the concentration of CO with the increase in ER is sharp, in the region of ER (0.20-0.40) used in this study. Increase in fluidization also decreases the concentration of fuel gases and increases the concentration of  $CO_2$  at any equivalence ratio (see Tables 4.4.4(a) and 4.4.4(b)). Increase in  $CO_2$  is due to the increase in degree of combustion at higher equivalence ratio and/or higher air fluidization velocity. At increased ER and/or air velocity, oxygen availability to the biomass and char are increased and thus more char is burned to form  $CO_2$  at the expense of CO,  $H_2$ ,  $CH_4$  and  $C_2H_m$ . Increase in ER and/or air velocity also increases nitrogen concentration in the gas [See Tables 4.4.4(a) and 4.4.4(b)]. As the air fluidization velocity increases, residence time for the char in the gasifier decreases, thereby losing some of the energy in the char, which would otherwise be in the form of fuel gases. It is found that the equivalence ratio of 0.20 and the air fluidization velocity of  $0.53 \text{ ms}^{-1}$  is the best. Incidentally, ER = 0.20 is the lowest recommended for air gasification.

**Table 4.4.4(a) : Average Gas Composition of Producer Gas (vol% dry basis)  
Feed Stock: Village Rice Husk**

Fluidization Velocity ( $\text{ms}^{-1}$ )	Equivalence Ratio $\phi$ (-)	H <sub>2</sub>	O <sub>2</sub>	N <sub>2</sub>	CH <sub>4</sub>	CO	CO <sub>2</sub>	C <sub>2</sub> H <sub>m</sub>
0.53	0.20	3.8	1.5	58.0	2.3	19.4	14.1	0.9
	0.25	3.5	1.5	59.8	2.2	17.5	14.8	0.7
	0.30	3.3	1.6	56.8	2.2	15.7	15.5	0.5
	0.35	3.2	1.6	61.9	2.1	14.7	16.0	0.5
	0.40	3.2	1.6	62.5	2.0	13.7	16.5	0.5
0.59	0.20	3.5	1.4	59.1	2.2	18.4	14.5	0.9
	0.25	3.4	1.4	60.7	2.1	16.6	15.1	0.7
	0.30	3.3	1.4	62.0	2.0	14.9	15.8	0.6
	0.35	3.2	1.3	62.7	1.9	14.0	16.3	0.6
	0.40	3.2	1.3	62.9	1.9	13.2	16.8	0.7
0.68	0.20	3.3	1.4	62.8	2.1	14.6	15.1	0.7
	0.25	3.3	1.4	63.3	2.0	13.8	15.5	0.7
	0.30	3.2	1.7	63.6	1.9	13.0	16.0	0.7
	0.35	3.1	1.7	63.7	1.8	12.4	16.7	0.6
	0.40	3.1	1.6	63.8	1.7	11.9	17.4	0.5
0.73	0.20	3.0	1.9	63.0	2.1	13.7	15.6	0.7
	0.25	3.0	1.8	63.7	1.9	12.8	16.1	0.7
	0.30	2.8	1.8	64.5	1.7	11.9	16.6	0.7
	0.35	2.7	1.8	64.8	1.6	11.5	17.0	0.6
	0.40	2.7	1.8	64.9	1.5	11.2	17.4	0.5

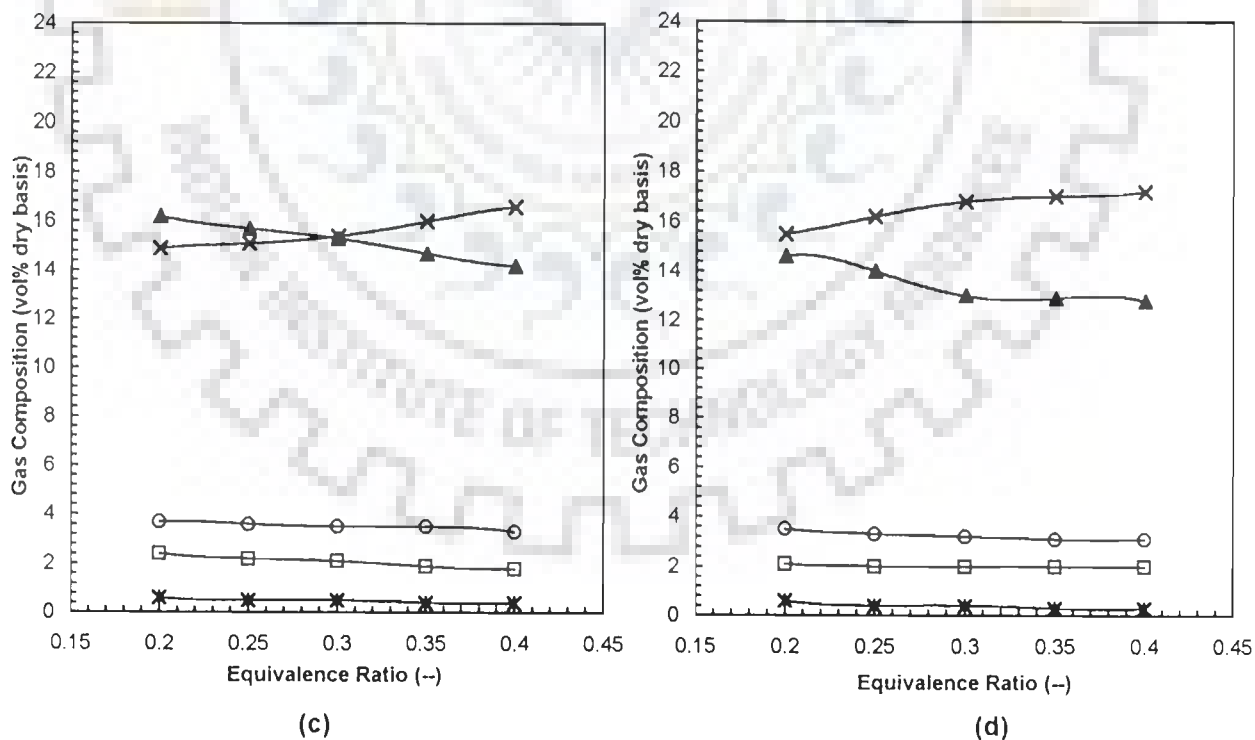
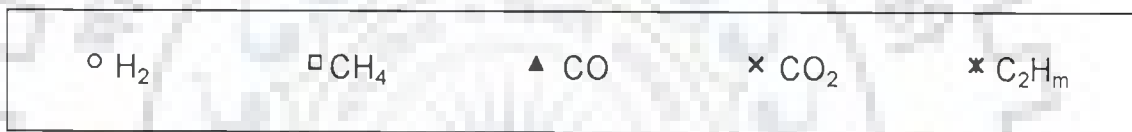
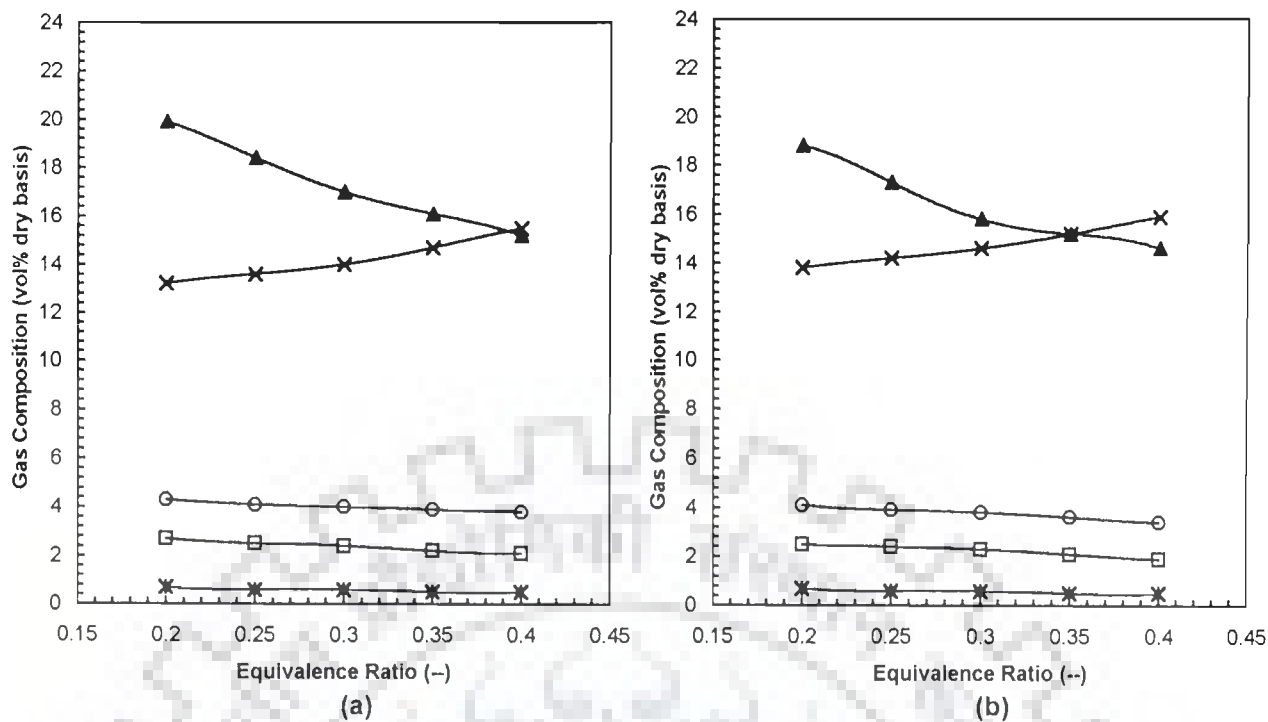
**Table 4.4.4(b) : Average Gas Composition of Producer Gas (vol% dry basis)  
Feed Stock: Sawdust**

Fluidization Velocity (ms <sup>-1</sup> )	Equivalence Ratio $\phi$ (-)	H <sub>2</sub>	O <sub>2</sub>	N <sub>2</sub>	CH <sub>4</sub>	CO	CO <sub>2</sub>	C <sub>2</sub> H <sub>m</sub>
0.53	0.20	4.3	1.2	58.0	2.7	19.9	13.2	0.7
	0.25	4.1	1.2	59.6	2.5	18.4	13.6	0.6
	0.30	4.0	1.3	60.7	2.4	17.0	14.0	0.6
	0.35	3.9	1.3	61.3	2.2	16.1	14.7	0.5
	0.40	3.8	1.5	61.4	2.1	15.2	15.5	0.5
0.59	0.20	4.1	1.4	58.7	2.5	18.8	13.8	0.7
	0.25	3.9	1.4	60.2	2.4	17.3	14.2	0.6
	0.30	3.8	1.5	61.4	2.3	15.8	14.6	0.6
	0.35	3.6	1.4	62.0	2.1	15.2	15.2	0.5
	0.40	3.4	1.4	62.3	1.9	14.6	15.9	0.5
0.68	0.20	3.7	1.5	60.7	2.4	16.2	14.9	0.6
	0.25	3.6	1.5	61.4	2.2	15.7	15.1	0.5
	0.30	3.5	1.7	61.5	2.1	15.3	15.4	0.5
	0.35	3.5	1.7	61.8	1.9	14.7	16.0	0.4
	0.40	3.3	1.8	61.9	1.8	14.2	16.6	0.4
0.73	0.20	3.5	1.5	62.2	2.1	14.6	15.5	0.6
	0.25	3.3	1.7	62.5	2.0	14.0	16.2	0.4
	0.30	3.2	1.7	62.9	2.0	13.0	16.8	0.4
	0.35	3.1	1.8	62.9	2.0	12.9	17.0	0.3
	0.40	3.1	1.8	62.8	2.0	12.8	17.2	0.3



(a) Fluidization Velocity = 0.53 ms<sup>-1</sup>, (b) Fluidization Velocity = 0.59 ms<sup>-1</sup>  
 (c) Fluidization Velocity = 0.68 ms<sup>-1</sup>, (d) Fluidization Velocity = 0.73 ms<sup>-1</sup>

**Fig. 4.4.3 : Variation of Gas Composition with ER and Fluidization Air Velocity  
 Village Rice Husk Gasification**



(a) Fluidization Velocity = 0.53 ms<sup>-1</sup>, (b) Fluidization Velocity = 0.59 ms<sup>-1</sup>  
 (c) Fluidization Velocity = 0.68 ms<sup>-1</sup>, (d) Fluidization Velocity = 0.73 ms<sup>-1</sup>

**Fig. 4.4.4 : Variation of Gas Composition with ER and Fluidization Air Velocity  
 Sawdust Gasification**

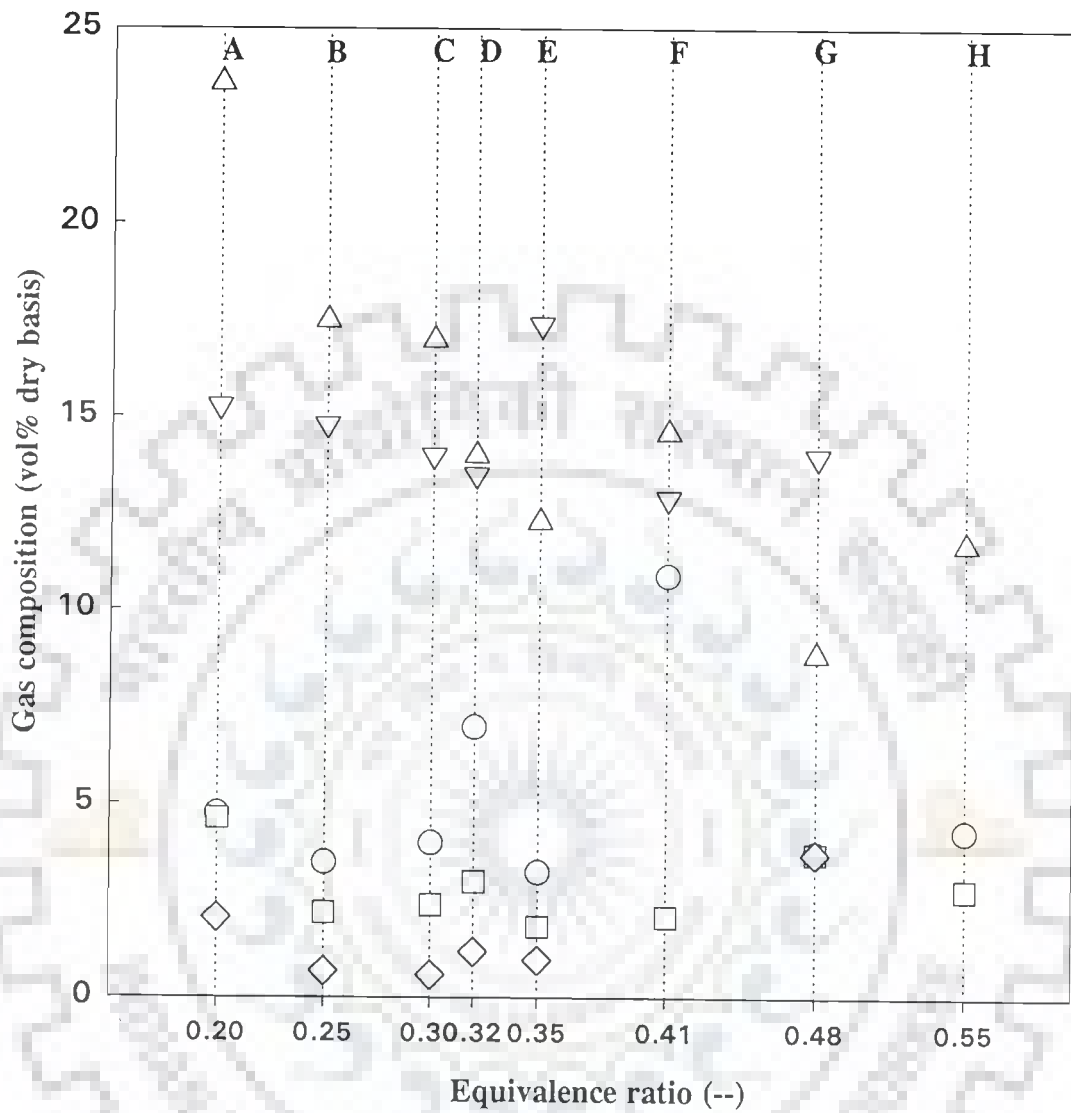


Fig.4.4.5 Comparison of Gas Composition at Different Equivalence Ratios Reported by Different Workers with the Present Work

○ H<sub>2</sub>    □ CH<sub>4</sub>    △ CO    ▽ CO<sub>2</sub>    ◇ C<sub>2</sub>H<sub>m</sub>

A: Ergudenler et al., 1997( Wheat straw)  
 B: Present work ( Village rice husk)  
 C: Present work (Sawdust)  
 D: Narvaez et al., 1996 (Pine sawdust)

E: Mansaray et al., 1999( Rice husk)  
 F: Jiang and Morey., 1992 ( Corn cobs)  
 G: Hartinaiti et al., 1989 ( Rice husk)  
 H: Sanchez and Lora, 1994 (Rice husk)



Desrosiers (1981), Maniatis et al. (1988), Schoeters (1989) Narvaez et al. (1996), Natarajan et al. (1998), Mansaray et al. (1999), and Gil et al. (1999) have shown that the highest concentrations of CO, H<sub>2</sub>, CH<sub>4</sub> and C<sub>2</sub>H<sub>m</sub> and the lowest concentration of O<sub>2</sub> are obtained in the temperature range of 650-750°C. Average bed temperatures in the present study varied between 675 and 782°C for VRH and between 680 and 791°C for sawdust. Narvaez et al. (1996) have graphically presented the variation in gas composition at different ERs for different biomass materials as reported by various researchers (Fig. 4.4.5). However, the effect of fluidization velocity has been ignored in this comparison. Gil et al. (1999) have shown that during pyrolysis of pine (*Pinus pinaster*) wood with 10-12 wt% moisture around 25% H<sub>2</sub> and around 50% CO (by volume on dry basis) was obtained. During air gasification, the concentrations of H<sub>2</sub> dropped to around 12 and 5% at ER = 0.2 and 0.5, respectively, and the concentration of CO dropped to around 20 and 10% at ER = 0.2 and 0.5, respectively. The present experimental results for VRH and SD show consistency with CO composition but give very low values of H<sub>2</sub>. Czernik et al. (1994) reported a value of 9.5 vol% (dry basis) for H<sub>2</sub> using pine sawdust. Higher values of hydrogen in the raw gas were obtained owing to injection of secondary air into the free board region and the use of calcined dolomite catalysts in the bed for the cracking of tar.

#### 4.4.3.3 Gas Higher Heating Value (HHV)

Higher heating values of the gas produced from VRH and SD are presented in Table 4.4.5 and plotted in Figs. 4.4.6(a) and 4.4.6(b), respectively. The HHV for SD is found to be higher than that for VRH at any ER and fluidization velocity. The higher heating value for VRH ranged from 2.93 to 3.85 MJNm<sup>-3</sup> between ER of 0.2 to 0.4 at a fluidization velocity of 0.53 ms<sup>-1</sup>. For the similar operating conditions, SD gave HHV in the range of 3.24 to 4.14 MJNm<sup>-3</sup>. Figs. 4.4.6(a) and 4.4.6(b) reveal that the HHV decreases with the increase of ER and/or fluidization velocity, giving almost a linear

**Table 4.4.5 : Higher Heating Value of the Gas Produced**

Fluidization Velocity (ms <sup>-1</sup> )	Equivalence Ratio (-)	Higher Heating Value (MJNm <sup>-3</sup> )	
		Sawdust	Village Rice Husk
0.53	0.20	4.14	3.85
	0.25	3.84	3.53
	0.30	3.61	3.26
	0.35	3.40	3.10
	0.40	3.24	2.93
0.59	0.20	3.89	3.64
	0.25	3.64	3.36
	0.30	3.39	3.10
	0.35	3.21	2.93
	0.40	3.04	2.83
0.68	0.20	3.47	3.10
	0.25	3.32	2.96
	0.30	3.21	2.79
	0.35	3.06	2.68
	0.40	2.93	2.57
0.73	0.20	3.12	2.95
	0.25	2.97	2.75
	0.30	2.84	2.53
	0.35	2.82	2.43
	0.40	2.81	2.35

Note : Nm<sup>-3</sup> = per unit volume (normal)

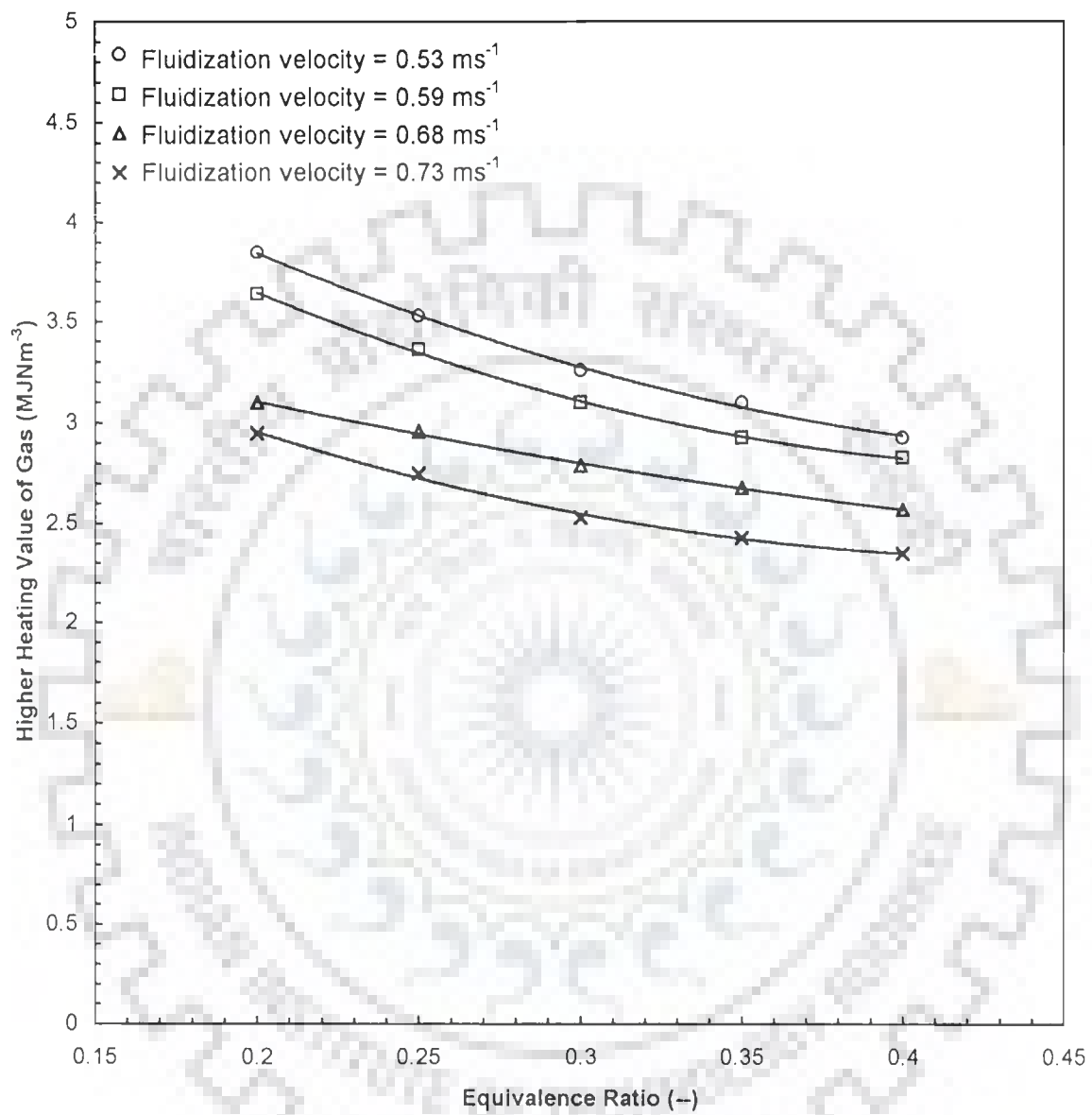


**Fig. 4.4.6(a) : Variation of Product Gas Heating Value with Equivalence Ratio and Fluidization Air Velocity**

**Feed Stock : Village Rice Husk**

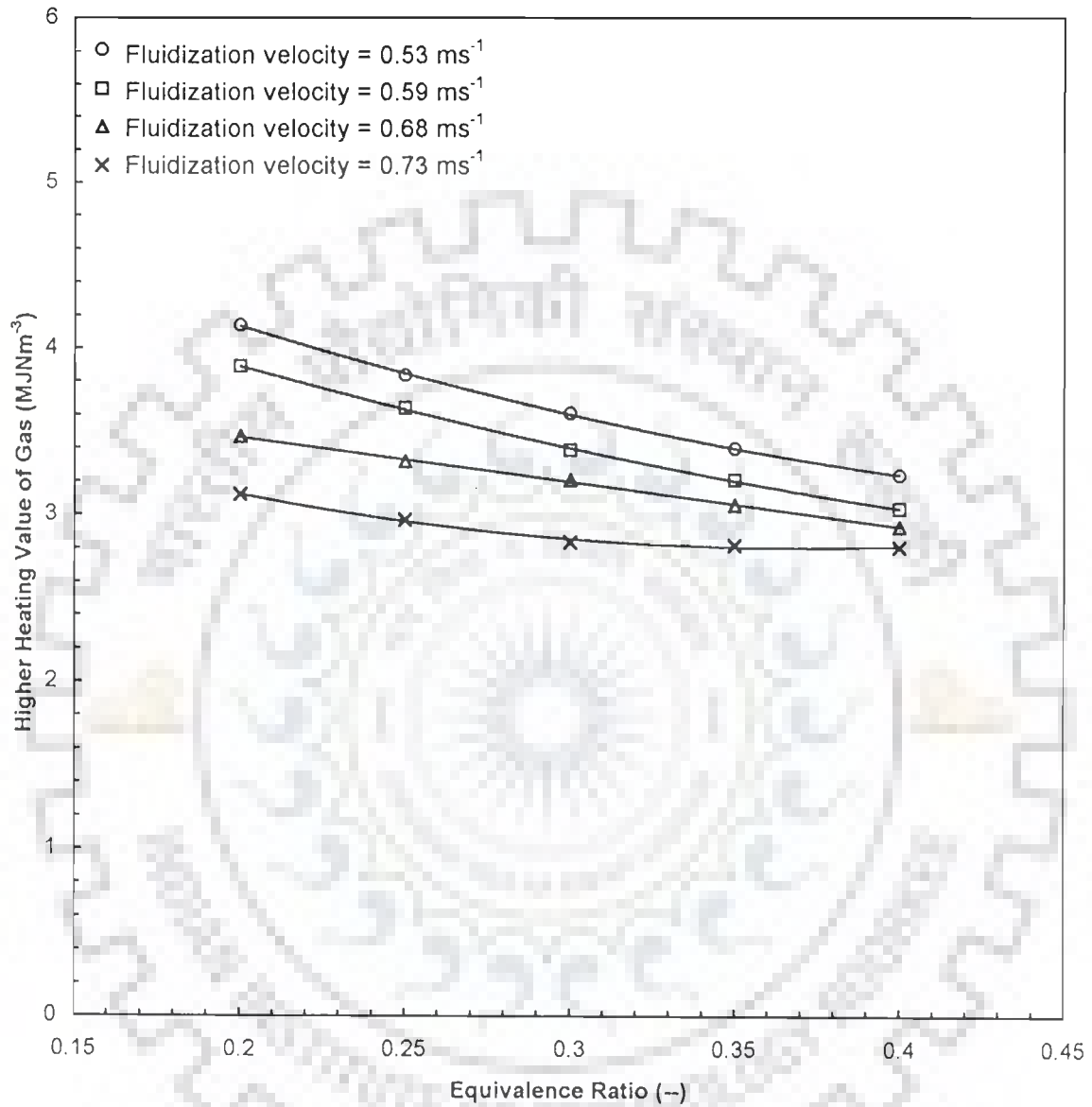


**Fig. 4.4.6(b) : Variation of Product Gas Heating Value with Equivalence Ratio and Fluidization Air Velocity**

**Feed Stock : Sawdust**

**Table 4.4.6 : Comparison of Higher Heating Value of the Gas Reported  
by Different Workers**

Feedstock	Gasifying Medium	HHV (MJNm <sup>-3</sup> )	Reference
Sawdust	Air	2.81-4.14	Present study
Village Rice husk	Air	2.35-3.85	Present study
Wood waste	Air + O <sub>2</sub>	1.4-8.0	Black et al. (1979)
Beach wood	Air	5.0-6.6	van den Aarsen et al.(1982)
Coconut shell	Air	3.4-6.2	Maniatis (1990)
Palm oil shell	Air	3.5-6.2	Maniatis (1990)
Rice hull	Steam	11.1-12.1	Boateng et al. (1992)
Wheat straw	Air	5.0-7.3	Ergudenler and Ghaly (1992)
Wood waste	Air	5.2	Czernik et al. (1994)
Municipal solid waste	Air	5.4	Czernik et al. (1994)
Rice husk	Air	3.1-5.0	Mansaray (1999)

Note : Nm<sup>-3</sup> = per unit volume (normal)

variation with ER at for any fluidization velocity. With the increase in fluidization velocity at any ER, the HHV decreases. With the increase in fluidization velocity and/or ER, the nitrogen content of the gas increases and the concentrations of methane and  $C_2H_m$  decrease. Nitrogen dilutes the raw product gas and reduces its energy content due to extraction of heat as sensible heat. The values of HHV reported by different authors for different feedstocks and gasifying media, alongwith the values from the present study are shown in Table 4.4.6. Some of the literature values, though from similar scale of operation, were obtained from experiments with external heat sources and the unburnt solid recycling mechanisms. Maniatis (1990) used an external heat source for heating the bed and the free board, while Aarsen et al. (1982) reintroduced coarse particles into the reactor bed after their separation from the gas stream.

Raman et al. (1980) and Walawender et al. (1985a) have used a radiant burner and jacketed heater to provide supplemental heat. Sakoda et al. (1981) used an electrical furnace to control the temperature in the bed.

#### 4.4.3.4 Gas Yield

The gas yields (amount of gas produced per unit mass of biomass) as obtained from experiments have been reported at 25°C and 1 atm pressure. The results are presented in Tables 4.4.7(a) and 4.4.7(b) for VRH and SD, respectively, for different fluidization velocities and equivalence ratios. Figs. 4.4.7(a) and 4.4.7(b) present gas yields as a function of ER for different fluidization velocities, for VRH and SD, respectively. The gas yield increased with increasing ER upto an ER = 0.35 and thereafter became almost constant upto ER=0.40, for any fluidizing air velocity for both VRH and SD. With increase in fluidization velocity, gas yield decreased, although only marginally. The effect of ER on the gas yield may be due to the greater production of gas in the initial biomass devolatilization, which is accelerated at higher ER, and to the endothermic reactions of gasification of char (Mansaray et al., 1999). At higher

**Table 4.4.7(a) : Gas Production Rate, Normalized Gas Production Rate, & Gas Yield  
Feedstock: Village Rice Husk**

Fluidization Velocity ( $\text{ms}^{-1}$ )	Equivalence Ratio, $\phi$ (-)	Density of Hot Gas ( $\text{kgm}^{-3}$ )	Temp. of Gas ( $^{\circ}\text{K}$ )	Feed Rate ( $\text{kgs}^{-1}$ )	Gas Production Rate ( $\text{m}^3\text{s}^{-1}$ )	Normalized Gas Production Rate ( $\text{Nm}^3\text{s}^{-1}$ )	Gas Yield ( $\text{Nm}^3\text{kg}^{-1}$ )	Gas Yield ( $\text{Nm}^3\text{kg}^{-1}\text{DAF}$ )
0.53	0.20	0.59	588	0.00486	0.01247	0.006321	1.30	1.90
	0.25	0.59	595	0.00388	0.01043	0.005227	1.34	2.00
	0.30	0.56	603	0.00319	0.00905	0.004474	1.40	2.08
	0.35	0.59	607	0.00277	0.00836	0.004108	1.48	2.13
	0.40	0.59	603	0.00250	0.00788	0.003899	1.55	2.14
0.59	0.20	0.60	589	0.00541	0.01382	0.006997	1.29	1.87
	0.25	0.59	594	0.00438	0.01150	0.005769	1.31	1.95
	0.30	0.59	602	0.00361	0.01005	0.004978	1.37	2.02
	0.35	0.59	606	0.00313	0.00925	0.004549	1.45	2.09
	0.40	0.59	609	0.00277	0.00836	0.004094	1.47	2.10
0.68	0.20	0.60	588	0.00625	0.01588	0.008052	1.28	1.83
	0.25	0.59	598	0.00500	0.01300	0.006481	1.29	1.91
	0.30	0.59	608	0.00416	0.01150	0.005636	1.35	1.98
	0.35	0.59	611	0.00355	0.01000	0.004905	1.38	2.05
	0.40	0.59	613	0.00311	0.00925	0.004497	1.44	2.06
0.73	0.20	0.60	593	0.00666	0.01650	0.008339	1.25	1.80
	0.25	0.59	605	0.00536	0.01422	0.007000	1.30	1.88
	0.30	0.58	618	0.00444	0.01226	0.005913	1.33	1.95
	0.35	0.58	623	0.00383	0.01089	0.005211	1.36	2.00
	0.40	0.57	628	0.00333	0.00983	0.004664	1.40	2.01

Table 4.4.7(b) : Gas Production Rate, Normalized Gas Production Rate, & Gas Yield  
Feedstock: Sawdust

Fluidization Velocity (ms <sup>-1</sup> )	Equivalence Ratio, $\phi$ (-)	Density of Hot Gas (kgm <sup>-3</sup> )	Temp. of Gas (°K)	Feed Rate (kgs <sup>-1</sup> )	Gas Production Rate (m <sup>3</sup> s <sup>-1</sup> )	Normalized Gas Production Rate (Nm <sup>3</sup> s <sup>-1</sup> )	Gas Yield (Nm <sup>3</sup> kg <sup>-1</sup> )	Gas Yield (Nm <sup>3</sup> kg <sup>-1</sup> DAF)
0.53	0.20	0.55	623	0.00458	0.01582	0.007568	1.65	1.96
	0.25	0.53	641	0.00366	0.01348	0.006269	1.71	2.03
	0.30	0.52	663	0.00305	0.01188	0.005341	1.75	2.08
	0.35	0.51	680	0.00263	0.01081	0.004740	1.80	2.13
	0.40	0.50	698	0.00227	0.00958	0.004090	1.80	2.13
0.59	0.20	0.54	638	0.00513	0.01797	0.008394	1.63	1.94
	0.25	0.53	659	0.00408	0.01529	0.006915	1.69	2.01
	0.30	0.51	683	0.00338	0.01341	0.005854	1.73	2.05
	0.35	0.50	686	0.00291	0.01173	0.005097	1.75	2.08
	0.40	0.51	693	0.00255	0.01039	0.004469	1.75	2.08
0.68	0.20	0.54	653	0.00583	0.02061	0.009400	1.61	1.91
	0.25	0.53	664	0.00466	0.01741	0.007813	1.67	1.99
	0.30	0.52	678	0.00388	0.01514	0.006658	1.71	2.03
	0.35	0.51	689	0.00333	0.01307	0.005656	1.69	2.01
	0.40	0.51	699	0.00291	0.01161	0.004953	1.70	2.02
0.73	0.20	0.54	663	0.00625	0.02201	0.009890	1.58	1.88
	0.25	0.52	674	0.00500	0.01855	0.008203	1.64	1.95
	0.30	0.51	698	0.00416	0.01633	0.006974	1.67	1.99
	0.35	0.51	703	0.00358	0.01407	0.005965	1.66	1.98
	0.40	0.50	713	0.00311	0.01249	0.005221	1.67	1.99



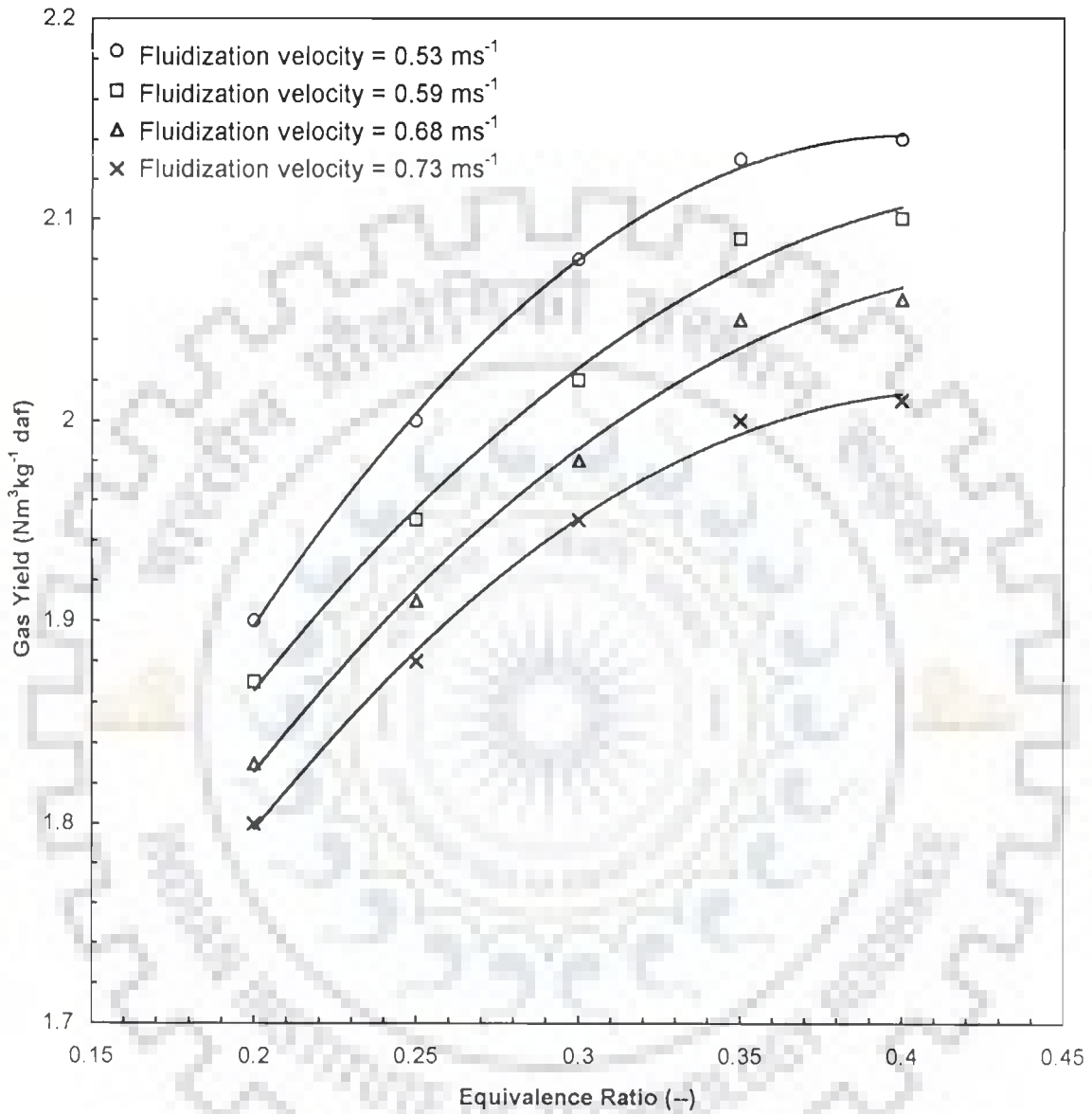


**Fig. 4.4.7(a) : Variation of Gas Yield with Equivalence Ratio and Fluidization Air Velocity**

**Feed Stock : Village Rice Husk**

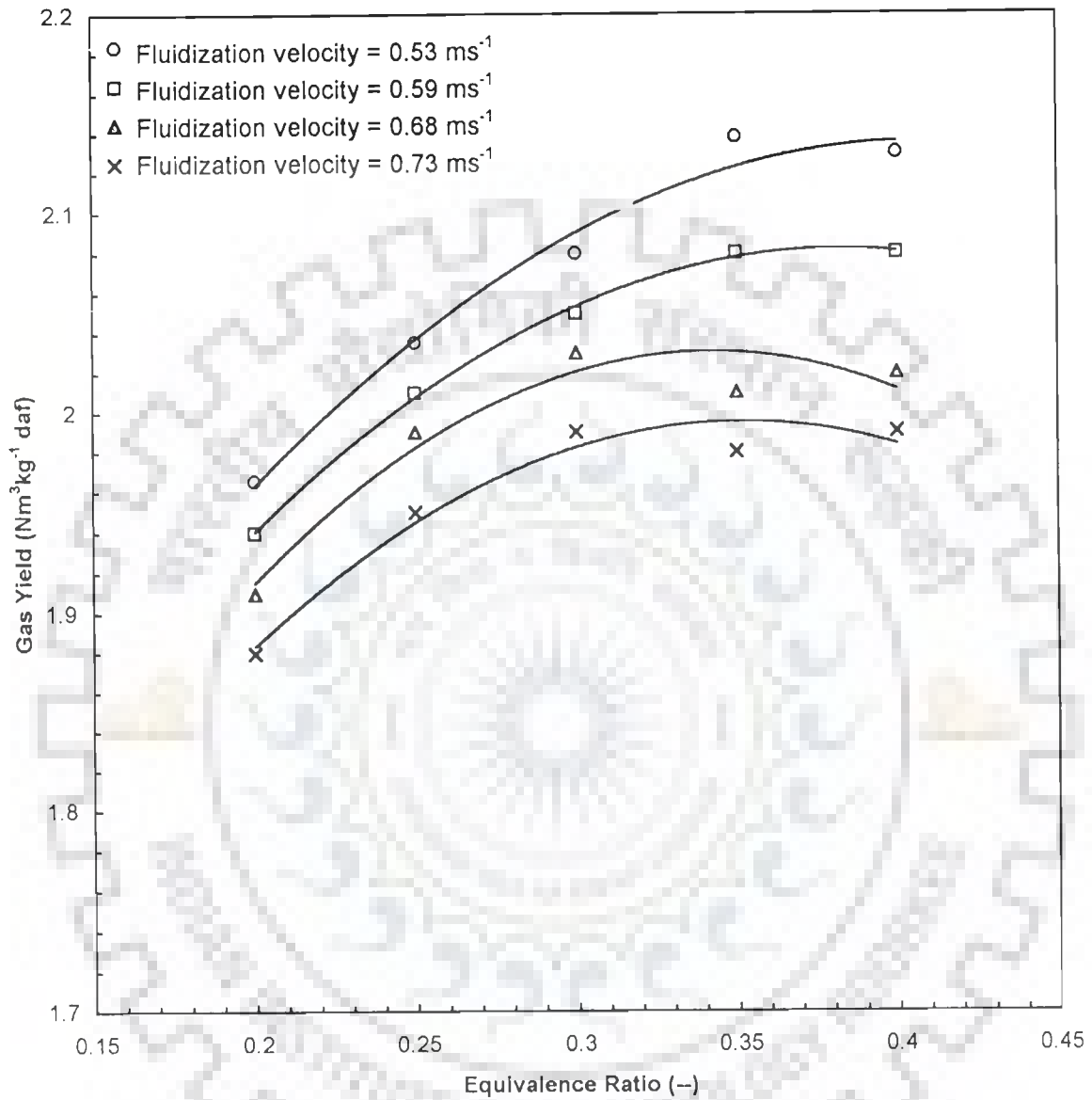


**Fig. 4.4.7(b) : Variation of Gas Yield with Equivalence Ratio and Fluidization Air Velocity**

**Feed Stock : Sawdust**

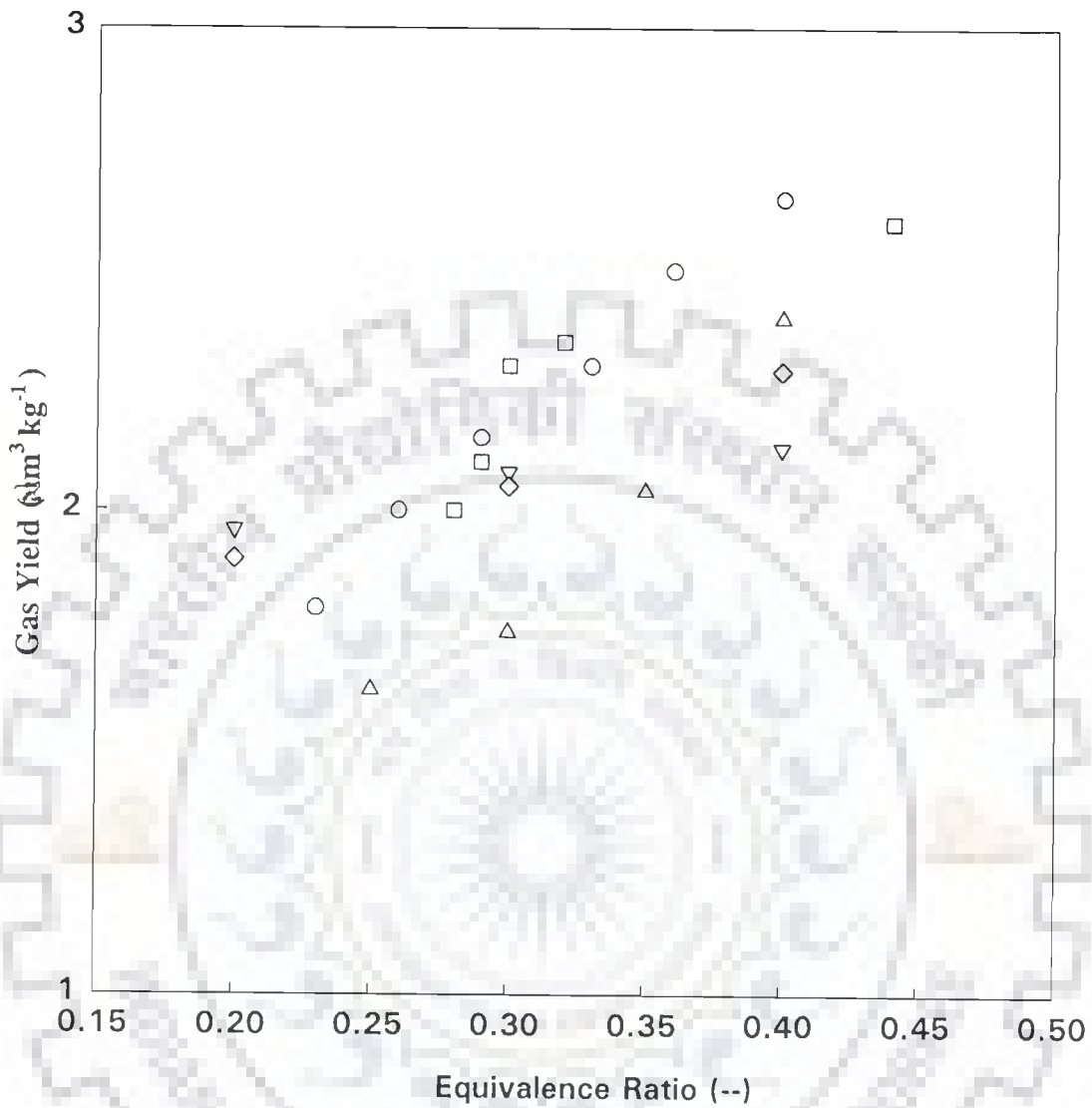


**Fig.4.4.8 Comparison of Gas Yield at Different Equivalence Ratios**

**With Some Reported Values**

- Maniatis et al.(1994)
- Narvaez et al.(1996)
- △ Ergudenler at al.(1997)
- ▽ Present work (sawdust)
- ◇ Present work(village rice husk)

temperatures, the tar cracking and steam reforming reactions are favoured with the resultant increase in gas yield. The gas yield varied between 1.83 and 2.13 Nm<sup>3</sup>kg<sup>-1</sup> DAF for SD, depending on the operating condition. The high yield of gas obtained for VRH may be due to the catalytic effect of the ash and its K<sub>2</sub>O content which favours the char-steam reaction (Mansaray et al., 1999). Increased bed temperature also favours enhanced gas yield. Fig. 4.4.8 presents the gas yield as reported by different workers along with the values obtained in the present work at a minimum fluidization velocity of 0.53 ms<sup>-1</sup>.

#### 4.4.3.5 Energy output

The energy value of the gas per kg DAF VRH and SD will provide the energy output of the gasifier. From Tables 4.4.5, 4.4.7(a) and 4.4.7(b) one can calculate the total energy output of the gas. For VRH, it varied between 4.7 and 7.3 MJkg<sup>-1</sup> DAF, while for SD, it varied between 5.6 and 8.1 MJkg<sup>-1</sup> DAF. The lowest values corresponded with the highest fluidization velocity of 0.73 ms<sup>-1</sup> and lowest ER of 0.20. Narvaez et al. (1996) have shown that the maximum total energy content of the produced gas from pine sawdust was at an ER = 0.32 producing 2.3 nm<sup>3</sup>kg<sup>-1</sup> DAF fuel with a LHV of 4.3 MJNm<sup>-3</sup>. This means the energy content was 9.9 MJkg<sup>-1</sup> DAF fuel. Hartiniati et al. (1989) have shown the maximum energy output of the gasifier bed with rice husk as 12.23 MJkg<sup>-1</sup> fuel at bed temperature of 785°C and ER = 0.35. Raman et al. (1980) have obtained the gasifier energy output as 10.55 MJkg<sup>-1</sup> DAF feed lot manure. However, it may be noted that the fluidizing medium was burner gas alongwith steam. Walawender et al. (1985) have reported that the fluidized bed gasifier energy output at around 750°C for corn stover and sorghum stover were around 10.8 and 12.7 MJkg<sup>-1</sup>DAF. In comparison to the reported values for other biomass, the energy outputs of the gas in the present study were lower. However, it may be noted that in the experiments of other investigators, air was either preheated or the reactor temperature was maintained by external heating.

#### 4.4.3.6 Carbon conversion

Carbon conversion is defined as the ratio of carbon in the fuel converted into carbonaceous gas products. Carbon conversion for VRH and SD are found to depend on the fluidizing velocity and the equivalence ratio, as can be seen from Table 4.4.8 and Figs. 4.4.9(a) and 4.4.9(b), respectively. As the fluidization velocity increases, carbon conversion decreases. The highest carbon conversion efficiency obtained in the present study were 65.94% for VRH and 66.93% for SD gasification, respectively. Equivalence ratio seems to have almost no effect on carbon conversion efficiency of saw dust, whereas for VRH, higher equivalence ratio gave higher carbon conversion.

Walawender et al. (1985a), Maniatis et al. (1988, 1989), Corella et al. (1989), and Mansaray et al. (1999) have reported results for carbon conversion in fluidized bed gasification. Walawender et al. (1985a) have shown that carbon conversion is dependent on bed temperature and it increases almost linearly with the temperature. They reported the values of 73.8% for sorghum stover, 63% for corn stover and 62.7% for wheat straw at the bed temperature of 1020 K. The results of the other investigators showed the carbon conversion values in the range of 50-85%. Mansaray et al. (1999) reported the highest carbon conversion of 81% at an ER = 0.35 and the lowest fluidization velocity of  $0.22 \text{ ms}^{-1}$ . They reported a lowest value of 55% at an ER = 0.25 and the fluidizing velocity of  $0.33 \text{ ms}^{-1}$ . The results of the present study indicate average values of carbon conversion.

Carbon conversion is reported to increase with the increase in bed temperature (Walawender et al., 1985a), free board height and particle residence time (Maniatis et al., 1989).

**Table 4.4.8 : Carbon Conversion Efficiencies for Village Rice Husk and Sawdust Gasification**

Fluidization Velocity (ms <sup>-1</sup> )	Equivalence Ratio (-)	Carbon Conversion Efficiency ,(%)	
		Village Rice Husk Gasification	Sawdust Gasification
0.53	0.20	61.78	66.62
	0.25	61.23	66.46
	0.30	61.76	65.86
	0.35	64.13	66.93
	0.40	65.94	66.52
0.59	0.20	60.12	64.53
	0.25	58.65	64.55
	0.30	59.27	63.76
	0.35	61.78	64.07
	0.40	62.15	63.90
0.68	0.20	53.95	60.78
	0.25	53.53	62.02
	0.30	55.31	63.12
	0.35	56.45	61.91
	0.40	59.00	62.28
0.73	0.20	52.03	57.18
	0.25	53.09	59.34
	0.30	53.29	59.59
	0.35	54.21	59.42
	0.40	55.71	59.96

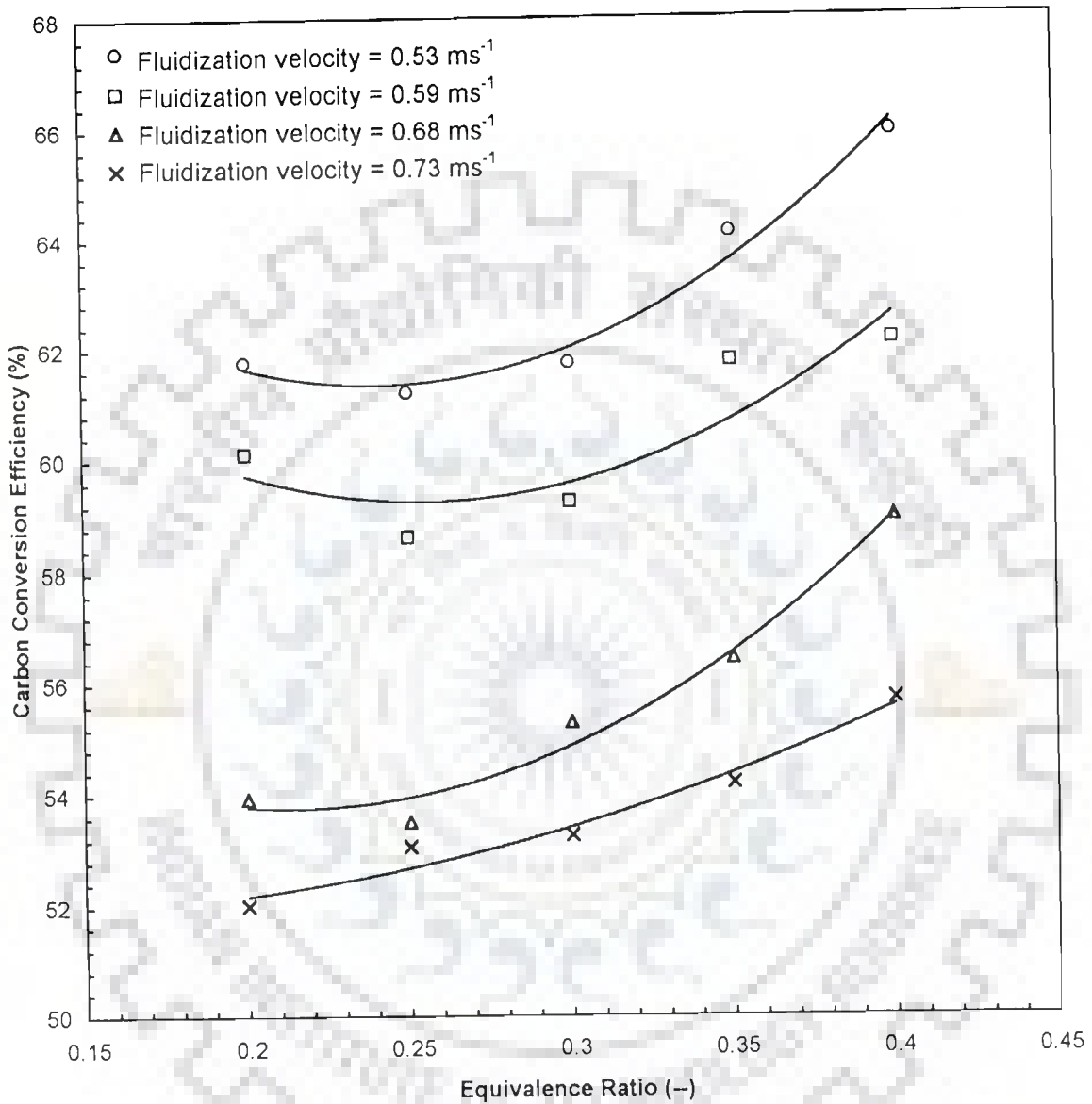


**Fig. 4.4.9(a) : Variation of Carbon Conversion Efficiency with Equivalence Ratio**

Village Rice Husk Gasification

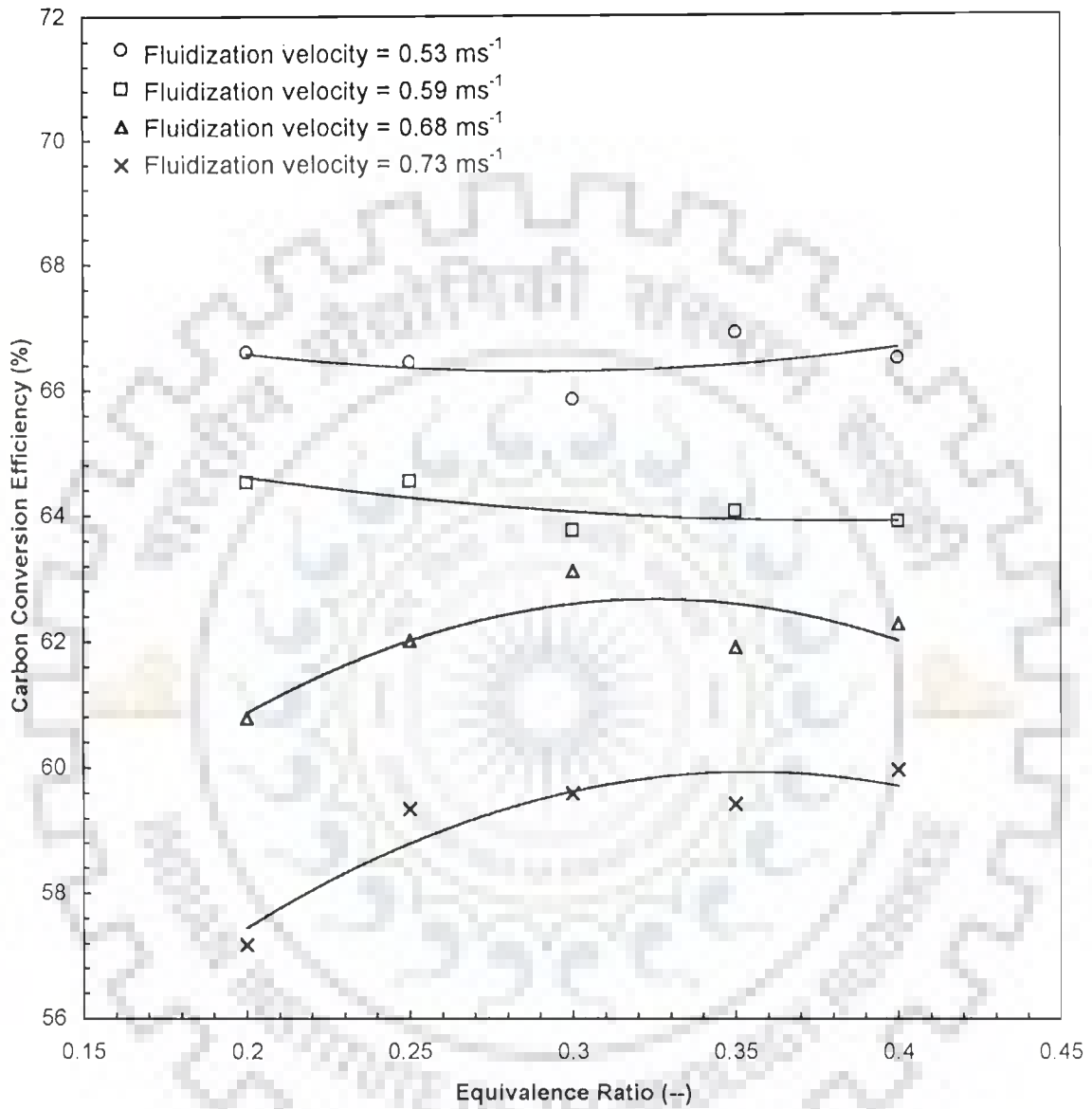


**Fig. 4.4.9(b) : Variation of Carbon Conversion Efficiency with Equivalence Ratio**

**Sawdust Gasification**



#### 4.4.3.7 Tar content of the gas

Figs. 4.4.10(a, b), Figs. 4.4.11(a, b) and Tables 4.4.9(a, b) present the variation in tar content of the product gas with equivalence ratio for various fluidization velocities, for VRH and SD fed gasifier, respectively. The sampling and gravimetric analysis of tar and particulate matter were carried out as per the draft protocol (Abatzoglou et al., 2000) and the suggestions received from Dr. Phillip Hasler, Verenum Research, Zurich (Switzerland) and Dr. J.P.A. Neeft, ECN-Netherlands Research Foundation. The gravimetric tar determination method used in the present study allowed for only the determination of high boiling tar compounds, as the glass bottle impingers were maintained at 0°C only.

As ER increases, slight reduction in tar content is observed. Highest amount of tar, 3.8 gNm<sup>-3</sup> is obtained with SD and 3.6 gNm<sup>-3</sup> for VRH at an ER = 0.20 and the highest fluidization velocity of 0.73 ms<sup>-1</sup>. At ER = 0.40, the tar content decreased to 3.15 and 3.05 gNm<sup>-3</sup> for SD and VRH, respectively. Fluidization velocity did not seem to have any effect on the amount of tar produced. This is seen from the Figs. 4.4.10(b) and 4.4.11(b) for the VRH and SD, respectively. Narvaez et al. (1996) have reported that the tar yield is high when the gasifier operates at temperatures lower than 850°C, and that the ER has then to be raised to about 0.30-0.40 to compensate for such an effect. They have reported that with the increase in H/C ratio of the fuel, the tar content of the gas decreases. They have reported that at the gasifier temperature of 800°C with an ER = 0.30, the tar content was between 4 and 18 gNm<sup>-3</sup>. Higher gasifier temperature facilitates tar cracking and steam reforming reactions of the type,



In the present study, the H/C ratio for VRH and SD were 0.16 and 0.14, respectively. The data for tar content at different ER values are plotted in Fig. 4.4.11(c), alongwith the data reported by Narvaez et al. (1996). The tar content data of Narvaez et al. (1996) were for pine sawdust and were obtained at bed temperature of 800 ± 20°C and the free board temperature of 550 ± 20°C.

Corella et al. (2001) have shown that with the fluidized bed gasification of coke with and without in-bed dolomite, tar content in the exit flue gas varies. With the temperatures of the bed higher than 830°C, tar contents are found to be ≤ 1gNm<sup>-3</sup>. At ER=0.30, tar content of 0.8 gNm<sup>-3</sup> was obtained.

**Table 4.4.9(a) : Tar Content of Producer Gas  
Feedstock: Village Rice Husk**

Fluidization Velocity, (ms <sup>-1</sup> )	Equivalence Ratio, $\phi$ (-)	Tar Content (gNm <sup>-3</sup> )	Particulate Matter (gNm <sup>-3</sup> )
0.53	0.2	3.5428	0.806
	0.3	3.2250	0.846
	0.4	3.0682	0.824
0.59	0.2	3.5224	0.842
	0.3	3.2248	0.864
	0.4	3.0438	0.872
0.68	0.2	3.5822	0.804
	0.3	3.2454	0.872
	0.4	3.0486	0.914
0.73	0.2	3.5894	0.832
	0.3	3.2438	0.960
	0.4	3.0516	0.804

**Table 4.4.9(b) : Tar Content of Producer Gas  
Feedstock: Sawdust**

Fluidization Velocity, (ms <sup>-1</sup> )	Equivalence Ratio, $\phi$ (-)	Tar Content (gNm <sup>-3</sup> )	Particulate Matter (gNm <sup>-3</sup> )
0.53	0.2	3.6606	1.1280
	0.3	3.3248	0.9380
	0.4	3.1280	1.2420
0.59	0.2	3.6858	0.904
	0.3	3.3426	0.806
	0.4	3.1140	1.024
0.68	0.2	3.7680	0.934
	0.3	3.3800	0.912
	0.4	3.1334	1.026
0.73	0.2	3.7822	0.824
	0.3	3.3960	0.802
	0.4	3.1304	0.849

Note : gNm<sup>-3</sup> = grams per unit volume (normal)

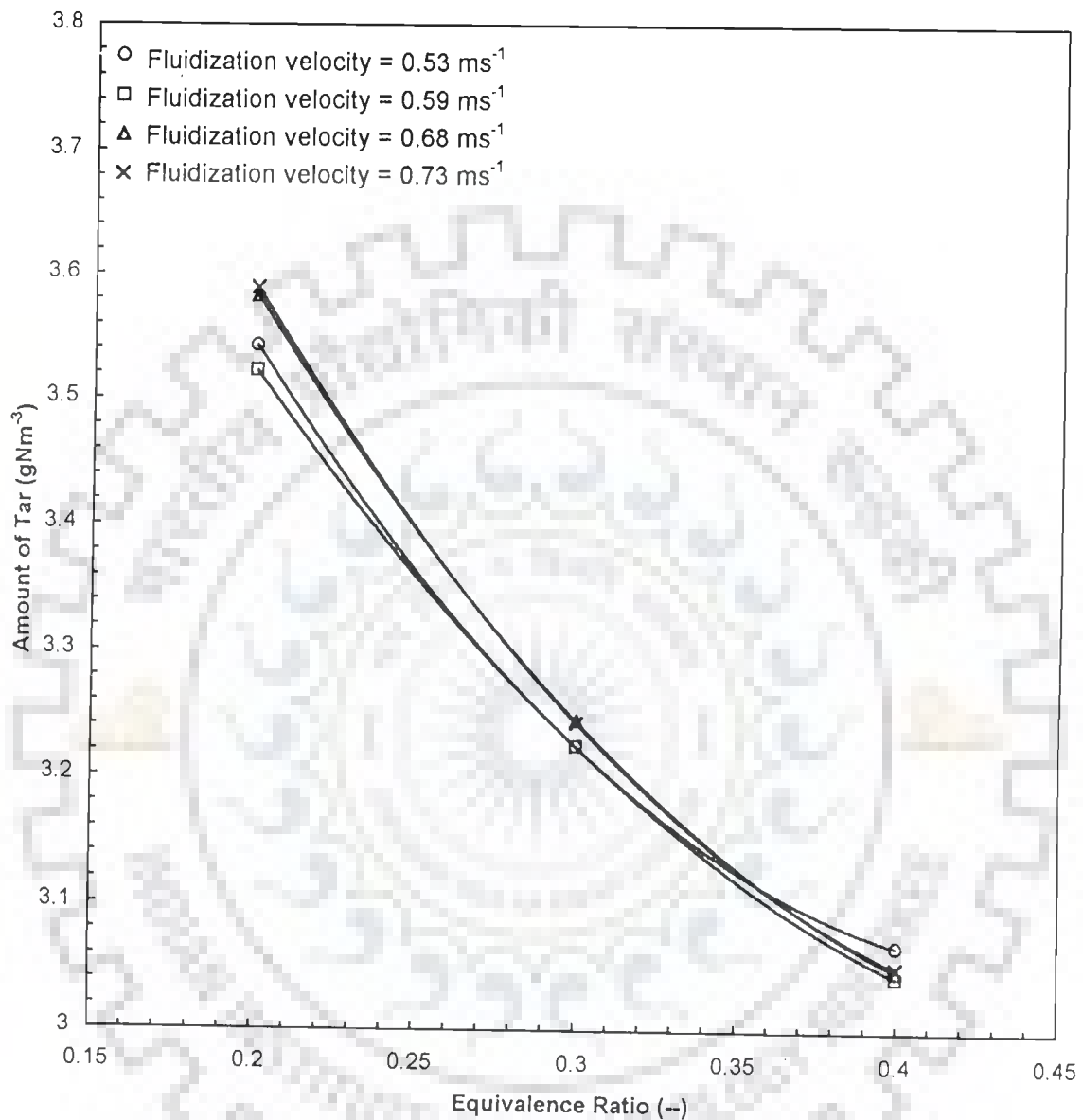


**Fig. 4.4.10(a) : Variation of Tar Content of Product Gas with Equivalence Ratio**

**Feed Stock : Village Rice Husk**

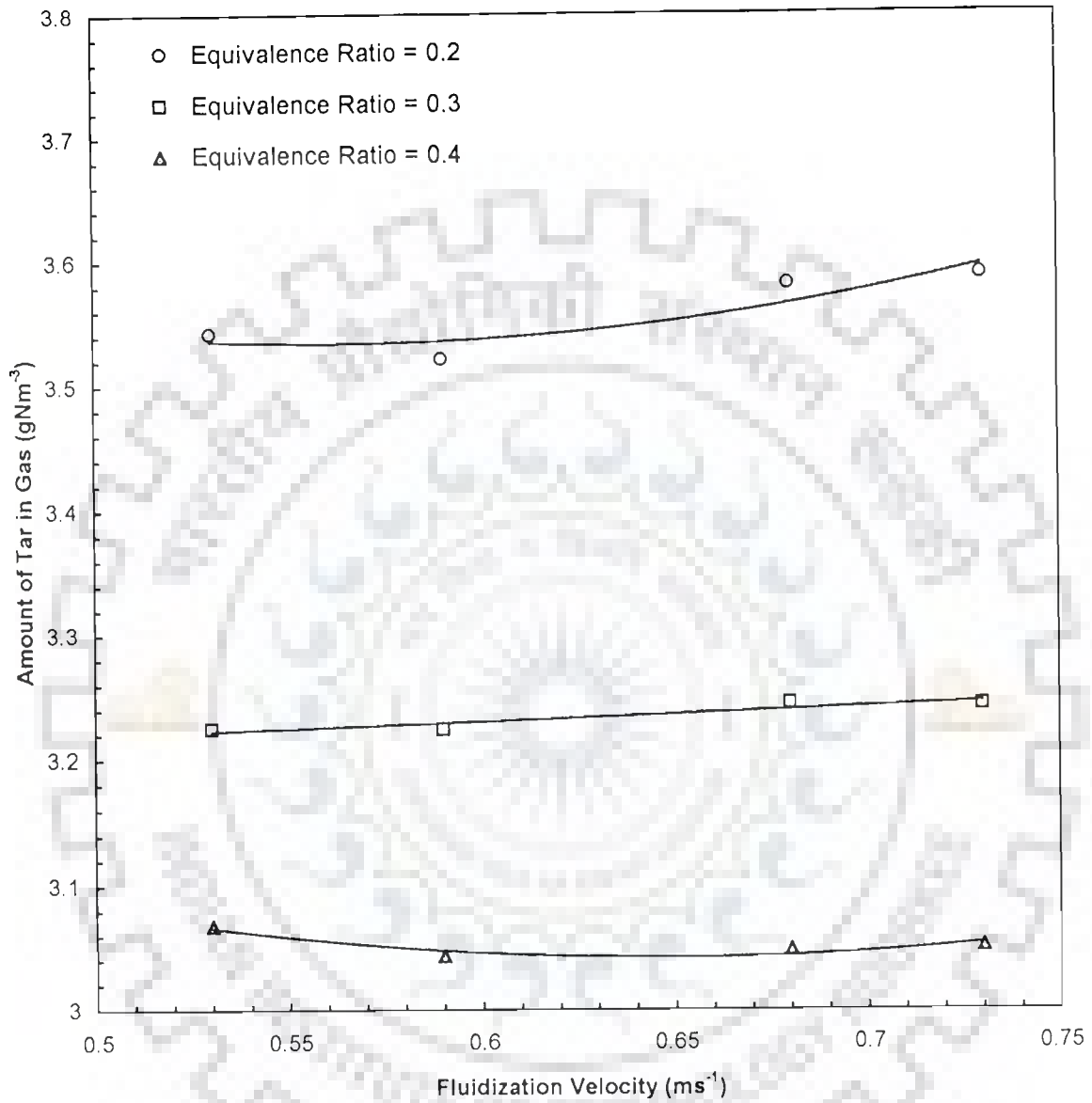
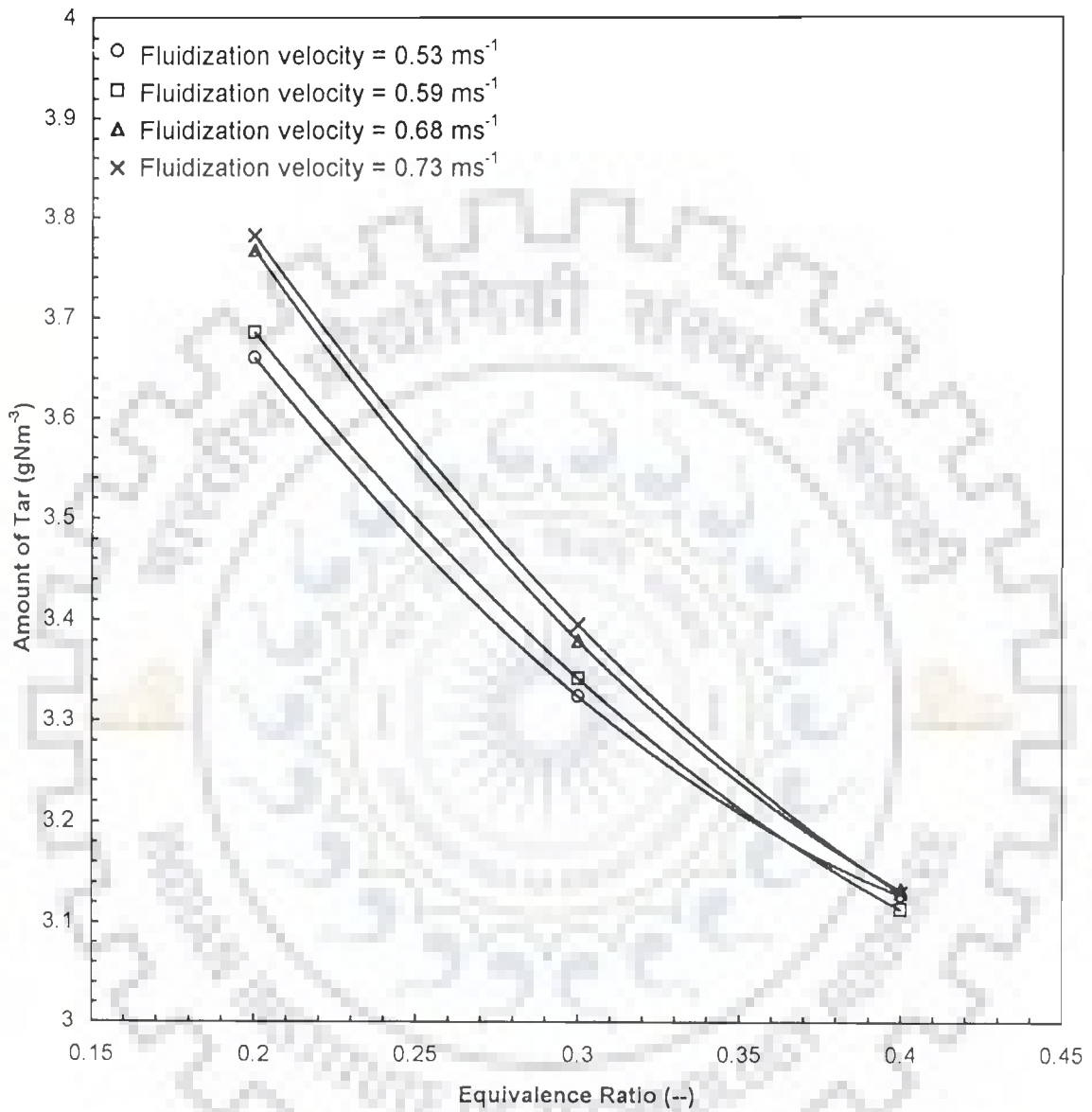


Fig. 4.4.10(b) : Variation of Tar Content in Gas with Fluidization Air Velocity

Feed Stock : Village Rice Husk



**Fig. 4.4.11(a) : Variation of Tar Content of Product Gas with Equivalence Ratio**

**Feed Stock : Sawdust**

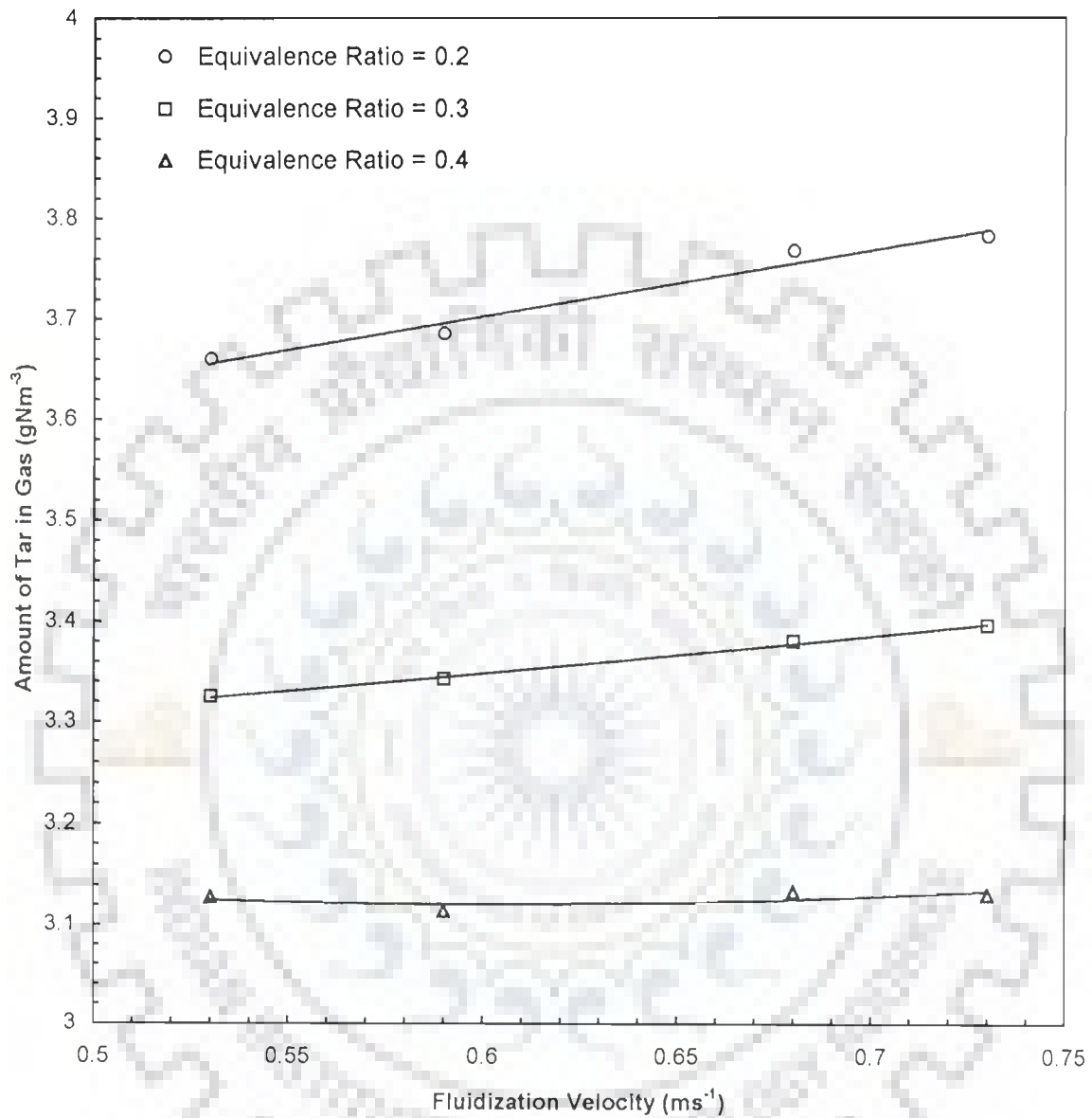


Fig. 4.4.11(b) : Variation of Tar Content in Gas with Fluidization Air Velocity

Feed Stock : Sawdust

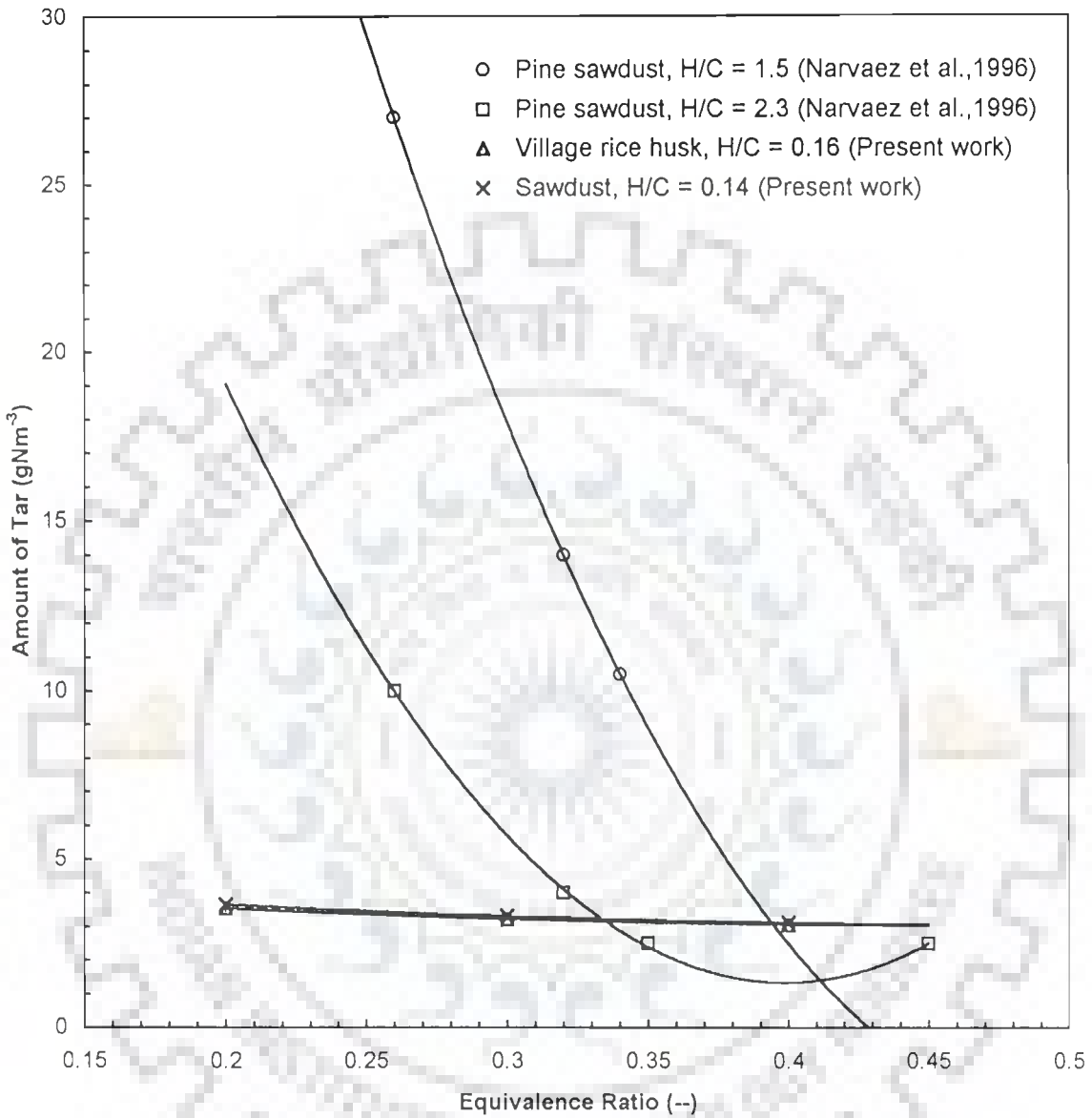


Fig. 4.4.11(c) : Variation of Tar Content of Product Gas with Equivalence Ratio Compared with Values Reported by Narvaez et al. (1996)

#### 4.4.3.8 Particulate matter in the gas

The particulate matter in the cleaned gas (i.e. the gas flowing in the pipe after the cyclone) consists of fine sand particles; unburnt/partially burnt biomass particles, and char particles and condensed tar particulates. The particulate matter content of the gas obtained by isokinetic sampling of the produced gas downstream of the cyclone, shows its steady value only. The particulate matter, sampled isokinetically, contains some amount of tar in particulate (condensed) form and some amount of tar adsorbed on other particles. The total particulate matter in the gas, as reported in Tables 4.4.9(a) and 4.4.9(b), show the amount of particulate matter minus the tar content, present in the gas. The total amount of particulate has been obtained after the complete extraction of tar with dichloromethane (DCM) in a Soxhlet apparatus.

It is found that the total particulate matter is almost insensitive to the equivalence ratio and the fluidization velocity. High particulate matter content of the gas indicates, that another gas-cleaning device (e.g. wet scrubber or fabric filter) may have to be used in conjunction with the cyclone, if the gas is to be used in a modern engine.

#### 4.4.3.9 Effect of residence time of gas on gas yield and gasifier efficiency

Figs. 4.4.12(a) and 4.4.12(b) show the gas yield as a function of the residence time for VRH and SD, respectively. The residence time used here has been calculated on the basis of the volumetric flow rate of the gas as measured at the gasifier outlet corrected for the average reactor temperature. The volume of the gasifier included the volumes of the fluidization column and that of the disengagement section. It is found that the gas yield from VRH gasification increases with the increase in the residence time. The plot for SD shows the tapering off of the gas yield beyond a residence time of 1.75 s for all the equivalence ratios. The effect of ER on gas yield could be seen clearly. As the ER increases, residence time decreases and the gas yield decreases. This is also seen from the data reported in Table 4.4.10.



Table 4.4.10 : Gas Residence Time for Sawdust and Village Rice Husk Gasification

Fluidization Velocity (ms <sup>-1</sup> )	Equivalence Ratio (-)	Gas Residence Time, (S)	
		Sawdust	Village Rice Husk
0.53	0.20	1.50	1.90
	0.25	1.76	2.28
	0.30	2.00	2.63
	0.35	2.20	2.84
	0.40	2.48	3.01
0.59	0.20	1.32	1.72
	0.25	1.55	2.07
	0.30	1.77	2.36
	0.35	2.02	2.57
	0.40	2.29	2.84
0.68	0.20	1.15	1.49
	0.25	1.36	1.83
	0.30	1.57	2.07
	0.35	1.82	2.36
	0.40	2.05	2.57
0.73	0.20	1.08	1.43
	0.25	1.28	1.67
	0.30	1.45	1.94
	0.35	1.69	2.18
	0.40	1.90	2.42

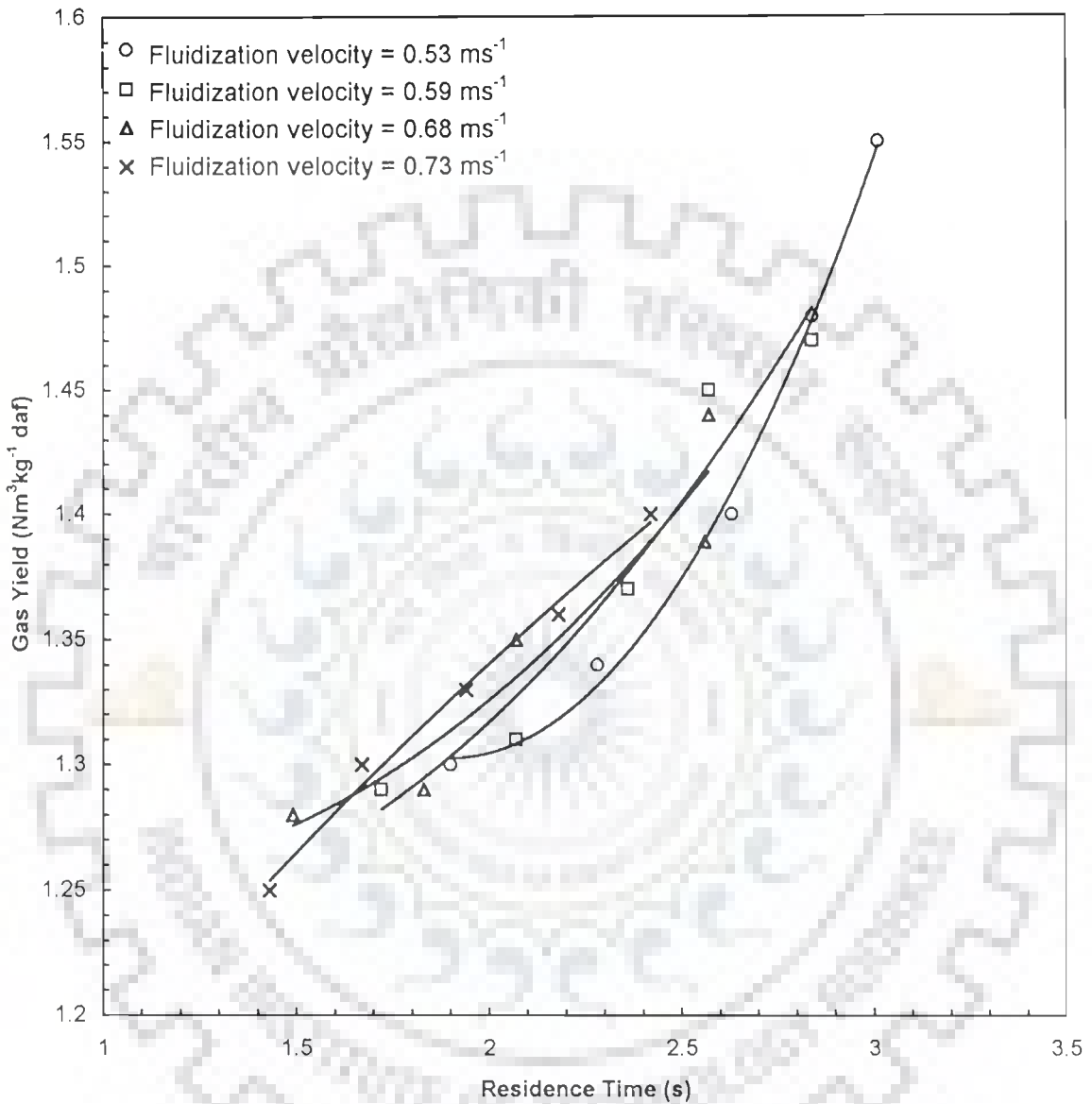


**Fig. 4.4.12(a) : Variation of Gas Yield with Residence Time and Fluidization Velocity**

**Feed Stock : Village Rice Husk**

#### 4.4.3.10 Gasifier thermal efficiency

Tables 4.4.11(a) and 4.4.11(b) present the effect of fluidization velocity and ER on the thermal efficiency of the gasifier. Thermal efficiency is found to decrease as the fluidization velocity increases. It seems to pass by a maximum in its variation with ER. It is due to the fact that the gas yield increases [Figs. 4.4.7(a) and 4.4.7(b)] and the high heating value decreases [Figs. 4.4.6(a) and 4.4.6(b)] with increase in ER at any fluidizing air velocity. For village rice husk, a maximum efficiency of ~57% at an ER=0.40 and the fluidization velocity of  $0.53 \text{ ms}^{-1}$  has been found. Lowest thermal efficiency of 37.4% is obtained at the fluidizing velocity of  $0.73 \text{ ms}^{-1}$  at an ER = 0.40. For saw dust, the highest efficiency of 72.3% was obtained at the lowest fluidizing velocity of  $0.53 \text{ ms}^{-1}$  and an ER = 0.25. Lowest efficiency was obtained at the highest fluidizing velocity of  $0.73 \text{ ms}^{-1}$  and the lowest ER of 0.20. Strom et al. (1982) reported a gasifier efficiency of 43% for gasification of wood shavings using preheated air as the gasifying medium in a circulating fluidized bed (CFB) gasifier operating at 0.18 MPa pressure. Lundquist (1993) found an efficiency of 82.43% for wood waste-fed circulating fluidized bed gasifier with preheated air at 2.48 MPa. The results reported by Strom et al. (1982) and Lundquist (1993) were for demonstration/commercial units. Baptista (1986) has reported an efficiency of 57% for BFB pilot plant gasifier using air-steam as the gasification agent. Overend et al. (1994) reported an efficiency of 61% for bagasse fed BFB using oxygen as a gasifying agent, at a pressure of 2.1 MPa. Sanchez and Lora (1994) have reported gasifier operation and design parameters for maximum efficiency conditions for fluidized bed gasifiers fed with rice husk, saw dust, spent coffee grounds and bagasse, being operated at the State University of Campinas, Brazil. They have reported a maximum efficiency of 65% at an ER of 0.55 for rice husk and 41% at an ER of 0.25 for saw dust fed fluidized bed gasifier. The bed temperatures for rice husk and saw dust were 759 and  $777^{\circ}\text{C}$ , respectively. Corella et al. (2001) have shown that the use of in-bed dolomite during the fluidized bed gasification of

Table 4.4.11 (b) : Gasifier Thermal Efficiency for Sawdust Gasification Experiments

Fluidization Velocity (ms <sup>-1</sup> )	Equivalence Ratio (-)	Energy in Feed		Chemical Energy in Gas		Thermal Efficiency, (%)
		Sawdust Feed Rate, (kg s <sup>-1</sup> )	Energy (MJ s <sup>-1</sup> )	Gas Production Rate (Nm <sup>3</sup> s <sup>-1</sup> )	Energy, (MJ s <sup>-1</sup> )	
0.53	0.20	0.00458	0.0833	0.0075	0.0600	71.94
	0.25	0.00366	0.0666	0.0063	0.0481	72.30
	0.30	0.00305	0.0555	0.0053	0.0394	71.11
	0.35	0.00263	0.0478	0.0047	0.0342	71.51
	0.40	0.00227	0.0413	0.0040	0.0283	68.70
0.59	0.20	0.00513	0.0933	0.0084	0.0622	66.69
	0.25	0.00408	0.0742	0.0069	0.0501	67.59
	0.30	0.00338	0.0615	0.0059	0.0405	65.85
	0.35	0.00291	0.0529	0.0051	0.0340	64.33
	0.40	0.00255	0.0464	0.0045	0.0284	61.39
0.68	0.20	0.00583	0.1061	0.0094	0.0619	59.40
	0.25	0.00466	0.0848	0.0078	0.0515	60.78
	0.30	0.00388	0.0706	0.0067	0.0434	61.58
	0.35	0.00333	0.0606	0.0057	0.0350	57.91
	0.40	0.00291	0.0529	0.0050	0.0298	55.89
0.73	0.20	0.00625	0.1137	0.0099	0.0585	51.43
	0.25	0.00500	0.0910	0.0082	0.0479	52.68
	0.30	0.00416	0.0757	0.0070	0.0396	52.42
	0.35	0.00358	0.0651	0.0060	0.0337	51.85
	0.40	0.00311	0.0566	0.0052	0.0296	52.37

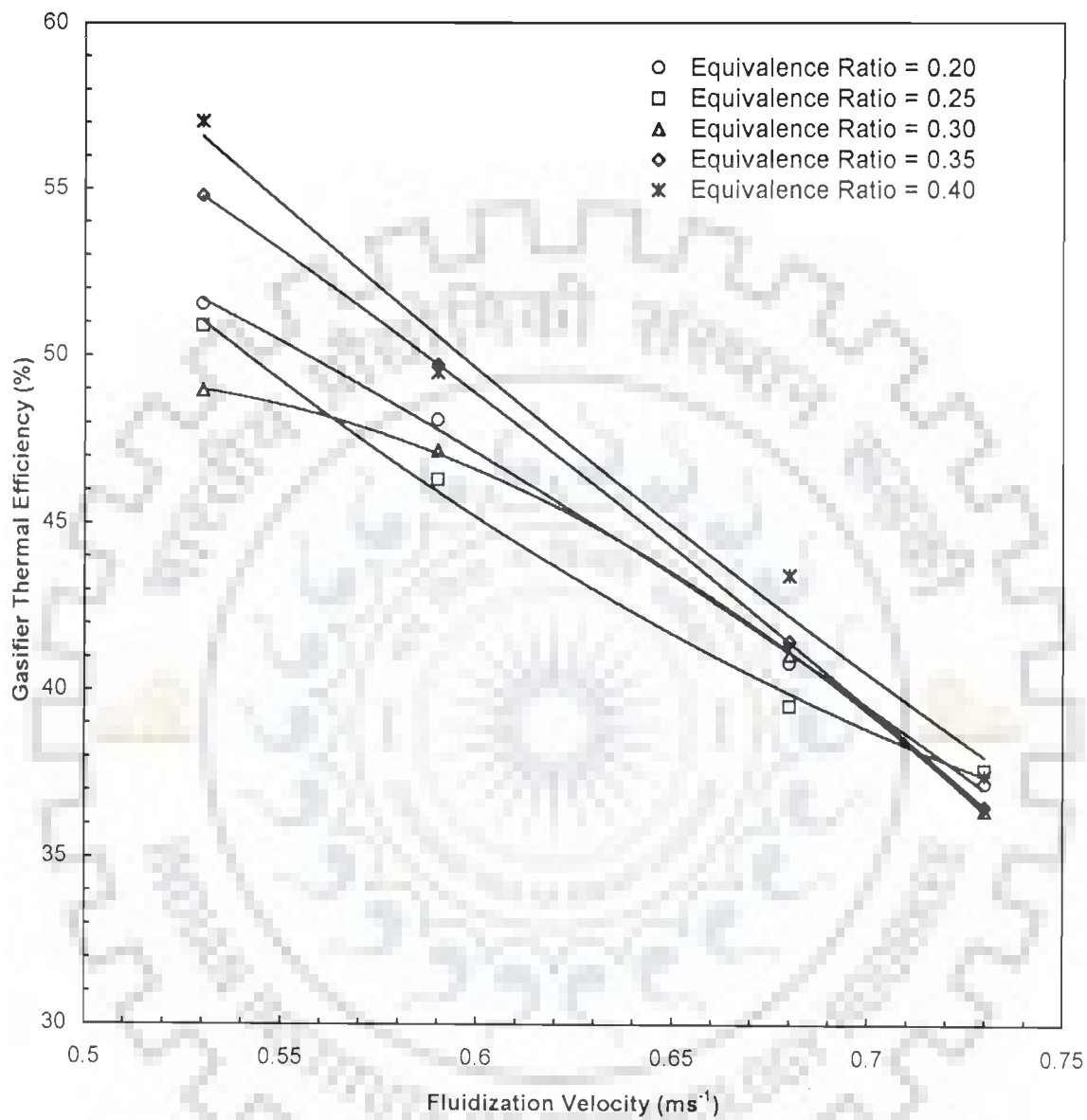


Fig. 4.4.13(a) : Variation of Gasifier Thermal Efficiency with Fluidization Air Velocity

Village Rice Husk Gasification

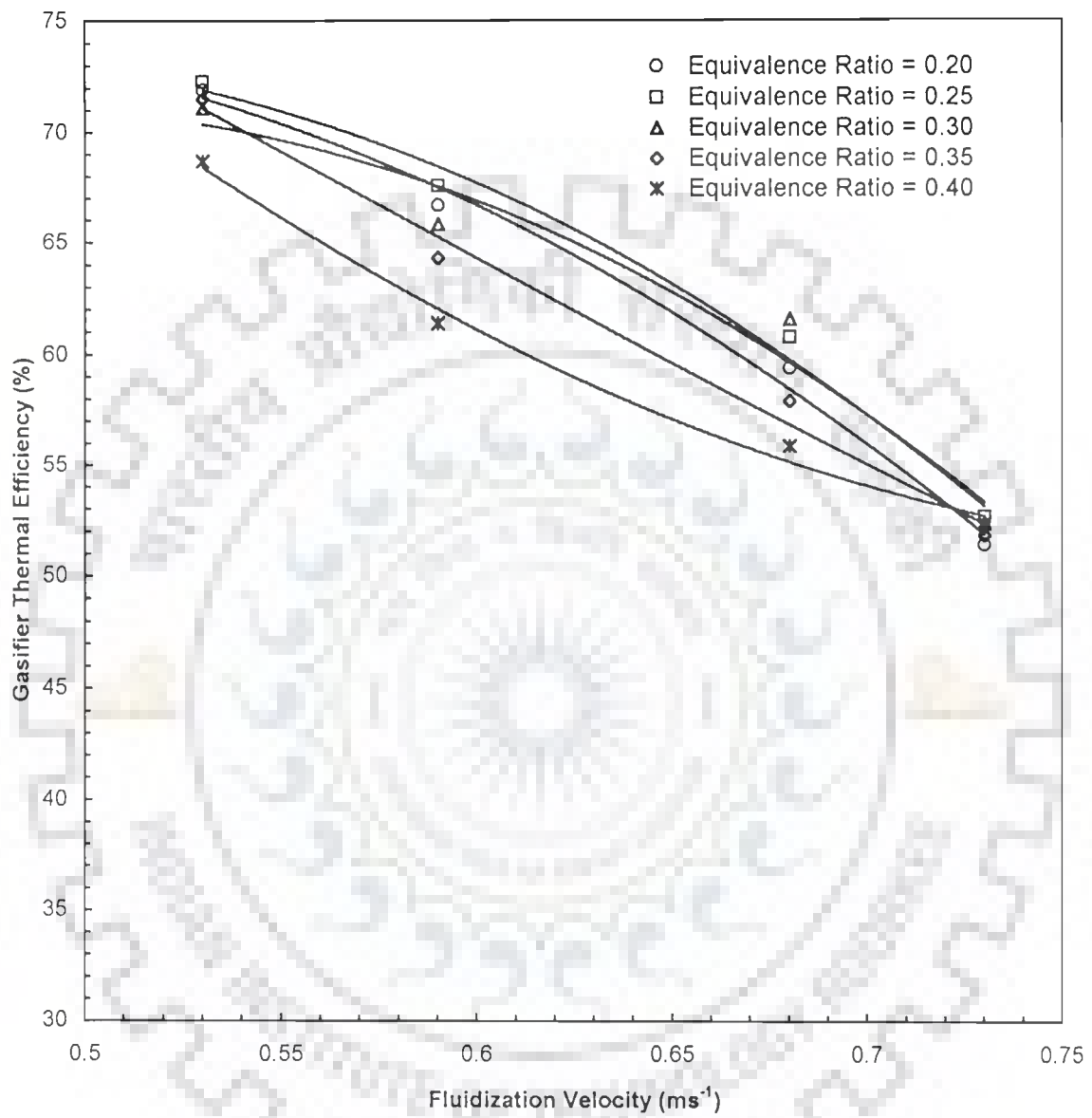


Fig. 4.4.13(b) : Variation of Gasifier Thermal Efficiency with Fluidization Air Velocity

Sawdust Gasification

petroleum coke shows a slight-parabolic increase in the apparent thermal efficiency with ER. The efficiency was found to pass through a maximum with the increase in ER, giving around 75% at an  $ER = \sim 0.34$ . The results from the present study [Figs. 4.4.13(a) and 4.4.13(b)] are in general agreement with the reported values in literature, although higher than the efficiency reported for rice husk and saw dust by Sanchez and Lora (1994).



---

---

## CONCLUSIONS AND RECOMMENDATIONS

### 5.1 PRELIMINARY EXPERIMENTS

Preliminary experiments were conducted to determine the physicochemical, physicochemical and thermochemical properties of the biomass materials relevant to their thermochemical conversion in a fluidized bed gasifier to assess their suitability and the feasible range of operating conditions. The physicochemical properties included bulk density, particle density, particle size, and angles of repose and slide. The physicochemical properties included the moisture, volatile matter, fixed carbon, ash and chemical elemental make up (C,H,O and N) of the biomass materials. The thermochemical properties included the heating values and the ash deformation and fusion temperatures.

#### 5.1.1 Physicochemical Properties

1. The bulk densities of the five biomass materials selected for study viz. village rice husk, mill rice husk, sawdust, bagasse and pressmud were in the range of 75 to 160  $\text{kgm}^{-3}$ . The biomass materials of the present study are powdery biomass materials, as they have the bulk densities less than 200  $\text{kgm}^{-3}$ . The particle densities of the biomass materials ranged from 961 to 1327  $\text{kgm}^{-3}$ .
2. The physical shapes and sizes of the biomass materials were complex. In the absence of a suitable established method of determining their sizes, the sieve analysis has been resorted to.
3. The angles of repose of the biomass materials were found to be between 29 to 33 degrees. The angles of slide ranged from 51 to 56 degrees.



### 5.1.2 Physicochemical Properties

1. The average volatile matter contents of the biomass materials were between 53.9 and 76% with bagasse and pressmud having the lowest values. Sawdust had the highest volatiles content. On comparison with the volatile matter content of coal available in India (20-30%), the volatile matter content of the biomass materials are on the higher side and hence are easily amenable to gasification with lesser amount of heat. Therefore the biomass materials of the present study are useful fuels for gasification.
2. The ash content of the biomass materials were found to be 20% for village rice husk and pressmud, 19.2% for mill rice husk, 11.1% for bagasse and 3.6% for sawdust. These values were comparable with reported values.
3. The nitrogen contents of the biomass materials varied from 0.34 to 1.32%. These are low concentrations and therefore the biomass materials of the present study are environmentally desirable fuels.

### 5.1.3 Thermochemical Properties

1. The higher heating values of the biomass materials ranged from 13.60 MJkg<sup>-1</sup> (pressmud) to 18.2 MJkg<sup>-1</sup>(sawdust). The lower heating values ranged from 11.98 MJkg<sup>-1</sup> (pressmud) to 15.66 MJkg<sup>-1</sup> (sawdust). It was observed that the heating value decreased with increase in the ash content.
2. In general, the heating values of the biomass materials were more than half of the heating value of average coal found in India. This factor makes them a potential source of energy.
3. The ash deformation and fusion temperatures of the biomass materials were found to be greater than 1200°C which are more than the normal operational temperature range of a fluidized bed gasifier (650-850°C).

## 5.2 FLUIDIZATION BEHAVIOUR OF BIOMASS MATERIALS

1. Powdery biomass is not fluidizable alone as a bed charge and a second carrier solid needs to be added to the bed charge to facilitate its fluidization.
2. The minimum fluidization velocities for the four carrier solids, namely sand of two sizes ( $d_p = -500 + 350 \mu\text{m}$  and  $d_p = -850 + 710 \mu\text{m}$ ) and bauxite of two sizes ( $d_p = -500 + 420 \mu\text{m}$  and  $d_p = -850 + 710 \mu\text{m}$ ) were found to be 0.41, 0.50, 0.38 and 0.47  $\text{ms}^{-1}$  respectively. No hysteresis was observed in the fluidization pattern of carrier solids.
3. For a carrier solid, the minimum fluidization velocity was observed to increase with increase in the particle size and density. The minimum fluidization velocity for sand ( $\rho_p = 2930 \text{ kgm}^{-3}$ ) was more than the minimum fluidization velocity for bauxite ( $\rho_p = 2100 \text{ kgm}^{-3}$ ) with both sand and bauxite having the same particle size ( $d_p = -850 + 710 \mu\text{m}$ ).
4. For a carrier solid, the ratio of bed height to its diameter did not seem to have any effect on the minimum fluidization velocity.
5. The effect of hysteresis was significant in the fluidization of binary mixtures of a carrier solid and a biomass. The minimum fluidization velocity, determined from the pressure drop versus superficial air velocity data obtained while decreasing the superficial air velocity from the fully fluidized state to its fixed bed state, was found to be slightly on the higher side than the minimum fluidization velocity determined from the data of pressure drop versus superficial air velocity obtained while increasing the superficial air velocity from the fixed bed state of the bed charge.
6. The minimum fluidization velocity increased with the percent mass (or volume) of biomass in the bed charge. When the mass of biomass present in the bed mixture exceeded 8 percent of the weight of the carrier solid in the bed, the mixture became 'non-fluidizable'. The segregation of biomass was significant at this percent content of biomass in the bed mixture.

### 5.3 CHARACTERISTICS AND KINETICS OF THERMAL DEGRADATION

1. TGA, DTG and DTA curves showed the number of distinct reaction zones during the thermal degradation process of the biomass. Natural break in the slope of the TGA is characterized by the change in the rate of weight loss due to drying, devolatilization and degradation of biomass components, namely hemicellulose, cellulose and lignin. The first DTG peak after the drying (dehydration) of biomass showed the degradation of hemicellulose, (smaller peak) at lower temperatures followed by a larger peak for the cellulose degradation at higher temperature. Lignin is found to degrade throughout the entire temperature range. Based on the nature of TGA, DTG and DTA curves, the number of reaction (degradation) zones could be easily identified for all the materials. The reaction zones (temperature zones) and the rate of degradation ( $\% \text{ weight loss min}^{-1}$ ) depend on the heating rate. Normally as the heating rate increased, the reaction zone temperature range increased. Change in atmosphere, i.e. from nitrogen for pyrolysis to air for oxidation reactions decreased the final residue.
2. For village rice husk (VRH), four reaction zones were identified, while only three reaction zones could be seen for mill rice husk. The maximum rate of degradation was found to be 11.7 and 23.1  $\text{wt}\% \text{min}^{-1}$  at 20 and 40°Cmin<sup>-1</sup> heating rates, respectively, for village rice husk pyrolysis. For mill rice husk pyrolysis, the maximum rate of degradation was found to be 37.5 and 59.7  $\text{wt}\% \text{min}^{-1}$  at 20 and 40°Cmin<sup>-1</sup> heating rates, respectively. For thermal degradation in air, only two reaction zones were identified. The first reaction zone showed very high maximum degradation rates of 14.9-17.5  $\text{wt}\% \text{min}^{-1}$  at 20°Cmin<sup>-1</sup> and 37.0-39.5  $\text{wt}\% \text{min}^{-1}$  at 40°Cmin<sup>-1</sup> heating rate for MRH and VRH samples. The second reaction zone degradation rates were much lower : 3.9-5.0  $\text{wt}\% \text{min}^{-1}$  and

zone degradation rates were much lower : 3.9-5.0 wt%min<sup>-1</sup> and 6.5-10.8 wt%min<sup>-1</sup> for 20 and 40°Cmin<sup>-1</sup> heating rate, respectively, for VRH and MRH samples. The increase in heating rate decreased the total residue at 700°C from around 29.6 to 15.6% for VRH and 32.5 to 15% for MRH at 40°Cmin<sup>-1</sup>.

3. For sawdust (SD), five clearly distinct zones were identified during pyrolysis. However, due to very slow first and fifth degradation zones, they were merged with other degradation zones and only three degradation zones were considered. The maximum rate of degradation was observed in the second reaction zone : 29.7 and 56.9wt%min<sup>-1</sup> at 20 and 40°Cmin<sup>-1</sup> heating rates, respectively. The residue was 17.5% at 20°Cmin<sup>-1</sup> and 25.0% at 40°Cmin<sup>-1</sup>. During thermal degradation in air, four distinct degradation zones (apart from drying) were identified. Maximum rate of degradation was observed during the second reaction zone – 46.6 and 51.6 wt%min<sup>-1</sup> at 20 and 40°Cmin<sup>-1</sup> heating rates, respectively. The total residue was 6.4% at 40°Cmin<sup>-1</sup> and 10.50% at 20°Cmin<sup>-1</sup>.
4. Three distinct pyrolysis zones were observed for bagasse (BG) with the second zone showing highest degradation rate of 22.5 and 49.6 wt%min<sup>-1</sup> at 20 and 40°Cmin<sup>-1</sup> heating rates, respectively. Bagasse residue was 18.6 and 11.5% at 20 and 40°Cmin<sup>-1</sup> heating rates, respectively. Air degradation showed five distinct zones with the second zone showing the highest degradation rates of 28.4 and 64.6%min<sup>-1</sup> at 20 and 40°Cmin<sup>-1</sup> heating rates, respectively. Only 2% residue was obtained at 700°C.

5. Pressmud, being sugar mill waste, showed distinct degradation behaviour in comparison to other biomass materials. However, for brevity, only three degradation zones were considered. Pyrolysis behaviour showed poor devolatilization, with the maximum devolatilization being 9.7 and 14.0 wt%min<sup>-1</sup> at 25 and 40°Cmin<sup>-1</sup> heating rates, respectively. At 850°C, the total residue obtained was around 50%. However, in oxidizing environment, the rate of degradation of pressmud was as high as 90.0 wt%min<sup>-1</sup> at 20°Cmin<sup>-1</sup> heating rate. The total residue at 40°Cmin<sup>-1</sup> heating rate was found to be 16.5 wt% only. This showed that the pressmud could be a very important source of clean energy through thermal gasification.

#### 5.4 KINETICS OF THERMAL DEGRADATION

1. TGA curves were used to determine kinetics of thermal degradation of the biomass materials in nitrogen and air atmospheres. Differential and integral methods were used. In all, six methods as proposed by Coats and Redfern (1964), Agarwal and Sivasubramanian (1987), Horowitz and Metzger (1963), Piloyan and Novikova (1967), Reich and Stivala (1982) and Freeman and Carroll (1958) were used to determine kinetic parameters. A simple, single-step, irreversible reaction was assumed to represent degradation in each temperature zone. The entire degradation zone was also represented by a single-step, irreversible reaction using Agarwal and Sivasubramanian approximation for the integral analysis of kinetics. For all the materials, at the two heating rates and under nitrogen and air atmospheres, the kinetic parameters were determined by using the least-squares best-fit approach. For the integral method of Coats and Redfern, and Agarwal and Sivasubramanian, the  $n$  was varied from zero to 3.0 to obtain the best-fit linear relation to determine the activation energy  $E$ , and the pre-

exponential factor,  $k_0$ . For any  $n$ , the value of  $E$  obtained by Coats and Redfern method and Agarwal and Sivasubramanian method were the same. The pre-exponential factor, however, differed slightly. From the results it is concluded that even the entire range of degradation could be represented by a single-step, irreversible reaction using Agarwal and Sivasubramanian (1987) approximation for integration, with reasonable confidence for all the biomass materials. It was found that as the value of  $n$  increased, the activation energy also increased for the best fit correlation using integral method. Therefore, it is not the activation energy alone, but the value of order of reaction  $n$  which gave the best fit for the TGA data, along with  $E$  and  $k_0$  should be taken for the design of pyrolysis and gasification reactor.

2. The kinetic parameters indicated that the best fit kinetic parameters varied in the range  $0.50 < n < 2.50$ ,  $27.84 < E < 132.9 \text{ kJmol}^{-1}$  and  $3.21 \times 10^1 < k_0 < 1.414 \times 10^{12} \text{ min}^{-1}$  for all the biomass materials. For air degradation, the values of  $E$  are found to be higher than those for pyrolysis at any value of  $n$ . The values of  $n$ ,  $E$  and  $k_0$  are found to be within the range reported by other investigators.

## 5.5 FLUIDIZED BED GASIFICATION OF VILLAGE RICE HUSK AND SAWDUST

1. The performance of the gasifier-unit, as a whole, was found to be satisfactory for both village rice husk and sawdust gasification. It may also be concluded that the fluidized bed gasifier is 'feed-flexible' and could take with equal ease both the kinds of biomass. The feed flow was very uniform without any bridging/arching.
2. The average bed temperature varied between 575 to 782°C for village rice husk gasification and 680 to 791°C for sawdust gasification. The average

free board temperatures were found to be lower than the average bed temperatures by 79 to 131°C for village rice husk and 81 to 92°C for sawdust. This was because of the absence of any external heat source to assist the gasification process, as has been employed by other investigators.

3. Gasifier temperatures increased with increase in the equivalence ratio and/or with increase in the fluidization velocity.
4. As the equivalence ratio increased, the concentration of CO<sub>2</sub> increased and the concentrations of fuel gases viz., CO, H<sub>2</sub>, CH<sub>4</sub> and C<sub>2</sub>H<sub>m</sub> decreased. Increase in fluidization velocity lead to the similar effect. Among the fuel gases, CO had the highest concentration (11.2-19.4% vol. for VRH; 12.8-19.9% vol. for SD) followed by H<sub>2</sub> (2.7-2.8% vol. for VRH; 3.1-4.3% vol. for SD), and CH<sub>4</sub> (1.5-2.3%vol. for VRH; 2.0 – 2.7% vol. for SD).
5. The higher heating value (HHV) of gas ranged from 2.35 to 3.85 MJNm<sup>-3</sup> for village rice husk (VRH) and 2.81 to 4.14 MJNm<sup>-3</sup> for sawdust (SD). The higher heating value of the product gas from both village rice husk and sawdust decreased linearly with increase in the equivalence ratio and fluidization velocity.
6. The gas yield varied from 1.8 to 2.14 Nm<sup>3</sup> kg<sup>-1</sup> DAF for village rice husk and 1.88 to 2.13 Nm<sup>3</sup> kg<sup>-1</sup> DAF for sawdust. In both cases, the gas yield increased with equivalence ratio (ER) upto ER=0.35 and thereafter it decreased.
7. The energy output (the energy value of the gas per kg of VRH or SD) were found to be in the range of 4.7 to 7.3 MJkg<sup>-1</sup> DAF for VRH and 5.6 to 8.1 MJkg<sup>-1</sup> DAF for SD. Carbon conversion efficiency varied from 52.03% to 65.94% for VRH and 57.18 to 66.93% for SD.

8. The gravimetric method allowed the determination of high boiling tar compounds only. The tar content of the raw product gas slightly decreased with increase in equivalence ratio for both village rice husk and sawdust. Fluidization velocity did not seem to affect the tar content. Particulate matter content of the gas did not exhibit any specific trend with either equivalence ratio or fluidization velocity.
9. The gasifier thermal efficiency ranged from 51.43 to 72.30% for sawdust gasification and 36.39 to 57.04% for village rice husk gasification.

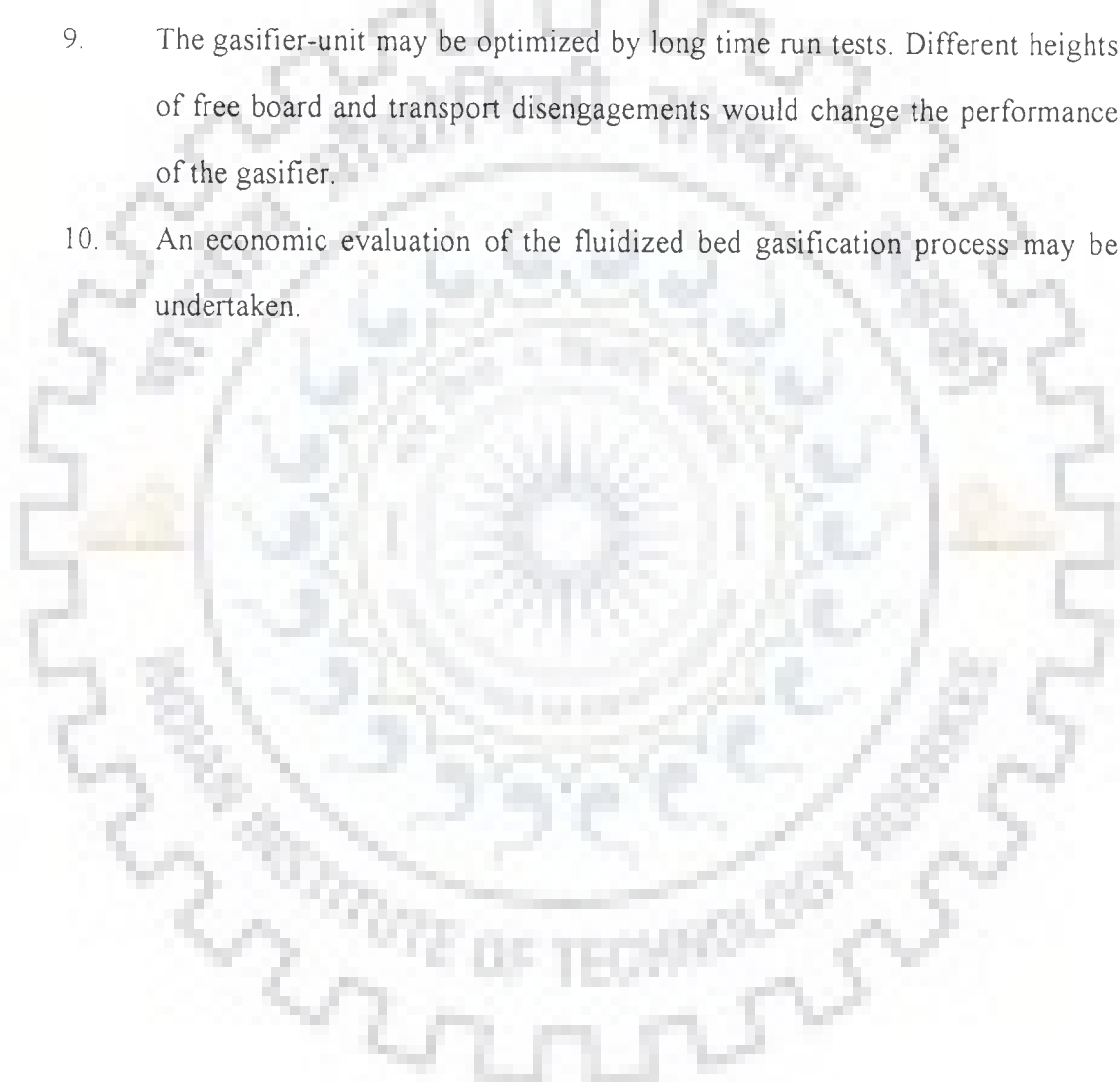
## 5.6 RECOMMENDATIONS

This study has brought forth a number of considerations which may be of interest for furthering the work in the area of fluidized bed biomass gasification.

1. An exhaustive data base on biomass of agricultural, agro-industrial and forestry origin available in plenty and perennially in different parts of India should be developed. Certain plants, shrubs and weeds which do not have fodder value may also be included.
2. The physico mechanical, physico chemical and thermochemical properties of such biomass be determined to assess their suitability for gasification.
3. The thermal degradation of such biomass be studied at different heating rates and in different atmospheres. The reaction kinetics of their thermal decomposition may also be studied for inert, oxidizing and reducing atmospheres.
4. The developed fluidized bed gasifier should be tested with different types of powdery biomass materials.
5. Efforts be made to run a diesel engine completely or partially on the product gas produced by the fluidized bed gasifier. The response time of the gasifier-unit to the load variation should be compared with that of the diesel engine. This will help in establishing the flexibility of the fuel.



6. Effect of secondary air injection either through the feeding screws or in the free board region on the gas quality should be studied.
7. The effect of the addition of catalytic materials like dolomite or limestone to the bed charge on the tar content of the gas should be studied.
8. The tar produced by the different feedstocks may be quantitatively analysed for its components or groups of components.
9. The gasifier-unit may be optimized by long time run tests. Different heights of free board and transport disengagements would change the performance of the gasifier.
10. An economic evaluation of the fluidized bed gasification process may be undertaken.



## REFERENCES

---

1. Aarsen van Den F.G., Beenackers, A.A.C.M. and van Swaij, W.P.M. In: Fluidization-V, Proceedings of 5<sup>th</sup> Engineering Foundation Conference on Fluidization, Elsinore, Denmark, Oestergaard K. and Soerenser, A. (Eds.), New York Engineering Foundation, p. 521 (1986).
2. Abatzoglou, N., Barker, N., Philip, H. and Knoef, H., "The development of a draft protocol for the sampling and analysis of particulate and organic contaminants in the gas from small biomass gasifiers", *Biomass & Bioenergy*, **18**, 5-17 (2000).
3. Agarwal, R.K. and Sivasubramanian, M.S., "Integral approximations for non-isothermal kinetics", *American Institute of Chemical Engineers Journal*, **33**, 7, 1212-1214 (1987).
4. Ahuja, P., Kumar, S. and Singh, P.C. "A model for primary and heterogeneous secondary reactions of wood pyrolysis", *Chemical Engineering Technology*, **19**, 272-282 (1996).
5. Ahuja, Pradeep, Singh P.C, Upadhyay, S.N. and Surendra Kumar, "Kinetics of biomass and sewage sludge pyrolysis – Thermogravimetric and sealed reactor studies", *Indian Journal of Chemical Technology*, **3**, 306-312 (1996).
6. Akita and Kase (1967) (Cited in Nishizaki et al., 1980).
7. Alves, S.S. and Figueiredo, J.L., "A model for pyrolysis of wetwood", *Chemical Engineering Science*, **44**, 2861 (1988).
8. Anon. Annual Books of ASTM Standards, American Society for Testing and Materials, Philadelphia, PA. 19103 (1993).
9. Antal, M.J. and Varhegyi, G, "Cellulose pyrolysis kinetics: the current state of knowledge", *Industrial Engineering Chemistry Research*, **34**, 703-717 (1995).

10. Antal, M.J., "Biomass pyrolysis – a review of the literature part II – lignocellulose pyrolysis" In: *Advances in Solar Energy*, Boer, K.W., Duffie, J.A., (Eds.), American Solar Energy Society, New York (1985).
11. Antal, M.J., "Thermogravimetric signatures of complex solid phase pyrolysis-mechanisms and kinetics" In: *Thermal Analysis Proceedings of the Seventh ICTA*; Miller, B. (Ed.), John Wiley, New York (1982).
12. Anthony, (1974) (Cited in Anthony et al., 1974).
13. Anthony, D.B. and Howard, J.B., *American Institute of Chemical Engineers Journal*, **22**, 625-656 (1976).
14. Anthony, D.B., Howard, J.B., Hottel, H.C. and Meissner, H.P., "Rapid devolatilization of pulverized Coal", Fifteenth Symposium (International) on Combustion, The Combustion Institute, Pittsburgh, PA, 1303 (1974).
15. Anuradha, G., Grover P.D. and Iyer, P.V.R., "Combustion and gasification characteristics of rice husk", *Fuel*, **71**, 889-894 (1992).
16. ASTM, *Annual Books of ASTM Standards*. American Society for Testing and Materials, Philadelphia, PA (1986).
17. Aznar, M., Gracia-Gorria, F.A. and Corella, J., "Minimum and maximum velocities for fluidization for mixtures of agricultural and forestry residues with a second fluidizing solid. Part I . Preliminary data and results with sand-sawdust mixtures. Part II. Experimental results for different mixtures", *International Chemical Engineering*, **32**, (1), 95-113 (1992a,b).
18. Baptista, M.A.C., "Gaseificacao de bagaco de cana-de-acucar : um estudo experimental", *Anais do XIV Encontro sobre Escoamento em Meios Porosos, UNI-CAMP*, 420-438 (1986).
19. Beenackers, A.A. C.M. and van Swaaij, W.P.M., "Gasification of biomass – a state of art review" *Thermochemical Processing of Biomass*, Bridgwater, A.V. (Ed.) Butterworths, London, 91-136 (1984).
20. Beenackers, A.A.C.M. and Bridgwater, A.V., "Gasification and pyrolysis of biomass in Europe". *Pyrolysis & Gasification International Conference*, 1989, Ferrero G.L. et al. (Ed.), Elsevier, London, 129-157 (1989).

21. Benson, S., "Thermochemical Kinetics" Wiley, NY (1968).
22. Berkowitz, N., Fuel, **39**, 47 (1960) (Cited in Anthony et al., 1974).
23. Bhatnagar, A.P., "Combustion and gasification of rice husk" In : International Conference on Biomass Energy Systems, 26-27 Feb. TERI, New Delhi, 225-237 (1996).
24. Bhattacharya, S.C., "State of the art of utilizing residues and other types of biomass as an energy source". RERIC International Energy Journal, **15**, (1), 1-21 (1993).
25. Bilbao, R., "Kinetics of weightloss by thermal decomposition of lignocellulosic materials", Thermochimica Acta, **165**, 103-117 (1990).
26. Bilbao, R., "Temperature profiles and weightloss in the thermal decomposition of large spherical wood particles", Industrial Engineering Chemistry Research, **32**, 1811-1817(1993).
27. Bilbao, R., Lezaun J and Abanades J.C., "Fluidization velocities of sand/straw binary mixtures", Powder Technology, **52**, 1-6 (1987).
28. Bilbao, R., Lezaun, J.L., Menendez M and Abanades., J.C., "Model of mixing/segregation of sand-straw mixtures in fluidized beds", Powder Technology, **56**, (1), 149-155 (1988).
29. Bining, A.S. and Jenkins B.M., "Thermochemical reaction kinetics for rice straw from an approximate integral technique", American Society for Agricultural Engineers, Paper Number 92-6029, St. Joseph, MI (1992).
30. Black, J.W., Bircher, K.G. and Chisholm, K.A., "Fluidized bed gasification of solid wastes and biomass: the CIL Program". In: Thermal Conversion of Solid Wastes and Biomass. American Chemical Society Symposium Series, **130**, 351-361 (1979).
31. Boateng, A.A., Walawender W.P and Fan L.T., In : Biomass for Energy and Industry, Grassi, G., Goosse, G. and dos Santos, G. (Eds.), Elsevier Applied Science, London (1990).

32. Boateng, A.A., Walawender, W.P., Fan, L.T. and Chee, C.S., "Fluidized bed steam gasification of rice hull", *Bioresource Technology*, **40**, 235-239 (1992).
33. Brandon, H.O., King, G.H. and Kinsey, D.V., "The role of thermochemical processing in biomass exploitation" In : *Thermochemical Processing of Biomass*, Bridgwater, A.V. (Ed.) Butterworths, 11-34 (1984).
34. Bridgwater, A.V., "The technical and economic feasibility of biomass gasification for power generation", *Fuel*, **74** (3), 631-653 (1995).
35. Bridgwater, A.V., "A Survey of thermochemical biomass processing activities", *Biomass*, **22**, 279-292 (1990).
36. Bridgwater, A.V., "Thermochemical processing of biomass", In: *Review of Thermochemical Biomass Conversion*, Butterworth, London (1984).
37. Campagnola, G., "RDF pellets gasification/gas clean-up development program", In: *Energy from Biomass- Progress in Thermochemical Conversion, Proceedings of the EC Contractors' Meeting held in Florence, Italy*, published by European Commission, Brussels, Luxembourg, 83-97 (1984).
38. Chakrabarti, S., Chakrabarti, P., Saha, S. and Datta, S., "Burning rice husk in a horizontal cyclone furnace: a case study", *Institute of Chemical Engineers Symposium Series*, **105**, 339-352 (1988).
39. Charley, E.L. and Warrington, S.B., "Thermal analysis – techniques and applications", Royal Society of Chemistry, London (1992).
40. Chatterjee, P.K., Datta, A.B. and Kundu, K.M., "Fluidized bed gasification of coal", *The Canadian Journal of Chemical Engineering*, **73**, (1), 204-210 (1995).
41. Chatterjee, P.K., *Journal of Polymer Science, Part A*, **3**, 4253 (1965) (Cited in Nishizaki et al. 1980).
42. Chen and Nuttal (1979) (Cited in Nishizaki et al., 1980).
43. Chen, J.L.P. and Keairns D.L., "Particle segregation in a fluidized bed", *The Canadian Journal of Chemical Engineering*, **53**, 395-402 (1975).

44. Cheremissinof, N.P. and Cheremissinoff, P.N., "Hydrodynamics of gas-solids fluidization" Gulf Publishing Company, London (1984).
45. Cherian, J., and Flanigan, V.J., "Effect of operating conditions on gas quality and conversion efficiency of a fluidized bed gasifier for wood, manure and peat" In : IGT-Symposium on Biomass and Wastes-VII, 412-431 (1983).
46. Cheung, L.Y.L., Nienow, A.W. and Rowe, P.N., Chemical Engineering Science, 29, 1301 (1974).
47. Chiba, S., Chiba, T., Nienow, A.W. and Kobayashi, H., "The minimum fluidization velocity, bed expansion and pressure-drop profiles for binary particle mixture", Powder Technology, 22, (2), 255-269 (1979).
48. Chowdhury, R., Bhattacharya, P. and Chakravarty, M., "Modelling and simulation of a downdraft rice husk gasifier", International Journal of Energy Research, 18, 581-594 (1994).
49. Clark, S.J. and Goodman, M.A., "Biomass gas fueling of spark ignition engine – carburettor development and testing", Paper ASAE, No. 85-3570, 1-27 (1985).
50. Coats, A.W. and Redfern, J.P., "Kinetic parameters from thermogravimetric data", Nature, 201, 68-69 (1964).
51. Cooley, S. and Antal, M.J. , "Kinetics of cellulose pyrolysis in the presence of nitric oxide", Journal of Analytical and Applied Pyrolysis, 14, 149-161 (1988).
52. Corella, J., Aznar, M.P., Delgado, J. and Aldea, E., "Steam gasification of cellulosic wastes in a fluidized bed with downstream vessels", Industrial Engineering Chemistry Research, 30, 2252-2262 (1991).
53. Corella, J., Caballero, M.A., Aznar, M.P. and Toledo, J.M., "Typical gas composition and characteristics in gasification with air of carbonaceous residues in circulating and atmospheric fluidized bed", Preprint of the Proceedings of Petro-Tech India, New Delhi, Jan. 9-11(2001).
54. Corella, J., Herguido, J. and Gonzalez-Saiz, "Stream gasification of biomass in fluidized bed-effect of the type of feedstock", In : Pyrolysis and Gasification, Ferrero,G.L., Maniatis,K, Beukens A and Bridgwater A.V (Eds.), Elsevier Science Publishers, London, UK, 619-623 (1989).

55. Czernik, S., Koeberle, P.G., Jollez, P., Bilodeau, J.F. and Chornet, E., "Gasification of residual biomass via the Biosyn fluidized bed technology", In : *Advances in Thermochemical Biomass Conversion*, Bridgwater, A.V. (Ed.) Blackie Academic and Professional, 423-437 (1994).
56. Davidson, J.F. and Harrison, D., "Fluidization" Academic Press, London (1971).
57. Desrosiers, R., "Thermodynamics of gas-char reactions" In: "Biomass Gasification Principles and Technology", Reed, T.B (Ed.) New Jersey, Noyes Data Corporation, 119-153 (1981).
58. Diblasi Colomba, Signorelli, G. and Portoricco, G., "Counter current fixed bed gasification of biomass at laboratory scale", *Industrial Engineering Chemistry Research*, **38**, 2571-2581 (1999).
59. Diblasi, Colomba and Branca, C., "Global degradation kinetics of wood and agricultural residues in air", *The Canadian Journal of Chemical Engineering*, **77**, 555-561 (1999).
60. Ebeling, J.M. and Jenkins B.M., "Physical and chemical properties of biomass fuels", *Transactions of the American Society of Agricultural Engineers*, **28**, (3), 898-902 (1985).
61. Engstrom, F. and Lee, Y.Y., "Future challenges of circulating fluidized bed combustion technology", In: *Circulating fluidized Bed Technology-111*, Basu, P. Horio, M. and Hasatani, M (Eds.), Pergamon Press (1991).
62. Ergudenler, A. and Ghaly A.E., "Quality of gas produced from wheat straw in a dual-distributor type fluidized bed gasifier", *Biomass and Bioenergy*, **3**, (2), 419-430 (1992).
63. Ergudenler, A., Ghaly, A.E., Hamdullahpur, F. and Al-Taweel, A.M., "Mathematical modeling of a fluidized bed straw gasifier: Part III- model verification" *Energy Sources*, **19**, 1099-1121 (1997).
64. Ergun, S., "Fluid flow through packed columns", *Chemical Engineering Progress*, **48** (1), 89-94 (1952).
65. Evans, R.J. and Milne, T.A. (1987) (Cited in Antal and Varhegyi, 1995).

66. Evans, R.J., Knight, R.A., Onischak, M. and Basu, S.P., "Process performance and environment assessment of the Renugas process", *Energy from Biomass and Wastes*, **10**, 677-694 (1987).
67. Faaiz, A. van Doorn J. , Curvers, T., Waldheim, L., Olsson E., Wijk, A. and Ouwens, C.D., "Characteristics and availability of biomass wastes & residues in the Netherlands for gasification", *Biomass & Bioenergy*, **12** (4), 225-240 (1997).
68. Feldman, H.F., Choi, P.S., Paisley, M.A., Chauhan, S.P., Robb, C.J., Folsam, D.W. and Kin, B.C., In: Symp. Papers Energy from Biomass and Wastes V, Lake Buena Vista, FL (1984) (Cited in Aznar et al., 1992a)
69. Flanigan, V.J., Shimon, J.E., Punyakumleard, A., "Low-Btu gas from a small scale fluidized bed reactor using saw dust feeds" In: Symposium on Energy from Biomass and Wastes-VI Institute of gas Technology USA, 645-665 (1982).
70. Flanigan, V.J., Xu, B.Y. and Huang, E., "Fluidized bed gasification of rice hulls", The Tenth Annual Energy-Sources Technology Conference and Exhibition, Dallas, Texas, 19-34 (1987).
71. Font, R., Marcilla, A., Verdu, E. and Devesa, Industrial Engineering Chemistry Process Design and Development, **25**, 491 (1986).
72. Freeman, E.S. and Carroll, B., "The application of thermogravimetric techniques to reaction kinetics. The thermogravimetric evaluation of the kinetics of the decomposition of calcium oxalate monohydrate", *Journal of Physical Chemistry*, **62**, 394 (1958).
73. Friedman, H.L., *Journal of Polymer Science Part C*, **6**, 183 (1965) (Cited in Nishizaki et al., 1980).
74. Gangawati, P.B., Prasad, B. and Mishra, I.M., "Fluidization characteristics of agricultural and forestry residue type biomass for thermal gasification". National Seminar on Future Trends in Mech. Engg. Research and Development organized by Deptt. of Mechanical and Industrial Engg., University of Roorkee(now IIT Roorkee), Roorkee and Institution of Engineers (India) Roorkee, Sept. 29-30, 651-656 (2000a).



75. Gangawati, P.B., Prasad, B. and Mishra, I.M., "Thermal gasification of biomass in fluidized bed" unpublished report, Chemical Engineering Department, Indian Institute of Technology, Roorkee (2000b).
76. Gaur and Reed (1994) (Cited in Antal and Varhegyi, 1995).
77. Gavalas, G.R., Industrial Engineering Chemistry Fundamentals, 20, 122 (1981) (Cited in Antal and Varhegyi, 1995)
78. Geldart, D., "Introduction" In: Gas Fluidization Technology, Geldart, D. (Ed.) John Wiley and Sons, New York, 1-9 (1986).
79. Ghaly, A.E. and Al-Taweel, A.M., "Physical and thermochemical properties of cereal straws", Energy Sources, 12, 131-145(1990).
80. Ghaly, A.E. and Ergudenler, A., "Thermal degradation of cercal straws in air and nitrogen", Journal of Applied Biochemistry and Biotechnology, 28/29, 111-126 (1991).
81. Ghaly, A.E., Ergudenler A. and Al-Taweel., A.M, "Determination of the kinetic parameters of oat straw using thermogravimetric analysis", Biomass and Bioenergy, 5 (6), 457-465 (1993).
82. Gibilaro, L.G. and Rowe, P.N., "A model for segregating gas fluidized bed", Chemical Engineering Science, 29, 1403 (1974).
83. Gil, J., Aznar, M.P., Caballero, M.A., Frances E. and Corella J., "Biomass gasification in fluidized bed at pilot scale with steam -O<sub>2</sub> mixture. Product distribution for very different operation conditions", Energy & Fuels, 11(6) (1997)
84. Gil, J., Corella, J., Aznar, M.P., and Caballero, A., "Biomass gasification in atmospheric and bubbling fluidized bed: Effect of the type of gasifying agent on the product distribution" Biomass and Bioenergy, 17, 389-403 (1999).
85. Gomez, E.O., Lora, E.S. and Cortez, L.A.B., "Constructive features, operation and sizing of fluidized bed gasifiers for biomass", Energy for Sustainable Development, III (4), 52-57 (1995).
86. Goosens, W.C.A., Dumont, G.L. and Spaepen, Chemical Engineering Progress Symposium Series, 67 (116) , 38 (1971).

87. Gorbachev, V.M., "A solution of the integral in the non-isothermal kinetics for linear heating", *Journal of Thermal Analysis*, **8**, 149 (1975).
88. Govindarao, V.M.H., "Utilization of rice husk – a preliminary analysis", *Journal of Scientific & Industrial Research*, **39**, 495-515 (1980).
89. Grace, J.R., "Advanced fluidization topics" Continuing Education, Montreal (1981).
90. Grover, P.D., "Biomass feed processing for energy conversion" In: *International Conference on Biomass Energy Systems*, 26-27 Feb. TERI, New Delhi, 177-195 (1996).
91. Grover, P.D., "Biomass: Thermochemical characterization for gasification" Report Chemical Engineering Department, I.I.T., New Delhi (1989).
92. Gumz, W., "Gas producers and blast furnaces" John Wiley and Sons, New York (1950).
93. Hall, D.O., "Biomass Energy", *Energy Policy*, 711-737 (1991).
94. Hamad, M.A., "Thermal characteristics of rice hulls", *Journal of Chemical Technology and Biotechnology*, **31** (3), 624-626 (1981).
95. Hartiniati, A., Soemardjo, A. and Youvial, M., "Performance of a pilot scale fluidized bed gasifier fuelled by rice husks", In: *Proceedings of International Conference on Pyrolysis and Gasification*, Ferrero, G.L., Maniatis, K. and Buekens, A (Eds.), Elsevier Applied Science, London, 257-263 (1989).
96. Hasler, P. and Nussbaumer, T., "Sampling and analysis of particles and tars from biomass gasifier", *Biomass & Bioenergy*, **18**, 61-66 (2000).
97. Hasler, P., Verenum Research Zurich Switzerland Personal Communication via e-mail (2000).
98. Hemati, M. (1985) (Cited in Aznar et al., 1992a).
99. Hemati, M., Spieker, K., Lagueric, C., Alvarez, R. and Pereira, F.A., "Experimental study of sawdust and coal particle mixing in sand or catalyst fluidized beds", *The Canadian Journal of Chemical Engineering*, **68**, 768-772 (1990).

100. Herguido, J., Corella, J. and Gonzalez, Saiz, "Steam gasification of ligno cellulosic residues in a fluidized bed at a small pilot scale- Effect of the type of feedstock", *Industrial Engineering and Chemistry Research*, **31**(5), 1274-1282 (1992).
101. Hiler, E.A., "On site energy production from agricultural residues", Centre for Energy and Minerals Resources, Texas A & M. Univ. College Station, TX, USA, Report: TENRAC/EDF-074 (1982).
102. Horowitz, H.H. and Metzger, G., "A new analysis of thermogravimetric traces", *Analytical Chemistry*, **35**, 1464 (1963) (Cited in Nishizaki et al., 1980).
103. Hos., J.J. and Groeneveld, M.J., "Gasification of various wastes in an annular co-current moving bed gasifier" In: "Energy from Biomass" Elsevier Applied Science, London, 406-409 (1983).
104. Houston, D.F., "Rice: chemistry and technology", Published by American Association of Cereal Chemists Incorporated, St. Paul, Minnesota (1972).
105. Hoveland et al, (1982) (Cited in Boateng et al., 1992)
106. Iyer, P.V.R., Rao, T.R., Grover, P.D. and Singh, N.P. (Eds.), "Biomass thermo-chemical characterization" Second Edition Biomass Gasifier Action Research Centre, Chemical Engineering Department, I.I.T., New Delhi. (1997)
107. Jain, A., Rao, T.R., Sambhi, S.S. and Grover, P.D., "Energy and chemicals from rice husk", *Biomass and Bioenergy*, **7**, 285-289 (1994).
108. Jain, A.K., Sharma S.K, and Daljeet Singh, "Reaction kinetics of paddy husk thermal decomposition", *Journal of Solar Energy Engineering (ASME)*, **121**(5), 25-30 (1999).
109. Jain, A.K., Sharma, S.K and Daljeet Singh, "Thermal analysis of paddy husk: Part I "Sensitivity of kinetic parameters to selection of stage transition points". Intersociety Energy Conversion Engineering Conference, Hawaii, USA, IECEC-97-98468, 2316-2321 (1997a).

110. Jain, A.K., Sharma, S.K and Daljeet Singh, "Thermal analysis of paddy husk Part II Order of reaction and other kinetic parameters", Intersociety Energy Conversion Engineering Conference, Hawaii, USA, IECEC-97-98469, 2322-2327 (1997b).
111. Jenkins, B.M. and Bhatnagar, A.P., "On the electric power potential from paddy straw in the Punjab and the optimal size of the power generation station", *Bioresource Technology* **37**, 35-41 (1991).
112. Jenkins, B.M. and Ebeling, J.M., "Correlation of the physical and chemical characteristics of terrestrial biomass with conversion", Symposium on Energy from Biomass and Wastes IX, Institute of Gas Technology, Chicago, Illinois, USA, 371-403 (1985).
113. Jenkins, B.M., "Fuel properties of biomass materials", International Symposium on Application and Management of Energy in Agriculture: The Role of Biomass Fuels, IIT, Delhi, India, May 21-23 (1990).
114. Jiang, H. and Morey R.V., "Air gasification of corncobs at fluidization", *Biomass & Bioenergy*, **3**(2), 87-92 (1992).
115. Jorapur, R.M. and Rajavanshi, A.K., "Development of a sugarcane leaf gasifier for electricity generation", *Biomass and Bioenergy*, **8**(2), 91-98 (1995).
116. Kapur, P.C., "Production of reactive bio-silica from the combustion of rice husk in a tube-in-basket burner", *Powder Technology*, **44**, 63-67 (1985).
117. Katyal, S.K. and Iyer, P.V.R., "Thermochemical characterization of pigeon pea stalk for its efficient utilization as an energy source", *Energy Sources*, **22**, 363-375 (2000).
118. Katyal, S.K., "Thermogravimetric analysis of pigeon pea stalk", *Indian Chemical Engineer, Section A*, **43**(1), T20-T24 (2001).
119. Kaupp, A., "The myths and facts about gas producer engine systems", *Producer gas : A collection of papers on producer gas with emphasis on application in developing countries*, Based on papers presented in the first international producer gas conference, Colombo, Sri Lanka, Published by the Beijer Institute, 25-46 (1982).

120. Kishore, V.V.N., "Thermal gasification of biomass- potential, problems and research needs", In : *Wealth from Wastes*, TERI Publication, New Delhi (1995).
121. Kissinger, H.E., "Reaction kinetics in differential thermal analysis", *Analytical Chemistry* **29**, 1702 (1957) (Cited in Nishizaki et al., 1980).
122. Koufopoulos, C.A., Maschio, G. and Lucchesi, A., "Kinetic modelling of the pyrolysis of biomass and biomass components", *The Canadian Journal of Chemical Engineering*, **67**, 75-82 (1989)
123. La Nauze, R.D., "A review of the fluidized bed combustion of biomass", *Journal of the Institute of Energy*, 66-76 (1986).
124. Lamorey, G.W., Jenkins, B.M. and Goss, J.R., "LP engine and fluidized bed gas producer performance", ASAE paper (as mentioned in Gomez et al., 1995) (1985).
125. Lee, T.V. and Beck S.R., "A new integral approximation formula for kinetic analysis of non isothermal TGA data", *American Institute of Chemical Engineers Journal*, **30**, 517 (1984).
126. Li chung-Hsuing, "An integral approximation formula for kinetic analysis of non-isothermal TGA data", *American Institute of Chemical Engineers Journal*, **31**(6), 1036-1038 (1985).
127. Lipska Quinn, A.E., Zeronian, S.H. and McGee, K.M., "Thermal degradation of rice straw and its components", In : "Fundamentals of Thermochemical Biomass Conversion", Overend, R.P., Milne, T.A. and Mudge, K.L. (Eds.), Elsevier Applied Science Publishers, Essex, England, 453-471 (1985).
128. Lundqvist, R.G., "The IGCC demonstration plant at Varnamo", *Bioresource Technology*, **46**, 49-53 (1993).
129. Maniatis, K., "Fluidized bed gasification of agricultural residues". In: *Papers presented at the International Symposium on Application and Management of Energy in Agriculture Role of Biomass Fuels*, New Delhi, India (1990).

130. Maniatis, K., and Kiritsis, S., "Gasification of cotton stalks in a fluidized bed", Proceedings of the 6<sup>th</sup> European Conference of Biomass for Energy, Environment and Industry (Athens, Greece, 1991), Elsevier Press, 806-810 (1992).
131. Maniatis, K., Bridgwater, A.V. and Buekens, A., "Fluidized bed gasification of wood: Performance of a demonstration plant. In: Ferrero G.L., Maniatis K., Buekens, A. and Bridgwater, A.V., (Ed.), Pyrolysis and Gasification. London: Elsevier Applied Science, 274-281 (1989).
132. Mansaray, K. G. and Ghaly, A.E., "Thermal degradation of rice husks in an O<sub>2</sub> atmosphere", Energy Sources, **21**, 453-466,(1999).
133. Mansaray, K.G. and Ghaly, A.E, "Thermogravimetric analysis of rice husks in an air atmosphere", Energy Sources, **20**, 653-663 (1998).
134. Mansaray, K.G., Ghaly, A.E., Al-Taweel, A.M., Hamdullahpur, F., and Ugursal, V.I., "Air gasification of rice husk in a dual distributor type fluidized bed gasifier", Biomass and Bioenergy, **17**, 315-332 (1999).
135. Maschio, G., Koufopoulos, C. and Lucchesi, A., " Pyrolysis, a promising route for biomass utilization" Bioresource Technology, **42**, 219-231 (1992).
136. Mehrling, P., and Reimert, R., "Synthetic fuel from wood via gasification in the circulating fluidized bed", Energy from Biomass Conference, 73-113 (1986).
137. Milosavljevic, I. and Suuberg, E.M., "Cellulose thermal decomposition kinetics: Global mass loss kinetics", Industrial Engineering Chemistry Research, **34**, 1081-1091 (1995).
138. Mishra, I.M., Deepak, D., Panesar, P.S. and Saraf, S.K., "Status of pollution in sugar industry" Departmental Report-2, Department of Chemical Engineering, IIT Roorkee, Roorkee (India) (1998).
139. Mohan, Sudhir and Meshram, J.R., "Biomass based power generation prospects in India", Energy Management, Jan.-March, 1-14 (1998).
140. Moreno, F.E and Goss, J.R., "Fluidized bed gasification of high ash agricultural wastes to produce process heat and electrical power" In: Symposium on Energy from Biomass and Wastes-VII , Institute of Gas Technology, USA, 515-537 (1983).

141. Mukunda, H.S. and Paul, P.J., "Fundamental combustion and gasification aspects of biomass and biomass derived gaseous fuels" In: Recent Advances in Biomass Gasification and Combustion, Interline Publishing, Bangalore, 109-117 (1994).
142. Mukunda, H.S., Paul, P.J., Dasappa, S., Srinivasa, U., Sharan, H., Buehler, R., Hasler, P. and Kaufman, H., "Results of an Indo-Swiss programme for qualification and testing of a 300 kW IISC-Dasag gasifier", Energy for Sustainable Development, 1 (4), 46-49 (1994).
143. Nagh, Z. B.A., Shamsuddin, I. and Fa, L.K., "Malaysian program on utilization of rice husks for power generation". Proceedings of the FAO/FHI regional technical consultation on agricultural wastes and solar technologies for farm energy needs", Published by FAO Regional Office for Asia and the Pacific, Bangkok, Thailand, 79-84 (1983).
144. Narvaez, I., Orio, A., Aznar M.P. and Corella, J., "Biomass gasification with air in an atmospheric bubbling fluidized bed. Effect of six operational variables on the quality of the produced gas", Industrial and Engineering Chemistry Research, 35(10), 2110-2120 (1996).
145. Nassar, M.M., "Kinetic Studies on thermal degradation of nonwood plants", Wood and Fiber Science, 17(2), 266-273 (1985).
146. Nassar, M.M., Ashour, E.A. and Wahid, S.S., "Thermal characteristics of bagasse", Journal of Applied Polymer Science, 61, 885-890 (1996).
147. Natarajan, E., "Experimental investigation on fluidized bed rice husk gasification system for power generation" unpublished Ph.D. thesis, Mechanical Engineering Department, Anna University, Chennai (1998).
148. Natarajan, E., Nordin, A. and Rao A.N., "Overview of combustion and gasification of rice husk in fluidized bed reactor". Biomass & Bioenergy, 14(5/6), 533-546 (1998).
149. Neef, John, ECN-Netherlands Energy Research Foundation Personal Communication via e-mail (2000).
150. Nienow, A.W., Rowe, P.N. and Cheung, L.Y.L., "A quantitative analysis of the mixing of two segregating powders of different density in a gas-fluidized bed", Powder Technology, 20(1), 89-97 (1978).

151. Nishizaki, H. Yoshida K and Wang, J.H., "Comparative study of various methods for thermogravimetric analysis of polysterene degradation", *Journal of Applied Polymer Science*, **25**, 2869-2877 (1980).
152. Noda, K., Uchida, S., Makino, T. and Kamo, H., "Minimum fluidization velocity of binary mixture of particles with large size ratio", *Powder Technology*, **46**, 149-154 (1986).
153. Omnifuel, Biomass Energy Technology, "Fluidized bed gasification systems", Technical Bulletin (1990).
154. Otero, A.R. and Corella, J., *An Quim*, **67**, 1221 (1971b) (Cited in Aznar et al., 1992a)
155. Otero, A.R. and Corella, J., *An Quim*, **67**, 1207 (1971a) (Cited in Aznar et al., 1992a)
156. Overend, R.P., Onischak, M., Trenka, A. and Kinoshita, C., "The U.S. Department of Energy and the Pacific International Centre for high technology research pressurized oxygen-air fluidized bed biomass gasification scale-up", In : *Advances in Thermochemical Biomass Conversion*, Bridgwater, A.V. (Ed.), Blackie Academic and Professional, 438-448 (1994).
157. Ozawa, T., *Bulletin of Chemical Society of Japan*, **38**, 1881 (1965) (Cited in Nishizaki et al., 1980).
158. Paisley, M.A., Feldmann, H.F., and Appelbaum, H.R., In : *Symposium on Energy from Biomass and Wastes-VIII*, Institute of Gas Technology, Illinois, USA (1984) (Cited in Aznar et al., 1992a).
159. Panaka, P., "Operating experience with biomass gasifiers in Indonesia", *Adv. Thermochem. Biomass Convers.*, Ed. By. Bridgwater, A.V, Blackie Publisher, Glasgow, UK, 392-402 (1994).
160. Parikh, P.P., "State of art report on biomass gasification", A report, Mech. Engg. Deptt., IIT Bombay (1989).
161. Patel, S.R. and Rao, C.S., "Development and performance of a 20 kW gasifier system using woody agricultural residues as feed stocks for power generation", In: *Proc. of IV National Technical Meet on Biomass Gasification held at Mysore, in January (1993)*.



162. Patil, K.N. and Rao, C.S., "Design and development of a 25000 kcal/h gasifier burner system for thermal applications in rural industries" Proceedings of National Solar Energy Convention, Vadodara, 244-247 (1993).
163. Peel, R.B. and Santos, F.J., "Fluidized bed combustion of vegetable fuels", Proceedings of International Conference on Fluidized Combustion: Systems and Applications, IIB.2.1-IIB.2.9 (1980).
164. Peiyi, J., "The application of paddy husk gas in rice mill", Proceedings of the FAO/FHI regional technical consultation on agricultural wastes and solar technologies for farm energy needs, held in Suzhou, China and Cabanatuan, Philippines in June 1982, Published by FAO Regional Office for Asia and the Pacific, Bangkok, Thailand, 91-100 (1983).
165. Perry, R.H. and Chilton, C.H., Chemical Engineers' Handbook, McGraw Hill-Kogakusha Ltd., Tokyo (1973).
166. Piloyan, G.O., Ryabchikov, I.D. and Novikova, O.S., "Determination of activation energies of chemical reactions by differential thermal analysis", Nature, 1229(1966).
167. Piloyan, G.O. and Novikova, O.S., Journal of Inorganic Chemistry, 12, 313 (1967) (Cited in Nishizaki et al., 1980)
168. Pitt, G.J., Fuel, 41 267 (1962) (Cited in Suuberg et al, 1979).
169. Prasad, B. and Sharma, M.P., "Development of downdraft gasifier energy management, 10, Oct.-Dec., 297-304. (1986).
170. Prasad, B.V.R.K. and Kuester J.L., "Process analysis of dual fluidized bed biomass gasification system". Industrial Engineering and Chemistry Research, 27(2), 304-310 (1988).
171. Preto, F., Anthony, E.J., Desai, D.L. and Friedrich, F.D., "Combustion trials of rice hulls in a pilot-scale fluidized bed", Proceedings of International Conference on Fluidized Bed Combustion, 2, 1123-1127 (1987).
172. Raissi, A.R. and Trezek, G.J., "Parameters governing biomass gasification" Industrial and Engineering Chemical Research, 26(2), 221-228 (1987).
173. Ramaih, M.V. and Goring, D.A.I., Cell. Chem. Technol., 1, 277 (1967) (Cited in Ramaih, 1970).

174. Ramaih, M.V., "Thermogravimetric and differential thermal analysis of cellulose, hemi cellulose and lignin", *Journal of Applied Polymer Science*, **14**, 1323-1337 (1970).
175. Raman, K.P., Walawender, W.P., Fan L.T and Howell J.A., "Thermogravimetric analysis of biomass-devolatilization studies on feedlot manure, *Industrial Engineering Chemistry Process Design Development*, **20** (4), 630-636 (1981).
176. Raman, K.P., Walawender, W.P. and Fan, L.T., "Gasification of feed lot manure in a fluidized bed reactor - The effect of temperature", *Industrial Engineering and Chemistry Process Design Development*, **19**(4), 623-629 (1980).
177. Raman, P., Dhingram, S. and Kishore, V.V.N., "A multi fuel-multipurpose prototype biomass gasifier system", *Proceedings of 2<sup>nd</sup> Technical Meet on Recent Advances in Biomass Gasification Technology*, Udaipur, Dec. 20-21, 99-119 (Cited in Kishore, 1995).
178. Rapagna, S. and Latif, A., "Steam gasification of almond shells in a fluidized bed reactor : The influence of temperature and particle size on product yield and distribution", *Biomass and Bioenergy*, **12**(4), 281-288 (1997).
179. Reed, T.B., "Biomass gasification-principles and technology", *Energy Technology Review No. 67*, Noyes Data Corporation, Park Ridge, New Jersey (1981).
180. Reich, L. and Levi, D.W., *Macromolecular Review*, **1**, 173 (1963) (Cited in Nishizaki et al., 1980).
181. Reich, L. and Stivala, S.S., "Computer determined kinetic parameters from TG curves", *Thermochimica Acta*, **36**, 103-105 (1980).
182. Reich, L. and Stivala, S.S., *Thermochimica Acta* **24**, 9 (1978) (Cited in Reich et al., 1980).
183. Reich, L. and Stivala, S.S., *Thermochimica Acta*, **52**, 337 (1982) (Cited in Agarwal and Sivasubramanian, 1987).

184. Reich, L., Journal of Polymer Science, Letters, 3, 231 (1965) (Cited in Nishizaki et al., 1980).
185. Rensfeld, E., "Cogeneration using gasification and diesel engines", Studsvik Energiteknik AB, Technical Bulletin (1988).
186. Rossi, A., "Fuel characteristics of wood and non-wood biomass fuels", In: Progress in Biomass Conversion, Tillman, D.A. and John, E.C. (Ed.), Academic Press, Orlando, FL, 5, 69-99 (1984).
187. Rowe, P.N. and Nienow A.W., (1975) (Cited in Rowe, P.N and Nienow, A.W., 1976)
188. Rowe, P.N. and Nienow A.W., (1978) (cited in Bilbao et al. 1988)
189. Rowe, P.N. and Nienow, A.W., "Particle mixing and segregation in gas fluidized beds – A Review", Powder Technology, 15(1), 141-147 (1976).
190. Rowe, P.N., Nienow, A.W. and Agbim, A.J., "The mechanisms by which particles segregate in gas fluidized beds – binary systems of near spherical particles" Transactions of Institution of Chemical Engineers, 50, 310-333 (1972).
191. Sakoda, A., Sadakata, M., Koya, T., Furusawa, T. and Kunii, D., "Gasification of biomass in a fluidized bed", The Chemical Engineering Journal, 22, 221-228 (1981).
192. Sanchez, C.G. and Silva, E.L., "Biomass fluidized bed gasification research in the State University of Campinas", Energy for Sustainable Development, 1(4), 31-34. (1994)
193. Schiefelbein, G.F., "Biomass thermal gasification research" Biomass 19(1), 145-159 (1989).
194. Schoeters, J. Maniatis, K. and A. Bueckens, A., "The fluidized bed gasification of biomass: Experimental studies on bench scale reactor", Biomass, 19(1), 129-143 (1989).
195. Schoeters, J., Maniatis, K. and Buekens, A., Proceedings of 2<sup>nd</sup> World Congress of Chemical Engineers, 1, Montreal, 313 (1981).
196. Sen, R. and Ghosh D.N, "Fluidization and combustion characteristics of rice husk", Indian Chemical Engineer, 34(4), 206-211 (1992).

197. Shafezadeh et al., In : Fuels from Waste, Anderson L.L. and Tilman D.A. (Eds.) (1977) (Cited in Shafizadeh, F., 1985).
198. Shafizadeh, F., "Pyrolytic reactions and products of biomass" In : Fundamentals of Thermochemical Biomass Conversion Overend, R.P., Milne, T.A. and Mudge, K.L. (Eds.), Elsevier Applied Science Publishers, London, UK, 183-217 (1985).
199. Sharma, A. and Rao T.R., " Kinetics of pyrolysis of rice husk", Bioresource Technology, 67, 53-59(1999).
200. Sharma, S.K., "Studies on biomass gasification", M.E. dissertation, Chemical Engg. Deptt., University of Roorkee (now I.I.T., Roorkee) (1988).
201. Sharma, S.K., Prasad, B. and Mishra, I.M., "Biomass gasification in a downdraft gasifier " Proceedings of Fourth National Convention of Chemical Engineers, The Institution of Engineers (India), Roorkee, Oct. 3-4 (1988).
202. Sharp, J.H. and Wentworth, S.A., "Kinetic analysis of thermogravimetric data", Analytical Chemistry, 41(14), 2060-2062 (1969).
203. Sharp, J.H. and Wentworth, S.A., "Kinetic analysis of thermogravimetric data", Analytical Chemistry, 41 (14), 2060-2062(1969).
204. Singamsetti, V. and Rajeshwara Rao, T., "Kinetics of thermal decomposition of rice husk", Indian Chemical Engineer, Section A, 42(4), T104-T109 (2000).
205. Singh, S.K., Walawender, W.P., and Fan, L.T., Wood and Fiber Science, 18(2), 327 (1986).
206. Skala, (1987) (Cited in Bilbao, 1990).
207. Soloman, P.R., Hamblen, D.G., Carangelo, R.M., Serio, M.A. and Deshpande, G.V., "A general model of coal devolatilization" Energy and Fuels, 2, 405 (1988).
208. Sridhar, G., Sridhar, H.V., Dasappa, S., Paul, P.J., Rajan, N.K.S., Srinivas, U. and Mukunda, H.S., "Technology for gasification of pulverized bio-fuels including agricultural residues", Energy for Sustainable Development, III(2), 9-18 (1996).

209. Srivastava, V.K., Sushil and Jalan, R.K., "Prediction of concentration in the pyrolysis of biomass material-III" *Energy Conversion & Management*, **37**(4), 473-483 (1996).
210. Strehler, D., "Results from research work in heat generation from wood and straw", In : *Energy from Biomass* Paiz, W., Coombs, J. and Hall, D.O. (Eds.) Elsevier Applied Science Publishers, London UK, 788-792 (1985).
211. Strom, E., Liinanki, L. and Sjostrom, K., "Gasification of biomass in the MINO Process", Technical Bulletin of the Royal Institute of Technology, Stockholm, Sweden (1982).
212. Suuberg, E.I., Petters, W.A. and Howard, J.B. , In : "Thermal Hydrocarbon Chemistry", Oblad et al., (Eds.) ACS Advances in Chemistry Series, **183** (1979).
213. Tang, W.K., "Effect of inorganic salts on pyrolysis of wood,  $\alpha$ -cellulose and lignin", US Department of Agriculture, Forestry Services Research paper FPL-71 (1967).
214. TEDDY, "TERI Energy Data Directory and Year book", Tata Energy Research Institute, New Delhi (2000-2001).
215. Teng, Hsisheng, Lin, H.C and Jui-Antto, "Thermogravimetric analysis of global mass loss kinetics of rice hull pyrolysis", *Industrial Engineering Chemistry Research*, **36**(9), 3974-3977 (1997).
216. Tia, S., Bhattacharya S.C and Wibulswas, P.B., "Thermogravimetric analysis of Thai-lignite-I pyrolysis kinetics", *Energy Conversion and Management*, **31**(3), 265-276 (1991).
217. Tillman, D.A., "Biomass combustion" In : "Regenerable Energy", Hall D.O. and Overend, R.P. (Eds.) John Wiley and Sons, NY, 203-219 (1987).
218. Tripathi, A.K., Iyer, P.V.R. and Kandapal, T.C., "A techno-economic evaluation of biomass briquetting in India", *Biomass & Bioenergy*, **14**(5/6), 479-488 (1998).
219. Tripathi, A.K., Iyer, P.V.R., Kandapal, T.C. and Singh, K.K., "Assessment of availability and costs of some agricultural residues used as feed stocks for biomass gasification and briquetting in India", *Energy Conversion and Management*, **39**(15), 1611-1618 (1998).

220. Uma, R., Kishore, V.V.N. and Mande, S. , In : International Conference on Biomass Energy Systems, 26-27 Feb. TERI, New Delhi (1996).
221. Vaid, R.P and Sen Gupta, P., “ Minimum fluidization velocities in beds of mixed solids” .The Canadian Journal of Chemical Engineering, 56, 292-296 (1978).
222. Van Den Aarsen (1982) (Cited in Boateng et al., 1992)
223. van Doorn, J., ECN-Netherlands Energy Research Foundation, personal communication (2000).
224. Van Fredersdoff, C.G. and Elliot, M.A., “Coal gasification” In: Chemistry of Coal Utilization, Lowry, H.H. (Ed.), John Wiley and Sons, New York, 892-1022 (1963).
225. van Krevelen, D.W., van Heerden, C. and Huntijens, F.J., Fuel, 30, 253 (1951) (Cited in Nishizaki et al., 1980).
226. van Swaaij, W.P.M., “Gasification – the process and technology” In : Energy from biomass, Palz, W., Chartier, P. and Hall, D.O. (Eds.), Applied Science Publishers, London and New York, 485-494 (1981).
227. Varhegyi, G., Antal, M.J., Szekely, T. and Szabo, P., “Kinetics of the thermal decomposition of cellulose, hemicellulose and sugarcane bagasse”, Energy and Fuels, 3, 329-335(1989).
228. Varhegyi, G., Szabo, P. and Antal, M.J., “Reaction kinetics of the thermal decomposition of cellulose and hemicellulose in biomass materials” In : Advances in Thermochemical Biomass Conversion Bridgwater, A.V., (Ed.), Blackie Academic and Professional, London, 2 (1994).
229. Walawender and Clark (1984) (Cited in Boateng et al., 1992)
230. Walawender, W.P., Dybing, Kyle and Fan, L.T., “Gasification of corn & sorghum stovers in a fluidized bed reactor”, Symposium on Energy from Biomass and Wastes-IX Institute of Gas Technology, USA, 541-572 (1985a).
231. Walawender, W.P., Hoveland, D.A. and Fan, L.T., “Steam gasification of alpha cellulose in a fluid bed reactor”, Chapter No. 49, (ch). Fundamentals of Biomass Conversion Overend R.P. (Ed.), 897-910 (1985b).

232. Walawender, W.P., Sudalaimuth, M.S. and Fan, L.T., in Symp. Papers Energy from Biomass and Wastes V, Lake Buena Vista, FL, 517 (1981).
233. Wang, J. and Kinoshita, C.M., "Experimental analysis of biomass gasification with steam and oxygen" Solar Energy 49(3), 153-158 (1992).
234. Wang, W. and Kinoshita, C.M., "Kinetic model of biomass gasification" Solar Energy, 51(1), 19-25 (1993).
235. Wen C.Y. and Y.H. Yu, "Mechanics of Fluidization" Chemical Engineering Symposium Series, No. 62, 100-111 (1966).
236. Wendlandt, W.W.M. . "Thermal Methods of Analysis", II Edition, John Wiley and Sons, New York (1974).
237. Williams, P.T. (1985) (Cited in Williams et al., 1993).
238. Williams, P.T. and Besler S., "The pyrolysis of rice husks in a thermogravimetric analyzer and static batch reactor", Fuel, 72, 151-159 (1993).
239. Xu , Bing Yan, Huang W.E., Flanigan, V.J. and Sitton, O.C., "Design and operation of a 6.0 inch fluidized bed gasifier for rice husks" Symposium on Energy from Biomass and Wastes – IX Institute of Gas Technology, Illinois, USA, 595-614 (1985).
240. Yang and Keairns D.L., (1982) (Cited in Bilbao et al., 1988)